

NOVEL DESIGN CRITERIA FOR DIRECT COAL LIQUEFACTION  
REACTORS

By

JOHN MICHAEL SHAW

B.A.Sc., The University of British Columbia, 1981

A THESIS SUBMITTED IN PARTIAL FULFILLMENT OF  
THE REQUIREMENTS FOR THE DEGREE OF  
DOCTOR OF PHILOSOPHY

in

THE FACULTY OF GRADUATE STUDIES  
Department of Metallurgical Engineering

We accept this thesis as conforming  
to the required standard

THE UNIVERSITY OF BRITISH COLUMBIA

January, 1985

© John Michael Shaw, 1985

22

In presenting this thesis in partial fulfilment of the requirements for an advanced degree at the University of British Columbia, I agree that the Library shall make it freely available for reference and study. I further agree that permission for extensive copying of this thesis for scholarly purposes may be granted by the head of my department or by his or her representatives. It is understood that copying or publication of this thesis for financial gain shall not be allowed without my written permission.

Department of METALLURGY

The University of British Columbia  
1956 Main Mall  
Vancouver, Canada  
V6T 1Y3

Date 01/04/85

ABSTRACT

A semi-batch Direct Coal Liquefaction facility was designed and constructed in order to examine the impact of process variables on coal liquefaction kinetics. A series of parametric investigations involving bituminous, sub-bituminous coals and lignite were performed. The process variables included solvent composition, catalyst to coal ratio, the intensity of turbulence, the initial dissolved hydrogen concentration, and the slurry residence time distribution. The results of these investigations showed that process variables have a significant impact on the rates of liquefaction reactions, and that reaction rates for coal and lignite are affected in a similar manner.

The overall rate and maximum extent of liquid and gas production was found to depend on the initial rate of molecular hydrogen transfer to the coal particles, and on the ratio of the intensity of turbulence to the level of catalysis. This latter finding led to the discovery of a persistent dispersed liquid phase within the coal liquefaction environment.

A reaction model, coupling these findings with a simple kinetic scheme, was found to correlate the liquefaction behaviour of bituminous and sub-bituminous coals and lignite, in diverse reaction environments. The experimental results and the reaction model were used to develop novel design criteria for Direct Coal Liquefaction Reactors. Two design

optima were identified. One optimum is closely approximated by an existing process. An alternative and potentially preferable optimum is proposed.



## TABLE OF CONTENTS

Abstract .....	ii
Table of Contents .....	iv
List of Tables .....	x
List of Figures .....	xii
Acknowledgements .....	xvii
Nomenclature .....	xviii
Quotation .....	xxiii
 1. Introduction	
1.1 General Introduction .....	1
1.2 Direct Coal Liquefaction - An Overview .....	5
1.2.0 Introduction .....	5
1.2.1 Coal Slurry Preparation .....	7
1.2.2 Coal Liquefaction .....	7
1.2.3 Product Separation .....	8
1.2.4 Solvent Treatment .....	9
1.2.5 Catalysis .....	10
 2. Literature Review .....	11
2.1 Direct Coal Liquefaction (DCL) Reactor Designs .....	11
2.1.0 Introduction .....	11
2.1.1 Liquefaction Reactor Design .....	22
2.1.1.0 Introduction .....	22
2.1.1.1 Pre-heaters .....	24
2.1.1.2 Contactor Design .....	28
2.1.1.3 Reactor Design Rationale .....	43
2.2 Liquefaction Reactions and Kinetics .....	43

2.2.0	Introduction .....	43
2.2.1	Coal Swelling and Solvent Absorption .....	44
2.2.2	Primary Dissolution .....	46
2.2.3	Secondary Dissolution .....	47
2.2.4	Hydrogenation .....	49
2.2.4.1	Hydrogenation Reactions .....	49
2.2.4.2	Heterogeneous Reactions .....	50
2.2.4.3	Homogeneous Reactions .....	51
2.2.5	Hetero-Atom Removal .....	53
2.2.5.1	Reactions .....	53
2.2.5.2	Catalytic Effects .....	54
2.2.6	Retrogressive Reactions .....	57
2.3	Catalysts and Catalysis .....	60
2.3.1	Catalytic and Solvolytic DCL Processes .....	60
2.3.2	The Role of Catalysis .....	60
2.3.3	Catalysts .....	61
2.3.4	Catalytic Activity of Metal Sulphides .....	64
2.4	Solvents.....	66
2.4.1	Chemical Composition .....	66
2.4.2	Physical Properties .....	67
2.4.2.0	Introduction .....	67
2.4.2.1	Gas Solubilities in Coal Liquids and Related Pure Aromatic Solvents at High Pressure .....	68
2.4.2.2	Solvent Density .....	81
2.4.2.3	Solvent Viscosity .....	82
2.5	Process and Kinetic Models .....	85
2.5.0	Introduction .....	87
2.5.1	Kinetic Models .....	88
2.5.2	Process Models .....	93

2.6 Coal Liquefaction Product Analysis .....	94
2.7 Summary .....	97
3. Objectives .....	100
4. Experimental .....	102
4.0 Introduction .....	102
4.1 Coal Liquefaction Experiments .....	104
4.1.1 Apparatus Design and Description .....	104
4.1.2 Operating Procedure .....	108
4.1.3 Materials .....	111
4.1.3.1 Catalysts .....	111
4.1.3.2 Coals/Lignite .....	112
4.1.3.3 Liquefaction Solvents .....	116
4.1.3.4 Analysis Solvent .....	116
4.1.3.5 Gases .....	116
4.1.4 Experiment Design .....	117
4.1.5 Result Analysis .....	121
4.1.5.0 Introduction .....	121
4.1.5.1 Gas Analysis .....	123
4.2 Fundamental Investigations .....	131
5. Experimental Results and Preliminary Discussion .....	134
5.0 Introduction .....	134
5.1 Data Precision .....	134

5.2	Gas Phase Phenomena .....	139
5.3	Reactor and Pre-heater Simulations .....	145
5.4	The Role of Cobalt Molybdate Catalysts in DCL Reaction Environments .....	158
5.5	The Intensity of Turbulence .....	163
5.6	Observations of a Dispersed Phase in a Model Solvent .....	171
5.7	Residual Solids Analysis .....	175
5.8	Summary .....	178
6.	A Novel Reaction Model for Direct Coal Liquefaction Kinetics .....	179
6.0	Introduction .....	179
6.1	An Outline of the Proposed Reaction Model .....	180
6.2	Mathematical Formulation of the Model .....	183
6.2.0	Introduction .....	183
6.2.1	Preliminary Reactions .....	184
6.2.2	Second Stage Reactions .....	189
6.2.3	Residence Time Distributions .....	194
6.2.4	Summary .....	194

6.3	Verification of the Model .....	195
6.3.0	Introduction .....	195
6.3.1	Experimental .....	198
6.3.2	Results and Discussion .....	200
6.4	Summary .....	219
7.	Direct Coal Liquefaction Reactor Design .....	221
7.0	Introduction .....	221
7.1	Pre-heater Design .....	221
7.2	Reactor Design .....	223
7.3	Catalysts .....	224
7.4	A Re-Evaluation of Existing DCL Reactor Designs .....	225
7.5	An Optimum Direct Coal Liquefaction Reactor Design .....	226
7.6	Summary .....	229
8.	Summary .....	230
8.1	Conclusions .....	230
8.2	Suggestions for Further Study .....	231
	References .....	233

Appendices .....	244
Appendix A: Hydrodynamic Calculations .....	245
Appendix B: Correlation Derivations .....	249
Appendix C: Liquefaction Trial Data .....	251
Appendix D: The Impact of Maceral Variations on the Liquefaction Behaviour of Byron Creek Coal .....	259

LIST OF TABLES

Table 2.1:	Direct Coal Liquefaction Process and Product Data .....	12
Table 2.2:	Wilsonville Pre-heater Design Data .....	26
Table 2.3:	H-Coal Product Slate Comparsion .....	31
Table 2.4:	Hydrodynamic Calculation Summary .....	33
Table 2.5:	CCLP Process Yields .....	42
Table 2.6:	Catalysts .....	63
Table 2.7:	Apparent Solubility Data .....	80
Table 2.8:	Coal Solvent Densities .....	84
Table 2.9:	Coal Liquefaction Reaction Models .....	89
Table 2.10:	Product Analysis by Solubility .....	96
Table 4.1:	Variables Investigated .....	103
Table 4.2:	Catalyst Particle Size Distribution .....	113
Table 4.3:	Proximate and Ultimate Analyses of the Test Coals .....	114
Table 4.4:	Apparent Gas Solubilities in Benzene .....	127

Table 5.1:	Result Repeatability .....	136
Table 5.2:	Water Gas Shift Reaction Data .....	142
Table 5.3:	Coal Conversion Statistics for Reactor and Pre-heater Simulations .....	149
Table 6.1:	Data Sets Selected for Model Verification .....	199
Table 6.2:	Optimum Parameters .....	213



# LIST OF FIGURES

Figure 1.1:	A Direct Coal Liquefaction Process Schematic .....	6
Figure 2.1:	H-Coal Process Schematic .....	14
Figure 2.2:	SRC I Process Schematic .....	15
Figure 2.3:	SRC II Process Schematic .....	16
Figure 2.4:	EDS Process Schematic .....	17
Figure 2.5:	Saarbergwerke Process Schematic .....	18
Figure 2.6:	Ruhrkohle Process Schematic .....	19
Figure 2.7:	CCLP Process Schematic .....	20
Figure 2.8:	Dow Process Schematic .....	21
Figure 2.9:	Flow Models .....	23
Figure 2.10:	Flow Regimes for Two-Phase Flow .....	25
Figure 2.11:	The H-Coal Contactor .....	30
Figure 2.12:	Catalyst Residence Time Distribution in a H-Coal Reactor .....	34
Figure 2.13:	Product Flexibility of the EDS Process .....	41
Figure 2.14:	Coal Liquefaction Phenomena .....	45

Figure 2.15: The Hydro de NOS Activity of Various Functionalities .....	55
Figure 2.16: Hydro de NOS Reaction Paths .....	55
Figure 2.17: Representative Retrogressive Reactions .....	58
Figure 2.18: Hydro de NOS Mechanism .....	65
Figure 2.19: Hydrogen Solubility in Pure Organic Solvents .....	71
Figure 2.20: Argon Solubility in Pure Organic Solvents .....	72
Figure 2.21: Ethane Solubility in Pure Organic Solvents .....	72
Figure 2.22: Nitrogen Solubility in Pure Organic Solvents .....	73
Figure 2.23: Carbon Dioxide Solubility in Pure Organic Solvents .....	73
Figure 2.24: Two Liquefaction Reaction Sequences .....	75
Figure 2.25: Hydrogen and Methane Solubilities in Coal Liquids .....	78
Figure 2.26: The Densities of Pure Organic Solvents.....	83
Figure 2.27: The viscosities of Pure Organic Solvents.....	85
Figure 4.1: Experimental Apparatus Schematic.....	105
Figure 4.2: Particle Size Distributions for the Test Coals.....	115

Figure 4.3: Continuous Flow Reactor Simulation Model.....	120
Figure 5.1: The Impact of Temperature Variations on Coal Conversion .....	137
Figure 5.2: The Impact of Residence Time Variations on Coal Conversion .....	138
Figure 5.3: Carbon Monoxide and Carbon Dioxide Production Contours .....	141
Figure 5.4: The Hydrocracking of Ethane .....	144
Figure 5.5: Relative Extents of CO and CH <sub>4</sub> Production During the Initial Stages of Liquefaction Reactions .....	146
Figure 5.6: Hydrogen Consumption During the Initial Stages of Liquefaction Reactions .....	147
Figure 5.7: Apparent Solubilities of Hydrogen in Product Liquids .....	154
Figure 5.8: The Influence of Catalysis on Coal and Lignite Conversion .....	161
Figure 5.9: The Influence of Stirring Rate on Coal and Lignite Conversion .....	165
Figure 5.10: The Influence of Stirring Rate on Residue Particle Size Distribution .....	168

Figure 5.11: Phase Distributions in a Model Two Phase Liquefaction Solvent at Room Temperature .....	173
Figure 5.12: Phase Distributions in a Model Two Phase Liquefaction Solvent at Elevated Temperatures ....	174
Figure 5.13: Sulphur Concentration Profiles in Spent Catalyst Particles .....	177
Figure 6.1: An Outline of the Model .....	181
Figure 6.2: The Temperature Dependence of DCL Rate Constants .....	192
Figure 6.3: The Modified Arrhenius Dependence of DCL Rate Constants .....	193
Figure 6.4: Result Summary for a Verification Trial with Fies Mine Coal .....	201
Figure 6.5: Result Summary for a Verification Trial with Hat Creek A Coal .....	202
Figure 6.6: Result Summary for a Verification Trial with Hat Creek B Coal .....	203
Figure 6.7: Result Summary for a Verification Trial with Middle Kittanning Coal .....	204
Figure 6.8: A Comparison of Predicted and Observed Results for Forestburg Coal Liquefied in Solvent 2 (I) .....	205

Figure 6.9: A Comparison of Predicted and Observed Results for Forestburg Coal Liquefied in Solvent 2 (II) .....	206
Figure 6.10: A Comparison of Predicted and Observed Results for Forestburg Coal Liquefied in Solvent 1 (I) .....	207
Figure 6.11: A Comparison of Predicted and Observed Results for Forestburg Coal Liquefied in Solvent 1 (II) .....	208
Figure 6.12: A Comparison of Predicted and Observed Results for Byron Creek Coal Liquefied in Solvent 2 (I) .....	209
Figure 6.13: A Comparison of Predicted and Observed Results for Byron Creek Coal Liquefied in Solvent 2 (II) .....	210
Figure 6.14: Result Summary for a Verification Trial with Saskatchewan Lignite .....	211
Figure 7.1: A Novel Direct Coal Liquefaction Reactor Design .....	228

### ACKNOWLEDGEMENTS

Many people have contributed to the success of this project. Special thanks are due Professor E. Peters for his guidance and encouragement throughout my tenure at the Metallurgy Department, Mr. G. Mojaphoko and Mr. G. Roemer, both undergraduate Metallurgy students, for volunteering many summer days and evenings in search of answers which frequently did not exist, and Mr. Peter Kemp who always found time to analyze a few more coal samples. I am also indebted to Professor R. Butters, and Mr. H. Tump. Their assistance with experimental difficulties was always timely and constructive.

The financial assistance, provided by B.C. Research and the Natural Sciences and Engineering Research Council is gratefully acknowledged.

NOMENCLATURE

$A, \bar{A}$	constants
$A'$	surface area of coal per unit volume, $m^{-1}$
$A_i, A_f$	mass fraction of ash in coal, residue.
$Ar$	argon, Archimedes number
$Ar_o, Ar_1, Ar_2$	argon mole fraction in initial gas, final high pressure sample, low pressure gas sample.
$b, \bar{b}$	constants
$C_i, \bar{C}_i$	mole fraction, average mole fraction
CAT	catalyst
CCLP	Chevron Coal Liquefaction Process
CSTR	continuous stirred tank reactor
$C_\theta$	normalized concentration $\equiv \int_0^\infty C_\theta dt = 1$
$D$	dispersion coefficient, $m^2 s^{-1}$ , impellor diameter, $m$ , molecular diffusion coefficient, $m^2 s^{-1}$ .
DCL	Direct Coal Liquefaction
$\bar{d}^\circ$	initial mean diameter of coal particles, $m$
$E_\theta$	frequency for a normalized probability distribution.

EDS	EXXON Donor Solvent
F	stirring rate Hz
$F_1$	a function defined by equation 4.5
g	gravitational acceleration $m\ s^{-2}$
H	hydrogen concentration moles $\cdot Kg^{-1}$ solvent
$H_0, H_1, H_2$	mole fraction of hydrogen in initial gas, final high pressure gas samples, low pressure gas samples.
$H_2^o, H_2^{eq}$	hydrogen concentration and equilibrium hydrogen concentration in a liquefaction solvent at zero time, under reaction conditions, moles $\cdot Kg^{-1}$ solvent.
HC	fraction of hydrogen consumed.
J	a function defined by Equation 6.11
$J_1$	a function defined by Equation 6.3
$J_2$	a function defined by Equation 6.10
$K, K_1, K_2, K_3, K_4$	constants
$K'$	overall mass transfer coefficient, moles $\cdot s^{-1}$
L	reactor length, m
M	molar mass, g
MAFC	moisture and ash free coal, g
mrt	mean residence time
N	the number of ideal stirred tanks, in series, which best simulate an experimental reactor



$P, P_c, P_r$	pressure, MPa, critical pressure, MPa, relative pressure
$P_o, P_1$	initial and final pressure, MPa
PFR	plug flow reactor
$Q$	gas flow rate, $m^3 s^{-1}$
$R$	universal gas constant
rtd	residence time distribution
$S$	solubility $moles \cdot Kg^{-1}_{solvent} \cdot Atm^{-1}$
$S_i$	the apparent solubility of a gas component in a solvent, the solubility of a gas in a single component of a complex solvent, $moles \cdot Kg^{-1} \cdot Atm^{-1}$
$S_{mix}$	solubility in a complex solvent,
SIR	slurry injection run $moles \cdot Kg^{-1} \cdot Atm^{-1}$
$Sh$	Sherwood number
$\bar{Sh}_{drop}$	average Sherwood number of dispersed phase droplets
$\bar{Sh}^o$	average initial Sherwood number for coal particles
$\bar{Sh}_o$	average initial Sherwood number for dispersed phase droplets evolving from coal particles
SNG	Synthetic Natural gas
SRC	Solvent Refined Coal

$T, T_c, T_r$	temperature, °K, critical temperature, °K, relative temperature
$T_b, T_{b50}$	normal boiling temperature, °K, average boiling temperature for complex mixtures, °K
TCC	total coal conversion
TINJECT	normalized time at which slurry injection is commenced
TIS	tanks in series
TPD	tonnes per day
$t, \bar{t}$	time, mean residence time, s
$t_1, t_2$	maximum and minimum residence times, s
U	superficial velocity, $\text{m s}^{-1}$
V	volume, $\text{m}^3$
$V_1, V_2, V_R$	gas volume in the reactor, apparent gas volume of the slurry phase, total reactor volume
$X_i$	mole fraction
Y(n)	constants for the coal liquefaction reaction model Chapter 6
Z	compressibility factor
$\theta$	normalized time $\equiv t/\bar{t}$
$\theta_1, \theta_2$	normalized mean residence time per pass, per reactor.
$\kappa$	first order rate constant $\text{s}^{-1}$

$\mu$	viscosity, poise
$\nu$	kinematic viscosity
$\rho, \rho^R$	density, reference density $\text{Kg m}^{-3}$
$\sigma$	the square root of the variance of a probability distribution, interfacial tension, $\text{Kg} \cdot \text{s}^{-2}$
$\omega$	eccentric factor

"There is, as every schoolboy knows in this scientific age, a very close chemical relation between coal and diamonds .... Both these commodities represent wealth; but coal is a much less portable form of property. There is ... a deplorable lack of concentration in coal .... At the same time, there is a fascination in coal, the supreme commodity of the age in which we are couped like bewildered travellers in a garish, unrestful hotel."

Joseph Conrad<sup>[1]</sup>

## Chapter 1

### 1. INTRODUCTION

#### 1.1 General Introduction

Coal is the only foreseeable energy resource which can be developed, on a global scale, to supplement or supplant mineral oil and natural gas consumption as the reserves of these latter two energy resources decline. Known and projected coal reserves contain between 1.5 and 7 times the energy remaining in mineral oil and natural gas reserves<sup>[92]</sup>. However, extensive use of raw coal presents a number of environmental and logistical problems. Foremost among these are:

- (1) sulphur, nitrogen and flyash emissions associated with coal combustion.
- (2) the unsuitability of solid fuels for transportation applications.
- (3) superfluous shipping costs related to ash, moisture and inert content.

Clearly, coal must be converted into conventional fuel analogs if the "hydrocarbon economy" is to survive beyond the 2000-2010 frontier projected solely on the basis of mineral oil and natural gas consumption<sup>[92]</sup>. The need to produce conventional fuels from coal will become increasingly compelling as mineral oil and natural gas reserves dwindle.

Direct Coal Liquefaction (DCL) is one technological alternative for the production of low sulphur and low ash gaseous, liquid and solid fuels from coal. Consequently, academic and industrial interest in this research area has intensified as the real cost of conventional clean energy resources has escalated. A potpourri of DCL process designs, utilizing different coal types and placing varying emphasis on oil, SNG, clean coal and chemical feedstock production, have been proposed. Many of these designs are derivatives or hybrids of the original process developed by Bergius et al during the 1920's, while others are adaptations of heavy oil processing technology. DCL processes, employing these design concepts, are currently undergoing laboratory examination; some are or have been demonstrated at pilot scale, but none of the processes have been commercialized.

Liquefaction reactor capital cost is the major technological impediment to the commercialization of DCL processes, as liquefaction reactions must be conducted under extreme conditions: temperatures greater than 680 K, pressures greater than 10 MPa; in a corrosive environment. Even under these conditions, liquefaction reactions are classified as "slow". So, it is not surprising that liquefaction reactors account for as much as 50% of the capital cost of DCL processes<sup>[2,89]</sup>. Despite this incentive, it is precisely in this one respect that DCL processes are most similar. In all cases, liquefaction reactors are sub-divided into two multiphase components: a pre-heater,

operated in slug flow, with a mean residence time of approximately 6 minutes, followed by an axially mixed contactor where the coal mean residence time is typically greater than 15 minutes. The choice of hydrodynamically similar reactor designs, for all processes, can only be rationalized on the basis of a limited conceptual grasp of coal-liquefaction reaction kinetics coupled with a traditional evaluation of process economics. Experimental evidence does not suggest that this design is optimal.

Process and reactor design development in particular has been hampered by the wax and wane of research fashion. Interest in DCL is only aroused during periods of perceived crisis (i.e.) prior to and during World War II, following the alleged oil crisis of 1973. Dominant themes in the literature reflect this sense of urgency. Both previous and current research emphasizes three issues:

- (1) can coals within a particular country or region be liquefied and if so, what is the product yield and distribution in existing processes
- (2) what catalysts or solvents optimize the production of particular products
- (3) what materials or mechanical problems must be resolved in order to scale-up existing processes

at the expense of others, such as:

- (1) what is the mechanism for coal liquefaction; do all coals liquefy in the same manner; if not, what raw coal parameters account for the difference

(2) where do the most critical reactions occur and are they controlled by mass transfer or kinetics

3) how does reactor hydrodynamics (axial mixing, the intensity of turbulence affect coal liquefaction kinetics)

which are rarely addressed. These latter issues must be addressed, comprehensively, if substantial improvements in the cost effectiveness of DCL processes are to be realized.

Currently, for example, it is difficult to predict liquefaction results for a single coal in similar reactors of varying size, and even more difficult to correlate liquefaction data for a single coal in reactors with different hydrodynamics. Present predictive models fail, in part, because they do not include the influence of physical phenomena (the intensity of turbulence, the extent of axial mixing, solvent properties, gas- liquid-solid mass transfer) on coal liquefaction kinetics. Optimal liquefaction reactor designs cannot be based on such poor predictive models.

This thesis, comprising a theoretical and experimental study, endeavours to identify process variables and physical phenomena that affect the productivity of DCL reactors for bituminous, sub-bituminous coal and lignite liquefaction. Mathematical models of likely reaction networks incorporating the effects of process variables and physical phenomena will then be compared with experimental results obtained in this and other



studies. A model which can account for the liquefaction behaviour of a broad range of coals and lignite is sought. Such a model would improve our limited understanding of coal liquefaction kinetics and yield more appropriate design criteria for DCL reactors. These new design criteria may lead to novel DCL reactor designs which liquefy coal more completely or have improved spacetime yields. Such reactors may reduce or eliminate the cost disincentive for commercialization of DCL processes and facilitate the transition from mineral to "synthetic" fuels.

## 1.2 Direct Coal Liquefaction - An Overview

### 1.2.0 Introduction

Before delving into detailed descriptions of many aspects of DCL reactor design, which comprise the following chapter, a brief introduction to DCL technology and terminology is warranted. Those already familiar with these topics may omit this section. The most effective way to introduce the technology and terminology associated with Direct Coal Liquefaction is to examine a typical process flow sheet. Figure 1.1, referenced throughout this preliminary discussion, is not based on any particular process and indicates only the most general features of DCL processing technology. For more complete descriptions of the various liquefaction processes, coal liquefaction reaction kinetics etc., the reader is referred to the appropriate sections of Chapter 2.

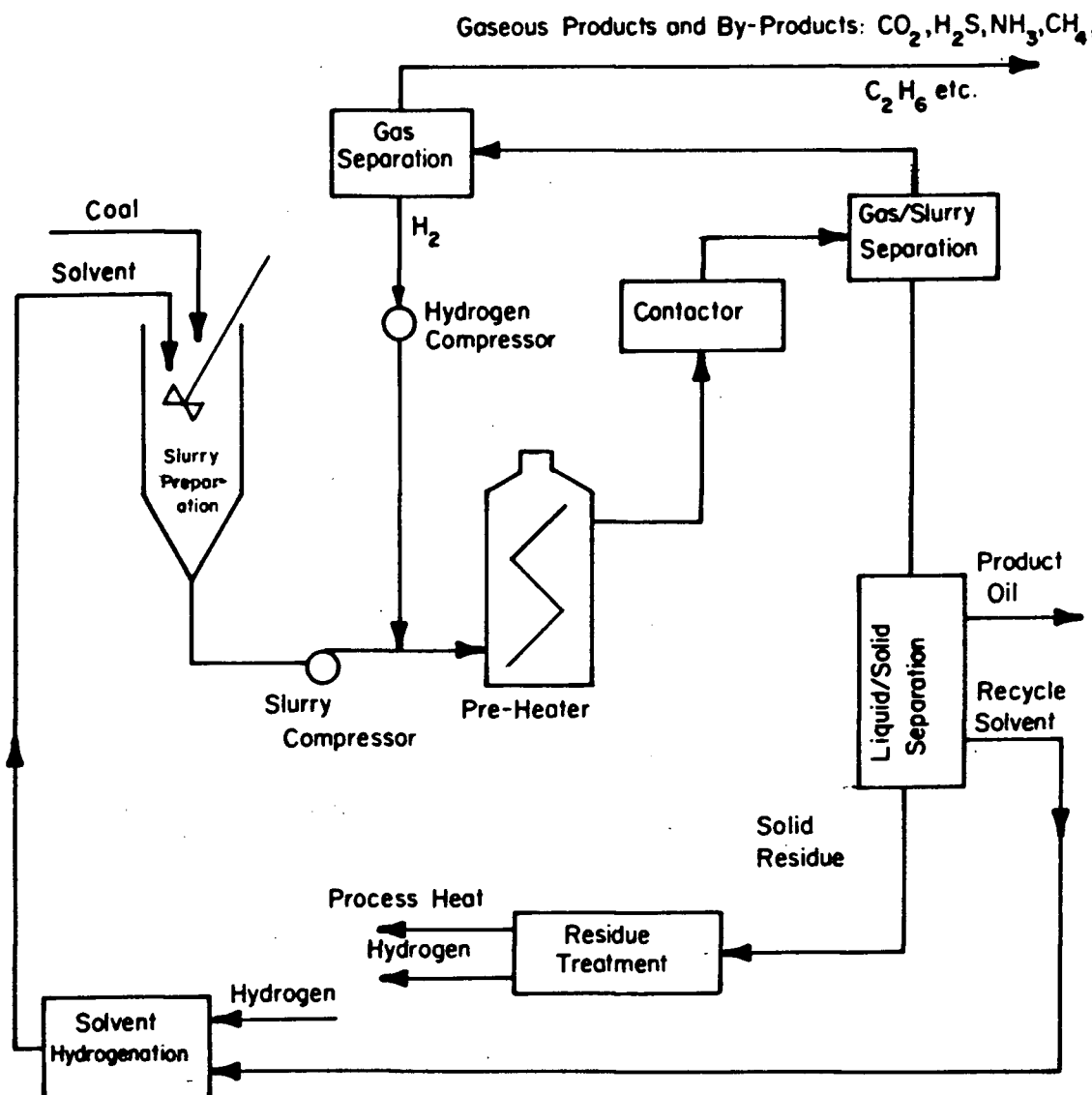


Figure 1.1: A Direct Coal Liquefaction Process Schematic

### 1.2.1 Coal Slurry Preparation

Slurry preparation is the first stage in a DCL process. Dried and pulverized coal or lignite is combined with a solvent to form a 20-40 wt% coal-in-solvent slurry. The solvent is typically a high boiling fraction of the oil produced from the coal itself and is called a recycle solvent. The solvent serves a number of roles throughout the various stages of DCL processes but acts primarily as a vehicle or carrier medium. The chemical and physical properties of solvents vary from process to process. In some processes, catalysts are also added to the coal at this point.

### 1.2.2 Coal Liquefaction

Coal slurry is compressed to between 10 and 30 MPa and combined with a gaseous hydrogen recycle stream. This multiphase mixture is then fed to the liquefaction reactor network. Coal oil, synthetic natural gas and by-product gases:  $\text{CO}$ ,  $\text{CO}_2$ ,  $\text{H}_2\text{S}$ ,  $\text{NH}_3$ , are generated by thermal decomposition of the coal or lignite and a subsequent series of homogeneous and heterogeneous reactions which occur in the pre-heater and contactor. The precise reaction paths vary from process to process. In some processes, gaseous or dissolved hydrogen reacts with coal fragments arising from thermal decomposition. These reactions are believed to occur principally on catalyst surfaces. In other processes, coal fragment-solvent interactions predominate. Solvent properties, whether or not a

catalyst is present and the precise operating conditions determine which path dominates. In general, liquefaction reactions are initiated in the pre-heater segment of the reactor and completed in the contactor.

Coal liquefaction reactions are exothermic, on balance, and a number of process variables such as slurry density, hydrogen recycle ratio, and pre-heater exit temperature, can be manipulated in order to control the reaction temperature. Consequently, the configuration and operating conditions of pre-heaters and contactors vary somewhat from process to process. Pre-heater exit temperatures are typically less than 420°C and contactor operating temperatures are normally greater than 440°C. Axial mixing patterns and the scale of turbulence are determined largely by the relative flow rates of hydrogen and slurry. Hydrogen recycle ratios vary from 2 to 4.

### 1.2.3 Product Separation

Product separation techniques vary greatly among existing DCL processes, and are not discussed, in detail, in this thesis. Much of the equipment is not radically different from separators encountered at conventional crude oil processing plants, although more specialized techniques, such as anti-solvent de-ashing are employed for ash and residua separation from the product liquid. Hydrogen is separated from the product and by-product gases, and recycled. Solvent is separated from the product oil and may contain residual catalyst. Solid residua and ash

report to a gasifier or furnace, and are used to produce hydrogen and/or process heat.

#### 1.2.4 Solvent Treatment

The physical and chemical properties of the solvent have an important influence on coal liquefaction kinetics. Consequently, some processes hydrogenate the recycle solvent in a catalytic reactor prior to recycle. Hydrogenation affects both the chemical and physical properties of a solvent. The mean molar mass of the solvent is reduced, the molar mass distribution is broadened, and the concentration of hydrogen donor molecules, (i.e.) molecules containing labile hydrogen atoms which can react with and stabilize coal fragments, increases as a result of hydrogenation. Physical properties, such as viscosity, density, the range of coal liquids soluble in the solvent, and hydrogen solubility are similarly affected. Processes which use hydrogenated solvents are referred to as solvolytic processes as they rely primarily on coal fragment-solvent interactions to complete liquefaction reactions. Processes which do not hydrogenate recycle solvents rely primarily on hydrogen-catalyst-coal fragment interactions and are called catalytic liquefaction processes. However both modes of reaction occur in both process types to varying degrees.

### 1.2.5 Catalysts

Metallic sulphides have been identified as the most active catalysts for direct coal liquefaction reactions. Since these compounds occur naturally and are frequently among coal constituents, catalysts are ubiquitous actors in DCL processes. Pyrite ( $\text{FeS}_2$ ) and trace metallic sulphates, which become metallic sulphides in situ, are the principle naturally occurring catalysts. Some processes enhance this "natural" catalytic effect by adding powdered metallic oxides (which sulphidize in situ), or aqueous metallic salt solutions (which produce colloidal metallic sulphides in situ) to the unreacted coal slurry. Catalysts employed in this way are either inexpensive or used sparingly. These added catalysts are rarely recovered and recycled. Other processes catalyse the solvent treatment or contactor stages selectively. These processes trap supported metallic sulphide pellets (typically cobalt, molybdenum, or nickel sulphides dispersed in an  $\alpha$ -alumina matrix) in a specific process unit, and rely on naturally occurring catalytic effects throughout the remainder of the process.

## Chapter 2

### 2. Literature Review

#### 2.1 Direct Coal Liquefaction (DCL) Reactor Designs

##### 2.1.0 Introduction

Industrial DCL process research has undergone a renaissance during the past decade. Older processes, based on the pioneering DCL research of F. Bergius et al, have been reviewed or revamped yielding the Saarberg Werke and Ruhrkohle processes<sup>[2,3,4]</sup>; heavy oil processing technology has been applied to DCL (i.e.) the H-Coal process; and a number of new ideas related to catalysts, catalyst use, and ash/oil separation have been tested. Process routes such as Synthoil, CCL, CSF were developed during this period and subsequently abandoned due to mechanical, scale-up and/or productivity problems<sup>[5,6]</sup>. Other processes, listed on Table 2.1, have met with experimental success and are actively researched. Hybrid processes, incorporating design features from the processes cited above, have also been considered<sup>[7,8,32]</sup>. Preliminary work is being conducted on the SRC-1/2 and the Lummus Clean Fuels from Coal Process (LCFFC) for example. The hydrogen consumption and gas yields for these processes are projected to be lower than the current processes and hetero-atom removal is expected to be improved. Fully integrated operating data is not yet

TABLE 2.1

## Direct Coal Liquefaction Process and Product Data

PROCESS NAME	OPERATING CONDITIONS								NET wt% YIELD (MAP BASIS)						
	Temperature °C		Pressure MPa	MRT <sup>1</sup> min	wt% COAL in slurry	Solvent	Catalyst	Gas Recycle Kg/Kg Coal	SNG	Hydrogen Consumed	LIQUIDS			Solids	
	Pre-Heater Exit	Reactor									Percent	Hetero-Atom Content			
												S	N		O
H-COAL		440-470	10-17	5-15		heavy dist.	Co-Mo/ $\alpha$ -Al <sub>2</sub> O <sub>3</sub>		12.	6.6	58.4	.26	.90		<16.6
SRC I	415	440	12	40	25	heavy dist.	mineral matter	0.1	8.2	3.	27.4	.6	1.3	4.1	52.4
SRC II		440	12	40		heavy dist.	mineral matter	> 0.1	18.	5.	48.5	.3	.8	4.	23.
EDS				40-90		middle dist.			7-20		45.		.1		
SAARBERG WERKE AG						heavy dist.	MO <sub>x</sub>		15.	5.5	54.				24.5
RUHRKOHLE	420	460-480	30	50	40	middle + heavy dist.	MO <sub>x</sub>	< 0.2	21.5	5.8	52.				21.2
CCLP <sup>2</sup>									8.	7.	60.	.013	.23		12.
DOW	420	460	14	35	40	middle + heavy dist.	colloidal MoS <sub>2</sub>		22.1	5.2	46.7	.51	.49	2.8	

<sup>1</sup> for a single pass<sup>2</sup> estimated.



available and the processes cannot be evaluated objectively at this time.

Current DCL processes are categorized arbitrarily in the literature as "catalytic" or "solvolytic" processes. While these labels can be misleading, refer to sections 1.2 and 2.3, the processes do present distinct design alternatives. Flow sheets, for the processes cited on Table 2.1, can be found on Figures 2.1-2.8. Many of the differences between the processes occur outside the liquefaction-reactor envelope, in the ancillary equipment (i.e.) hydrogen and process heat generation, de-ashing techniques, solvent hydrogenation; these differences are discussed at length elsewhere<sup>[7,9,10]</sup>. Within the liquefaction-reactor envelope the processes share a number of design criteria:

- (1) A pre-heater precedes the contactor(s) in all cases,
- (2) A large quantity of hydrogen is recirculated and has the following roles:
  - i) controlling reaction temperature
  - ii) promoting mixing
  - iii) providing a hydrogenation medium,
- (3) The solvent is a high-boiling fraction of the product oil
  - i) permitting liquid quality improvement by recycle
  - ii) providing a suitable coal dissolution medium,
- (4) The contactors are axially mixed with respect to the slurry phase
- (5) Catalyst species are dispersed and move freely within the contactor(s),
- (6) Process operating conditions (temperature, pressure, nominal mean

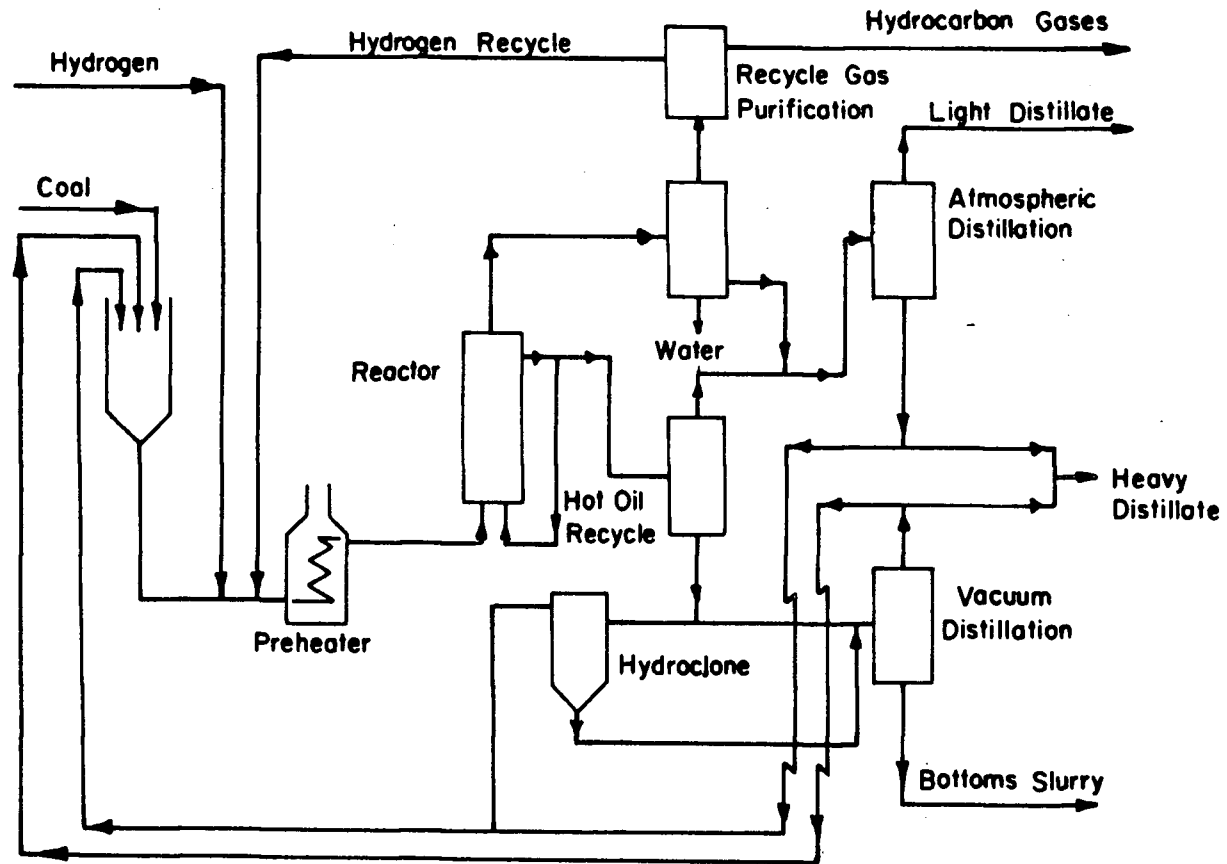


Figure 2.1: H-Coal Process Schematic

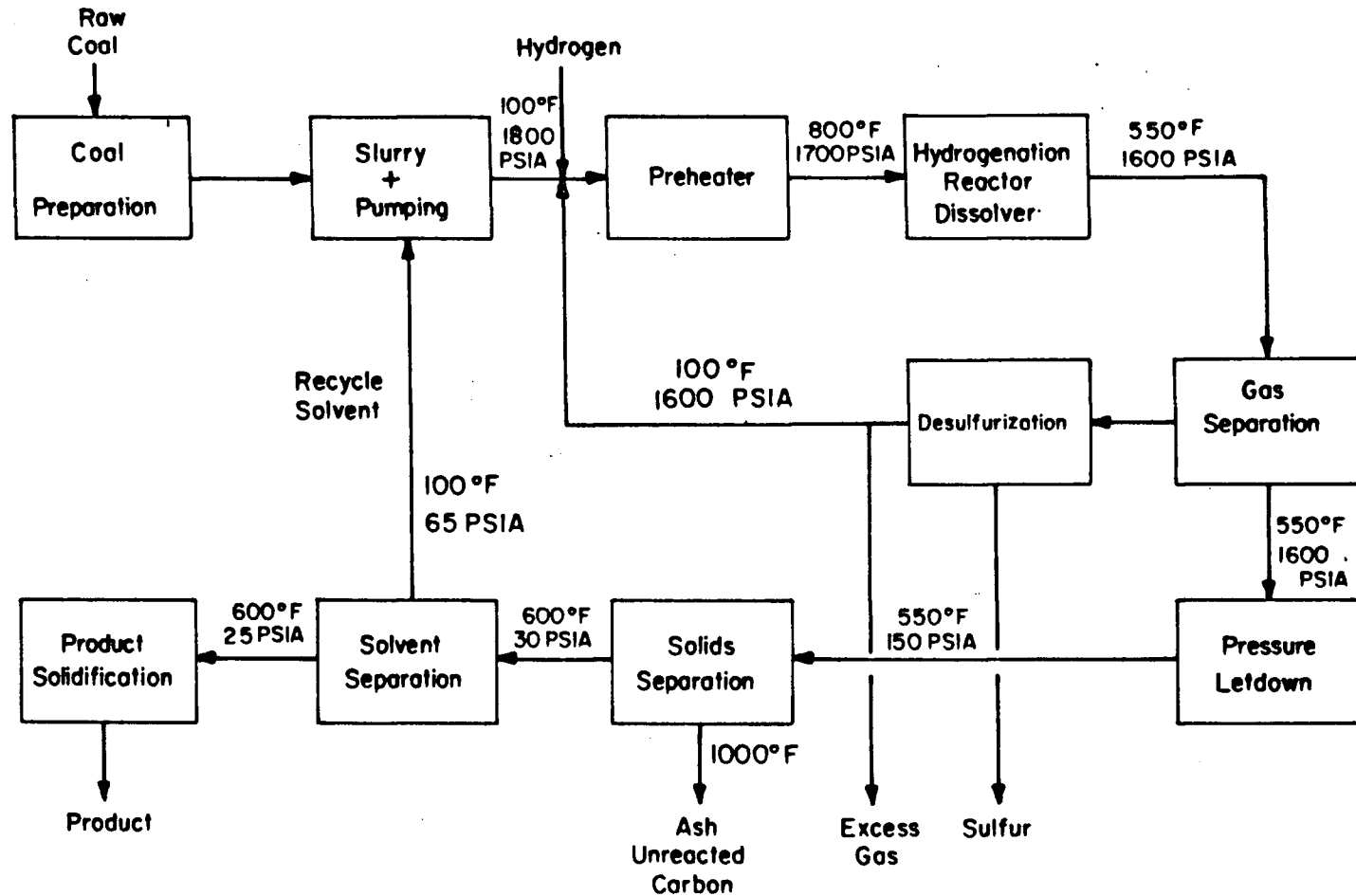


Figure 2.2: SRC I Process Schematic

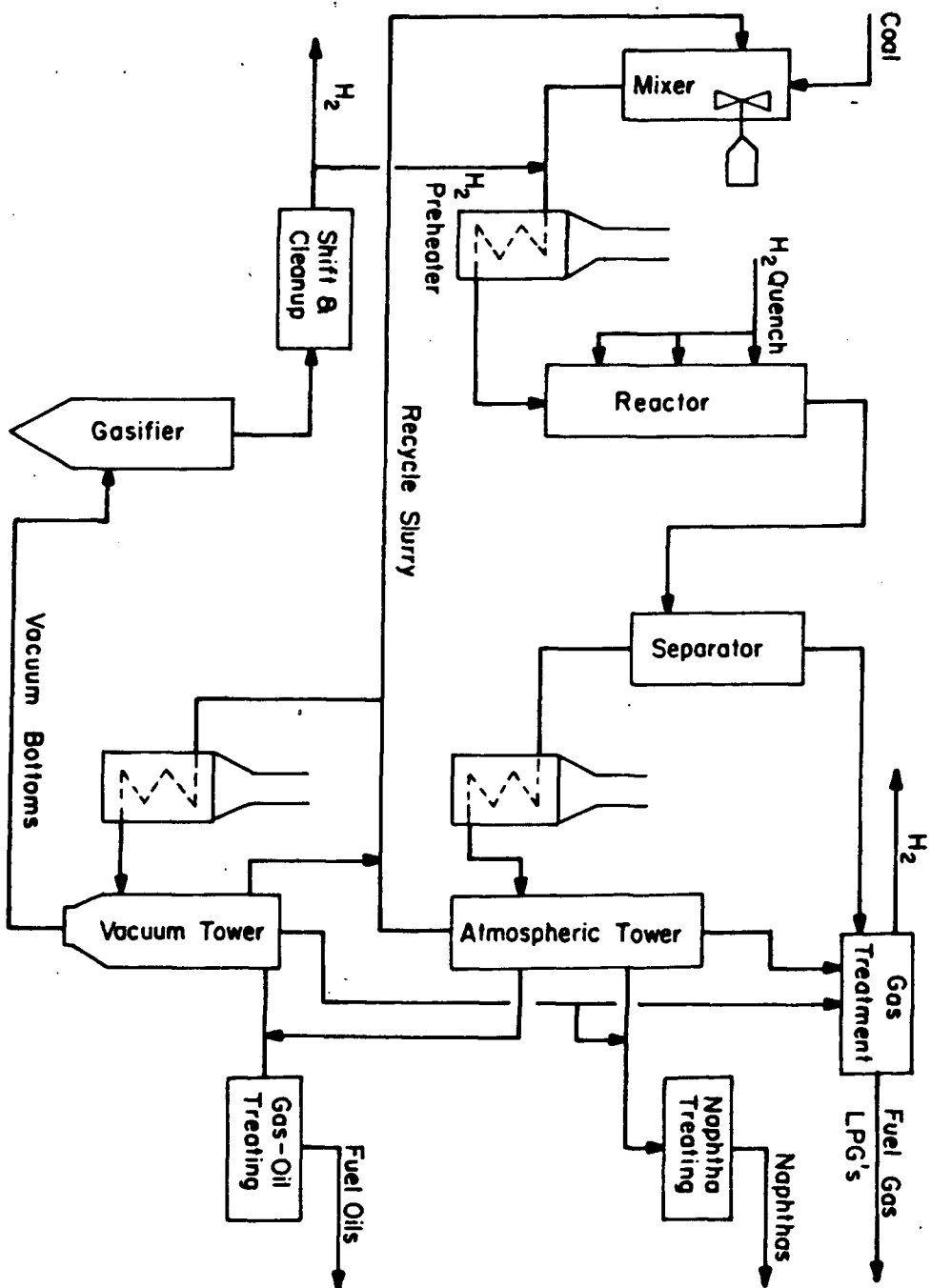


Figure 2.3: SRC II Process Schematic

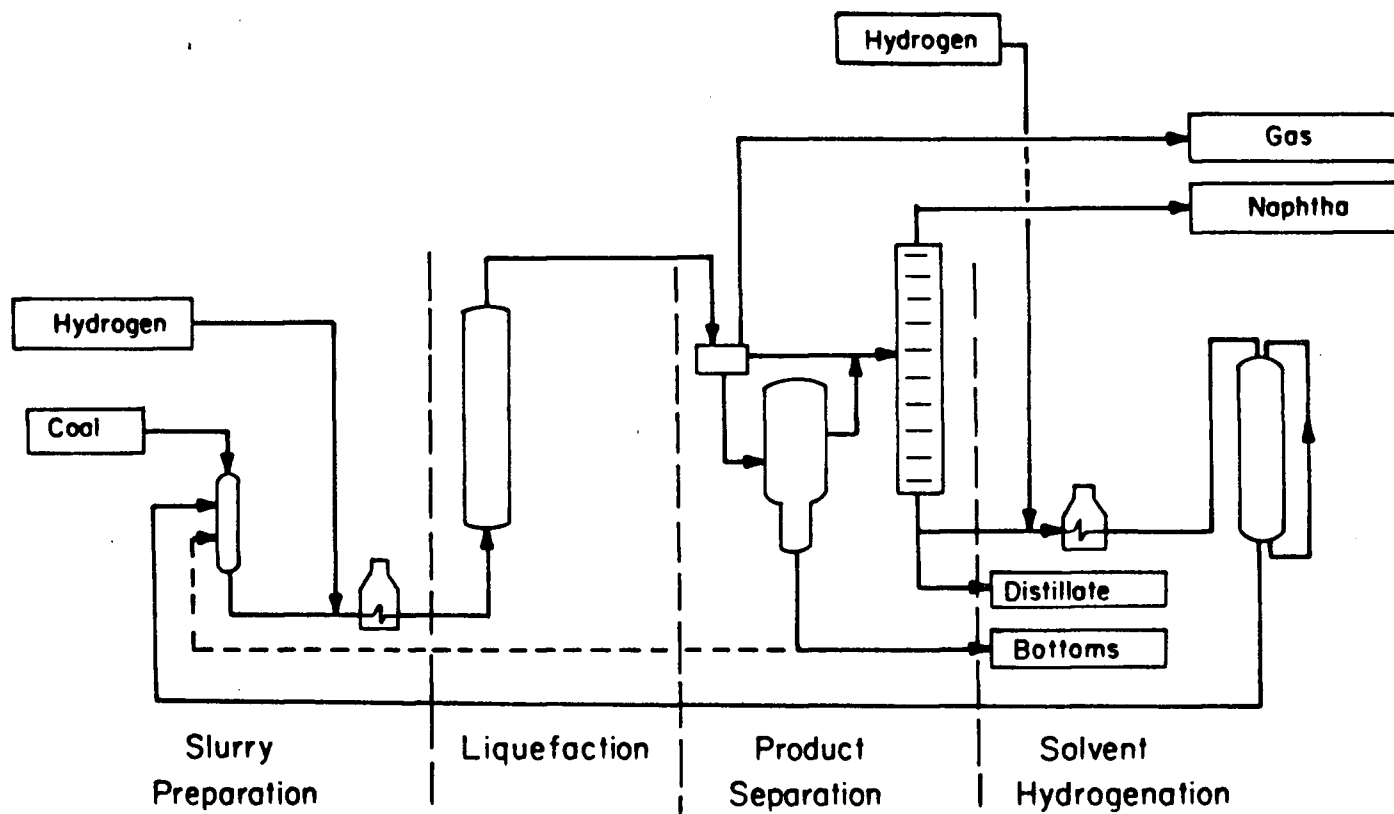


Figure 2.4: EDS Process Schematic

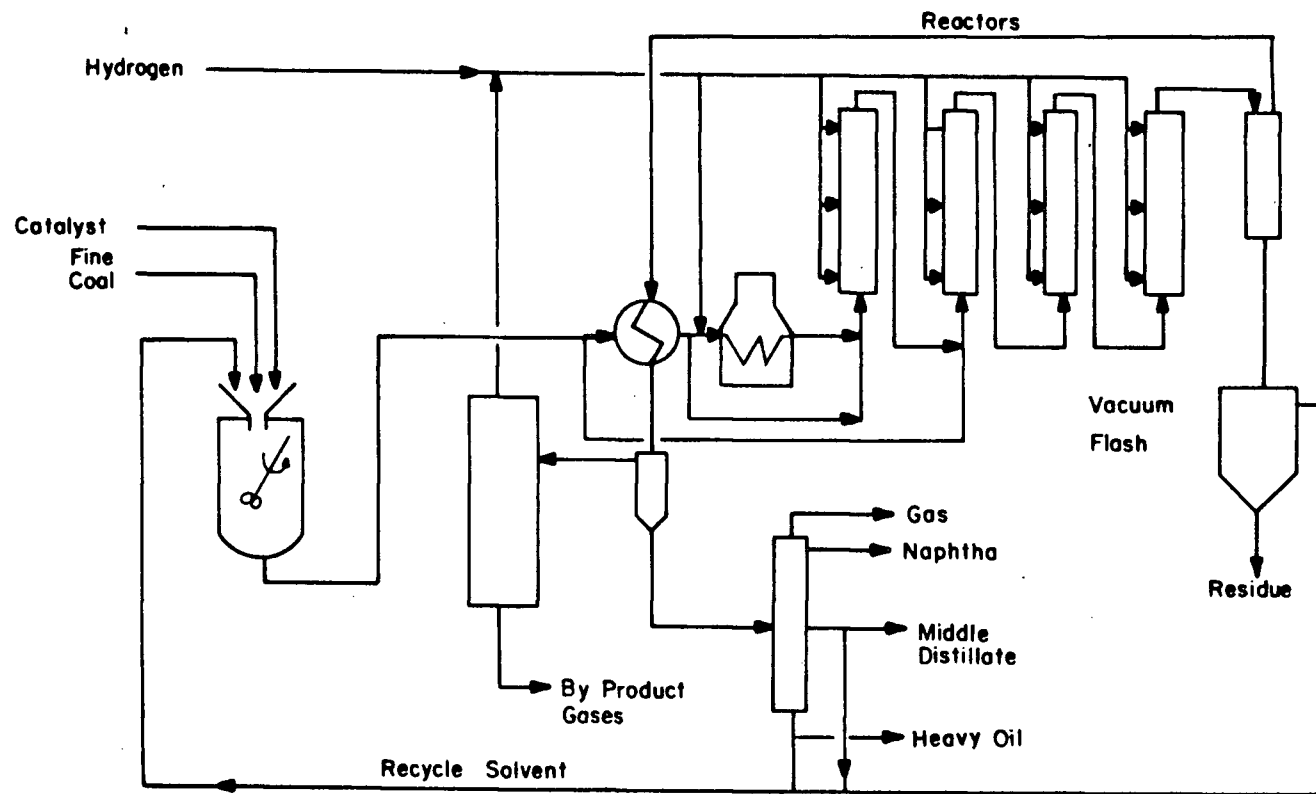


Figure 2.5: Saarbergwerke Process Schematic

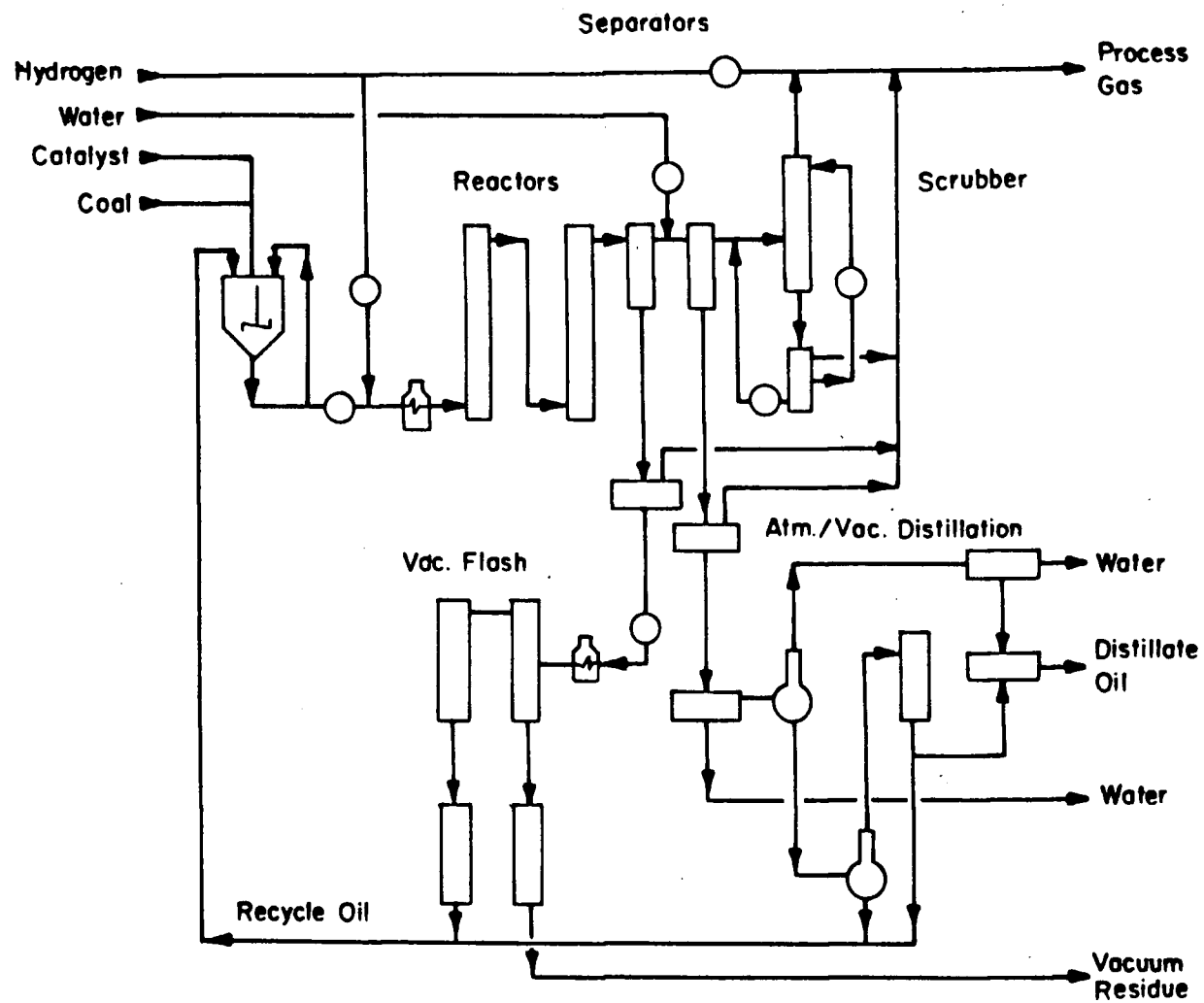


Figure 2.6: Ruhrkohle Process Schematic

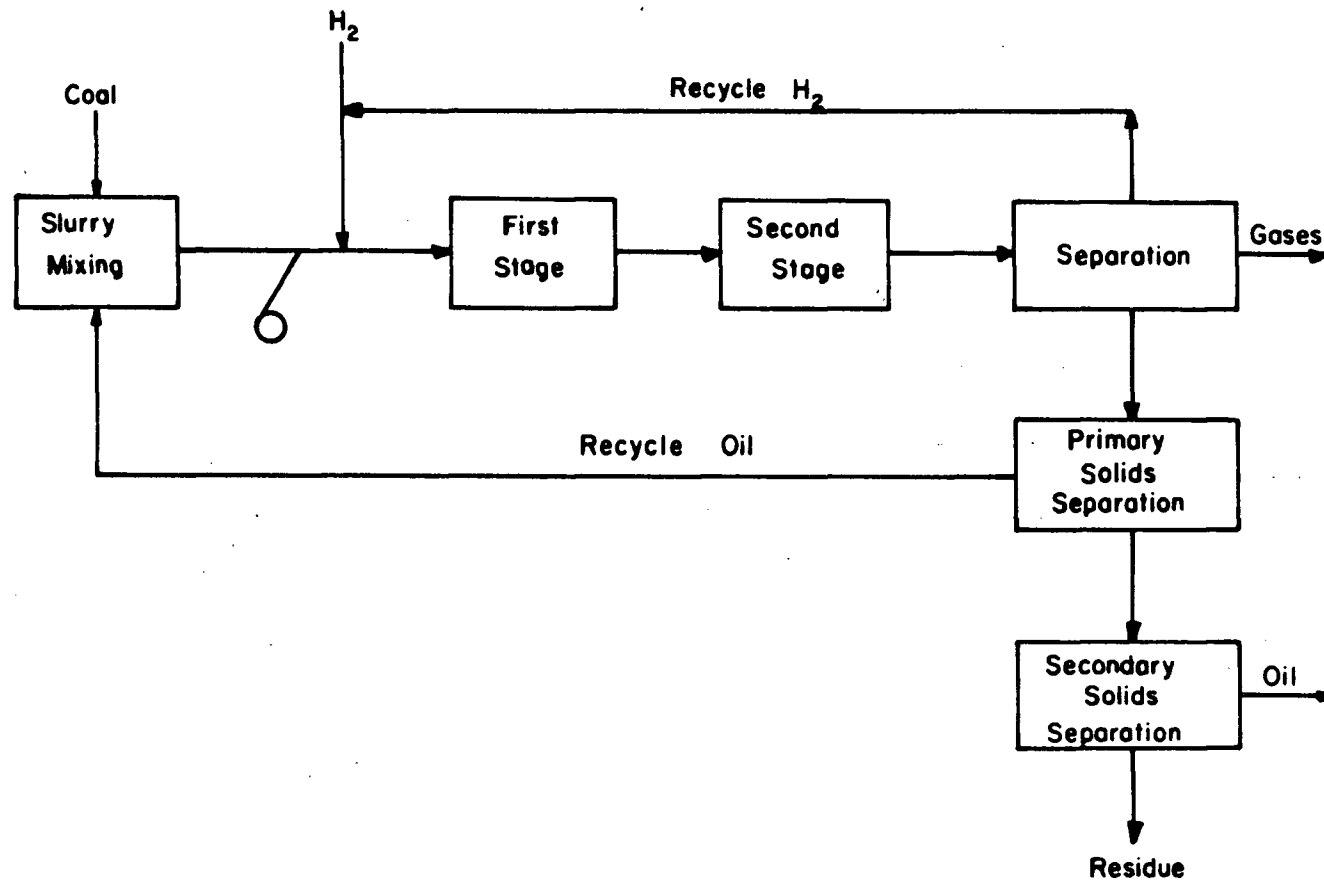


Figure 2.7: CCLP Process Schematic



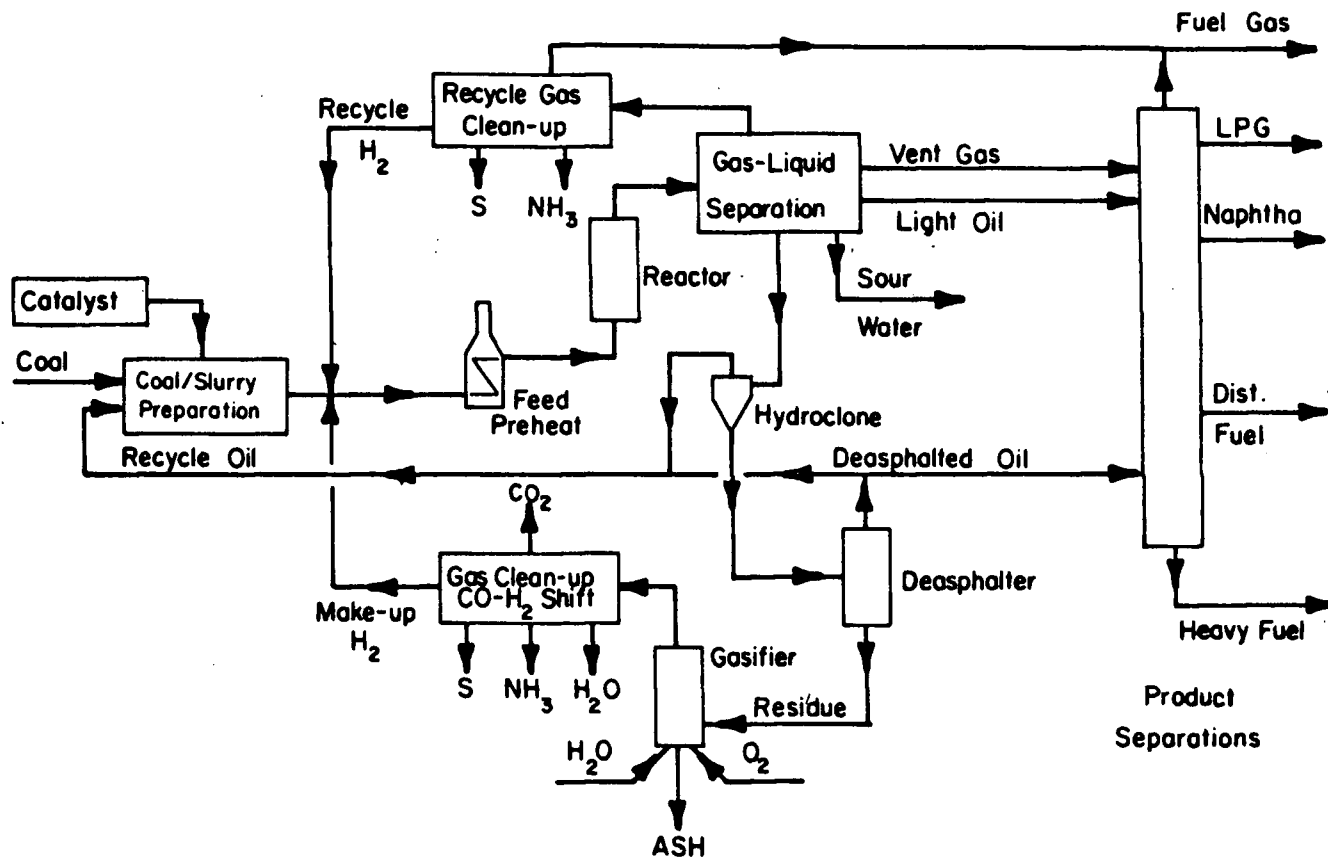


Figure 2.8: Dow Process Schematic

residence time, etc.) are comparable, yet liquefaction yields and product distributions vary widely among the different processes (refer to Table 2.1). Variations in product yield and distribution can only be related to details such as the extent of axial mixing, the intensity of turbulence, solvent composition or the precise catalyst composition. Perhaps operating conditions also play an important role in conjunction with the other process variables. General aspects of DCL reactor design and the influence of design on product yield and distribution are analysed in this section. Product yield and distribution variations attributed to solvent composition, catalysts etc. are discussed separately.

### **2.1.1 Liquefaction Reactor Design**

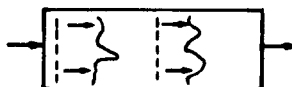
#### **2.1.1.0 Introduction**

The description and analysis of reactor hydrodynamics invariably involves process flow models. The following discussion is not an exception. Five flow models, the plug flow model, the dispersed flow model, the recirculation model, the continuously stirred tank reactor (CSTR) model and the tank in series (TIS) model are used to describe fluid flow patterns for various DCL reactors and pre-heaters. Pictorial descriptions of these models can be found on Figure 2.9. The equations, defining the associated flow patterns, are discussed elsewhere, in detail<sup>[16]</sup>, and are simply introduced in the text as they are required.

Plug Flow Model

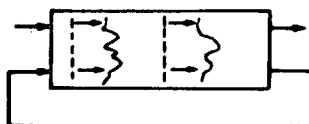


Dispersion Model



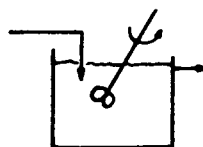
eqn 2.2

Recirculation Model



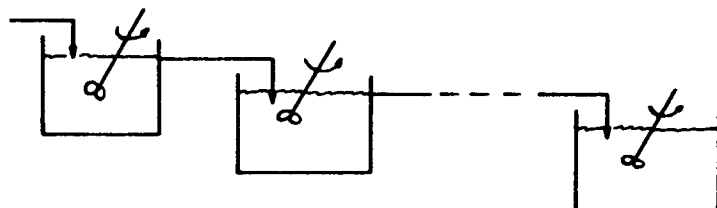
eqn 2.3

Continuous Stirred Tank Model



eqn 2.4

Tank in Series Model



eqn 2.5

Figure 2.9: Flow Models

#### 2.1.1.1 Pre-heaters

Pre-heaters are among the common features of all DCL reactor designs (refer to Figures 2.1-2.8). This piece of equipment is intended to heat the coal-oil-gas mixture to reaction conditions, initiate the coal conversion process without causing the coal, or recycle oil to coke. The pre-heater comprises a gas fired boiler, typically, where the coal-oil-gas reaction mixture flows through coiled boiler tubes and is heated from  $\sim 20^{\circ}\text{C}$  to at least  $350^{\circ}\text{C}$ . The nominal mean-residence time (mrt) of the slurry in the pre-heater rarely exceeds 8 minutes; less than 3 minutes of this time is spent at a kinetically active temperature (i.e.)  $T_{\text{slurry}} > 250^{\circ}\text{C}$ .

Pre-heater heating efficiency and susceptibility to coking depends on the phase distribution within the boiler tubes and boiler tube orientation. Possible flow regimes are illustrated on Figure 2.10. Precise design data could only be obtained for the pre-heater at the 6 TPD SRC pilot plant, Wilsonville, Alabama (Table 2.2). From overall operating data, pre-heaters for the other processes appear to operate under comparable conditions<sup>[19]</sup>. Flow pattern mapping of three phase flow systems has been performed, exclusively, with air-water-inert solid combinations at atmospheric conditions. This work suggests that liquid phase dispersion coefficients are unaffected by superficial liquid velocity and solids concentration, and that solid and liquid phase dispersion coefficients are equal regardless of

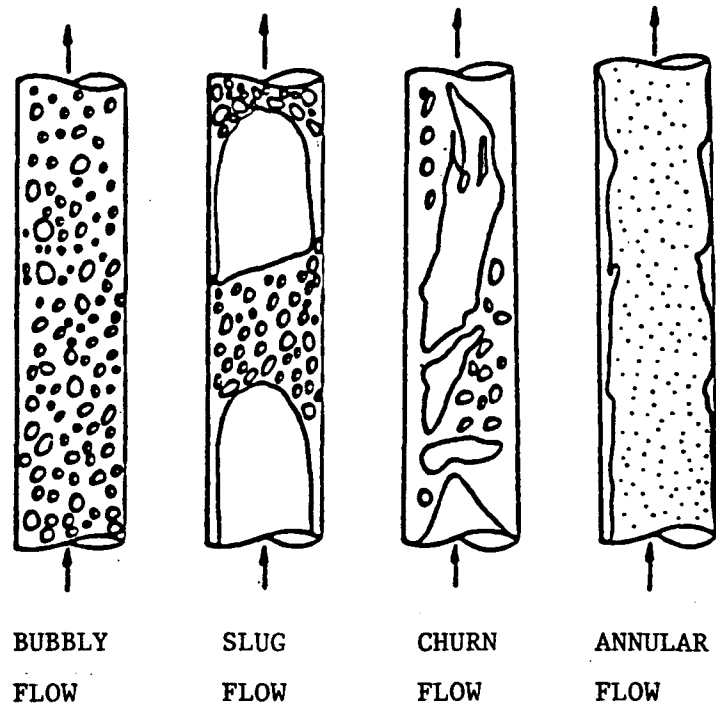


Figure 2.10: Flow Regimes For Two Phase Flow<sup>[15]</sup>

TABLE 2.2Wilsonville Pre-Heater Design Data

Design Specification	Value
Pre-heater length	77.m
Pre-heater diameter	3.25 cm
Superficial slurry velocity	20.cm s <sup>-1</sup>
Superficial gas velocity	100.cm s <sup>-1</sup>
Pressure	12.MPa

flow regime<sup>[12]</sup>. If these results can be extended to oil-coal-hydrogen systems at high temperatures and pressures, one need only consider analogous two-phase flow systems. One flow pattern mapping study, performed with methane-oil flow at 7.7 MPa, and 38°C, in a vertical, 2.5 cm diameter column, suggests that the Wilsonville pre-heater operates in the "slug flow" regime<sup>[13]</sup>. Results obtained from studies performed with air-water systems, in the same diameter tubes at atmospheric conditions, concur - for horizontal, inclined and vertical tubes<sup>[13,14,15]</sup>. It is therefore probable if not conclusive that pre-heaters operate in the slug flow regime.

The slurry phase residence time distribution, (rtd), can be predicted from the dispersion coefficient<sup>[12]</sup>,

$$D = v \cdot 800 [\log (g^{1/3} Q v^{-5/3}) - 4.331]^{3.2} \quad (2.1)$$

and the dispersed flow model<sup>[16]</sup>

$$C_{\theta} = \frac{1}{2(\pi D/UL)} \cdot \exp \frac{-(1-\theta)^2}{4(D/UL)} \quad (2.2)$$

The Wilsonville pre-heater slurry phase rtd fits a narrow Normal distribution ( $\sigma = 0.04$ ). Thus slug flow imparts strong local mixing but very little slurry phase dispersion. All of the slurry passes through the pre-heater network within the interval  $8 \pm 0.65$  minutes, if solvent evaporation and coal volatilization is ignored.

Coal conversion reactions and the extent of reaction occurring in the pre-heater depends on the gas volume flux, the slurry flux, the coal concentration in the slurry, pre-heater exit temperature and solvent composition, in a complex manner<sup>[17,18]</sup>. Short-residence-time, batch-autoclave experiments, performed with bituminous coals (Illinois #6, Kentucky #14), indicate that coal conversion, to pyridine soluble products, exhibits a weak dependence on slurry Reynolds number but is independent of hydrogen pressure and hydrogen : slurry mass ratio<sup>[17]</sup>. Results, from short residence time experiments conducted in flow apparatus, note the influence of solvent quality on the extent of coal conversion to pyridine soluble material, and the hydrogenation potential of the initial products<sup>[18]</sup>. The difference in the hydrogen dependence between batch and flow apparatus may be attributed to differences in solvent composition, and the role hydrogen plays in establishing the scale of turbulence and heat transfer characteristics in flow apparatus. The presence of hydrogen should have little impact on slurry hydrodynamics in a vigorously stirred autoclave. However, the precise role of solvents and hydrogen, in pre-heaters, is not resolved in the literature.

#### **2.1.1.2 Contactor Design**

##### **2.1.1.2.0 Introduction**

The contactor segment of the liquefaction reactor is intended to complete the liquefaction reactions and generate sufficient recycle solvent



to permit continuous operation of the liquefaction reactor<sup>\*</sup>. Contactor designs, for the processes cited on Table 2.1, are proprietary. Precise design and operating data for these processes is scant, but sufficient data do exist to permit a hydrodynamic characterization of each process and to contrast the different processes.

#### 2.1.1.2.1 Single Stage Contactors

##### 2.1.1.2.1.1 The H-Coal Reactor

The major design features and dimensions of the H-Coal contactor<sup>[90,91]</sup> are illustrated on Figure 2.11. The unique features of the contactor include an annular ebullated catalyst bed and forced internal recirculation of processed oil. The broad spectrum of operating data, Table 2.1, actually reflect two distinct modes of operation, synthetic crude oil and low sulphur fuel oil production, realized at or near the extrema of the processing conditions. Low sulphur fuel oil is obtained at the lower temperature and short contact time extremum, while synthetic crude oil production requires more severe processing conditions. A product slate comparison for these two modes of operation can be found on Table 2.3.

---

<sup>\*</sup>Co-processing of heavy mineral oils and coal is under investigation regionally [20]. For this specific case, a "recycle solvent" is not necessary.

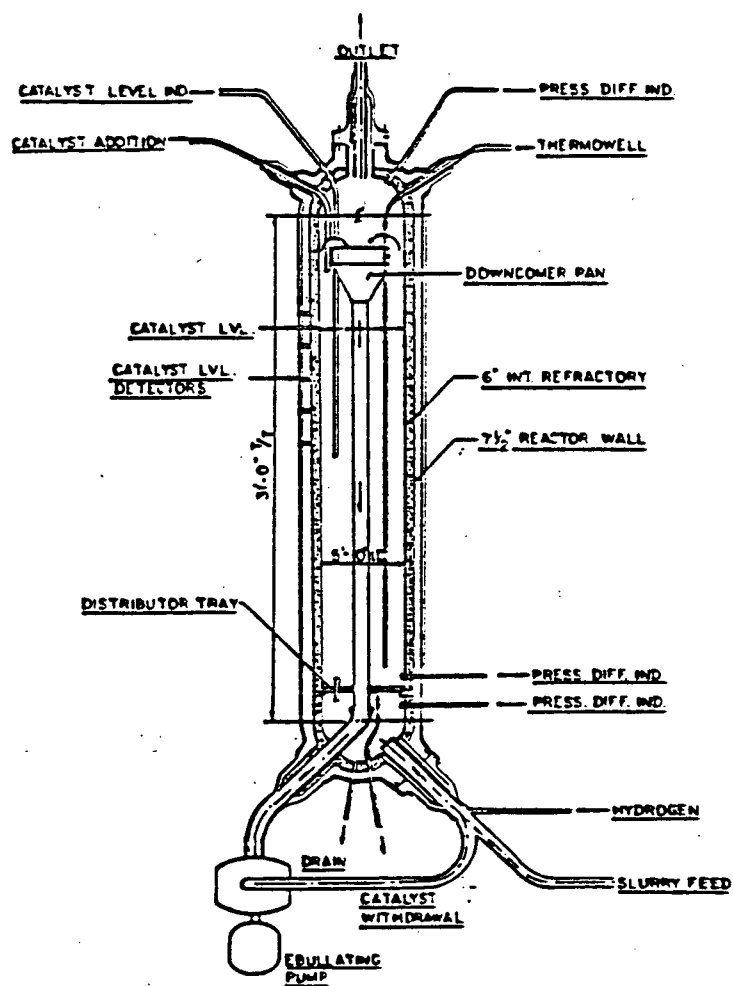


Figure 2.11: The H-Coal Contactor<sup>[90]</sup>

TABLE 2.3H-Coal Product Slate Comparison

Coal	Illinois Bituminous	
Desired Product	Synthetic Crude	Low-Sulphur Fuel Oil
<u>Normalized Product Distribution (wt%)</u>		
C <sub>1</sub> -C <sub>3</sub> Hydrocarbons	10.7	5.4
C <sub>4</sub> - 205°C Distillate	17.2	12.1
205°C-343°C Distillate	28.2	19.3
343°C-524°C Distillate	18.6	17.3
524°C + Residual Oil	10.0	29.5
Unreacted Ash-Free Coal	5.2	6.8
H <sub>2</sub> O, NH <sub>3</sub> , H <sub>2</sub> S, CO, CO <sub>2</sub>	<u>15.0</u>	<u>12.8</u>
Total (100.0 + H <sub>2</sub> Reacted)	104.9	103.2
Conversion, %	94.8	93.2

H-Coal Contactor<sup>[90,91]</sup> hydrodynamics are constrained by the necessity to keep the catalyst bed fluidized and are independent of the mode of operation - Table 2.4 comprises a summary of hydrodynamic calculations found in Appendix A.1. The slurry superficial velocity, in the absence of recycle, is less than one-tenth the minimum superficial fluidization velocity. The minimum recycle ratios required to achieve fluidization are 12:1 and 36:1 for fuel oil and synthetic crude oil production respectively. In both cases, the residence time distribution, described by equation 2.3

$$E_{\theta} = N e^{-(N\theta_1 + \theta_2)} \sum_{m=1}^{\infty} \frac{(N\theta_1)^{mN-1}}{(mN-1)!} \quad (2.3)$$

ensures a minimum slurry-catalyst contact time (approximately 0.5 min) prior to recycle but is otherwise indistinguishable from the CSTR residence time distribution, equation 2.4

$$E_{\theta} = e^{-\theta} \quad (2.4)$$

One can infer, from the H-Coal process development unit catalyst rtd<sup>[21]</sup> (Figure 2.12)<sup>\*</sup>, that the contactor is operated at or near the minimum fluidization condition cited above. The catalyst rtd shows evidence of low frequency gross recirculation which is typical hydrodynamic behaviour for asymmetrically fluidized beds operating near the minimum fluidization velocity<sup>[22]</sup>.

---

\*Bickel and Thomas fitted their data to the CSTR rtd model. The fit is poor and perhaps invalid because of the injection and sampling procedures used in their study: the tracer was injected as a plane distribution rather than as a flux, and catalyst was removed from the contactor batch-wise - a continuous outlet stream was not sampled [23]. In addition, significant catalyst losses occurred during the course of the tracer study.

TABLE 2.4Hydrodynamic Calculation Summary for the H-Coal Reactor

(for details refer to Appendix A.1)

Superficial Liquid Velocities	Value
Minimum fluidization velocity	2.3 - 3.5 cm s <sup>-1</sup>
Slurry velocity:	
syn-crude mode	0.06 - 0.10 cm s <sup>-1</sup>
boiler fuel mode	0.19 - 0.30 cm s <sup>-1</sup>

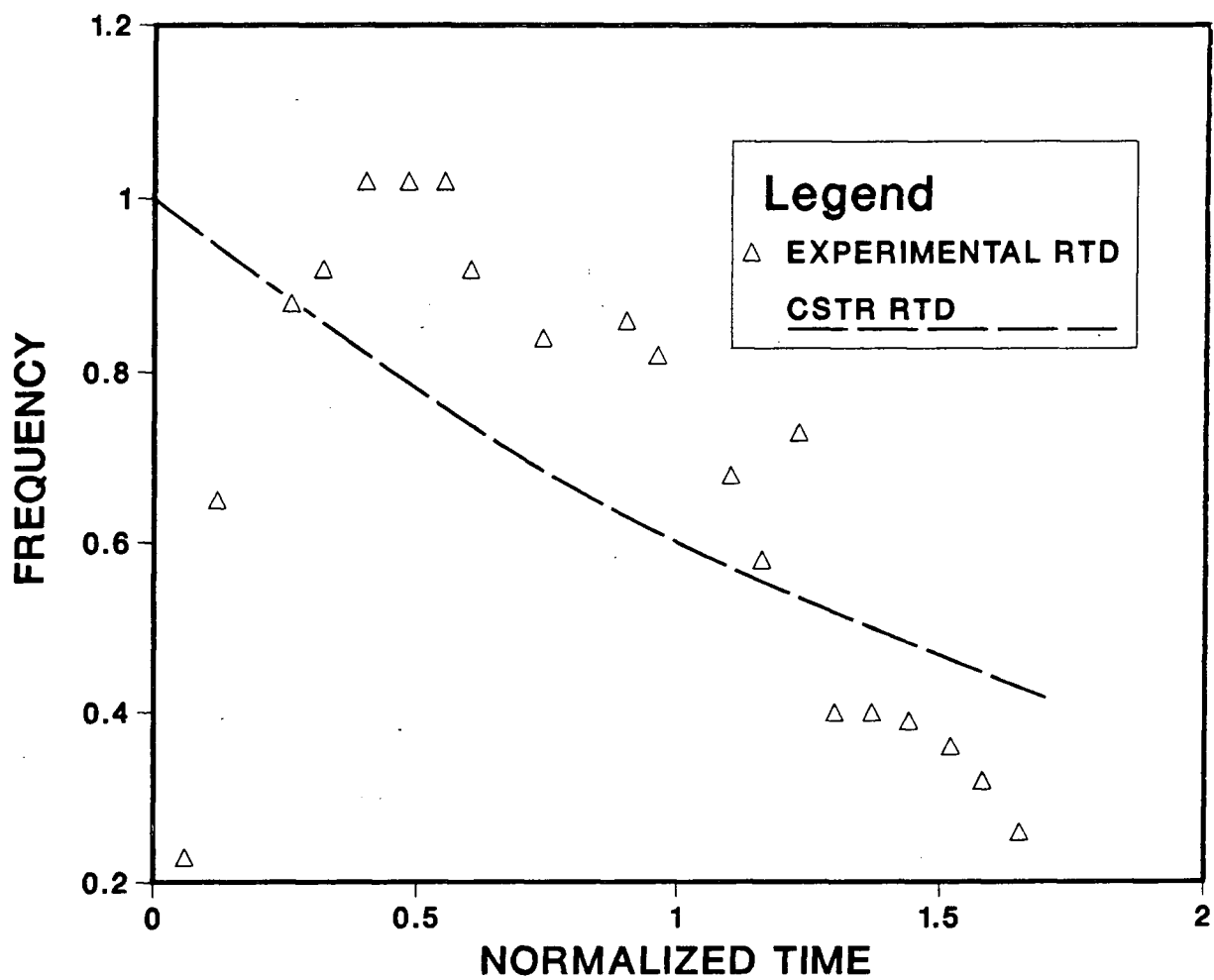


Figure 2.12: Catalyst Residence Time Distribution in a H-Coal Contactor

The advantages of the H-Coal contactor design occur principally in the syncrude mode. Relatively short times, 15 min, produce high yields of hydrogenated liquids that are easily upgraded. Over 34% of the liquid product can be used as a petrochemical feedstock - a percentage 1.5 times greater than the nearest rival, SRCII<sup>[24]</sup>. The disadvantages of the process include the high costs associated with slurry recirculation and catalyst use (elutriation losses caused by particle abrasion, catalyst deactivation and replacement), and poor slurry distributor design. Improved distributor design could reduce or eliminate catalyst bed recirculation, thus minimizing particle abrasion and shortcircuiting.

#### **2.1.1.2.1.2 The Solvent Refined Coal Contactor (SRC I & II)**

The SRC I and SRC II processes share a common contactor design. The contactor is an open vertical tube with gas injection ports mounted on the sides; it is operated at constant temperature<sup>[25]</sup>. The differences between the two processes parallel the differences between the two operating modes of the H-Coal Process. The SRC I process is intended to produce a synthetic refined coal (SRC) - low in ash and sulphur. This product objective requires a minimum extent of reaction. Consequently, ash bearing process streams are not returned to the contactor. Distillate oils are the primary products of the SRC II process; high ash process streams containing unreacted coal, distillate bottoms etc., are recycled to the contactor to enhance catalytic effects and improve overall yields. Operating data for both processes can be found on Table 2.1.

The SRC contactor is susceptible to hydrodynamic differences arising from changes in scale. The 5.45 tonne per day Wilsonville plant operating data suggests that all the gas enters with the slurry at the base of the contactor<sup>[11]</sup>. Calculations, employing equation 2.1 and the tank-in-series flow model (TIS)<sup>[16]</sup>, equation 2.5,

$$E_{\theta} = \frac{N(N\theta)^{N-1}}{(N-1)!} e^{-N\theta} \quad (2.5)$$

predict a slurry rtd equivalent to the TIS model with the number of tanks in series,  $N$ , approximately equal to 1.24. Lee et al<sup>[11]</sup> fitted a flow and kinetic model to typical Wilsonville product yields and distributions. Their dispersion analysis results correspond to a tank in series residence time distribution with  $N=1.35$ . Gas jets are positioned at intervals along the sides of the larger (45.5 tonne per day) Fort Lewis contactor<sup>[25]</sup> and one cannot assign a single dispersion coefficient to the entire contactor. Experimental slurry phase rtd data was obtained, for this contactor, by injecting a radio active tracer at the mid point of the contactor and measuring the tracer concentration as a function of time at the summit and base<sup>[26]</sup>. These results indicate a maximum mixing velocity of  $0.95 \text{ cm.s}^{-1}$  and  $0.67 \text{ cm.s}^{-1}$  in the top and bottom portions of the contactor. The difference in mixing velocity can be attributed to differences in gas flux, the effect of slurry flux on counter current bulk diffusion (the mean slurry velocity is in the range  $0.16 - 0.48 \text{ cm.s}^{-1}$ ), or both. In either case, the contactor exhibits extensive axial mixing and is likely to have a residence time distribution which corresponds to a recycle flow model or a TIS model with  $N < 2$ , depending on the influence of macro-mixing and micro-mixing effects.



The SCR I and SRC II processes have commercial prospects only on a regional basis. The mean residence times are long and the product slate is restricted. Bituminous coals with catalytically active mineral matter appear to be the only suitable feed materials.

#### **2.1.1.2.1.3 The Dow Contactor**

Few construction or operation details are available for the Dow Contactor<sup>[27]</sup>. The contactor is described as "a back-mixed, pressure vessel of open tube design"; the hydrodynamics should be comparable to the SRC contactor. The coal is hydrogenated in the presence of an (oil in water) emulsion catalyst. The emulsion is used to carry and dispense an inorganic molybdate salt which precipitates as colloidal  $\text{MoS}_2$  in situ. Molybdenum levels in the slurry are in the range of 100 ppm.. Processing conditions are summarized on Table 2.1.

The Dow contactor produces a broad range of products well suited to the process requirements of a large chemical plant: petrochemical feed stocks, clean fuels for electricity generation, process steam etc..

#### **2.1.1.2.2 Multi-Stage Contactors**

##### **2.1.1.2.2.1 The Ruhrkohle Contactor**

Two contactor designs have been tested for the Ruhrkohle process:

the 0.5 tonne per day experimental plant at Bergbau-Forschung contains a vertical up-flow tubular contactor<sup>[2]</sup>, the 200 tonne per day pilot plant at Bottrop employs three up-flow tubular contactors in series<sup>[28]</sup>. The Bergbau-Forschung contactor operates at constant temperature and contains magnetically driven impellers to promote local mixing. In the absence of forced agitation, the slurry and dispersed metal oxide catalyst rtd would resemble the TIS flow model rtd with  $N \approx 1.3$  (see Appendix A.3). With agitation, local recirculation patterns are established about each impeller, slurry dispersion is reduced, and the apparent number of stages in series,  $N$ , increases<sup>[29]</sup>. More explicit process data is required to evaluate the slurry rtd in the B-F plant contactor. Each stage of the 3 stage pilot plant contactor operates on the same principle as a bubble column and is axially mixed. The stages operate at constant but different temperatures and the overall residence time distribution approximates  $4^+$  tanks in series.

The Ruhrkohle process is at an advanced stage of development, and high yields of light and middle distillate oils are obtained (refer to Table 2.1). Possible debilities of this process include a long mean residence time, and high gas and residue yields. However, the process can be used to upgrade heavy mineral oils, at 5 times the production rate of oil from coal, with minor modifications.

#### 2.1.1.2.2.2 The Saarbergwerke Contactor

The Saarbergwerke contactor differs significantly from the other multistage contactors (Figure 2.5). A portion of the slurry feed by-passes the pre-heater and the first stage of the contactor to enter at the base of the second stage. There are 4 stages in total, each an up-flow tubular reactor<sup>[2]</sup>. Optimum ranges for pressure, temperature slurry mean-residence-time, and gas flow rates have not been published. The absence of hydrodynamic data precludes an evaluation of axial mixing effects, and there is insufficient data to review the contactor critically.

#### 2.1.1.2.2.3 The EDS<sup>\*</sup> Contactor

The EDS contactor has a staged configuration<sup>[30]</sup>, which is not shown on the simplified flow sheet, Figure 2.4. The contactor comprises a multi-stage dissolver, the number of stages is not specified, and a fixed-bed, catalytic hydrogenation unit - operated as a CSTR. A vacuum distillation unit separates the dissolver from the hydrogenation unit. Light hydrocarbons ( $T_b < 204^\circ\text{C}$ ) and coal residues (unreacted coal, ash and liquefaction products with a boiling temperature greater than  $500^\circ\text{C}$ ) by-pass the hydrogenation unit permitting smooth operation of the fixed-catalyst-bed and minimizing synthetic natural gas formation.

---

\*The EDS process outlined here is not the original one, proposed by EXXON during 1966, but a process variant developed later where a large fraction of the vacuum bottoms is recycled to the dissolver.

The contactor can operate in two processing modes: "high naphtha" and "mixed mode". Approximately the same liquid yield is realized in both modes, Figure 2.13, but under high naphtha conditions the liquid products are primarily  $C_4$  to  $T_b < 204^\circ\text{C}$  liquids. The interplay between dissolver and hydrogenation unit operating conditions required to achieve the processing modes is not specified but (1) hydrogen consumption is substantially greater in the "high naphtha" mode (a more hydrogenated liquid is produced, 3 to 4 times as much SNG is produced), (2) the slurry mean residence time is longer, (3) hydrogenation conditions are more severe.

Advantages of the EDS process include product slate and coal feed flexibility<sup>[30]</sup>, and high yields of light oils. The disadvantages include a complex reactor network, and long residence time - especially when the hydrogenation unit residence time is included.

#### 2.1.1.2.2.4 The Chevron Coal Liquefaction Process (CCLP) Contactor

CCLP is a recent process<sup>[31]</sup>. The contactor has two stages: the first an uncatalyzed dissolver, the second a catalytic hydrogen unit; the processing conditions for both stages can be optimized separately. No operating data has been published.

The high liquid yields, suggested by the data on Table 2.5, can be misleading. The data was obtained from a 23 kg per day laboratory scale

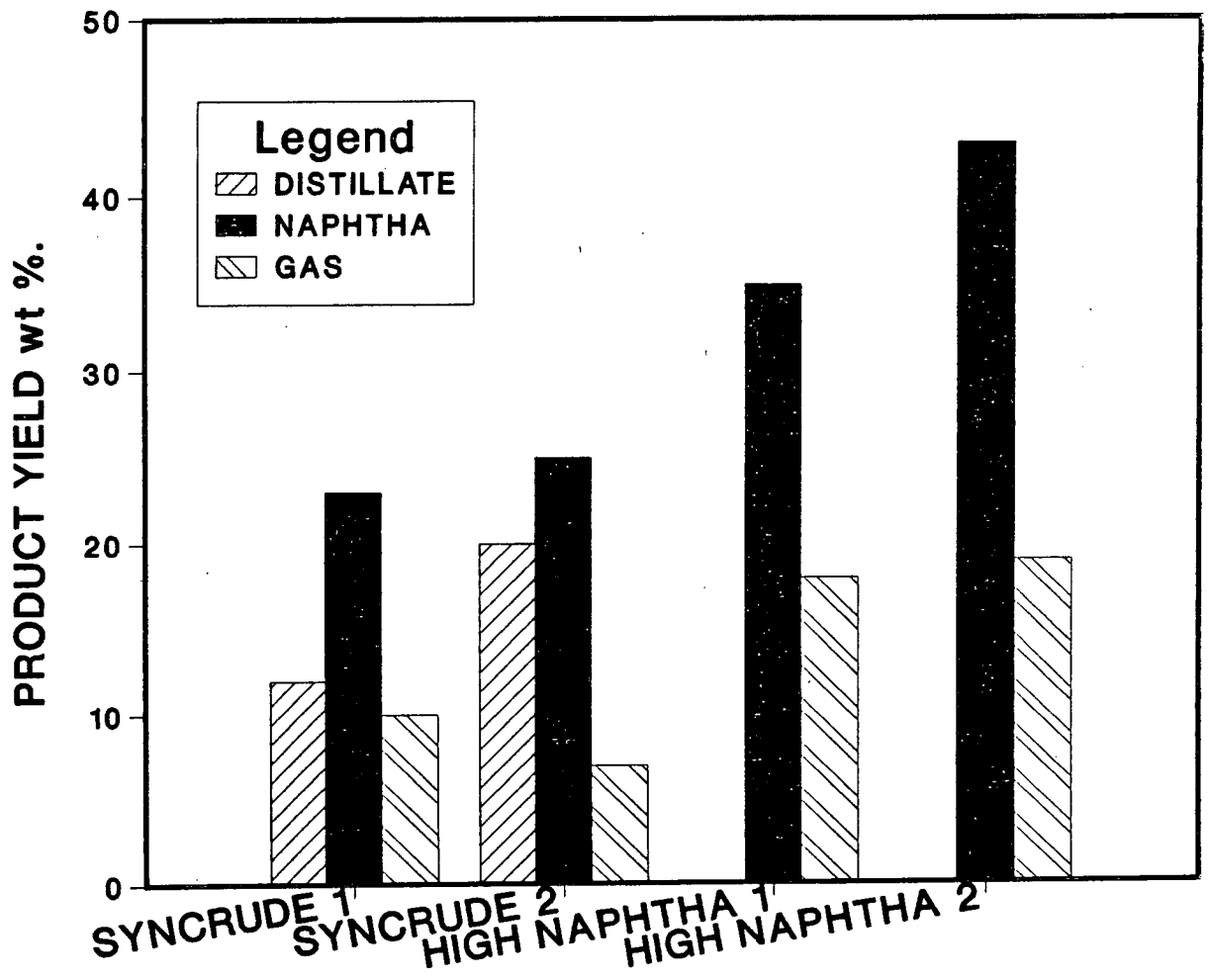


Figure 2.13: Product Flexibility of the EDS Process

TABLE 2.5

CCLP Process Yields

Feed Coal	Illinois No.6 (Burning Star)	Illinois No.2 (Sunspot)	Dietz No.1 (Decker)	Australian Brown Coal (Morwell)
Products (wt%)				
C <sub>1</sub> - C <sub>3</sub>	7.4	6.8	10.7	10.2
> C <sub>4</sub> liquid	73.7	79.6	65.2	66.1
Undissolved coal *	9.8	4.2	11.8	4.5
H <sub>2</sub> O, CO, CO <sub>2</sub>	15.3	17.8	20.0	28.0
H <sub>2</sub> S, NH <sub>3</sub>				
Hydrogen Consumption	5.9	8.1	7.4	8.7
Oil Yield (BBL tonne <sup>-1</sup> MAF Coal)	4.6	5.2	4.2	4.4

\* Ethyl-acetate insoluble material

integrated pilot plant: hydrogen and process heat were not generated from the coal and "liquids" with  $T_b > 500^\circ\text{C}$  are included in the distillate product. Realistic estimates of the liquid yields would be lower by perhaps 15%. The process does not present a distinct advantage over the processes cited above.

#### **2.1.1.3 Reactor Design Rationale**

The liquefaction reactor designs cited above reflect the extreme operating conditions required for Direct Coal Liquefaction and the desire to employ existing heavy oil processing facilities as DCL plants. Heavy oils are and have been upgraded in very similar reactors. In addition, applications of simple 1st or 2nd order kinetic models to the complex coal liquefaction reaction network has led to the conclusion that little benefit accrues beyond segmenting a reactor into the equivalent of 4 tanks in series<sup>[106]</sup> (i.e.) the marginal cost of additional reactor segmentation is not recouped by increases in the yield of oil etc. from the coal.

### **2.2 Liquefaction Reactions and Kinetics**

#### **2.2.0 Introduction**

Coal undergoes a complex sequence of physical and chemical processes as it is liquefied and hydrogenated. To date, research has focussed on an

analysis of the dissolution and kinetic behaviour of bituminous coals. The events, listed on Figure 2.14, reflect the current understanding of the overall liquefaction sequence for bituminous coals (sub-bituminous coals appear to experience a comparable sequence<sup>[33,34]</sup>). While the liquefaction "events", cited on Figure 2.14, are not disputed, there is little agreement in the literature on the reaction mechanisms, reaction paths, or on the correct theoretical approach to adopt in evaluating the reaction kinetics connecting them. Many of the disparities can be attributed to hydrodynamic effects and other incompatable differences in reacting environments, or product analysis which act as hidden variables. Other disparities, inhibiting the correlation of data obtained under comparable conditions, are caused by the presence of multiple regression minima. Often two or more sets of kinetic parameters "optimize" the fit of a reaction model to experimental data<sup>[35]</sup>. Alternatively, several different models may fit the data equally well<sup>[35]</sup>. Current kinetic studies are of limited use for design purposes. One must rely on an understanding of the fundamental liquefaction phenomena, "events" and the factors which influence them.

### 2.2.1 Coal Swelling and Solvent Absorption

Four to ten fold transient increases in slurry viscosity have been reported for a variety of 30-40% coal-oil slurries<sup>[36,37,38]</sup>\* on initial

---

\*Kentucky 9 and Illinois 6, both bituminous coals, and a Japanese coal Shin-Yubari.



1. SOLVENT ABSORPTION
2. PRIMARY DISSOLUTION
3. SECONDARY DISSOLUTION
4. HYDROGENATION
5. HETERO-ATOM REMOVAL
6. RETROGRESSIVE REACTIONS

Figure 2.14: Coal Liquefaction Phenomena

heating through the 280–380°C temperature range and at elevated pressures (approximately 15 MPa). This effect has been attributed to the formation of viscous liquid products derived from thermal decomposition of coals<sup>[33]</sup>. However, coal particle swelling was observed by Droege et al<sup>[36]</sup> and the increases in apparent viscosity are consistent with values predicted by slurry transport correlations for 50 to 100% increases in coal particle size<sup>[39]</sup>. The swelling can result from solvent-coal interactions<sup>[40,41,42]</sup> and/or thermal decomposition of the coal<sup>[43]</sup>. Both causes of swelling can account for the predicted increases in particle size and oil absorption individually.

### 2.2.2 Primary Dissolution

As more reactive macerals, volatile matter, continue to interact with the solvent and dissolve or evolve, less reactive maceral and mineral matter fragments become detached from the original coal particles, particle size is reduced and the viscosity transient subsides<sup>\*</sup>. The destruction of coal particles, in this manner, supports the widely held view that initial particle size has little influence on the rate of coal liquefaction, and highlights the importance of coal-solvent interactions during the initial stages of reaction. In poor hydrogen-donor solvents or donor depleted

---

<sup>\*</sup>There is no experimental evidence related to the method of particle destruction. Hydrodynamic effects (i.e.) the intensity of turbulence may determine the extent of particle destruction or the particles may "explode" due to gas evolution etc..

solvents, for example, high-molecular-weight, viscous, liquid products can be formed by condensation reactions between solvent molecules and coal derived radicals or by inter or intra- radical reactions<sup>[33,52]</sup>. These "condensed" products can precipitate during the initial stages of reaction (at low temperatures or in poor physical solvents) to form SRC<sup>[44]</sup>. The condensed products formed by such reactions, including SRC, can be re-hydrogenated during subsequent stages of reaction<sup>[45]</sup> but reduce space-time yields of lower-molecular-weight, liquid products (oils, naphthas). Primary dissolution reactions are completed within the first 2 to 10 minutes of high temperature contact time<sup>[37,18]</sup>; the controlling variables appear to include the contact temperature, coal type, and the solvent composition. These reactions are highly exothermic and generally occur before the slurry enters the contactor.

### 2.2.3 Secondary Dissolution

The cleavage of less reactive bonds and kinetically slower reactions, occurring within the dispersed coal fragments or SRC particles (precipitated during primary dissolution), leads to secondary coal dissolution. Abundant physical and chemical evidence supports the existence of this phenomenon:

- 1 Coal is not structurally homogeneous<sup>[46,47]</sup>. Constituent macerals exhibit a broad range of reactivities<sup>[42]</sup> under DCL conditions. Coals with comparable elemental compositions can have radically different maceral distributions and hence different average reactivities and hydrogenation potentials.

- ii Dissolution-reaction-order has been observed to fluctuate as dissolution progresses<sup>[48]</sup>.
- iii The apparent activation energy of the dissolution reaction increases with the extent of dissolution<sup>[49]</sup>.
- iv The dissolution potential for a coal is temperature dependent, particularly under solvolytic liquefaction conditions. Two temperature ranges (350-400°C, 400<sup>+</sup>°C) with characteristically different dissolution kinetics have been identified<sup>[35,50]</sup>. At lower temperatures dissolution is dominated by ether bond rupture<sup>\*</sup>; at higher temperatures, dissolution has been shown to include methyl group cleavage<sup>[50,51]</sup>.
- v Reaction models, not incorporating secondary dissolution effects, frequently exhibit poor or skewed fits to experimental dissolution data<sup>[33-35]</sup>.

It is difficult to estimate the coal fraction involved in secondary dissolution. By analyzing experimental results, fit with reaction models not including this effect, between 5 and 20 percent of the reactive coal appears to dissolve in this way. However, the percentage is highly variable even for the same coal; solvent effects, limits on experimental reproducibility, and differences in result analysis (i.e. coal dissolution can be defined on the basis of pyridine, THF or Benzene solubility) impair

---

<sup>\*</sup>Some low rank bituminous coals do not appear to possess reactive ether linkages<sup>[51]</sup>.

an accurate assessment. Secondary dissolution reactions occur for the most part in DCL contactors as they can require 2 or more hours to reach completion.

## 2.2.4 Hydrogenation

### 2.2.4.1 Hydrogenation Reactions

Curran et al<sup>[53]</sup> proposed a free radical mechanism for the transfer of hydrogen from solvents to coal and coal derived liquids. This work has been extended by other researchers<sup>[54-56]</sup> and provides a helpful framework for examining coal hydrogenation reactions. Coal and coal derived liquids are hydrogenated by reactions with:

- 1) hydrogen donor molecules present in the solvent, (tetralin, dihydropyrene, etc.)<sup>[44,33-35,57]</sup>.
- 2) dissolved molecular hydrogen<sup>[54]</sup>.
- 3) solvent or coal derived products hydrogenated insitu<sup>[57]</sup>.

The reactions are initiated and propagated by free radicals which occur both heterogeneously and homogeneously. The relative importance of the three reaction paths and the dominance of heterogeneous or homogeneous reaction is determined by the specific coal-solvent-catalyst-gas system,

reactor hydrodynamics, and operating conditions. The most reactive path dominates. As hydrogenation progresses a sequence of reaction paths exert different kinetics and dependencies on extensive and intensive system properties.

#### 2.2.4.2 Heterogeneous Reactions

Two types of heterogeneous reactions occur within DCL reactors. The first occurs at the onset of coal dissolution within coal particles or on the surface of coal fragments. Coal derived free radicals are stabilized by reactions 1-3 above or by condensation reactions. The second type of heterogeneous reaction occurs on catalyst, ash, autoclave surfaces<sup>[58,60]</sup>. Dissolved, low-molecular-weight, coal-derived molecules (phenols, catechols, planar benzoid molecules<sup>[59]</sup>) are adsorbed on Co-Mo-alumina catalyst and metal/metal oxide/metal sulfide surfaces<sup>[58,59]</sup>. Adsorbed molecules can undergo three distinct reaction sequences depending on local hydrodynamic phenomena:

- (1) dehydrogenation followed by rapid rehydrogenation
- (2) dehydrogenation followed by polymerization
- (3) hydrogenation and/or hydrogenolysis

Reaction sequence (1) is best exemplified by catechol adsorbed on high-speed stirrer surfaces<sup>[59]</sup>. The catechol forms a surface stabilized free

radical by donating a hydride to a coal derived radical or molecule. The surface radical is rehydrogenated rapidly in the hydrogen saturated environment. Adsorbed organic molecules reacting in this way act as catalysts. Reaction sequence (2) leads to the formation of coke or coke precursors. The dehydrogenation step is the same as for sequence (1). However, in the absence of a rehydrogenating medium or in a poorly hydrogenating medium, adsorbed radicals undergo condensation/polymerization reactions<sup>[60]</sup>. Coke is invariably associated with quartz-calcite deposits in SRC reactors<sup>[60]</sup> and forms on Co-Mo-alumina catalyst particles in the H-Coal reactor<sup>[21]</sup>. Reaction mode (3) includes several classes of hydrogenolysis and hydrogenation reactions. These reactions are discussed in sections 2.2.5 and 2.3.

#### 2.2.4.3 Homogeneous Reactions

Coal free radicals, stabilized on initial dissolution, may possess additional reactive bonds<sup>[35]</sup>. Further, homogeneous, thermal cleavage, followed by hydrogenation, reduces the average molecular weight and raises the hydrogen to carbon atomic ratio of the liquid products. However, retrogressive reactions also occur. These reactions reduce space-time yields of low molecular weight products and/or reduce the liquefaction potential of a coal. Ideally, such reactions could be eliminated if radicals were hydrogenated as rapidly as they were formed. Petrakis et al<sup>[55]</sup> obtained residual free radical concentrations for a

variety of bituminous and sub-bituminous coals and lignite in a broad range of solvents under DCL conditions. They concluded that residual free radical concentrations could only be minimized, and that the rate of hydrogenation is controlled by the rate of hydrogen transfer to radicals. This conclusion is supported by Guin et al<sup>[66,67]</sup> who found that coal liquid hydrogenation could be controlled by molecular hydrogen transfer to the solvent, or the extent of solvent hydrogenation. Other researchers have concluded that the rate of coal dissolution, (i.e.) radical formation, limits the rate of hydrogenation<sup>[53]</sup>.

These two contradictory conclusions reflect differences in experimental conditions and illustrate the temperature, pressure, catalytic sensitivity of many coal-solvent-catalyst-gas DCL systems. Free radical generation has a high activation energy. The rate of radical formation increases rapidly in the temperature range 350-450°C<sup>[68]</sup>. At low temperatures within this range, radical generation occurs slowly and good donor solvents hydrogenate radicals as they form. Such systems are not sensitive to (1) the presence or pressure of a hydrogen or inert gas cover<sup>[57]</sup>, (2) the solvent to coal ratio<sup>[61]</sup>. At higher temperatures, the rate of radical generation can exceed the rate at which solvent alone can donate hydrogen. Under these conditions, liquefaction yields are sensitive to solvent composition, the rate of solvent rehydrogenation and hydrogen pressure<sup>[57,63,75]</sup>. Other hydrogenation reaction paths become important<sup>[57]</sup>, and retrogressive reactions become more significant<sup>[61]</sup>.



These effects are accentuated in poor donor solvents<sup>[62]</sup>, or in solvents, such as tetralin, which are subject to thermal degradation and hydro-cracking at elevated temperatures and pressures<sup>[64,65]</sup>. Catalysis and retrogressive reactions are discussed separately.

## 2.2.5 Hetero-Atom Removal

### 2.2.5.1 Reactions

The removal of hetero-atoms, oxygen, nitrogen, and sulphur, from coal liquids is an important aspect of direct coal liquefaction. Hydro-de NOS reactions consume large quantities of hydrogen and are considered to be the rate limiting reactions for the production of clean fuels from coal<sup>[67]</sup>. The reactions occur primarily on catalytically active surfaces<sup>[66,69,70]</sup>; homogeneous hydro-de NOS reactions and thermal decomposition of N-, O-, S- compounds are not important reaction paths<sup>[70]</sup>. Only marginal hetero-atom removal is realized in the absence of mineral matter or other catalysts<sup>[66,69]</sup>. The Dow emulsion phase hydrogenation catalyst does not appear to be effective in hydro-de NOS reactions<sup>[27]</sup>. The catalytic nature of the reactions restricts the molecular size<sup>[70]</sup> and geometry<sup>[58]</sup> from which hetero-atoms can be abstracted.

Rollman<sup>[71]</sup> analyzed the reactivity of several classes of N-, O-, S-compounds, with structures resembling those found in coal liquids, and

established a hydro-de NOS hierarchy, Figure 2.15. He also established reaction paths for the hydro-de NOS reactions of hetero-cyclic compounds under DCL conditions, Figure 2.16, which are in general agreement with work reported by Weisser and Landa<sup>[72]</sup>, and Badilla-Ohlbaum et al<sup>[81]</sup>. The hydrogen consumption of hydro-de NOS reactions for hetero-cyclic compounds is temperature sensitive. At 344°C, the reactions are selective: O and N removal is preceded by hydrogen saturation and rupture of the hetero-cyclic ring, and saturation of the adjacent ring as shown on Figure 2.16; S removal only necessitates hydrogen saturation and rupture of the hetero-cyclic ring. At higher temperatures, 400°C, the selectivity is reduced and S N O removal from hetero-cyclic compounds can produce aromatic or saturated structures. Specific hydrogen consumption is less for S removal than N or O removal, especially at lower temperatures, but hydrogen consumption is minimized at higher temperatures.

#### 2.2.5.2 Catalytic Effects

Hydro-de NOS catalysts promote hydrogenolysis (cleavage) and hydrogenation reactions for compounds found in coal liquids. Both catalytic reactions are subject to synergistic effects in the presence of alternate adsorbed species,  $H_2S$ ,  $H_2O$ ,  $NH_3$ ,  $CO$ :

1. Hydro-deoxidation of phenol, for example, occurs by hydrogenolysis in the absence of other adsorbed species, while ring hydrogenation preceeds hydrogenolysis in the presence of adsorbed  $H_2S$ ,  $H_2O$  etc<sup>[70]</sup>.

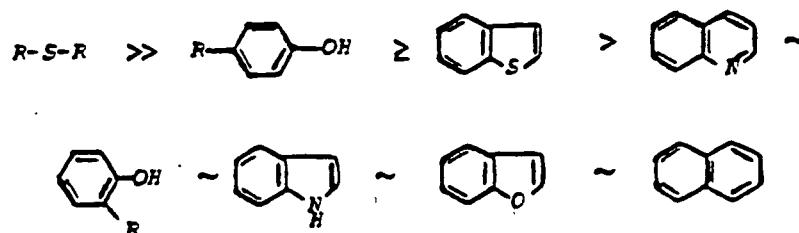


Figure 2.15: The Hydro de NOS Activity of Various Functionalities [71]

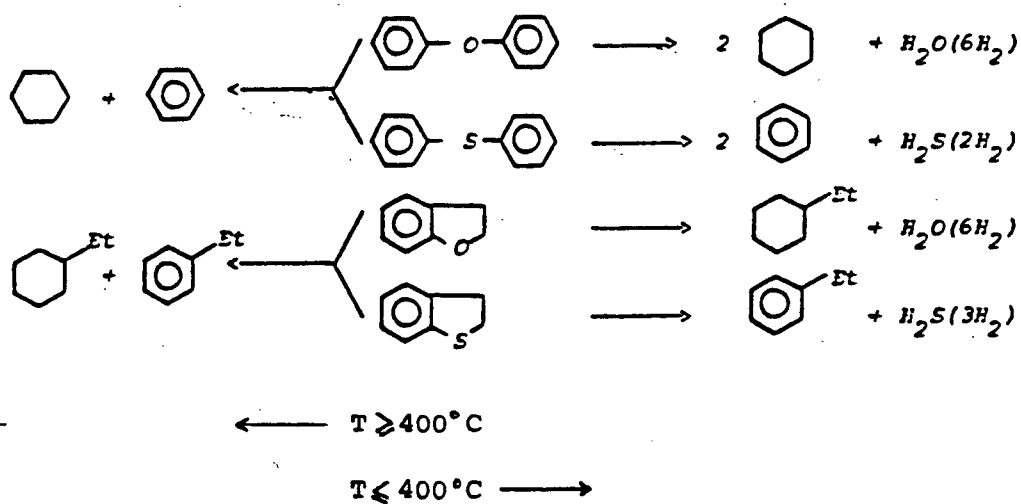


Figure 2.16: Hydro de NOS Reaction Paths [71]

- ii. The rate of hydro-denitrification and hydrodeoxidation is synergistically enhanced in the presence of  $H_2S$  and sulphided Mo-Co-alumina catalyst<sup>[70]</sup>.
- iii. The rate of hetero-atom removal from coal liquids is reduced with increasing pressure under DCL conditions<sup>[73]</sup>. The adsorption of  $NH_3$ ,  $H_2S$  etc. on catalyst surfaces increases with pressure and inhibits hydro-de NOS reactions<sup>[74,66,67]</sup>.
- iv. Direct hydro-deoxidation (hydrogenolysis) of phenols is inhibited synergistically if both sulphided Mo-Co alumina and hetero-cyclic nitrogen compounds are present. This effect is mitigated if  $H_2O$  is also present<sup>[70]</sup>.

These effects are less important at temperatures greater than  $400^\circ C$ <sup>[70]</sup>. Reverse reactions,  $H_2S + \text{Liquid product} \rightarrow \text{Sulphided Liquid product}$ , have been shown to occur under DCL conditions<sup>[66]</sup>. These reactions may or may not be surface catalyzed.

Studies, performed with commercial hydro-de NOS catalysts of the  $MO_x$  and  $MS_x$  type, where M is Co and/or Mo, have shown that catalyst reactivity is altered by catalyst composition<sup>[70]</sup>, the presence and structure of the support<sup>[70,71]</sup>, and whether the catalyst is present in the oxide or sulphide form<sup>[70,74]</sup>. Reactivity variations among catalysts are reflected by differences in the rate of hydro-de NOS reactions for the various

structures<sup>[71]</sup>, or by differences in the extent of product hydrogenation<sup>[70]</sup>. Sulphided catalysts are more susceptible to  $H_2S$ ,  $CO$ ,  $NH_3$  adsorption<sup>[74]</sup> and are, therefore, more likely to promote hydrogenation reactions.

### 2.2.6 Retrogressive Reactions

Retrogressive reactions include all reactions which increase the average molar mass of the liquid products or reduce the solubility of the liquid products in the solvent. Both bituminous and sub-bituminous coals and coal liquids are subject to retrogressive reactions, although sub-bituminous coals/coal liquids are more adversely affected under equivalent DCL conditions<sup>[52]</sup>. These reactions occur throughout the liquefaction circuit: in pre-heaters<sup>[18]</sup>, and contactors<sup>[21]</sup>. Experimental studies have shown the potential for retrogressive "ageing" reactions in solvent storage tanks, transfer lines and in the solvent recycle loop<sup>[76,77,78]</sup>. The effects and extent of retrogressive reactions can only be minimized by maintaining a hydrogenating reaction environment in the liquefaction reactor and by minimizing the hetero-atom content of product liquids.

Some retrogressive reactions, occurring in pre-heaters (solvent adduction by coal radicals<sup>[33,52]</sup> coal radical interactions<sup>[52]</sup> and contactors (reforming and heterogeneous coke formation), were mentioned previously. Other reactions which compete with hydrogenation and hydrogenolysis reactions are those depicted on Figure 2.17<sup>[60]</sup>. Water can prevent methyl bridge

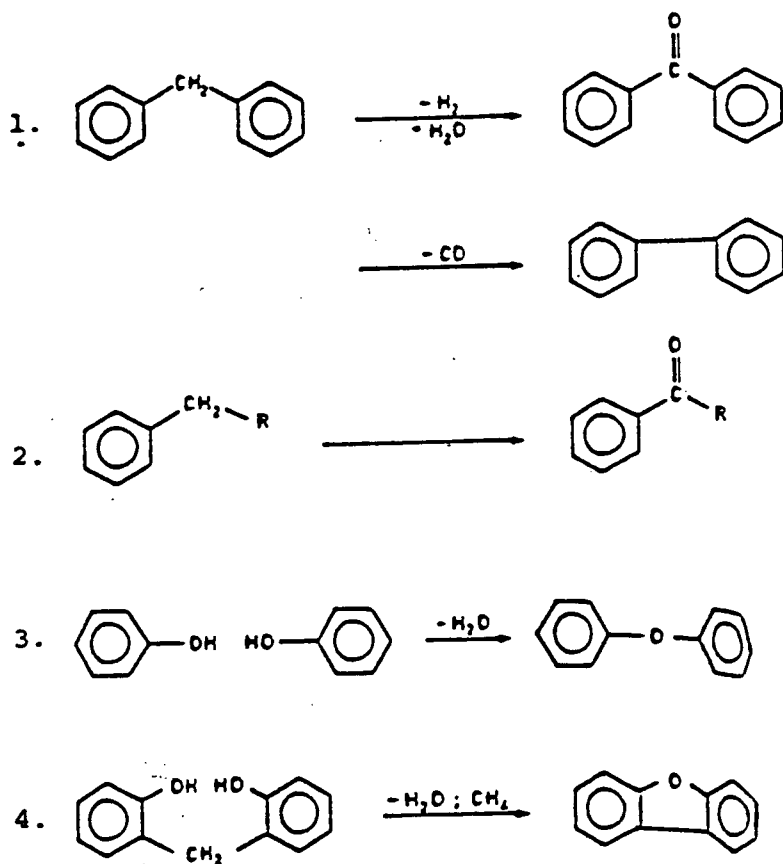


Figure 2.17: Representative Retrogressive Reactions [60]

cleavage and phenolic functional groups are prone to condensation reactions.

Coal liquid ageing is most pronounced in the presence of oxygen, where the oxidative coupling of phenols<sup>[77,78]</sup>, and the production of carbonyl groups (which form hydrogen bonds with phenols etc<sup>[76]</sup>) is realized. In the absence of oxygen, auto-oxidation/polymerization reactions, initiated and propagated by residual free radicals are thought to occur<sup>[78]</sup>. Alkylated heterocyclic nitrogen compounds, present in coal oil, are also thought to cause product degradation<sup>[97]</sup>. Ageing rates increase with temperature<sup>[76,78]</sup> and oxygen partial pressure<sup>[78]</sup>. However, ageing reactions progress slowly. At temperatures less than 60°C, several hours to several days are required to produce noticeable changes in product quality. At higher temperatures extensive degradation and coke formation can occur at short contact times by pyrolysis reactions<sup>[79]\*</sup>.

---

\*The yield of coke from coal-liquids, under pyrolysis conditions, increases with the age of the coal liquids [80].

## **2.3 Catalysts and Catalysis**

### **2.3.1 Catalytic and Solvolytic DCL Processes**

The distinction, made in the literature, between solvolytic and catalytic DCL processes is misleading. Mineral matter constituents, present in most coals, promote hydrogenation, hydrogenolysis and hydro-de NOS reactions in much the same way as commercial catalysts. Direct coal liquefaction processes should be treated as a continuum. The catalytic effects occurring in the solvolytic processes are simply not emphasized.

### **2.3.2 The Role of Catalysis**

Catalytic requirements for DCL processes are complex. In order to minimize hydrogen consumption, a catalyst must promote:

- i. hydrogenation reactions for solvent range compounds (naphthalene, pyrene, etc),
- ii. hydrogenolysis reactions for multi cyclic compounds while avoiding excessive hydro-cracking of low-molecular-weight liquids and the attendant production of SNG,
- iii. efficient hydro-de NOS reactions for compounds containing hetero-atoms,

selectively. However, these catalytic requirements are mutually exclusive.



A catalyst, promoting the hydrogenolysis reactions desirable for ii and iii, would cause dehydrogenated donor-solvent molecules to undergo hydro-cracking rather than rehydrogenation reactions - reducing solvent quality. Conversely, a catalyst which promotes hydrogenation reactions causes the hydrogen consumption for ii and iii to increase sharply. The conflicting nature of the desired catalytic reactivities limits the choice of catalysts for the current generation of DCL processes and has led in part to the different DCL reactor design philosophies. In the EDS process, for example, only the middle distillate product is hydrogenated/hydro-cracked catalytically, while in the H-Coal process the multi-pass ebullated bed reactor permits lighter components, present in the gas phase, to bypass the catalyst.

### 2.3.3 Catalysts

Catalysts, active within DCL reactors, include a broad range of metallic sulphides, mixed metallic sulphides and coal mineral matter constituents (Table 2.6). Catechols have also demonstrated catalytic activity under special circumstances (refer to section 2.2.4.2). Metallic sulphides exhibit greater catalytic activity for hydro-de NOS, hydrogenation and hydrogenolysis reactions than the principle catalytically active mineral matter components: pyrrhotite, pyrite, "ash"<sup>[69,66]</sup>. However, the reactivity of all the catalysts depends on catalyst particle size, composition, and if a support is present, the composition and structure of

the support<sup>[66,69,70]</sup>. Metal sulphide catalysts are subject to de-activation through the deposition of ash and coke, and the adsorption of  $H_2S$ ,  $NH_3$  etc. as discussed in sections 2.2.5 and 2.1.1.2.1.1.

Some of the more important effects, related to the catalysts cited on Table 2.6 are summarized below:

- i. Micron and sub-micron metal sulphide particles (Mo, Co, Ni, W, Fe, Va), introduced into the DCL reactor as sulphates present in the coal or as dissolved-salt emulsion catalysts which are sulphided insitu<sup>[27,66]</sup>, perform well as hydrogenation/hydrogenolysis catalysts but have little impact on hydro-de NOS reactions. Larger metal sulphide particles (Co, Mo, supported Co-Mo, Fe) promote hydro-de NOS reactions but have a lower specific catalytic reactivity with respect to hydrogenation and hydrogenolysis reactions than fine particles<sup>[27,66,69]</sup>.
- ii. Alumina supported Co-Mo catalysts promote hydro-de NOS reactions for asphaltenes selectively; promotion by FeS is non selective<sup>[69]</sup>.
- iii. FeS acts principally as a hydrogenolysis catalyst. The rate of low-molecular-weight liquid formation increases in the presence of FeS but hydrogen consumption remains unchanged<sup>[67,69]</sup>.
- iv. Pyrrhotite has been shown to promote both hydrogenation<sup>[66,67]</sup> and dehydrogenation reactions<sup>[69]</sup>.

TABLE 2.6Catalysts

Catalytic Action	Catalysts
Hydrogenation/Hydrogenolysis	FeS Sn (sulphides) Co-Mo/ $\gamma$ -Al <sub>2</sub> O <sub>3</sub> Ni-Mo/ $\gamma$ -Al <sub>2</sub> O <sub>3</sub> Pyrite* SRC Residue
Hydro-de-NOS Activity	Co-Mo/ $\alpha$ -Al <sub>2</sub> O <sub>3</sub> Ni-Mo/ $\alpha$ -Al <sub>2</sub> O <sub>3</sub> FeS SRC Residue
Dehydrogenation	Pyrrhotite

\* Trace amounts of Ni and Mo are frequently encountered in lattice positions, and pyrite (FeS<sub>2</sub>) decomposes under DCL conditions to produce pyrrhotite (FeS) and H<sub>2</sub>S.

### 2.3.4 Catalytic Activity of Metal Sulphides

The catalytic activity of metal sulphide catalysts, active in DCL processes, has been associated with the lattice defects of non-stoichiometric sulphides ( $\text{Fe}_7\text{S}_8, \text{Co}_9\text{S}_8$ )<sup>[66]</sup>. An alternate and more complex activity model has been proposed, by Weigold<sup>[70]</sup>, to explain the bi-fuctionality of sulphided Co-Mo- $\text{Al}_2\text{O}_3$  catalysts, which promote both hydrogenation and hydrogenolysis reactions. The postulated active sites include a molybdenum and a cobalt atom. The reaction mechanism for hydro-de NOS reactions, Figure 2.18, requires competitive co-ordination of the substrate on one of the metal atoms, rearrangement of the substrate from a  $\sigma$  to a  $\pi$  "bonded" state, and the presence of a co-ordinatively unsaturated metal atom to accept the hydroxyl or thio group. If competitive ligands ( $\text{H}_2\text{O}, \text{H}_2\text{S}, \text{NH}_3$ ) saturate the metal atoms, hydrogenolysis reactions will not occur; the  $\pi$  bonded substrate molecule undergoes hydrogenation instead, as this only requires hydride transfer from the catalyst to the substrate. This mechanism is supported experimentally:

- (1) Meta-substituted NOS-compounds exhibit very slow rates for hydro-de NOS reactions<sup>[58,70]</sup>. Such molecules would have the greatest steric interference for the  $\sigma \rightarrow \pi$  transition.
- (2) Increasing the ligand/catalyst ratio, where ligands include NOS compounds, can reduce the rate of hydro-de NOS reactions significantly<sup>[58]</sup>. High substrate concentrations should inhibit the  $\sigma \rightarrow \pi$  transition.

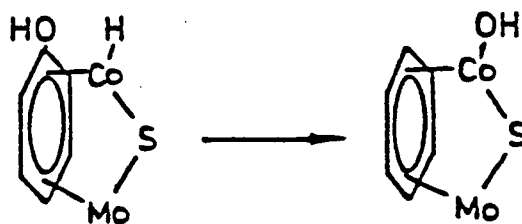
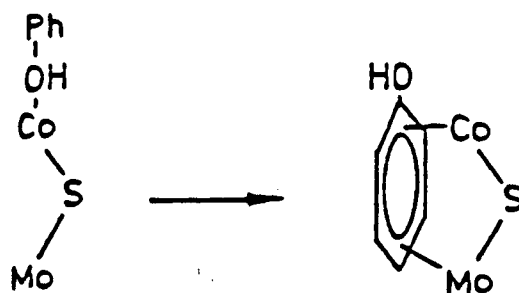


Figure 2.18: Hydro de NOS Mechanism<sup>[70]</sup>

A third activity model, proposed by Sapre and Gates<sup>[82]</sup>, concurs mechanistically with the Weigold model but limits the reactive site to a single exposed metal atom.

## 2.4 Solvents

### 2.4.1 Chemical Composition

Coal liquefaction solvents envisioned for use in industrial DCL processes are high or middle boiling fractions<sup>[2,27,30,31]</sup> of the coal liquids produced in DCL reactors. These solvents contain complex mixtures of aromatic and hydroaromatic compounds<sup>[85-88]</sup>, which vary with coal and process type. Some laboratory experimental programs have endeavoured to duplicate envisioned industrial conditions with complex coal-derived solvents<sup>[33,34,61]</sup>. Others have used model compounds to simulate the functions of the different classes of compounds present in industrial solvents<sup>[44,45,49,57,61]</sup>. This work has led to the development of solvent quality indices for complex solvents<sup>[30]</sup>, and has identified desirable solvent properties. Solvents should

- i. be good physical solvents for the liquefaction products - phenolic and polycyclic compounds are suitable, (i.e.) phenol, fluoranthene and carbazole pyrene; tetralin is a poor physical solvent<sup>[44]</sup>
- ii. contain labile hydrogen in the form of hydro-aromatics<sup>[33]</sup>, and aromatics which are readily hydrogenated to produce hydro-

aromatics<sup>[44,57]</sup>\* - hydro-aromatics include compounds such as tetralin, the aromatics include pyrene like compounds which can act as hydrogen donors or "shuttlers"<sup>[44]</sup>; solvents such as "anthracene oil"<sup>[33]</sup> are poor hydrogen donors

- iii. be stable under the conditions of use - tetralin, for example, decomposes at elevated temperatures<sup>[64,65]</sup>.

## 2.4.2 Physical Properties

### 2.4.2.0 Introduction

Solvent properties rarely considered with respect to coal liquefaction reactor design and of potential importance are:

- (1) Solvent density
- (2) The solubility of hydrogen and other gases in a solvent
- (3) Solvent viscosity

as functions of chemical composition and temperature. Without knowing solvent density it is difficult to determine slurry mean residence time in continuous contactors or pre-heaters. The equilibrium concentration of hydrogen influences reaction kinetics in batch reactors and the potential for gas-liquid mass transfer in continuous flow apparatus. Similarly, the solubility of gases such as  $H_2S$ ,  $CO_2$ ,  $NH_3$  etc. impact on catalyst efficiency and the reaction paths they promote. Solvent viscosity

---

\*This phenomenon is temperature sensitive in some cases [85].

influences the scale of turbulence in a reactor and may affect particle break-up and the degree of axial mixing. Without considering these physical properties effects arising from changes in solvent composition may be attributed to an improper source.

#### **2.4.2.1 Gas Solubilities in Coal Liquids and Related Pure Aromatic Solvents at High Pressure**

##### **2.4.2.1.0 Introduction**

The solubilities of hydrogen, low molar mass hydrocarbon gases, and by-product gases such as carbon dioxide, carbon monoxide, nitrogen, argon, hydrogen sulphide, and ammonia, in aromatic solvents, exhibit complex and disparate dependencies on the chemical composition and mean molar mass of solvents, and on temperature. Available high pressure data for hydrogen, argon, ethane, nitrogen, carbon dioxide, carbon monoxide solubilities, in pure organic solvents, comprise Figures 2.19 - 2.24 respectively. These data emphasise, wherever possible, solubilities in compounds commonly associated with coal liquefaction solvents. Solubilities in aliphatic hydrocarbon compounds are included for comparison.

The solubilities of these gases cover a broad range at a given temperature, depending on solvent composition, and exhibit three distinct types of temperature dependence. Hydrogen, nitrogen, carbon monoxide



solubilities increase with temperature; methane and argon solubilities remain constant or decline with temperature; carbon dioxide and ethane solubilities decline rapidly with temperature. Ammonia, hydrogen sulphide and propane solubilities in aromatic compounds are also expected to decline with temperature. Clearly, the solubility behaviour of these gases does not correspond to the anticipated behaviour suggested by "ideal" solubility theory<sup>[108]</sup>, which states that gas solubilities decline as temperature increases and are inversely proportional to solvent molar mass. Gas solubility behaviour in DCL systems must be analysed without the aid of this frequently helpful theoretical framework.

In order to facilitate data presentation and comparison, all solubilities are expressed as pseudo Henry's Law constants. Deviation from Henry's Law behaviour for methane, hydrogen, carbon monoxide, and carbon dioxide solubility, in organic solvents is less than 10% for the pressure ranges considered (25-100 ATM)<sup>[98,99,107]</sup>. This deviation is ignored in all cases as the probable error associated with solubility measurements is 5-10%.

#### **2.4.2.1.1 The Effect of Temperature on Gas Solubility**

The effect of temperature on gas solubility can be examined in absolute as well as relative terms. Pure solvents of the same class exhibit the same solubilities at the same relative temperature, whereas gas solubilities decline at constant absolute temperature for solvents of the

same class as solvent molar mass increases. Figure 2.19 illustrates this phenomenon for hydrogen solubilities, where aromatic solvents are divided into three classes: single ring aromatic compounds; double ring aromatic compounds; and aromatic compounds comprising three or more rings, or aromatic compounds containing oxygen, sulphur or nitrogen atoms. A similar tendency is noted, with respect to relative and absolute temperature, for hydrogen solubility in straight chain aliphatic hydrocarbons. Hydrogen solubility in n-hexane and n-hexadecane differs by less than 50% at the same relative temperature, whereas the difference exceeds 200% at the same absolute temperature.

Figures 2.19 - 2.23, which include data for hydrogen, argon, ethane, nitrogen and carbon dioxide, suggest that the temperature dependence of gas solubilities is consistent for both aliphatic and aromatic solvents. So, despite the scarcity of solubility data for methane, carbon dioxide, carbon monoxide, propane, ammonia and hydrogen sulphide, the general temperature dependence of solubility for these gases can be inferred from available data involving only one solvent class. The influence of temperature, on gas solubility, is appreciable - except for methane and argon solubilities. Hydrogen and nitrogen solubilities in Benzene, for example, double between 20°C and 100°C. Carbon dioxide and ethane solubilities, in the same solvent, drop by a factor of 5 and 2 respectively over the same temperature interval.

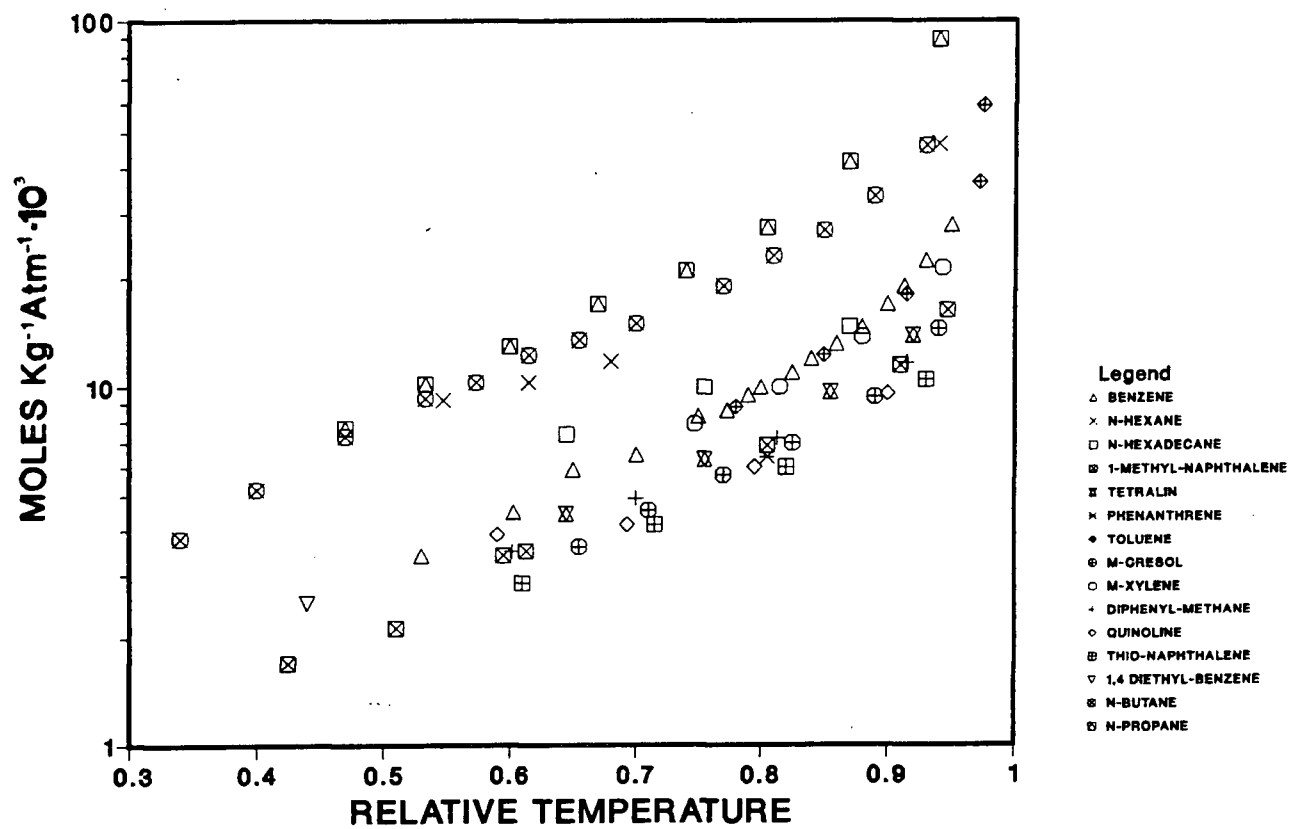


Figure 2.19: Hydrogen Solubility in Pure Organic Solvents

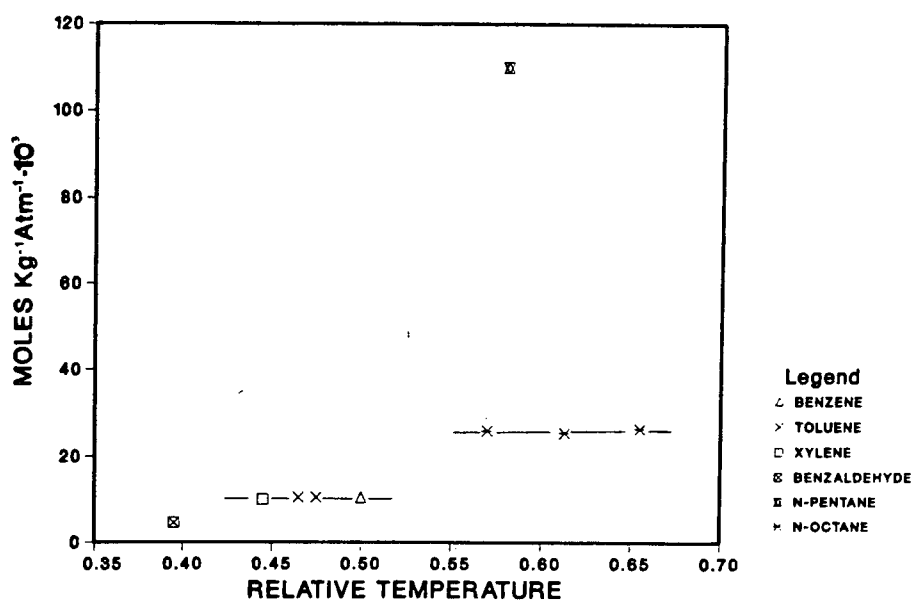


Figure 2.20: Argon Solubility in Pure Organic Solvents

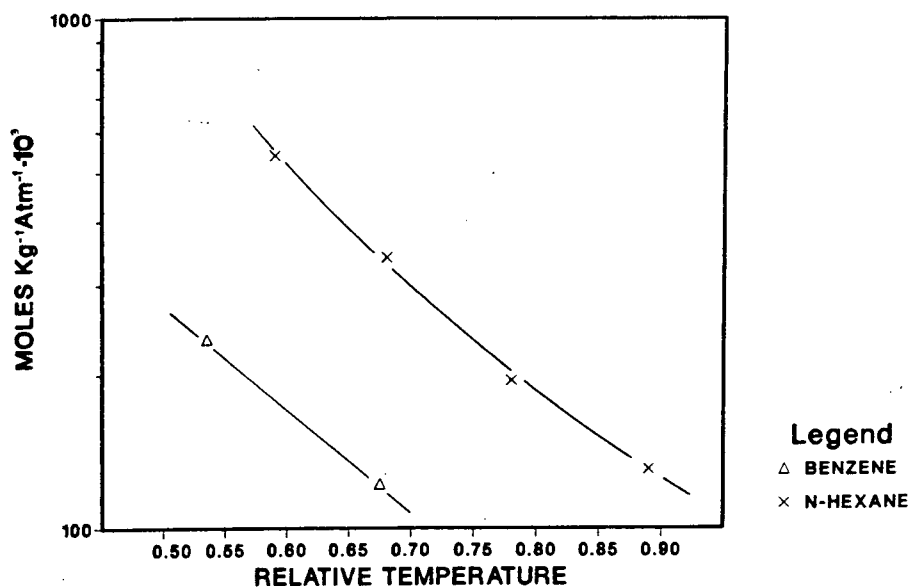


Figure 2.21: Ethane Solubility in Pure Organic Solvents

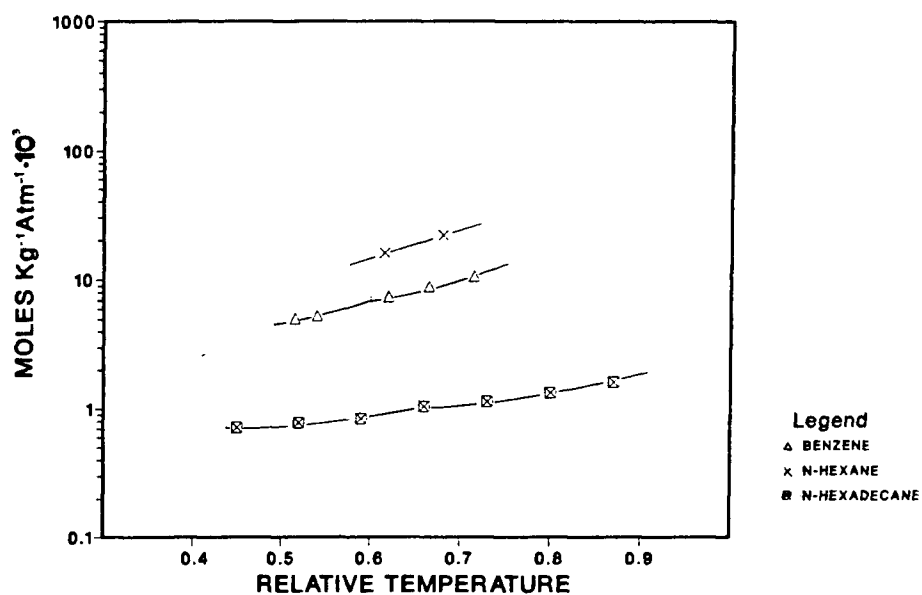


Figure 2.22: Nitrogen Solubility in Pure Organic Solvents

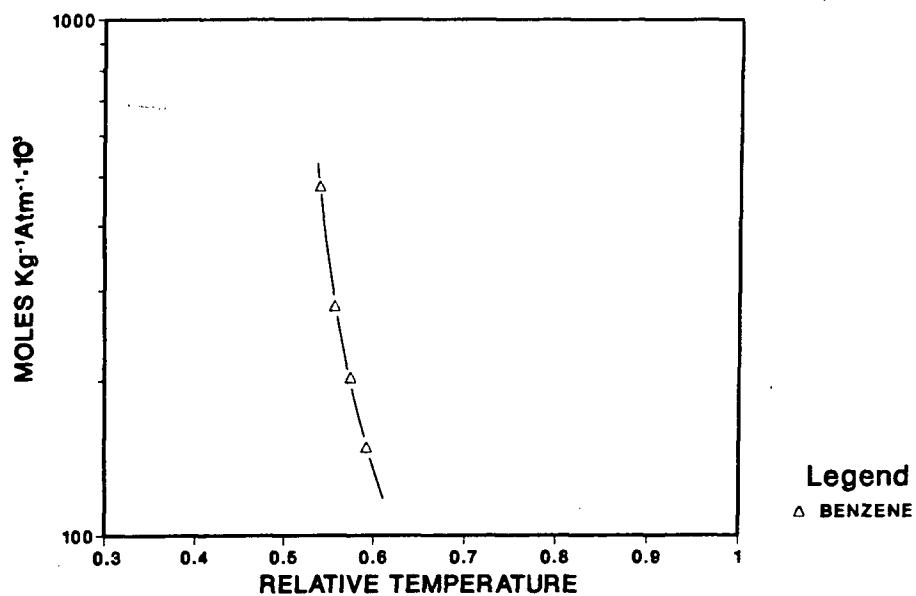
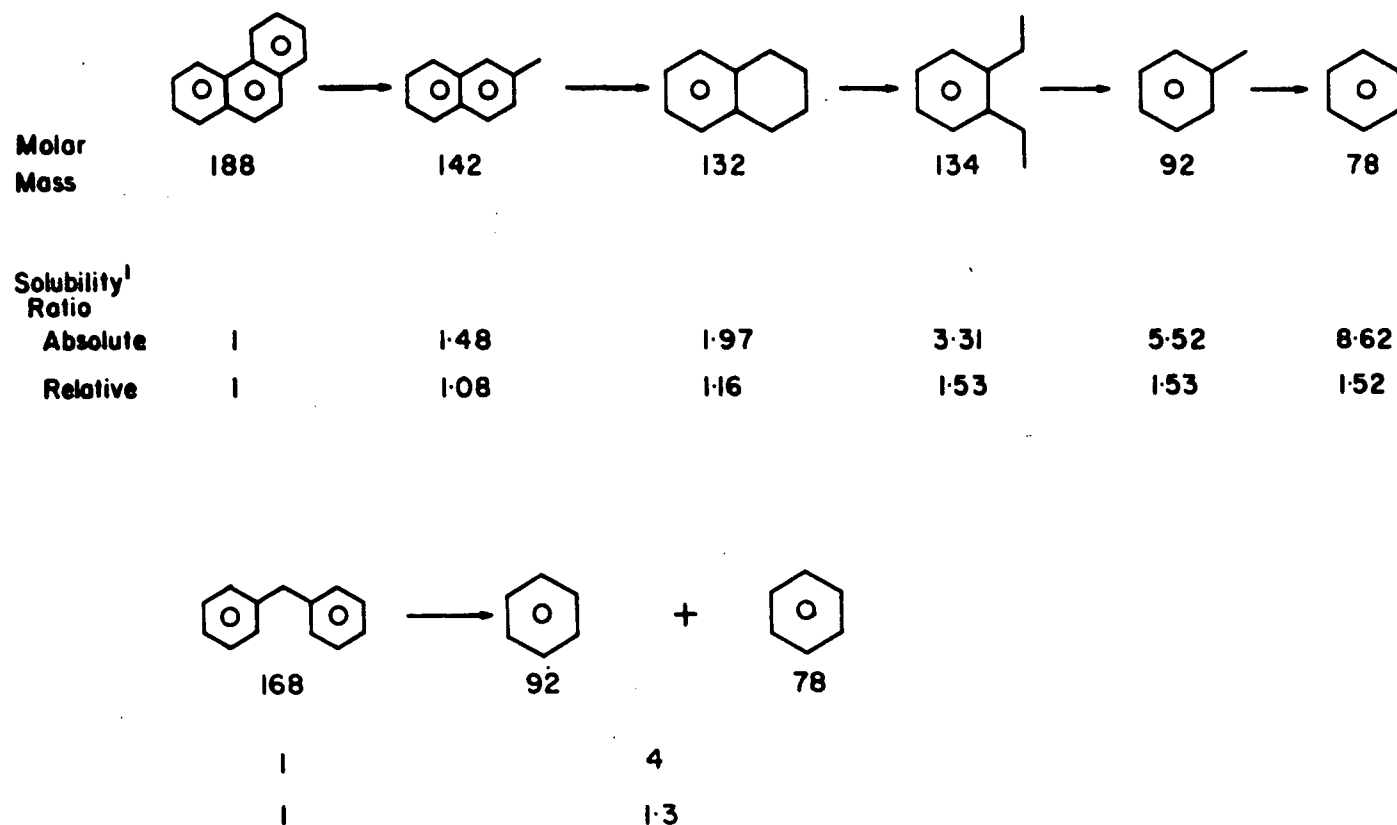


Figure 2.23: Carbon Dioxide Solubility in Pure Organic Solvents

#### 2.4.2.1.2 The Effect of Solvent Composition on Gas Solubility

Solvent composition affects the molar mass, the elemental composition, and the molecular structure of a solvent, thus determining its class and the relative temperature. Gas solubilities in solvents of different classes can be radically different at the same relative or absolute temperature even if solvent molar mass and molecular structure are similar. Hydrogen solubility in m-xylene ( $C_8H_{10}$ , mm = 106) is 53% greater at the same relative temperature and 122% greater at the same absolute temperature than hydrogen solubility in m-cresol ( $C_7H_8O$ , mm = 108). Similar differences are encountered for hydrogen solubility in diethyl benzene ( $C_{10}H_{14}$ , mm = 134) vs hydrogen solubility in thio-naphthalene ( $C_8H_6S$  mm = 134) - 65% and 140% respectively. Comparable differences are noted for other gas solubilities.

Figure 2.24 illustrates the effect of 2 typical liquefaction reaction sequences on hydrogen solubility. The molecular structure and composition of the compounds remains similar but the molar mass is reduced. The solubility ratios cited on Figure 2.25 vary somewhat depending on the temperature range considered but the magnitude of the change in solubility realized by cleaving the aromatic structure is enormous. 5 to 10 fold increases in hydrogen solubility result at constant temperature, simply by reducing the molar mass by 50%. The increase in solubility would be much less (i.e.) 1.5-2 fold if hetero-atoms remain within the molecular structure.



1. Solubility ratios are reported at the same absolute and relative temperatures with respect to the initial species in each sequence.

Figure 2.24: Two Liquefaction Reaction Sequences

The solubility results for hydrogen can be used to interpret the solubility behaviour of other gases. Carbon monoxide<sup>[107]</sup> and nitrogen solubilities behave in a manner similar to hydrogen solubility. Solubility increases resulting from reductions in molar mass or hetero-atom content are reinforced by a corresponding increase in relative temperature. The solubilities of other gases argon, methane, carbon dioxide, ethane, propane etc. do not behave in a similar manner. Increases in solubility caused by reductions in molar mass, or hetero-atom content are not reinforced by a corresponding increase in relative temperature. On the contrary, the solubilities of these gases remain constant or decline as temperature increases. Therefore, the solubilities of these gases will only tend to increase when the solvent changes from a class with a low solubility to another of much higher solubility. Gas solubility will decline if the solvent remains within the same class after the molar mass or hetero-atom content has been reduced.

#### **2.4.2.1.3 Gas Solubilities in Mixed Solvents**

##### **2.4.2.1.3.0 Introduction**

Mixed solvents such as coal liquids comprise innumerable compounds with broad ranges of molar mass, molecular structure and chemical composition. Fortunately, gas solubility trends in mixed solvents parallel trends encountered with pure solvents<sup>[108]</sup>. In general,



$$S_{\text{mix}} \cong \prod_{i=1}^n S_i^{x_i} \quad (2.6)$$

where  $S_{\text{mix}} \equiv$  solubility in a mixed solvent

$x_i \equiv$  the mole fraction of component  $i$  in the solvent

$S_i \equiv$  the solubility in pure  $i$

$n \equiv$  the number of components in the mixed solvent

Despite the limitations and restrictions implicit in an equation as simple as equation 2.6 it was used to derive a semi-empirical equation for correlating gas solubility data in complex solvents. The details related to the derivation of equation 2.7 can be found in Appendix B1.

$$S_{\text{mix}} = \bar{A} \exp \left\{ \frac{\bar{b}}{1.495 \frac{T}{T_{B50}}} \right\} \quad (2.7)$$

where:  $\bar{A}$  and  $\bar{b}$  are constants

$1.495 T_{B50}$  approximates the critical temperature of the mixture

$T$  is the absolute temperature (K)

#### 2.4.2.1.3.1 Gas Solubilities in Coal Liquids

Very little data on gas solubilities in coal liquids has been published. However, available data for hydrogen and methane solubility in coal liquids and narrow boiling fractions comprise Figure 2.25. Hydrogen

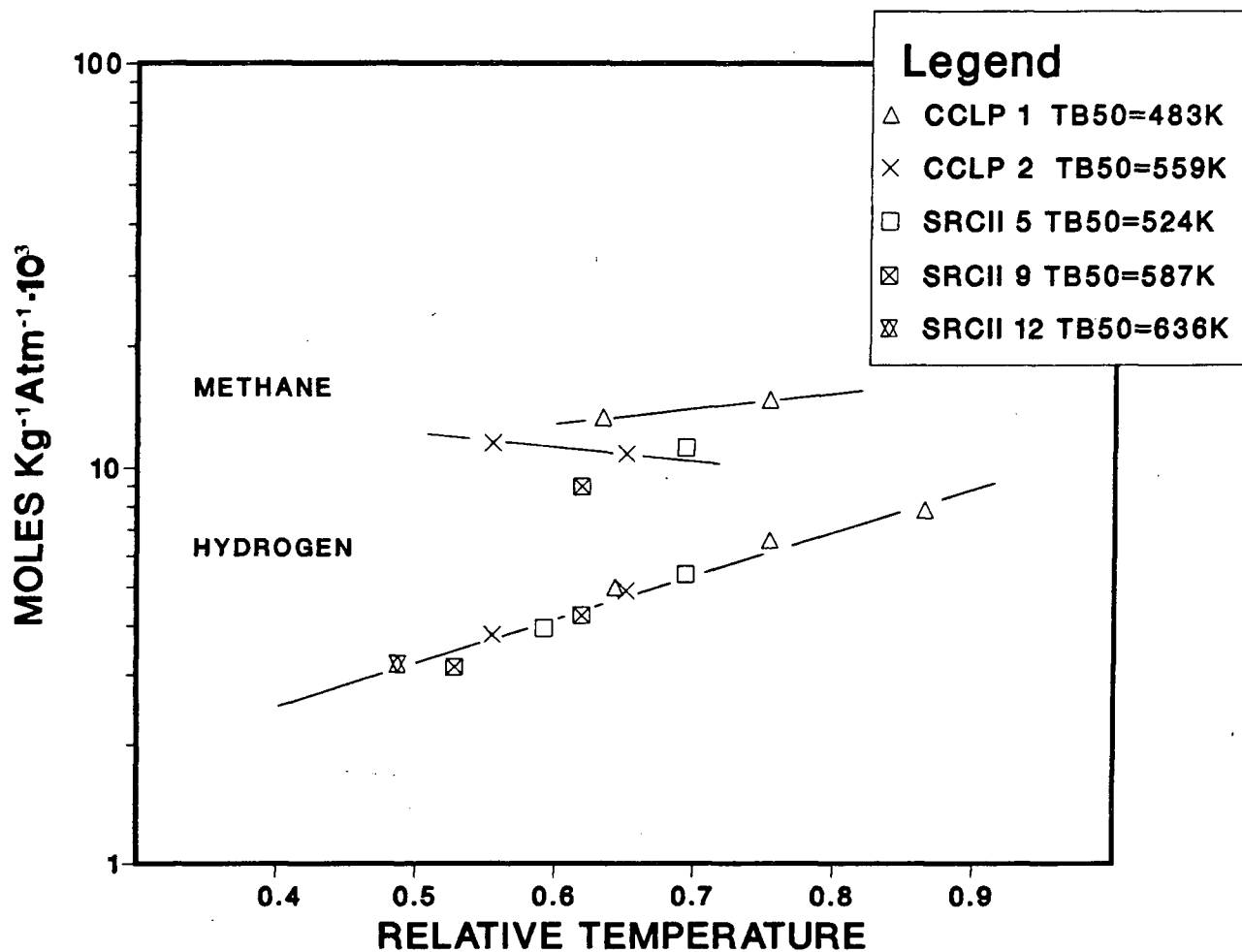


Figure 2.25: Hydrogen and Methane Solubilities in Coal Liquids

solubilities in all of the liquids are accurately correlated by equation 2.7. Methane solubilities form stratified curves according to the mean molar mass of the solvent.

The effect of trace components on gas solubility is a further consideration. Gas solubilities in compounds such as hexane, pentane, butane, propane can be as great as 200 times gas solubilities in aromatic solvents at the same temperature. A 5 mole % (1 wt%) addition of some combination of these compounds to a phenanthrene like solvent would yield a 25-50% increase in hydrogen solubility according to equation 2.6. There is insufficient data to quantify the effect of such additions on the solubilities of other gases.

#### 2.4.2.1.4 Apparent Solubility

All of the solubility data presented so far was obtained from apparatus with a gas phase comprising gaseous solvent and a single pure solute. In general the gas phase was 98<sup>+</sup> mole % solute, and less than 2 mole % vapourized solvent. Solubility data obtained in conjunction with liquefaction experiments and of greater relevance to process design and development is not realized in this manner. Solubility determinations involve complex gas phases with widely varying composition. Solubilities obtained from complex gas phases must be distinguished from solubility data obtained with a relatively pure gas phase. These solubilities are referred to as "apparent solubilities".

TABLE 2.7  
Apparent Solubility Data

Compound Pair	Solvent	Gas Consumption mole fraction		Solubility moles.Kg <sup>-1</sup> solvent ATM <sup>-1</sup> x10 <sup>3</sup>	
H <sub>2</sub> + CO	A mixture of straight chain alcohols C <sub>12</sub> - C <sub>16</sub> @ 315°K and 60 ATM	H <sub>2</sub>	CO	H <sub>2</sub>	CO
		.69	.31	2.37	4.32
		.515	.485	2.35	4.55
		.43	.57	2.54	4.63
H <sub>2</sub> + CH <sub>4</sub>	Tetrahydro- naphthalene  @ 462.4°K & 50 ATM	H <sub>2</sub>	CH <sub>4</sub>	H <sub>2</sub>	CH <sub>4</sub>
		.8892	.1033	4.36	12.23
		1.000	0.00	4.40	-

Apparent solubility data for two binary gas phases is presented on Table 2.7. The variation of solubility for each gas component with composition is small, less than 7%, and reflects the variation of activity coefficient with pressure more so than interactions between gas phase constituents. Activity coefficients for gas solubilities do not stray appreciably from unity as noted in section 2.4.2.1 and this effect was neglected as secondary. Apparent solubility data is scant but fluctuations in activity coefficients with gas phase composition appear to be equally secondary. Despite the probable similarity between apparent and pure gas phase solubilities, it is important to note that they are qualitatively different.

#### 2.4.2.2 Solvent Density

Reid et al<sup>[109]</sup> reviewed a number of correlations for estimating pure-liquid densities. They found that the Gunn-Yamada correlation, equation 2.8,

$$\rho = \rho^R \frac{v_r^{(o)R}}{v_r^o} \frac{(1 - \omega \Gamma^R)}{(1 - \omega \Gamma)} \quad (2.8)$$

where:

$$\Gamma^R = 0.29607 - 0.09045 T_r - 0.04842 T_r^2$$

$$v_r^o = \begin{cases} .33593 - .33953 T_r + 1.5191 T_r^2 - 2.02512 T_r^3 \\ + 1.11422 T_r^4 & 0.2 < T_r < 0.8 \\ 1.0 + 1.3 (1 - T_r)^{1/2} \log (1 - T_r) - .50879 (1 - T_r) \\ - 0.91534 (1 - T_r)^2 & 0.8 < T_r < 1.0 \end{cases}$$

provided the most accurate and consistent results for the temperature range  $0.2 < T_r < 0.99$ . Density values predicted by equation 2.8 are typically within 3% of experimental values. Figure 2.26 illustrates the change in density between room temperature and coal-liquefaction conditions for tetralin, naphthalene and other pure compounds associated with model solvent studies and DCL experiments. Densities for these compounds drop from  $1 \text{ g cm}^{-3}$  at room temperature to between  $0.5$  and  $0.65 \text{ g cm}^{-3}$  at  $700\text{K}$ . There are no general methods for treating densities of complex mixtures and little data appears in the open literature. However, one would not expect such large reductions in solvent density with temperature, especially in continuous process equipment - lighter, more volatile solvent components tend to be stripped from the solvent by the recirculating hydrogen stream. The densities of DCL recycle solvents, at elevated temperatures, are less than their respective room temperature densities, Table 2.8, but greater than  $0.7 \text{ g cm}^{-3}$  at  $700\text{K}$ .

#### 2.4.2.3 Solvent Viscosity

Viscosities of pure solvents are readily estimated as a function of temperature<sup>[110]</sup>. At temperatures removed from the critical point, (i.e.)  $T_r < 0.74$ ,

$$\log (\mu) = A \left\{ \frac{1}{T} - B \right\} \quad (2.9)$$

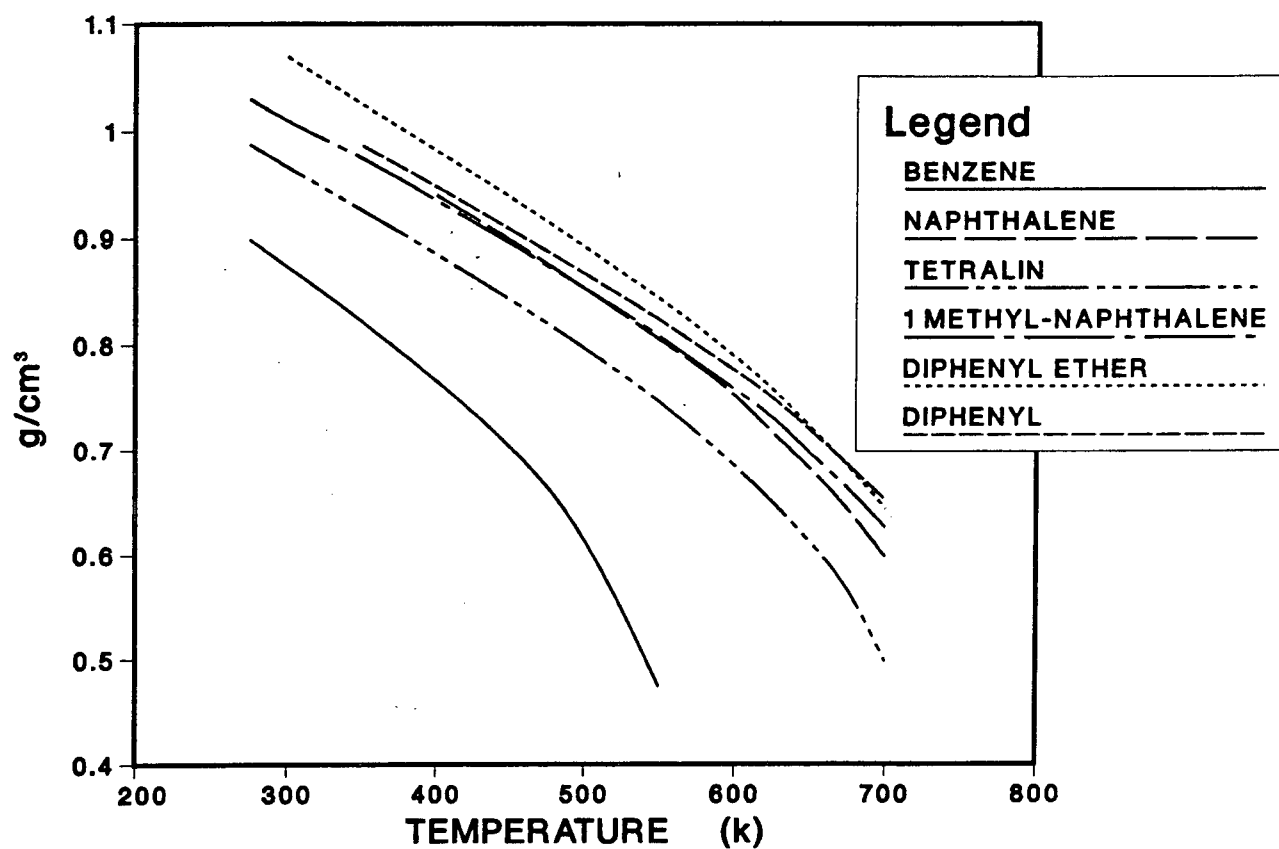


Figure 2.26: The Densities of Pure Organic Solvents

TABLE 2.8

Coal Solvent Densities

Coal Liquid	Physical Properties <sup>[98]</sup>		
	Mean Molar Mass g	T <sub>B50</sub> (K)	density g cm <sup>-3</sup> at 15°C
CLPP-A5	154.34	483.	0.9320
CLPP-A5	182.30	558.	0.9844
SRC II #5	182.	524.	0.9826
SRC II #9	212.	587.	1.0306
SRC II #12	252	636.	1.091



viscosity data for most compounds correlate well with equation 2.9. As the critical point is approached, viscosity drops rapidly with temperature and a more complex equation is required:

$$\mu = \frac{M^{1/2} P_c^{2/3}}{T_c^{1/6}} \{ .015174 - .02135 T_r + .0075 T_r^2 + \omega (0.42552 - .07674 T_r + .0340 T_r^2) \} \quad (2.10)$$

Equation 2.10 is appropriate for the relative temperature range  $0.74 < T_r < .98$ . These correlations estimate viscosities within 15% of experimental values. Kinematic viscosities for a variety of aromatic and hydro-aromatic compounds and several coal derived liquids are shown on Figure 2.27. Under DCL conditions the kinematic viscosities of pure 2 ring solvents are in the range of 0.15 cSt. The kinematic viscosity of anthracene, a 3 ring aromatic, is approximately 0.25 cSt, and the viscosities of higher-boiling, coal-derived liquids are likely to be greater still. At room temperature viscosities can be 1 to 2 orders of magnitude greater. The very high viscosities exhibited by some of the coal liquids at room temperature is not unusual. Many pure compounds undergo large increases in viscosity near the freezing point.

## 2.5 Process and Kinetic Models

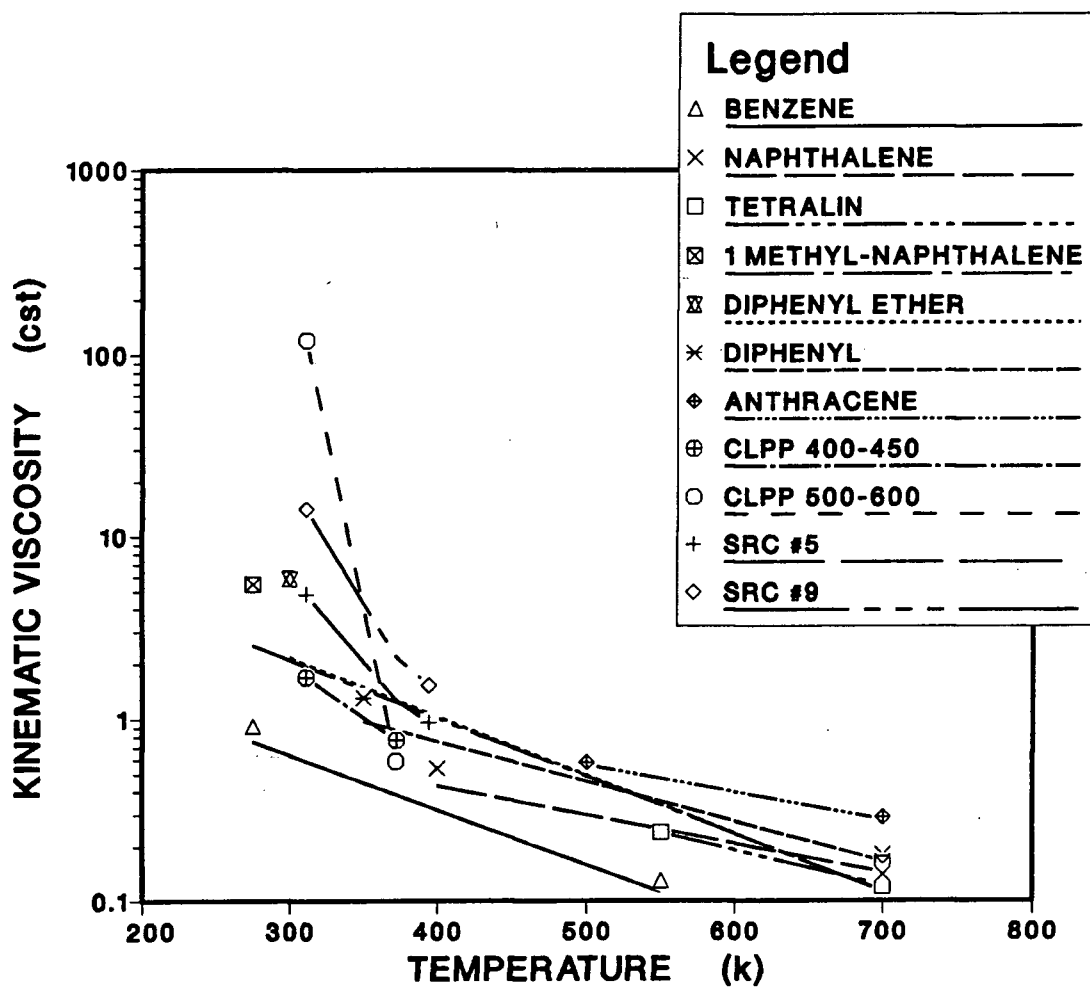


Figure 2.27: The Viscosities of Pure Organic Solvents

### 2.5.0 Introduction

Many kinetic models, with varying degrees of complexity and sophistication, have been proposed to describe coal liquefaction kinetics (Table 2.9). Some of the models simply endeavour to predict overall coal conversion to gases + liquids, while others endeavour to predict yields of individual liquid and gaseous fractions - fractions based on solubility: asphaltenes, pre-asphaltenes, oils; or chromatographic fractions: multi-functionals, hydroxyls, ethers, aromatics, nitrogens. The number of fitted parameters vary with the complexity of the predictions. Simple models comprise as few as 2 parameters; more complex models employ more than 30 parameters. All models have had some success in describing coal liquefaction behaviour, but restrictions must be imposed on:

- (1) reactor operating conditions (temperature, pressure)
- (2) coal or coal type
- (3) reactor design

A general model which can treat a variety of coals under a broad range of conditions, has not yet been devised. Despite these limitations such models have been incorporated into process models in order to evaluate process design alternatives and economics.

### 2.5.1 Kinetic Models

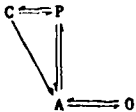

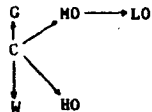
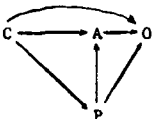
The kinetic models cited on Table 2.9 highlight the lack of consensus in the literature with respect to the specific mechanism(s) for coal liquefaction. The only common feature of all the models is that coal decomposes/reacts irreversibly. It has not been resolved whether or not coal behaves as a single monolythic species or if different coal components react according to different reaction networks. Neither is there a consensus on the products produced directly from coal, or the order of these initial reaction(s). Equally unresolved is the necessity or desirability of incorporating secondary reactions (i.e.) asphaltenes → oils etc.. Should such reactions be included in a model, are they reversible or irreversible, and what reaction order should be assigned to them? Yet, each of these models has been fitted to experimental data, successfully, and is therefore verified in a narrow sense.

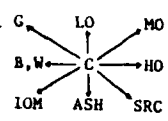
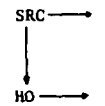
The extreme specificity of the models is best illustrated by a few examples:

- (1) Mohan and Silla<sup>[35]</sup> proposed two models to describe the liquefaction kinetics of Illinois #6 coal. One based on product separation by high pressure liquid chromatography; the other based on product separation by solubility. Both models have two complete sets of parameters. One to describe liquefaction behaviour at high temperatures, the other only valid at low temperatures. The

**TABLE 2.9**  
**Coal Liquefaction Reaction Models**

Models	Kinetic Scheme	Number of Parameters	Assumptions	Coal	Solvent	Comments
<u>Simple Models</u> <sup>[35]</sup>						
Hill et al	$C \rightarrow A + O$	2	- first order kinetics - a single thermal decomposition	"Utah"	tetralin	
Curran et al	$\begin{array}{c} C_1 \searrow \\ C_2 \nearrow \end{array} A + O$	4	- coal is best characterized as comprising two different reactive species	Pittsburg	tetralin	
Liebenberg et al	$\begin{array}{c} C \rightarrow A \\ \searrow \\ O \end{array}$	4	- coal produces A & O by separate reaction sequences	"bituminous"	tetralin	
Yoshida et al	$C \rightarrow A \rightarrow O$	6	- coal produces A & O by separate reaction sequences	Japanese	anthracene oil	red mud and sulphur added as catalysts
<u>Complex Models</u>						
Mohan et al <sup>[35]</sup>	$1) \begin{array}{c} H \\ \nearrow \\ C \rightarrow N \\ \searrow \\ AR \end{array} \begin{array}{c} N \\ \nearrow \\ E \end{array}$	18	- gas generation ignored - coal decomposes irreversibly into large fragments	Illinois #6	tetralin	- the authors propose two models (1) based on chromatographic separation of liquids (2) based on solubility separation.
	$2) C \rightarrow \begin{array}{c} A \\ \nearrow \\ P \\ \searrow \\ O \end{array}$	10	- large fragments react reversibly to form lighter components			- Model (2) fits the data better - a batch reactor was used for the experiments

Gertenbach et al <sup>[111]</sup>		14	<ul style="list-style-type: none"> <li>- reactions occurring in the pre-heater are not included</li> <li>- the reversible reaction C → P is not truly reversible. P can form coke which cannot be distinguished from coal</li> </ul>	Kentucky #9	250°C Vacuum cut of SRCII liquids	<ul style="list-style-type: none"> <li>- efforts were made to fit the model to the data of other researchers. The fit was poor even with their own data</li> <li>- the model predicts a significant increase in oil yield in plug flow reactors.</li> </ul>
Cronauer et al <sup>[34]</sup>		12	<ul style="list-style-type: none"> <li>- all reactions are first order and irreversible</li> <li>- no distinction made for reactions in the pre-heater</li> </ul>	Bell Ayre sub-bituminous	<ul style="list-style-type: none"> <li>- hydrogenated anthracene oil</li> <li>- hydrogenated phenanthrene oil</li> </ul>	<ul style="list-style-type: none"> <li>- completely different set of parameters fitted the results for the two solvents</li> <li>- a slug flow pre-heater followed by a CSTR were employed</li> </ul>
Shah et al <sup>[112]</sup>		10	<ul style="list-style-type: none"> <li>- all reactions involving coal are first order</li> <li>- hydrocracking reactions are 0th or 1st order</li> </ul>	Big Horn sub-bituminous	process derived liquid	<ul style="list-style-type: none"> <li>- a slug flow pre-heater followed by a CSTR were employed</li> <li>- a proprietary catalyst was used</li> <li>- Dispersion Number was a parameter and varied with slurry rtd and H<sub>2</sub> flux</li> </ul>
Shalabi et al <sup>[45]</sup>		12	<ul style="list-style-type: none"> <li>- irreversible first order reaction kinetics</li> </ul>	Kentucky	tetralin	<ul style="list-style-type: none"> <li>- short heat-up time batch experiments were performed.</li> </ul>

Singh et al <sup>[113]</sup>	<p>1</p>  <p>2</p> 	34	<p>- 2 stage kinetics:</p> <p>i: instantaneous break-up of coal to fixed fractions of various components</p> <p>ii: slow conversion of SRC and HO to lighter components</p> <p>- irreversible first order kinetics</p> <p>- pre-heater has no impact on kinetics</p>	Pohatan #5	Vacuum tower bottoms from SRCII plant	<p>- a slug flow pre-heater and a CSTR were employed</p> <p>- This model has been used to simulate the SRCII process.</p>
------------------------------	---	----	--	------------	---------------------------------------	---

**Legend for Kinetic Schemes on Table 2.9**

A      asphaltenes

AR     aromatics

B      by product gases

C      coal

E      ethers

G      gases

H      Hydroxyls

HO     heavy oil

IOM    inert organic matter

LO     light oil

M      multi-functionals

MO     middle oil

N      nitrogens

O      oil

P      pre-asphaltenes

SRC    solvent refined coal

W      water

solvent, the coal and all other process variables are unchanged.

- (2) The model proposed by Cronauer et al<sup>[34]</sup> requires two unrelated sets of parameters to describe the liquefaction behaviour of a single coal in two different solvents. All other process variables are held constant.
- (3) The model proposed by Gertenbach et al<sup>[111]</sup> correlates data obtained by other researchers poorly and has even greater difficulty correlating their own data under a variety of operating conditions.

Further examples of specificity can be cited but this approach does not resolve the main issue, which is, why are these models so specific?

The diversity of model functional forms and parameters can be attributed in part to data precision. Liquefaction result repeatability, a parameter frequently quoted in the literature, is often  $\pm 3$  wt% for any liquid or gaseous fraction produced, when normalized with respect to the initial coal mass. Thus a fraction comprising 20 wt% of the initial coal mass has a mean error of  $\pm 15\%$ . Data, this imprecise, may be fitted, empirically, by any curve which follows the general trend of the results. Differences in product analysis also contribute to the diversity of models and parameters. Refer to section 2.6 for details. Data processing introduces two additional contributing factors:



- (1) the existence of multiple regression minima may yield more than one set of equally good parameters from the same data base when models are fitted to experimental data. This problem becomes more severe as the number of fitting parameters increases.
- (2) differences in the fitting function can yield radically different "optimum" parameters (i.e.) minimizing the absolute value of the error instead of the absolute value of the % error produces a skewed parameter set which fits observed data with larger values much better than observed data with smaller values.

Differences in observed kinetics may also be attributed to incompatible differences in experimental conditions (i.e.) dominant reaction path(s) vary with experimental conditions (Section 2.2).

However, effects such as these cannot account wholly for the extreme specificity of the kinetic models. Unfortunately, none of the models satisfactorily accounts for the observed kinetic phenomena described in section 2.2. In particular, the role of primary and secondary coal dissolution and the influence of operating conditions on kinetics is ignored in all cases.

### 2.5.2 Process Models

Singh et al<sup>[113]</sup> employed their kinetic model as part of process models intended to simulate various aspects of the SRCII process. They simulated: the SRCII Recycle System<sup>[114]</sup>, the reactivity of liquefaction

products<sup>[115]</sup>, the steady state and dynamic thermal behaviour of the SRCII contactor<sup>[116,117]</sup>, and flows and compositions of process stream<sup>[118]</sup>. Their models ignore the changing influence of reactor hydrodynamics on liquefaction kinetics as the processing conditions are altered.

Lee et al<sup>[11]</sup> also modeled the SRC reactor but applied the dispersion model to the contactor to allow for variations in slurry residence time distribution with changing gas flow rates. Their model predicts a 3% reduction in total conversion, for the same mean residence time as  $N_D$  decreases from 0.97 to 0.1<sup>\*</sup>. Contactor simulations performed by Gertenbach et al<sup>[111]</sup>, based solely on kinetics, suggest only modest differences between total conversions for a CSTR and a PFR at high temperatures (450°C) but a much larger difference at 400°C - approximately 1% and 10% respectively. The results of these latter two studies are distorted because the kinetic models were fitted to data obtained from reactors which included plug flow pre-heaters. Generalization of their data, in this way, may not be valid.

## 2.6 Coal Liquefaction Product Analysis

Apart from SNG yields which are invariably analyzed by gas-solid chromatography, comparison of experimental liquefaction results is often complicated by incompatible differences in product analysis. Liquid/solid products are categorized, variously, on the basis of functionality<sup>[35]</sup> or

---

\* $N_D \equiv 0.1$  implies the reactor is equivalent to a CSTR

$N_D \equiv 0.97$  implies the reactor is almost equivalent to a CSTR

solubility. When categorized by functionality, 6 compound groups are normally identified by high pressure liquid chromatography (HPLC): saturates, aromatics, ethers, nitrogens, hydroxyls, multifunctionals. Solubilities subdivide liquid/solid products into the classic fractions: oils, asphaltenes pre-asphaltenes - see Table 2.10. These two classification techniques are not readily inter-related. In addition, non-standard total liquid yield definitions are frequently encountered in the literature. These definitions are based on quinoline solubility<sup>[61]</sup>, cresol solubility<sup>[66]</sup>, tetralin solubility<sup>[83]</sup>, etc..

Table 2.10Product Analysis by Solubility

Product Category	Definitions
Oils	n-pentane soluble liquids <sup>[34,45,47]</sup> <sup>1</sup> n-hexane soluble liquids <sup>[35,69]</sup>
Asphaltenes	benzene soluble liquids <sup>[34,35,45,67,69]</sup> toluene soluble liquids <sup>[47]</sup> <sup>1</sup>
Pre-asphaltenes <sup>2</sup>	tetrahydrofuran (THF) soluble liquids <sup>[35,45]</sup> <sup>1</sup> pyridine soluble liquids <sup>[34,67-69]</sup>

## Notes to Table 2.10:

<sup>1</sup> Less Hazardous alternative according to NIOSH/OSHA Standards [84]. These materials all attack the eyes, skin respiratory system, and the central nervous system:  
pentane < toluene < THF.

<sup>2</sup> THF soluble material ≠ Pyridine soluble material. Raw coal is soluble in Pyridine but not in THF [45,69].

## 2.7 Summary

Even a cursory review of the literature related to Direct Coal Liquefaction reactor design leaves one in a mild state of confusion. Industrial liquefaction reactor designs comprise a very narrow range of alternatives. Such designs, employing back-mixed reactors with large gas recycle ratios, are normally associated with gas-liquid mass-transfer limited reaction-kinetics. Mathematical models, for DCL kinetics, suggest that the same designs are optimal or near optimal but base this conclusion on simplistic approximations of coal liquefaction kinetics. The role of catalysis, gas-liquid mass transfer and other physical phenomena is all but ignored in these models. Since data for these models was generally obtained from reactors which are hydrodynamically similar to industrial designs, these effects, though implicitly included in the models, can be treated as constants if only a limited range of reactor designs is considered. However, these models also fail to include the pre-heater as an integral component of the overall reactor design, and do not predict liquefaction results except under very narrowly defined reaction conditions. The models also fail to account for the apparent necessity to recycle large quantities of hydrogen in industrial reactors.

Observed kinetic phenomena tend to conflict, in whole or in part, with both the kinetic models and the choice of industrial liquefaction reactor designs. These observations highlight the importance of physical phenomena such as:

(1) the intensity of turbulence

- relative flow rates of gas and slurry, in pre-heaters, influences liquefaction reaction kinetics

(2) the extent of axial mixing

- the kinetics of hetero-atom removal reactions are slow. The presence of hetero-atoms reduces the saleability of liquid products. Consequently, these reactions limit the productivity of DCL reactors.

(3) coal liquid - solvent interactions

- poor physical solvents tend to yield lower rates and extents of conversion.

on coal liquefaction kinetics. These observations also suggest that pre-heaters are important components of DCL reaction networks.

Such a level of conflict, between observed kinetic phenomena, kinetic models, and industrial liquefaction reactor designs, provides a poor basis for reactor design and scale-up of DCL processes. Until the role of physical phenomena is resolved, little progress can be made towards quantifying coal liquefaction kinetics or designing efficient DCL reactors. It may happen that the current designs are near optimal or that even radical changes in reactor design have little effect on the final distribution or yield of liquefaction products. In this event, a clear understanding of the physical phenomena, related to direct coal liquefaction will provide a coherent framework for optimizing current

liquefaction reactor designs. Conversely, a detailed analysis of physical phenomena may lead to significantly improved design principles for direct coal liquefaction reactors.

## Chapter 3

### 3. Objectives

Coal liquefaction reaction kinetics and the relationship between reaction kinetics and process variables are so poorly understood that research in a number of diverse areas is warranted. This thesis, comprising a theoretical and experimental study is limited to the following objectives:

(1) Identification of Consequential Process Variables.

The impact of gas-phase moisture content and synergistic effects associated with the extent of axial mixing, the intensity of turbulence, catalysis, solvent composition and coal particle size distribution are investigated. A semi-batch, backmixed autoclave and auxillary equipment are employed for this component of the study.

(2) Development of a Quantitative Kinetic Model for Coal Liquefaction.

A quantitative kinetic model, based on likely reaction paths and observed dependencies on process variables, is used to correlate coal liquefaction results obtained from this work and from the literature. The role of chemical reactions and physical phenomena occurring in pre-heaters is emphasized. A variety of coal-solvent systems are considered.



(3) Development of Improved Design Criteria for Direct Coal Liquefaction Reactors.

Liquefaction results, obtained from simulated, axially-mixed pre-heaters and reactors are combined with the kinetic model in order to characterize rate controlling phenomena in existing DCL processes and predict optimal reactor designs for bituminous and sub-bituminous coal and lignite liquefaction.

## Chapter 4

### 4. Experimental

#### 4.0 Introduction

The motivation and intent of this study are discussed in the previous chapters. In order to achieve the stated objectives, accurate comparative data for the liquefaction behaviour of bituminous and sub-bituminous coals and lignite are required, for a variety of reactor configurations and sets of values for process variables. The principal independent variables include: the amount of catalyst, the reaction temperature, slurry phase residence time and residence time distribution, the intensity of turbulence (stirring rate), solvent composition and gas phase composition. A single reactor network was designed to accommodate an investigation of these variables. The objective variables, employed throughout the reactor and pre-heater simulations, to determine the importance of process variables, were the liquid and gas yields from the test coals.

A multivariable study of this type, can lead rapidly to an unwieldy number of experiments, if one were to complete the matrix of experiments suggested on Table 4.1. However, this study comprises a series of discrete enquiries, aimed at elucidating effects caused by individual process variables in conjunction with a sparse matrix of experiments for each coal.

**TABLE 4.1****Variables Investigated**

Variable	Values Tested
Gas Phase Composition	5 MPa H <sub>2</sub> (cold) 5 MPa H <sub>2</sub> + varying amounts of H <sub>2</sub> O
Gas Phase Pressure	Let reactor Pressure Vary Maintain Initial Pressure by Adding H <sub>2</sub>
Axial Mixing	Plug Flow Simulation (mrt ± 2 min) Axially mixed Simulation (mrt ± mrt) Axially mixed Pre-heater + Plug Flow Reactor
Reaction Time	2.5 min 5.0 min 15.0 min 30.0 min
Catalyst Particle Size	cylinders 3 mm dia. x 3 cm long ground to 4 µm
Temperature	425°C 400°C 375°C
Solvent	SRC oil + 30 wt% tetralin SRC oil
Amount of Catalyst	20 grams 40 grams 80 grams 0 grams 5 grams 10 grams
Stirring Rate	8.33 Hz 16.67 Hz 25.00 Hz
Coal	Forestburg Sub-bituminous Byron Creek Bituminous Saskatchewan Lignite

In addition, anticipated similarities in the dependence of lignite, sub-bituminous and bituminous coals, on process variables, further reduces the total number of experiments. Most of the exploratory experiments are performed with a single coal. Consequently, as few as 80 experiments are required to complete the experimental program.

The remainder of this chapter is devoted to a detailed description of the apparatus and experimental techniques.

## 4.1 Coal Liquefaction Experiments

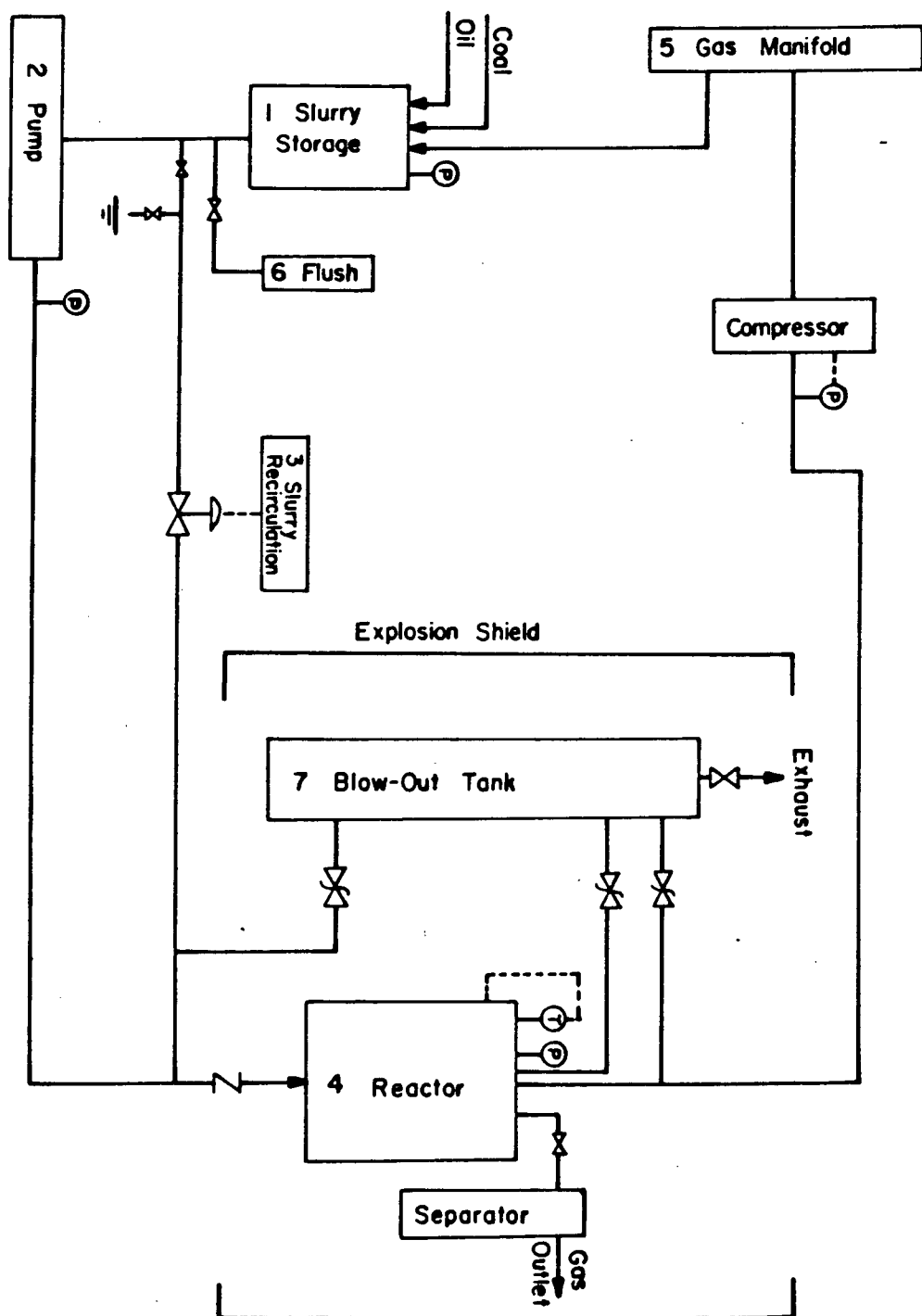
### 4.1.1 Apparatus Design and Description

Direct Coal Liquefaction experiments were conducted in a versatile semi-batch reactor. The apparatus possesses a number of desirable features. However, the extreme operating conditions of DCL processes (450°C, 20 MPa) and the need to transport dense coal slurries constrained the selection and configuration of equipment components. Commercial components were chosen and assembled to minimize potential mechanical problems, and mass balance distortions, and to facilitate cleaning. The major design features of the apparatus are outlined on Figure 4.1. A detailed description of the apparatus, keyed to Figure 4.1, follows.

#### 1. Slurry Storage

A 2ℓ, mechanically-stirred, Parr autoclave (#488) is used for coal slurry storage. The autoclave can be pressurized to 7 MPa in order to control the feed pressure to the slurry pump.

Figure 4.1: Experimental Apparatus Schematic



## 2. Slurry Pump

The slurry pump, a variable-stroke, reciprocating, Milroyal pump (Model A ), pressurizes the slurry and meters slurry flow at an average rate between  $1.75\text{--}3.5\text{ cm}^3\text{ s}^{-1}$  by pulsing a variable fluid volume 44 times per minute. The pump, the smallest available pump with a sufficiently high exit pressure, cannot operate at lower flow rates or with coal particles greater than  $90\text{ }\mu\text{m}$  in diameter because the particles tend to clog a series of ball valves inside the pump.

## 3. Slurry Recirculation Loop

In order to simulate axially mixed reactors and pre-heaters, slurry flow rates as low as  $0.30\text{ cm}^3\text{ s}^{-1}$  are required. Since the minimum pumping rate is  $1.75\text{ cm}^3\text{ s}^{-1}$ , a slurry recirculation loop was installed. A cascaded-relay controlled solenoid valve (Skinner V5 Series) was used, at first, to recirculate a portion of the slurry to the pump. This valve was subject to plugging and did not shut or open readily. Efforts were made to improve the reliability of this device, by modifying the seat and plunger, but it was finally replaced with a manually operated valve.

## 4. The Reactor

Slurry is fed from the recirculation loop in through the base of a modified, 2l PPI reactor (AOH 34220). Design features include a variable speed, magnetically driven stirrer, internal cooling coils and a temperature controlled external heating mantle. These

features permit rapid and controlled manipulation of reactor temperature. Steady state temperatures can be controlled to within  $\pm 1^\circ\text{K}$ . The reactor is depressurized through a gas-liquid separator. The design of the separator was later refined so that entrained slurry could be collected and incorporated into the mass balance.

## 5. Gases

Gases are fed from cylinders and pressurized, if necessary, with a PPI compressor (model #1038) to the desired operating pressure. Gas flow to the reactor can be controlled in two ways:

- i. the reactor can be pressurized cold and sealed.
- ii. the feed back pressure controller, on the compressor, can be used to maintain a fixed gas pressure under conditions of net gas consumption.

Gases can be sampled at the reactor sample port, or at the cylinders.

## 6. Slurry Line Flush

Once the slurry is injected, the slurry lines are flushed with oil under nitrogen pressure to recover unused slurry and clean the slurry lines.

## 7. Safety

- i. the reactor and all transfer lines are connected via 30 MPa rupture discs to a 27ℓ blow-out tank.
- ii. the reactor and blow-out tank are encased in an exhausted explosion shield fabricated from 1.07 m gas pipeline stock.

#### 4.1.2 Operating Procedure

The operating procedure followed for all slurry injection experiments, is summarized below:

1. The strip chart recorders, the gas chromatograph, the pressure transducer are all switched on and the cold junction for the reactor temperature controller is filled with ice water. Ambient pressure is recorded.
2. The reactor is charged with 150 g of solvent and catalyst (if desired). The mass of solvent and catalyst is recorded.
3. The reactor is placed under vacuum (using an aspirator) and flushed twice with hydrogen to remove air. The reactor is then sealed and pressurized to 5.0 MPa. A gas sample is extracted and analysed; the initial pressure, and the reactor temperature are recorded.
4. The stirrer is set at 1000 rpm and the heater is turned on. The temperature control point is set 25°K above the desired operating temperature.
5. While the reactor is heating
  - i. a coffee break is taken (20 minutes)
  - ii. dried coal (~ 230 g) is combined with solvent (575 g SRC oil, or 403 g SRC oil + 172.5 g THN) in a 2 l beaker. The precise



solvent to coal ratio is 2.5:1. The slurry is then agitated with a hand mixer to remove lumps. A 10 g coal sample is retained for analysis. The coal and solvent masses are recorded.

- iii. The pre-mixed slurry is poured into the slurry storage tank, which is then sealed. The stirrer is turned on to prevent settling. The mass of slurry charged is recorded.
- iv. The flush tank is filled with solvent using a squeeze bottle. The gas/liquid separator is weighed and replaced. A catchall bottle is weighed and placed under the slurry line drain. All masses are recorded.

6. Once the reactor has reached the temperature set point:

- i. The slurry storage tank is flushed and pressurized with nitrogen (3 MPa).
- ii. The pump is primed by flowing slurry through the recycle loop and collecting a small quantity of slurry at the drain (catchall).
- iii. The temperature set point is reset to the operating temperature and the stirring rate is changed if desired.
- iv. The reactor is sub-cooled to the operating temperature by flowing cold water through the internal cooling coils.

7. Slurry flow rate is selected, and slurry injection is commenced.

Cooling water is applied, as necessary, during slurry injection, to maintain the operating temperature. In order to assure reliable valve operation, during axially mixed reactor trials, slurry should be injected into the reactor in at least 10 stroke bursts .

8. The slurry inlet line to the reactor is sealed once slurry injection is completed. While the liquefaction reactions progress
  - i. unused slurry is collected by forcing it from the storage tank through the recycle loop to the drain.
  - ii. the slurry lines are flushed with solvent.
  - iii. the slurry storage tank is depressurized and cleaned.
  - iv. the total mass of slurry + flush solvent collected at the drain, and the mass of slurry retrieved from the slurry storage tank is recorded.
9. Once the trial is completed, the reactor is cooled to 600 K, within 200s, using the internal cooling coils, and is at room temperature, in about one hour. Lunch is eaten while the reactor cools.
10. The stirrer is turned off and a gas sample is extracted from the reactor. The reactor is then depressurized, rapidly, through the separator. The stirrer is switched on again for 10 seconds and a second gas sample is extracted. These samples are analysed on the gas chromatograph.
11. The lid is removed from the reactor, a small stirrer is placed inside and two slurry samples (~ 30 g each) are extracted while the reactor contents are being agitated. The remaining slurry is collected and filtered, and a small liquid sample is retained for analysis. The mass of the slurry samples is recorded.

12. The slurry samples are dissolved in 200 g of THF for 1 hour, at room temperature in a beaker equipped with a magnetically driven stirrer. The resultant slurry is filtered through Gooch crucibles. The solid residua is dried overnight in a vacuum oven and retained for analysis.
13. The apparatus is cleaned with varsol and paper towels. Particular attention is paid to the slurry transfer line and valve at the base of the reactor.
14. The mass of the slurry in the separator is recorded, and mass balance calculations are completed.
15. Coal, residua, and product liquids are submitted for external analysis as necessary. Appropriate ASTM standards are employed.

#### **4.1.3 Materials**

##### **4.1.3.1 Catalysts**

A cobalt-molybdenum catalyst, supported on alumina, was the principal catalyst employed in coal liquefaction experiments. The catalyst comprised 12 wt%  $\text{MoO}_3$  and 3 wt%  $\text{CoO}$  in an  $\alpha$ -alumina matrix. This catalyst, supplied by Alpha Products in the form of 3 mm diameter x 3 mm long pellets, was typically ground prior to use. The volume mean particle

diameter of the ground catalyst is approximately  $1.41\text{ }\mu\text{m}$  (see Table 4.2). Whole catalyst pellets and an unsupported  $\text{MoO}_3 \cdot 1/2\text{ H}_2\text{O}$  catalyst were also employed in selected experiments. All catalysts were sulphidized in situ.

#### 4.1.3.2 Coals/Lignites

The liquefaction characteristics of Forestburg sub-bituminous coal, Byron Creek bituminous coal and Saskatchewan lignite were investigated. Slurry handling difficulties limited the maximum coal particle size to  $90\text{ }\mu\text{m}$ . Pulverized samples of Forestburg and Byron Creek coal were obtained. A significant fraction of the Forestburg coal was greater than  $90\text{ }\mu\text{m}$  in diameter. This coal was wet screened through a  $90\text{ }\mu\text{m}$  screen using a custom designed semi-automatic screening/settling device. Only the  $-90\text{ }\mu\text{m}$  fraction was retained. Virtually all of the Byron Creek coal was less than  $90\text{ }\mu\text{m}$  in diameter; it was simply dry screened using a Tyler Ro-Tap Sieve Shaker. Since pulverized Saskatchewan lignite could not be obtained, it was ground in a Fritsch automatic mortar. Only a small quantity of lignite could be prepared in this way. Clearly, the test "coals" resemble but are not identical to the parent "coals". Proximate and ultimate analyses of the test coals are listed on Table 4.3. Particle size distributions for the coal and lignite samples are shown on Figure 4.2.

**TABLE 4.2****Catalyst Particle Size Distribution**

Mean Diameter ( $\mu\text{m}$ )	Number of Particles	Volume Fraction (%)
0.29	214	2.10
0.88	138	37.94
1.46	28	35.16
2.05	5	17.38
2.64	1	7.42
3.22	0	0.

**TABLE 4.3****Proximate and Ultimate Analyses of the Test Coals**

	Forestburg Coal	Bryon Creek Coal	Saskatchewan Lignite
Proximate Analysis (dry basis)			
Ash	16.19	16.26	19.91
Fixed Carbon	46.52	62.25	43.27
Volatile Matter	37.29	21.49	36.82
Ultimate Analysis			
C	66.63	83.84	69.21
H	4.87	4.63	4.91
N	1.46	1.23	1.24
O	26.38	9.97	23.97
S	0.66	0.32	0.68

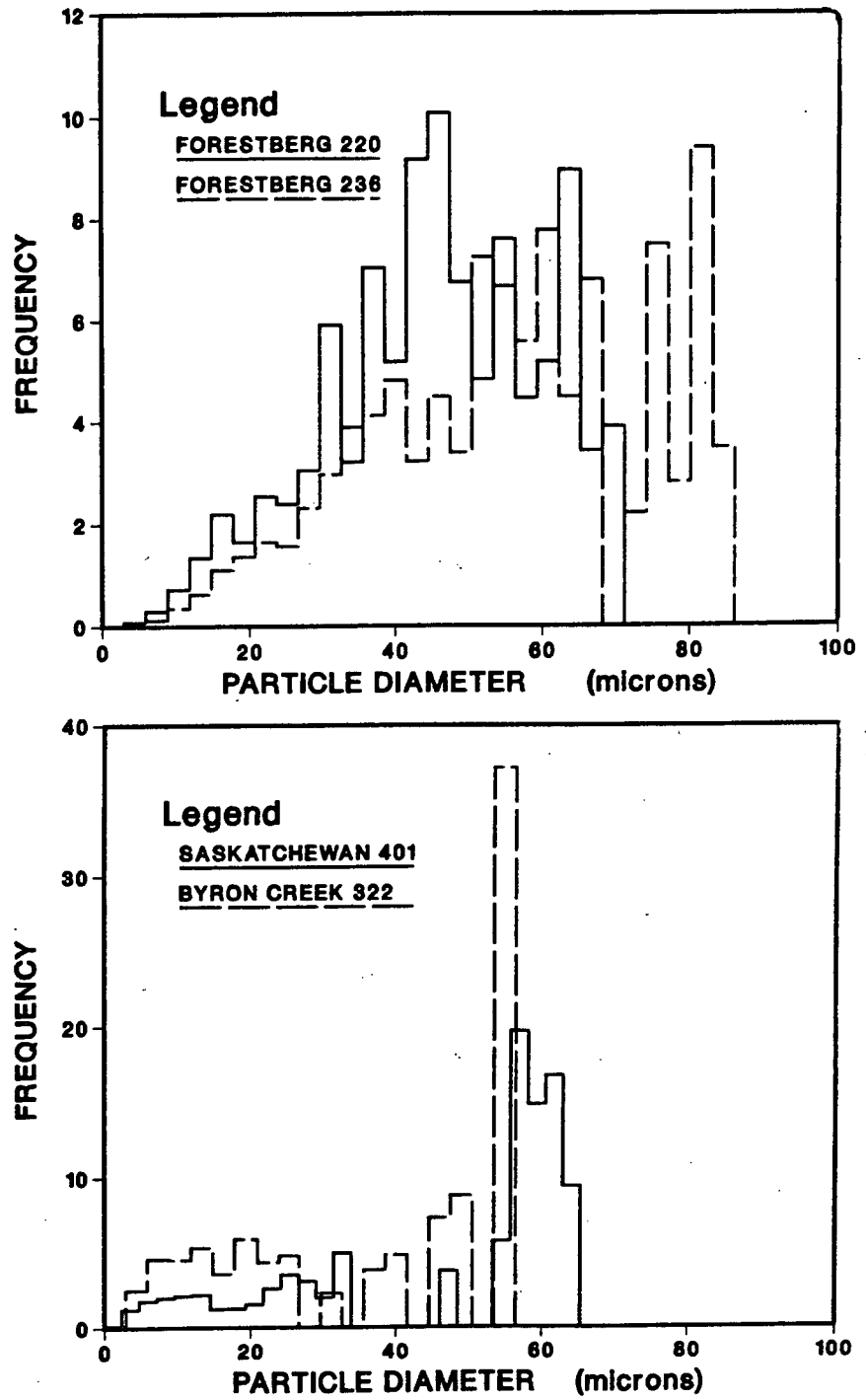


Figure 4.2: Particle Size Distributions for the Test Coals

#### 4.1.3.3 Liquefaction Solvents

One of the objectives of this study is the simulation of industrial liquefaction environments. Industrial processes employ heavy oils or hydrogenated heavy oils as the recycle solvent. Such solvents have been shown to be suitable vehicles for DCL reactions, and recycling heavy oils yields a greater fraction of more valuable light oils. Consequently, two solvents were selected for this study. Solvent 1, comprising SRC oil obtained from the Wilsonville pilot plant combined with 30 wt% tetrahydronaphthalene tetralin, is used to simulate a hydrogenated process solvent. Solvent 2, comprising 100 wt% SRC oil, simulates an untreated recycle solvent. The SRC oil was distilled prior to use in order to remove water. Technical grade tetralin was added to the SRC oil to form Solvent 1.

#### 4.1.3.4 Analysis Solvent

Tetrahydrofuran solubility was used to define the base line for coal conversion. Pre-asphaltenes, asphaltenes, oils etc. are all soluble in THF; raw coal is not. Raw coal is soluble in pyridine, the other solvent frequently employed for this purpose.

#### 4.1.3.5 Gases

Dry hydrogen comprises 90<sup>+</sup>% of the initial gas phase for the majority of experiments. Nitrogen, used to pre-pressurize the coal slurry,



enters the reactor with the slurry and comprises approximately 5%. Argon, added to the hydrogen cylinder, acts as a tie substance and comprises about 2%. The remaining fraction is vapourized solvent. Nitrogen, argon, and hydrogen are supplied by Linde and are at least 99.9% pure. A standard gas, containing fixed percentages of methane (5.08%), carbon dioxide (5.01%), ethane (1.00%), carbon monoxide (2.00%), argon (2.01%), nitrogen (0.97%) and hydrogen (balance), was used for solubility tests, and to calibrate a Beckman GC1 Gas Chromatograph. This gas was supplied by Matheson.

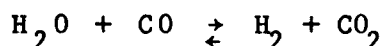
#### 4.1.4 Experiment Design

The experimental program was subdivided into three phases:

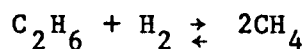
1. preliminary experiments,
2. investigations of gas phase phenomena,
3. investigations of slurry phase phenomena.

Preliminary experiments established operating limits for the liquefaction reactor network, resolved problems related to result analysis and mass balances, and suggested apparatus modifications and procedural changes. Results from these preliminary experiments have little meaning in themselves and are not reported. However, modifications and adjustments suggested by these experiments are responsible for the accuracy and repeatability of experiments reported in the following chapters.

Investigations of gas phase phenomena consider the potential role of the water gas shift reaction



and hydrocracking reactions (e.g.)



as representative sources and sinks for hydrogen. These reactions influence hydrogen consumption patterns if long gas phase residence times are employed in DCL reactors. Currently, the gas phase passes through industrial reactors very quickly - relative to the slurry mean residence time.

Investigations of various slurry phase phenomena comprise the remainder of this thesis. Four issues, which are not resolved by the literature, are addressed:

1. The number of active phases in DCL reactors is unknown. Variation of stirring rate and solvent composition is used to investigate the effect of the intensity of turbulence and solvent composition on gas-liquid and liquid-liquid or liquid-solid mass transfer, and the distribution of coal derived products between the phases present.

2. Possible synergistic alterations of coal liquefaction kinetics, caused by slurry phase axial mixing, are investigated. Axially mixed and plug flow reactors and pre-heaters are simulated by varying the mean residence time of the slurry and the rate of slurry injection into the reactor. A computer model has been developed to relate pumping rate to an approximate number of tanks in series, for a normalized mean residence time. The model, shown on Figure 4.3, indicates the time of initial slurry injection and the duration of injection. Slurry flow rate is simply adjusted to fit these bounds.
3. The role of catalysts in DCL reactors is investigated by varying the amount and type of catalyst in conjunction with coal and solvent composition.
4. Reaction temperature is varied in order to observe possible transitions in DCL kinetics. 425°C is the maximum safe operating temperature for this apparatus because the reactor must be superheated prior to slurry injection.

These investigations are by their very nature discrete, and aimed at providing bases for modelling the DCL reaction environment.

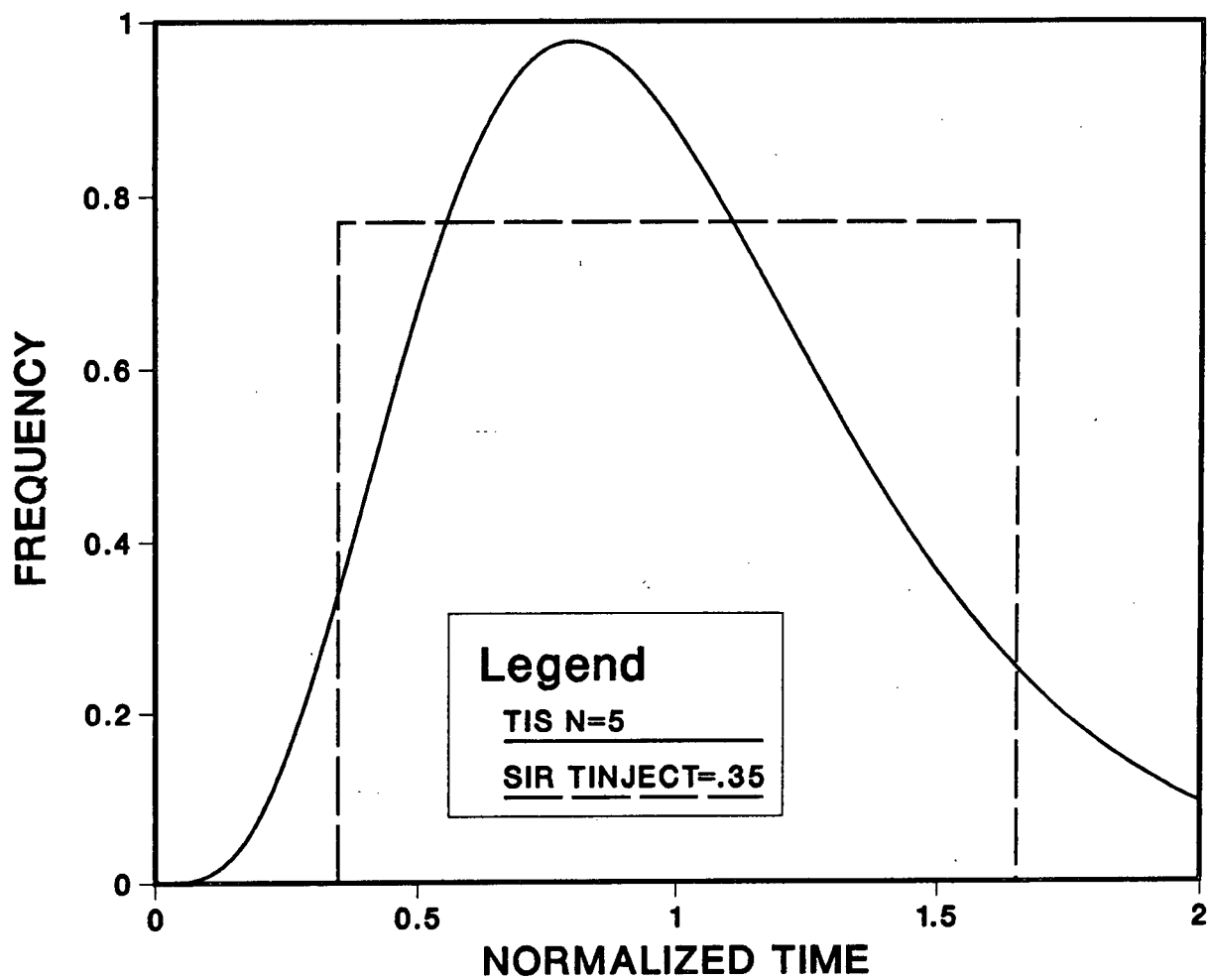


Figure 4.3: Continuous Flow Reactor Simulation Model

#### 4.1.5 Result Analysis

##### 4.1.5.0 Introduction

Coal liquefaction experiments present a number of analytical problems which account, in part, for the poor result repeatability frequently quoted in the literature. The source of these problems is the sensitivity of various parameters to the overall mass balance. However, these problems can be circumvented once they are recognized. Two recurrent problems are:

- (1) Evaluation of the amount of hydrogen consumed and gases produced during liquefaction experiments.
- (2) Evaluation of total coal conversion.

Gas analysis is invariably performed once the reactor is cooled (after batch laboratory experiments). Some researchers simply extract a gas sample from the reactor while it is still pressurized. This procedure ignores gas solubility in the product liquids, causing hydrogen consumption to be overestimated and gas production to be underestimated. The magnitude of the systematic errors varies with the solubility of the gas components and reactor geometry. As much as 50% of ethane and carbon dioxide may be dissolved in the product oil. Other researchers, recognizing this problem, depressurize the reactor into a large balloon. Though this improves the accuracy of gas phase measurements, the improvement is less than one expects because the gas remaining in the autoclave has much higher concentrations of the more soluble gases than the

gases collected in the balloon. This fact is often overlooked. Furthermore, a fraction of the slurry is entrained with the gas as it exits the reactor which can cause concurrent problems with slurry phase analysis. Gas analysis problems appear to be much less severe in a continuous flow apparatus.

Analytical problems related to the evaluation of total coal conversion also vary with the reactor type and the analytical method employed. In flow apparatus, for example, one must assume that representative samples of the ingoing and outgoing slurry streams can be obtained, and that flow surges do not occur, or have a very high frequency with respect to the sample time. Inevitably, flows and compositions vary. Since conversion is sensitive to these fluctuations, large errors can result. In batch reactors, the amount of coal in the reactor is known by direct measurement. Following an experiment, some researchers extract the "entire" slurry phase from the reactor and base conversion on the total amount of organic residua retrieved. However, some slurry remains in the reactor or transfer apparatus, and some is entrained with the gas. Conversion is overestimated and errors vary widely from experiment to experiment. Other researchers extract slurry samples from the reactor and base conversion on the composition of the solid residua. This approach is more precise. An additional problem with slurry phase analysis is that few researchers sample the ingoing coal with sufficient frequency. Small variations in ash or moisture content from run to run also contribute to the uncertainty of liquefaction results.

The semi-batch apparatus, described previously, and the analysis techniques adopted for this study endeavour to combine the potential accuracy of batch apparatus with the experimental versatility of flow apparatus. A description of analytical techniques follows.

#### **4.1.5.1 Gas Analysis**

##### **4.1.5.1.0 Introduction**

Accurate estimates of the amount of gases produced and hydrogen consumed can only be obtained if the composition and volume of the gas phase are known, and the composition and apparent volume of gas dissolved in the product slurry are known. The gas phase volume and composition are readily obtained in a semi-batch reactor network by

- 1) extracting a gas sample at pressure
- 2) subjecting it to chromatographic analysis
- 3) determining the density and mass of the slurry phase

Estimation of the dissolved gas composition and volume is more difficult, as it involves a determination of gas solubility or apparent solubility in the product slurry.

##### **4.1.5.1.1 Solubility Estimation**

Gas solubility estimates are obtained indirectly. The estimation technique relies on the accuracy of mass balances and assumes that gas

samples extracted from the reactor, once it is depressurized, are representative of the dissolved gas composition. The overall mole fraction of a gas component,  $\bar{C}_1$ , is defined as

$$\bar{C}_1 = \frac{C_{11} + C_{12} (V_2/V_1)}{(1 + V_2/V_1)} \quad (4.1)$$

where  $V_1$  is the gas phase volume .

$V_2$  is the apparent gas volume of the liquid phase

$C_{11}$  and  $C_{12}$  are the mole fractions of component 1 in the two phases respectively.

Equation 4.1 can be incorporated into the hydrogen and argon molar balances to obtain two equations for the fraction of hydrogen consumed during reaction, HC.

$$HC = 1 - \frac{Ar_o}{H_o} \left( \frac{H_1 + H_2 (V_2/V_1)}{Ar_1 + Ar_2 (V_2/V_1)} \right) \quad (4.2)$$

$$HC = 1 - \frac{H_1 V_1 P_1 T_o}{T_1 H_o V_o P_o} \left( 1 + \frac{H_2 V_2}{H_1 V_1} \right) \quad (4.3)$$

Combining equations 4.2 and 4.3 yields equation 4.4

$$\frac{T_1 V_o P_o Ar_o}{T_o V_1 P_1 H_2} \left( \frac{H_1 + H_2 (V_2/V_1)}{Ar_1 + Ar_2 (V_2/V_1)} \right) - \frac{H_1}{H_2} - \frac{V_2}{V_1} = 0 \quad (4.4)$$



which must be solved iteratively for  $V_2$ . If a gas of known composition is used for solubility testing,  $V_2$  can be obtained from equation 4.1 directly. Once  $V_2$  is obtained the fraction of component 1 dissolved in the liquid phase,  $F_1$ , is

$$F_1 = \frac{C_{12} V_2}{C_{11} V_1 + C_{12} V_2} \quad (4.5)$$

and the solubility,  $S_1$ , becomes

$$S_1 = \frac{V_R}{M_s} - \frac{1}{\rho_s} \frac{1}{1/F_1 - 1} \frac{1}{ZRT_1} \quad (4.6)$$

where  $V_R$  = reactor volume  $\ell$

$M_s$  = slurry or oil mass Kg

$\rho_s$  = slurry or oil density Kg/ $\ell$  or g cm<sup>-3</sup>

$Z$  = gas compressibility factor (1-1.03)

$R$  = the universal gas constant (.08206  $\ell \cdot \text{Atm} \cdot \text{mol}^{-1} \text{K}^{-1}$ )

$S_1$  = solubility of component 1 moles Kg<sup>-1</sup>  $\cdot \text{Atm}^{-1}$

Apart from uncertainties associated with mass balances, the solubilities estimated by equation 4.6 are predicated on the assumption that representative "dissolved gas" samples can be extracted from the depressurized reactor. This may or may not be feasible. A mathematical model, which considers two extreme depressurization cases:

1) plug-flow depressurization

gases evolving from the slurry phase force gas in the gas phase out of the reactor. The two gases do not mix.

2) completely backmixed depressurization

gas evolving from the slurry phase mixes intimately and completely with the gas already present in the gas phase and exits the reactor in proportion to its content in the gas phase.

was formulated to address this issue. The results obtained from this mathematical treatment are summarized on Table 4.4. The possible bounds, on depressurization behaviour are too broad to provide a definitive answer to this question except in the event of very high or very low gas solubilities. However, the results do not preclude the possibility of obtaining representative dissolved gas samples over a broad range of solubilities. If one were to consider the plug-flow extreme, for example, as little as 2% of the gas need be dissolved in order to obtain a representative sample\*.

A number of experimental observations suggested that reactor depressurization approximates the plug-flow extreme, and the method was verified by determining the solubility of a calibrant gas in benzene - Table 4.4. Solubilities calculated as outlined above are compared with results obtained using two other experimental methods, and results selected

---

\*The final, cold reactor pressure is typically 25 to 50 times atmospheric pressure.

**TABLE 4.4****Apparent Gas Solubilities in Benzene**

Compound	Solubility (moles Kg <sup>-1</sup> · Atm <sup>-1</sup> ) x 10 <sup>3</sup>									
	Literature Values	Method I			Method II			Method III		
		1	2	3	1	2	3	1	2	3
Ar	10.5 <sup>[100]</sup>	9.71	8.97	8.63	9.74	8.74	9.75			
N <sub>2</sub>	5.0 <sup>[102]</sup>	5.27	8.08	4.47	2.21	4.48	8.13			
CH <sub>4</sub>	-	18.7	15.3	17.3	23.0	21.5	22.0			
CO	-	4.77	4.28	4.65	7.51	10.5	4.14			
C <sub>2</sub> H <sub>6</sub>	193 <sup>[101]</sup>	54.7	48.0	55.4	140.	147.	129.			
CO <sub>2</sub>	-	47.2	37.3	43.9	98.4	87.6	87.6			
H <sub>2</sub>	3.2 <sup>[99]</sup>	2.8	2.1	2.4	0.91	1.48	3.63			
S̄		5.01	4.06	4.58	5.24	5.63	7.26	5.87	5.89	5.92

from the literature. Data for these comparisons were collected by injecting calibrant gas, comprising argon, nitrogen, carbon monoxide, methane, ethane, carbon dioxide and hydrogen, into the reactor over a known mass of benzene. This gas was sampled and the pressure recorded. The reactor was then stirred at 1000 rpm for approximately 15 minutes. The stirrer was stopped, a second gas sample extracted, and the pressure recorded. Finally, the reactor was depressurized rapidly to room temperature and a low pressure gas sample was extracted. Three trials were performed.

Calculation Method I is the method described above. Method II only employs high pressure gas compositions and solubilities are defined by equation 4.7

$$S_1 = \frac{V_1}{ZRT K_{g_{BZ}}} \left( \frac{\bar{C}_1 P_o}{C_{1l} P_1} - 1 \right) \quad (4.7)$$

Calculation Method III, based on differential pressure measurements, only predicts a mean solubility for all of the gases combined - equation 4.8.

$$\bar{S} = \frac{V_1}{ZRT K_{g_{BZ}}} \left( \frac{P_o}{P_1} - 1 \right) \quad (4.8)$$

Calculation Methods I and II are sensitive to air leaks into the gas samples and this accounts for the scatter of the results. Method I, selected for use in this thesis, provides the greatest accuracy and

consistency for gases with low and moderate solubility (i.e.) argon, hydrogen, carbon monoxide, nitrogen and methane. The solubilities of very soluble gases i.e. ethane, carbon dioxide are badly underestimated. Solubilities of all gases are systematically underestimated:

- argon, methane, carbon dioxide, hydrogen and nitrogen solubilities are underestimated by approximately 20% on an absolute scale with a relative random error of 15%.
- carbon dioxide and ethane solubilities are underestimated by ~ 50% and 60% respectively on an absolute scale with a relative random error of 15%.

Gas production and consumption results are not corrected for these systematic errors as they have a minimal effect on the overall mass balance. Without this correction, overall gas production is underestimated by less than 10% with a random error of approximately 3%. The precise values vary with the composition of the gas phase.

#### 4.1.5.2 Slurry Analysis

The apparatus is a flow device with respect to the slurry phase. Consequently, the precise quantity of slurry entering the reactor can only be estimated. However, the bounds on this estimate are very narrow. The amount of slurry placed in the storage tank, that does not report to the slurry drain, overestimates the amount of slurry entering the reactor: a residual amount of slurry remains in the storage tank (~ 15 g), about 5 g remain in the flushed recycle loop, and 8 to 10 g lodge in connecting

tubing. The amount of slurry retrieved from the reactor, at the end of an experiment, underestimates the amount of slurry entering the reactor. Material clings to the cooling coils, the reactor wall, and passes through the gas/liquid separator on depressurization. This material cannot all be retrieved and the amount varies from experiment to experiment. After performing a number of pumping tests, the minus 30 gram mass balance was adopted as the standard for all experiments (i.e.) slurry mass entering the reactor  $\equiv$  slurry mass charged to the reactor

- slurry mass reporting to the drain
- 30.0 grams

This equation cannot have an uncertainty greater than  $\pm 3$  g out of approximately 750 g. The mass of coal entering the reactor is determined within 1 g from the estimated slurry mass and the composition of the slurry obtained by direct measurement.

Residual solid analysis is based on a similar principle. The composition of the residual solids is more reliable than the quantity or density of slurry retrieved from the reactor. Thus, the total coal conversion, TCC, is defined by equation 4.9

$$TCC \equiv 1 - \frac{A_1 (1 - A_F)}{(1 - A_1) A_F} - \frac{CAT (1 - A_F)}{MAFC \cdot A_F} \quad (4.9)$$

where  $A_1$  = ash content of the moisture free coal (wt fraction)

$A_F$  = ash content of the moisture free residual solids (wt fraction)

CAT = catalyst charged to the reactor (g)

MAFC = moisture and ash free coal charged to the reactor (g)

Total coal conversion for direct coal liquefaction experiments performed as part of this study are repeatable to within 0.3 to 0.5%. This uncertainty is a factor of 10 smaller than the uncertainty quoted in the literature.

## 4.2 Fundamental Investigations

A number of fundamental investigations were undertaken with respect to slurry phase analyses. I am indebted to Mr. G. Roemer and Mr. I. Mojaphoko, both undergraduate metallurgy students, who performed two projects as part of their 398 course work. The results of these investigations are reported in Chapter 5.

Mr. Mojaphoko analysed solid residua particles using an ETEC scanning electron microscope in an effort to identify residual coal, ash and catalyst particles, and examine particle cross-sections in search of cross penetration effects. Some of the effects sought included: coke deposition on catalyst and ash particles, and catalyst penetration into "coal" particles. Chemical interferences and the poor resolution of the ORTEC analyser hampered much of this work.

Mr. Roemer analysed organic residua particle size distributions, as a function of the intensity of turbulence in the reactor, using a LEITZ image analyser. If these particles had formed a dispersed liquid phase under DCL

reaction conditions, the mean particle size would decline as the stirring rate increased - at the same extent of conversion. If the particles were solid, or "exploded" during reaction, stirring rate would have little effect on the mean particle size. He dispersed coal, ash, catalyst and residua particles on slides with acetone, and placed them under a microscope which is connected to the image analyser through a video camera. He found that by adjusting the grey level, ash particles could be distinguished from organic matter, even when partially coated with coke, and that catalyst particles are much smaller than ash or "organic coal" particles. Manual image manipulation coupled with a software package thus enabled Mr. Roemer to obtain reproducible particle size distributions for organic residua and coal particles.

Catalyst and spent catalyst pellets were analysed with a JOEL microprobe to determine the distribution of phases and examine the rate of catalyst sulphidization in the reactor. This work endeavoured to address the nature of the catalytically active sites on various catalyst surfaces.

The unusual behaviour of DCL kinetics in solvent 1 (30 wt% THN, 70 wt% SRC oil) prompted an investigation of the number of liquid phases present at room temperature and under DCL reaction conditions. Small glass capillaries were manufactured from .76 cm OD .15 cm ID glass tubing. These capillaries were partially filled with THN and a small quantity of SRC oil and then sealed under vacuum. Capillaries were placed on an



alumina oxide bed inside an explosion shield and heated to 700 K. A thermocouple was placed in a capillary adjacent to the test capillaries. A temperature time history of the phases present was recorded photographically.

## Chapter 5

### 5. Experimental Results and Preliminary Discussion

#### 5.0 Introduction

Experimental results, presented in this chapter, are summarized on Figures and short Tables, which illustrate key findings of the various components of the experimental program outlined in Chapters 3 and 4. Complete sets of results and operating conditions for individual trials can be found on the Tables collected in Appendix C. Tables C.1 to C.3 contain product distribution data and process variables for trials with Forestburg sub-bituminous coal, Byron Creek bituminous coal and Saskatchewan lignite respectively. Tables C.4 to C.6 contain estimated solubility data for the gas phase constituents in the product liquids. Trial numbers mentioned in the text refer to this set of Tables.

#### 5.1 Data Precision

Before discussing the experimental results in detail, it is important to note the precision of the data presented in this chapter, as a number of the effects examined are normally obscured by the poor repeatability associated with coal liquefaction experiments. Four liquefaction trials with Forestburg coal were duplicated in this work.

The total conversion and gas yield results obtained from these experiments are compared on Table 5.1. Total coal conversion is repeatable to within 0.3 wt%, a precision at least an order of magnitude better than the  $\pm 3$  to 5 wt% encountered in the literature. A comparable improvement in total gas yield precision is also realized. Gas yield is repeatable to within 10% of the value reported, although the composition of the gas varies with the water content of the gas phase and the mean residence time, as discussed in Section 5.2.

The repeatability of liquefaction results attests to the accuracy of the analytical procedures adopted for this study and the precision of the control of operating conditions. As Figures 5.1 and 5.2 suggest, coal conversion is sensitive to changes in the reaction temperature and the mean residence time. 2°K differences in reaction temperature between "duplicate" trials can cause 1.5 to 2 wt% fluctuations in total conversion and 0.15 to 0.2 wt% fluctuations in gas yield for Forestburg sub-bituminous and Byron Creek bituminous coal. One minute differences in mean residence time introduce comparable result variations, particularly at short residence times. Uncertainties introduced by the analysis procedures compound these fluctuations and together they obscure effects related to solvent composition, catalyst:coal ratio, intensity of turbulence, and axial mixing variations. The slurry injection apparatus and the analytical procedures employed in this work permit precise control of reactor temperature and mean residence time and minimize the impact of "error"

TABLE 5.1Result Repeatability

Duplicate Set	Gas Yield (wt%)	Total Coal Conversion (wt%)
205	6.26	89.64
213	6.26	89.94
208	6.34	90.10
209	7.03	89.98
221	5.39	70.36
223	5.28	69.74
224	6.98	86.16
226	6.80	86.35

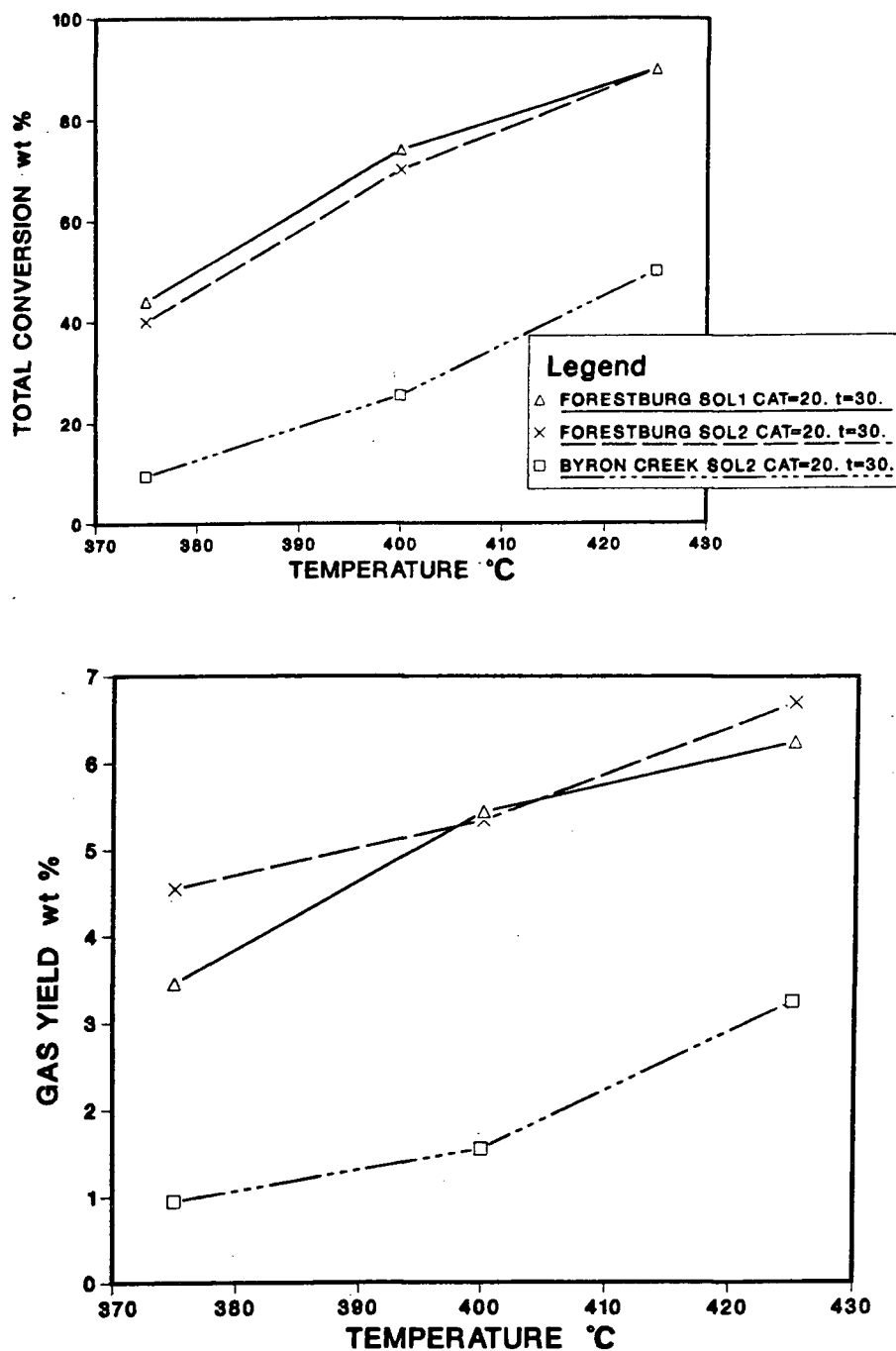


Figure 5.1: The Impact of Temperature Variations on Coal Conversion

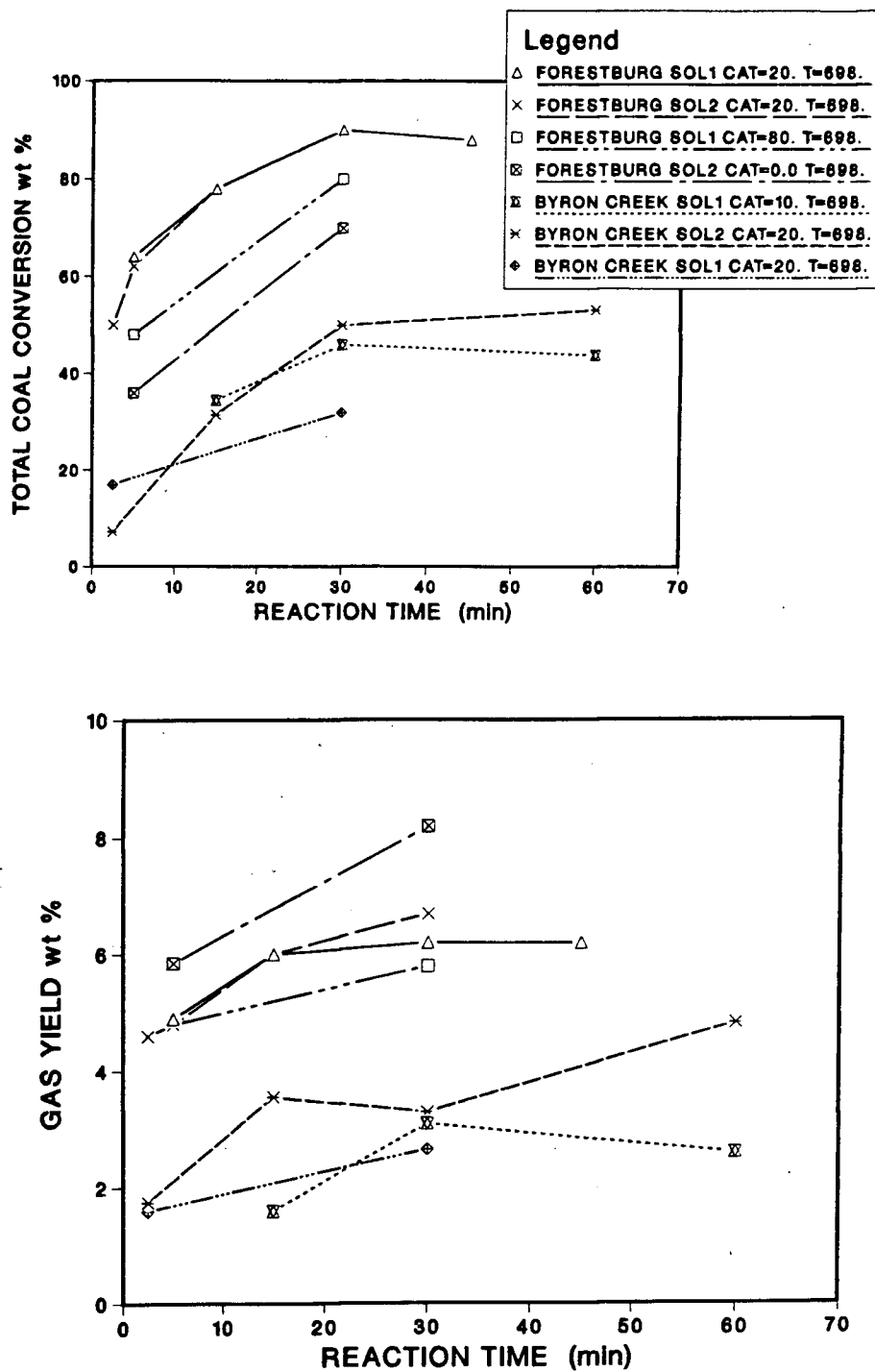
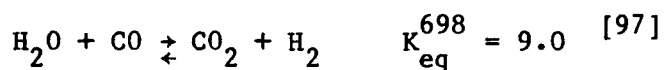


Figure 5.2: the Impact of Residence Time Variation on Coal Conversion

supposition on experimental results. Secondary effects, causing as little as 0.6 wt% differences in total conversion can be observed reliably.

## 5.2 Gas Phase Phenomena

Current DCL reactor designs purify and recycle large quantities of hydrogen. Consequently, the gas phase residence time is short and any reactions occurring among gas phase constituents are relatively unimportant. In batch-laboratory reactors and possible design alternatives for DCL reactor networks, gas phase residence times may be much longer and reactions occurring in the gas phase cannot be ignored. In this work, the impact of two representative gas phase reactions: the water gas shift reaction



and hydrocracking reactions (i.e.)



on hydrogen availability and consumption are considered.

The role or potential role of the water gas shift reaction, in direct coal liquefaction reactors, is disputed in the literature. Batchelder and Fu<sup>[89]</sup> and Kriz<sup>[103]</sup> have proposed the use of synthesis gas, in which CO and H<sub>2</sub>O become a source of hydrogen, while the prevailing opinion is that the water gas shift reaction does not occur to an appreciable extent and CO cannot act as a hydrogen source. Results from this work suggest that the water gas shift reaction is superimposed on the intrinsic production rates of CO and CO<sub>2</sub> from coals. However, the rate of this reaction, in the presence of a sulphidized Co-Mo catalyst at 698K, is not sufficiently rapid for it to approach equilibrium within 30 minutes.

The superposition hypothesis was tested and confirmed by plotting the relative amounts of CO and CO<sub>2</sub> produced, during reaction, against the moisture content of the coal fed to the reactor, at constant molar extents of CO + CO<sub>2</sub> production - Figure 5.3. The linearity of the iso-production contours is supported by the zero moisture intercepts - Table 5.2. The iso-production contours and the CO + CO<sub>2</sub> production intercepts coincide. Further evidence of superposition can be obtained from the slope of the iso-production contours, also listed on Table 5.2. The ratio  $\frac{\partial \text{CO}_2}{\partial \text{H}_2\text{O}} / \frac{\partial \text{CO}}{\partial \text{H}_2\text{O}}$  fluctuates with the extent of CO + CO<sub>2</sub> production, suggesting that the water gas shift reaction, and CO and CO<sub>2</sub> production occur simultaneously.



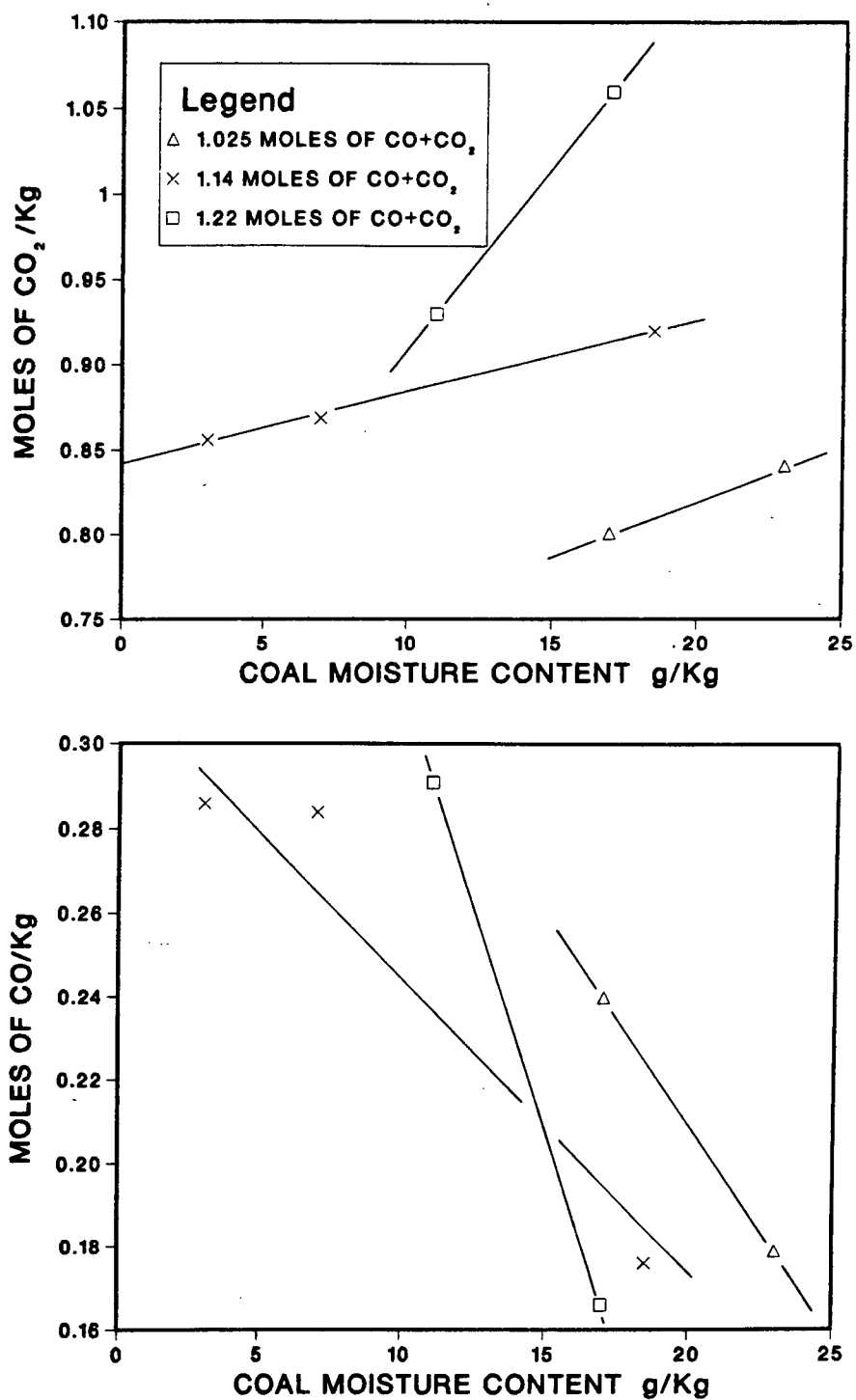


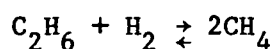
Figure 5.3: Carbon Monoxide and Carbon Dioxide Production Contours

TABLE 5.2Water Gas Shift Reaction Data

Experiment Groups	201,210	204,213	205,209
Iso-production moles (CO + CO <sub>2</sub> )	1.03	1.14	1.22
Zero Moisture Intercepts (moles)			
- (CO + CO <sub>2</sub> )	1.08	1.15	1.23
- (CO)	0.389	0.313	0.510
- (CO <sub>2</sub> )	0.687	0.841	0.715
CO:CO <sub>2</sub>	0.57	0.36	0.714
$\frac{\partial \text{CO}_2}{\partial \text{H}_2\text{O}}$ $\frac{\partial \text{CO}}{\partial \text{H}_2\text{O}}$	-0.76	-0.59	-1.06

Despite the impact of the water gas shift reaction on gas composition at longer gas phase residence times, it has only a marginal influence on hydrogen availability. As much as 0.5 moles of CO are produced per Kg of coal which could yield a maximum of 0.5 moles of hydrogen. Yet,  $15^+$  moles of hydrogen can be consumed during liquefaction reactions. Less than 3% of the required  $H_2$  can be realized from this source without artificially supplementing both the CO and  $H_2O$  content of the reaction mixture and selectively catalyzing this reaction. Gas handling and processing equipment would also have to be redesigned to accommodate a much larger gas flow rate.

Excessive hydrocracking, particularly of low molar mass aliphatic hydrocarbons, can lead to substantial increases in hydrogen consumption and a reduction in gas product value. One such reaction



is readily observed in slurry injection experiments - Figure 5.4. This reaction does not reach equilibrium within 60 minutes at 698K but the trend is evident. Excessive hydrocracking, associated with long gas phase mean residence times, can counteract the beneficial hydrogen generation effect resulting from the water gas shift reaction.

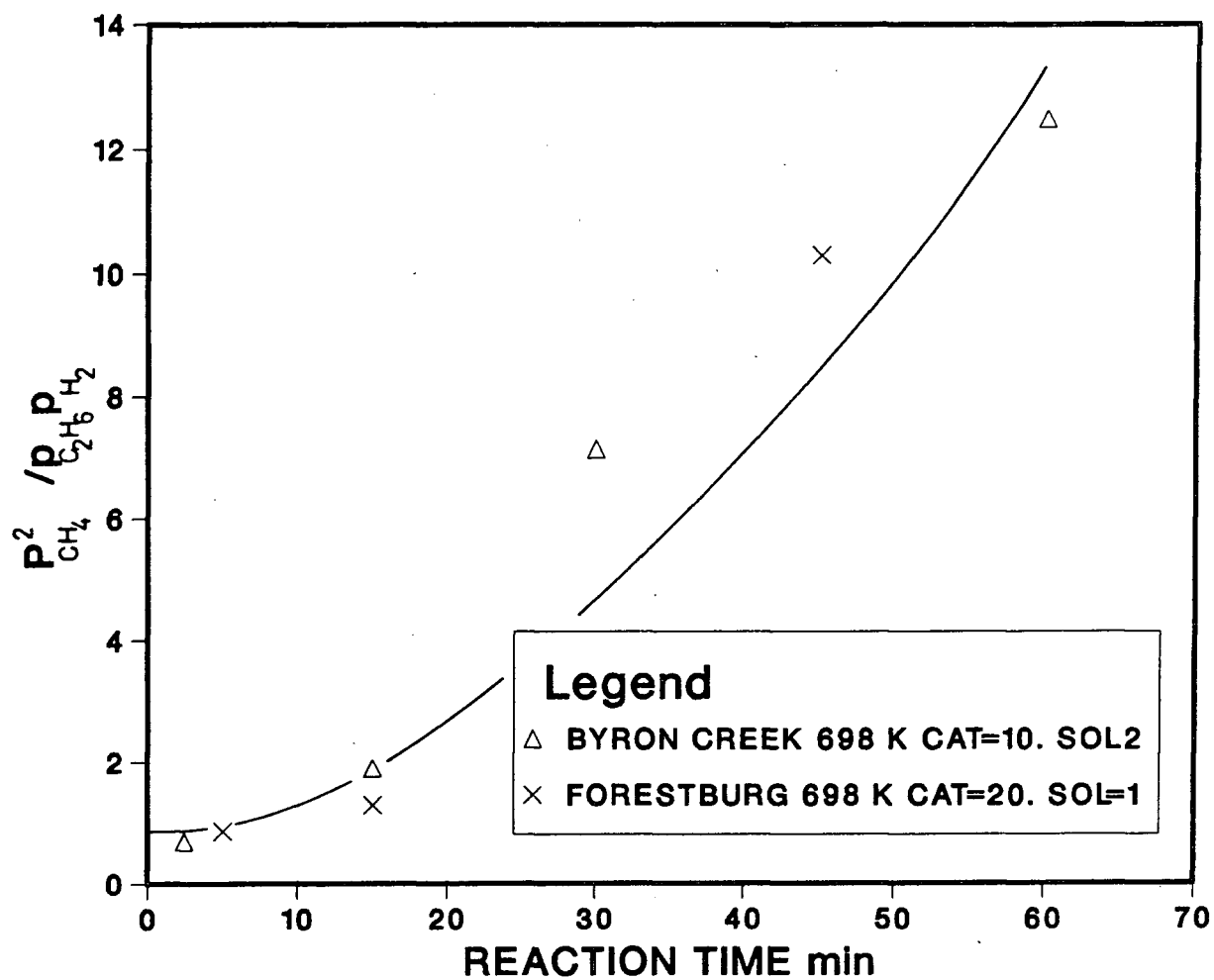


Figure 5.4: The Hydrocracking of Ethane

Clearly, synthesis gas would only be a desirable hydrogenation medium if the water gas shift and hydrocracking reactions could be separated. This can be done, at least in principle, because CO tends to be produced during the initial moments of reaction while  $\text{CH}_4$  evolves more slowly from the reaction mixture - Figure 5.5. Synthesis gas could be recycled through the first stage of a DCL reactor having a short mean residence time for the coal slurry, while gases evolved during subsequent stages would be permitted to pass rapidly through the remaining stages of the reactor. The limiting constraint on the use of synthesis gas is that it could only be employed if the water gas shift reaction was catalysed and rapid, as greater than 50% of the hydrogen consumption, 5 to 15 moles of  $\text{H}_2$  per Kg of coal, occurs within the first 3 minutes of reaction even in the presence of a "donor" solvent - Figure 5.6.

### 5.3 Reactor and Pre-heater Simulations

A number of experiments were performed in an effort to simulate axial mixing patterns, for slurries, in continuous flow apparatus. Pre-heaters were simulated by isothermal experiments with 5 minute mean residence times, while 30 minute mean residence times were used to simulate various reactor and pre-heater combinations. The operating temperatures for the reactor and pre-heater components of a combined simulation need not be the same. Two extreme axial mixing patterns were considered:

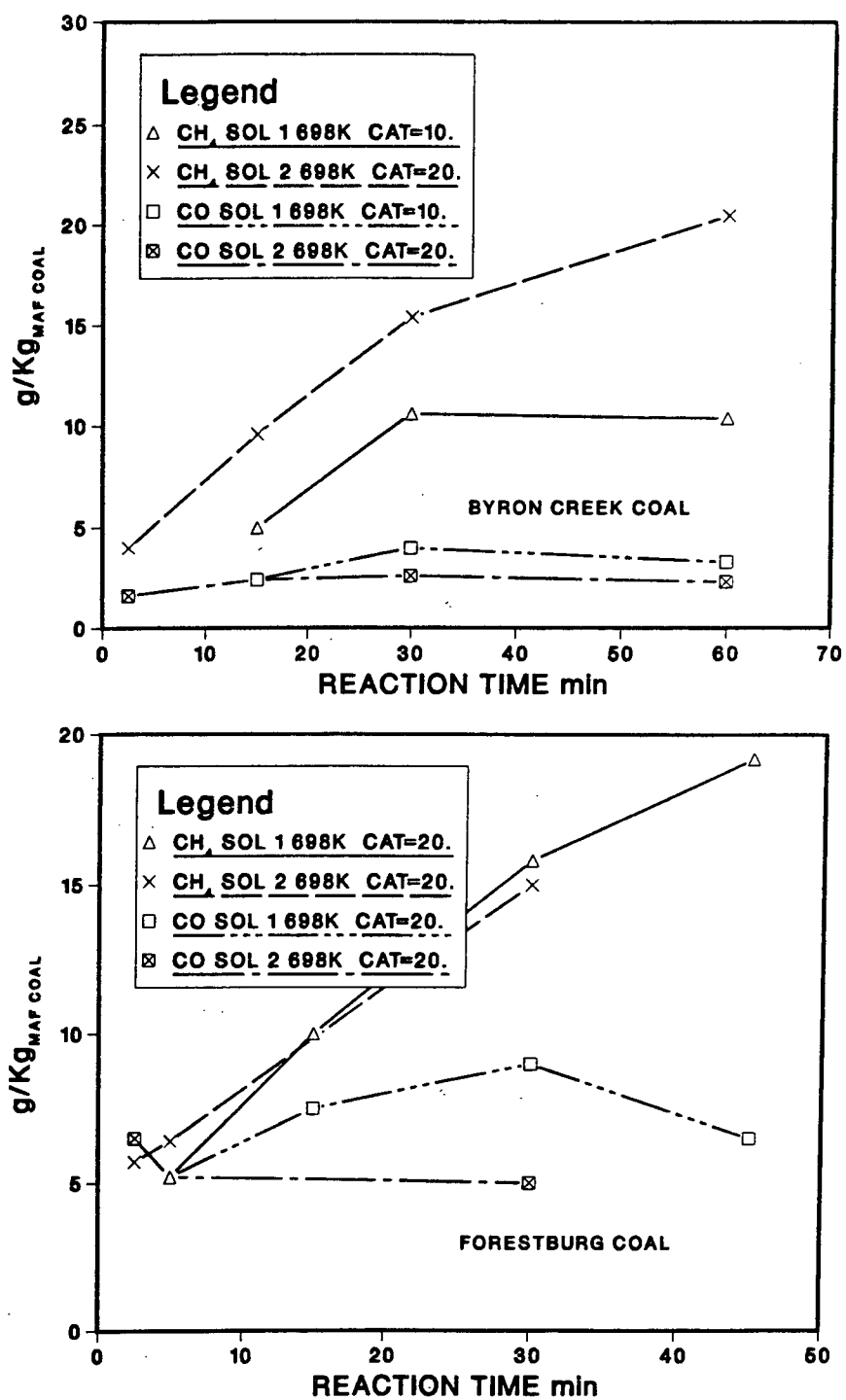


Figure 5.5: Relative Extents of CO and methane Production During the Initial Stages of Liquefaction Reactions

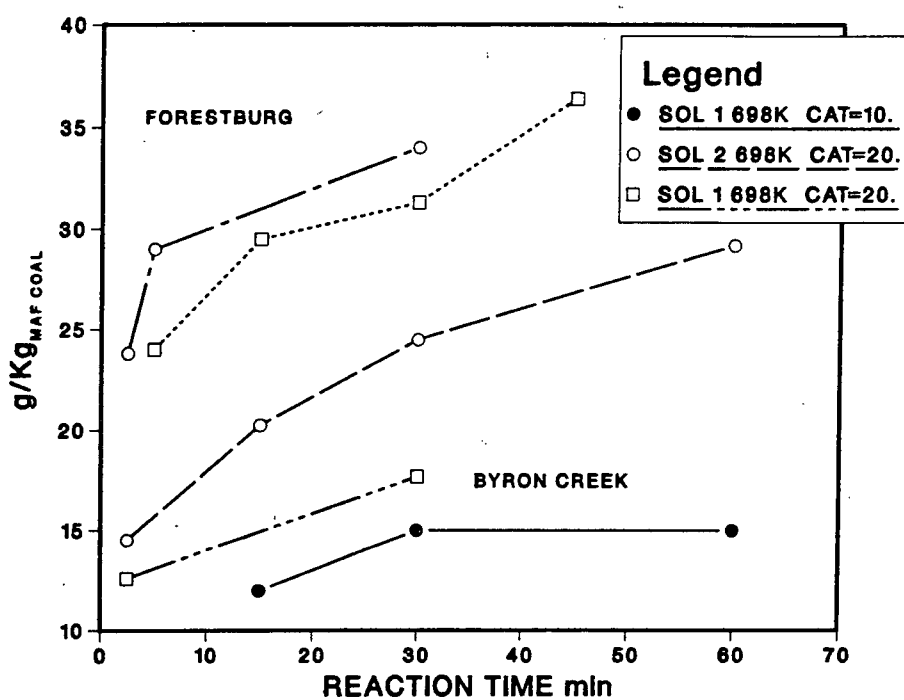


Figure 5.6: Hydrogen Consumption During the Initial Stages of Liquefaction

- plug flow (i.e.) all of the slurry has a residence time within 2 minutes of the mean.
- "axially mixed" (i.e.) all of the slurry has a residence time within the interval 0 to  $2\bar{t}$ .

Existing processes, for example, employ a pre-heater with a plug flow residence time distribution for the coal slurry, followed by an axially mixed contactor. This design is approximated by results obtained from axially mixed reactor simulations. Several other design variants were also modelled - Table 5.3.

The need to simulate axial mixing patterns in pre-heaters as well as reactors is evident from the liquefaction results shown on Figure 5.1. Greater than 50% of Forestburg coal and 15% of Byron Creek coal is liquefied within 2.5 minutes at 698K, and greater than 50% of the hydrogen consumption occurs simultaneously. Experiments, with shorter mean residence times could not be performed with this apparatus, but pre-heaters are clearly an integral component of liquefaction reactor networks.

The reactor and pre-heater simulations illustrate the extreme importance of axial mixing in DCL reactor networks and provide a number of clues with respect to the nature of coal liquefaction kinetics. However, at first glance, the results appear to present a jumble of inconsistencies,



TABLE 5.3

Coal Conversion Statistics for Reactor and Pre-heater Simulations

Simulation	Total Coal Conversion and Gas Yield wt%			
	Forestburg Sub-bituminous Coal		Bryon Creek Bituminous Coal	
	Solvent 1	Solvent 2	Solvent 1	Solvent 2
Plug flow reactor + pre-heater	(89.64,89.94), ( 6.26, 6.26)	(90.10,89.97), ( 6.34, 7.03)	45.81,3.09	49.95,3.32
Plug flow pre-heater (648K) + reactor (698K)		84.69, 5.40		
Axially mixed pre-heater + plug flow reactor	90.54, 6.37	89.91, 5.8		
Plug flow reactor + pre-heater at constant pressure		91.42, 8.18		
Axially mixed reactor	0.00, 0.00	84.35, 7.30	51.57,3.53	47.83,3.74
Plug flow pre-heater	64.13, 4.96	62.05, 4.83		
Axially mixed pre-heater	64.70, 5.20	59.63, 5.30		

particularly if one examines them from the point of view of current kinetic and process models outlined in Chapter 2. Current coal liquefaction reaction models cannot account for the divergent behaviour of the two solvents when liquefaction results from simulated axially mixed and plug flow pre-heaters are compared. Total conversion of Forestburg coal increases from 64.1 to 64.7 wt%, in solvent 1 (70 wt% SRC oil + 30 wt% THN), if an axially mixed pre-heater is substituted for a plug flow one, whereas total conversion for the same coal declines from 62.05 to 59.63 wt%, under similar conditions, when liquefied in solvent 2 (100 wt% SRC oil). In addition, current coal liquefaction models could not predict the excessive "coke" formation resulting in failure of axially mixed reactor trials for Forestburg coal liquefaction in solvent 1, or the enhanced conversion of Byron Creek coal, from 45.81 to 51.57 wt%, in a simulated axially mixed vs plug flow reactor. Only if one considers the underlying physical phenomena, which act as "hidden" variables in these trials, can the apparent inconsistencies become comprehensible.

One factor, contributing to the apparent inconsistencies, is the analysis method itself. Coal conversion to products soluble in an arbitrary solvent is, at best, a primitive measure of the extent of coal reaction. The Forestburg coal which "coked" and plugged the reactor during the axially mixed reactor simulations, with solvent 1, obviously reacted, even though it did not report as THF soluble or "converted" material.

Similar though less dramatic differences between reacted and "converted" material are observed in a number of other reactor and pre-heater simulations. Clearly, coal conversion statistics only include a fraction of the coal that undergoes hydrogenation or hydrogenolysis reactions. Coal which undergoes polymerization reaction, "coking", or decomposes into species that are not soluble in the carrier solvent are lumped together with the truly unreactive material. The conversion differences to be explained are, therefore, merely differences arising from the distribution of the reactions which the coal undergoes. It is also clear, from Table 5.3, that a portion of coal constituents undergoing one class of reactions may subsequently undergo reactions of the other class. The reduction in coal conversion, realized in an axially mixed pre-heater simulation for Forestburg coal liquefaction in solvent 2, is "recovered" if a plug flow reactor follows the pre-heater. Figure 5.1 illustrates a reverse example of this phenomenon. Forestburg and Byron Creek coal conversion begins to decline at long mean residence times when these coals are liquefied in solvent 1.

The considerations outlined above focus the search for hidden variables on system properties that are most affected by changes in the degree of axial mixing. The composition of the carrier solvent is the most important property likely to be affected by slurry phase axial mixing, as it in turn alters the solubility of hydrogen and coal derived molecular species in the carrier solvent. These latter two variables can impact

directly on observed coal liquefaction kinetics.

The extremely high hydrogen consumption rate, and the similarity of this rate, during the initial coal liquefaction reactions in both solvents, suggests that molecular hydrogen mass transfer across either the gas-liquid or liquid-dispersed phase interface, may limit the initial rate of coal liquefaction reactions - Figure 5.6. In general, the gas-liquid mass transfer resistance can be neglected in stirred autoclaves and bubble columns<sup>[95]</sup>. However, in this case the slurry entering the reactor does not contain dissolved hydrogen. Therefore, the initial dissolved hydrogen concentration is between zero and the saturated concentration of the seed oil (i.e.)  $[H_2^o] \approx 0.2 [H_2^{eq}]$ , but quickly rises to the saturated concentration. If the initial rate of coal liquefaction reactions is so fast that the initial dissolved hydrogen concentration cannot quench the coal radicals as rapidly as they are formed, one would expect that by increasing the initial hydrogen concentration the initial observed coal conversion would increase (i.e.) the fraction of the coal undergoing polymerization and other undesirable reactions would decrease. Just such an effect was observed for Byron Creek coal liquefaction in solvent 2. Two experiments with 2.5 minute slurry mean residence times were performed at 698K. The first experiment performed in the usual way, yielded a total coal conversion of 7.32 wt%, while the second experiment, employing a hydrogen saturated slurry (at 290K, 4 MPa) with  $[H_2^o] \approx 0.4 [H_2^{eq}]$ , yielded a total coal conversion of 13.93 wt%.

Clearly, the initial rate of coal liquefaction reactions, at 698K, is controlled by molecular hydrogen transfer to a dispersed condensed phase. An additional experiment was performed to test whether hydrogen mass transfer limited reaction rates beyond the first moments of reaction but this proved not to be the case. The experiments mentioned so far are "batch" with respect to the gas phase, and reactor pressure declines by about 30% during reaction. For this single experiment hydrogen was injected continuously into the reactor to maintain the high initial hydrogen pressure. After a 30 minute plug flow reactor + pre-heater simulation, with Forestburg coal in solvent 2, total coal conversion was 91.42 wt% vs 90.0 wt% when the gas pressure was allowed to drop. Much of the difference in yield is in the form of gas yield - Table 5.3.

The carrier solvent-dispersed condensed phase mass transfer limitation on the initial rate of coal liquefaction reactions is also supported by the apparent solubility data for hydrogen in the two solvents, as the reactions progress. These data, presented on Figure 5.7, were obtained once the reactor was cooled to room temperature. Hydrogen solubilities at reaction temperature, 698K, would be greater, as shown on Figures 2.19 and 2.25. Solubility differences would also be amplified under reaction conditions. Hydrogen solubility in solvent 1, measured at 290K, drops by about a factor of 2 during the first 5 minutes of reaction at 698K, but by increasing the extent of slurry phase axial mixing, the peak hydrogen demand is reduced and the total conversion in the pre-heater increases slightly. Hydrogen solubility in solvent 2 drops below the

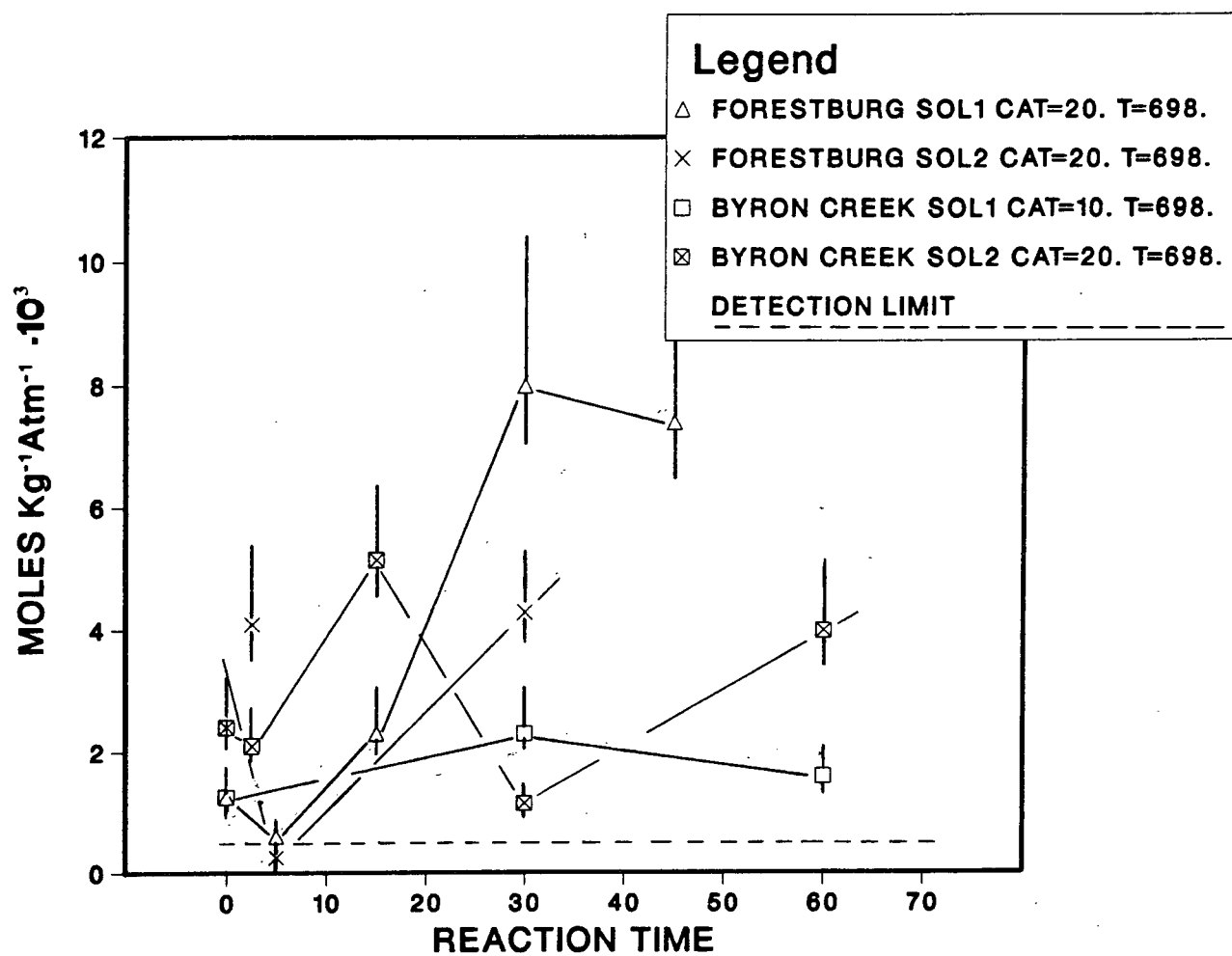


Figure 5.7: Apparent Solubilities of Hydrogen in Product Liquids at 290K

detection limit within the same time interval, as liquefaction reactions progress. So, even though the peak hydrogen demand is reduced, in an axially mixed pre-heater, the last coal entering the pre-heater encounters a very low dissolved hydrogen concentration and a net decrease in coal conversion results.

Apparent hydrogen solubility differences can also account, in part, for the observed differences in coal conversion obtained from axially mixed and plug flow reactors. Byron Creek coal, liquefied in an axially mixed reactor with solvent 1, encounters a hydrogen solubility of  $3 \times 10^{-3}$  moles  $\text{H}_2 \cdot \text{Kg}_{(\text{solvent})}^{-1} \cdot \text{Atm}^{-1}$ , which is at least double the hydrogen solubility encountered during the opening moments of a plug flow reactor/pre-heater simulation. Consequently, the initial coal conversion increases. The apparent hydrogen solubilities, encountered by Forestberg and Byron Creek coal during an axially mixed reactor simulation are  $1.06$  and  $1.80 \times 10^{-3}$  moles  $\text{H}_2 \cdot \text{Kg}_{(\text{solvent})}^{-1} \cdot \text{Atm}^{-1}$  respectively. These solubilities are much lower than the initial hydrogen solubility encountered during plug flow reactor simulations, and the initial coal conversion is reduced. Hydrodynamic effects are superimposed on the differences in initial conversion (i.e.) conversion in plug-flow reactors should be greater than conversion in axially mixed reactors, if simple nth order reaction kinetics are applicable.

The liquefaction of Forestburg coal, during axially mixed reactor simulations with solvent 1, presents a more complex situation. The failure of these two trials cannot be treated as a spurious result or as a reflection of mechanical problems. Both trials failed approximately 1/3 of the way through slurry injection. No blockages were observed anywhere in the slurry recycle loop, which was dismantled following both trials, but "coking" occurred at the slurry entry port at the base of the reactor. This material was not dislodged by a differential pressure exceeding 15 MPa and the slurry line rupture disc failed during both trials. What experimental factors can account for the failure of these two trials? As mentioned in Chapter 2, large changes in hydrogen solubility reflect significant changes in solvent composition. The solvent composition encountered by the Forestburg coal during an axially mixed reactor simulation has a very high hydrogen solubility, suggesting that it has both a low mean molar mass and hetero-atom content. The initial liquefaction products comprise large, complex molecules with an appreciable hetero-atom content. Such species, particularly those containing a high hetero-atom content are unlikely to be miscible with such a solvent and may form flocs, micelles, or a separate liquid or solid phase. The close proximity of these species could easily lead to retrogressive reactions and "coke" formation. The same phenomenon is not observed during axially mixed trials with Byron Creek coal, because it has a much lower hetero-atom content, Table 4.3, and less catalyst was employed during trials involving this coal (i.e.) less solvent hydrogenolysis and hydrogenation occurs during these trials. Some coal derived products also appear to "condense" near the end



of plug flow reactor simulations, with solvent 1, if slurry phase mean residence time is sufficiently long - Figure 5.1. These two effects are probably related, as Cobalt-Molybdenum catalysts catalyse hydrogenation and hydrogenolysis reactions for mid-range compounds selectively. Large molecules, which contain most of the hetero atoms present in a solvent<sup>[119]</sup> are either introduced into or remain in a progressively less amenable solvent and a greater fraction of these species become insoluble. This topic is addressed again in sections 5.5 and 5.6.

The reactor and pre-heater simulations have, of necessity, been restricted to an evaluation of the importance of slurry phase axial mixing. Other variables: the catalyst to coal ratio, the stirring rate, reaction temperature, etc., were held constant if not identical for each coal/solvent system. Efforts were made to employ optimal or near optimal catalyst to coal ratios for each coal/solvent system. However, all of the variables are interdependent to some degree and axial mixing cannot be examined in complete isolation. The other variables, no doubt, exert an influence on these trials. Nevertheless, the simulations have provided a number of insights into the nature of the coal liquefaction reaction environment and established a framework for evaluating other experimental results. The major findings related to these trials are:

1. The initial coal liquefaction reactions can be controlled by molecular hydrogen transfer to coal or coal fragments, regardless of the donor solvent content of the liquefaction solvent.

2. The fraction of molecular species, produced by initial decomposition of coal, that reports as "converted" material depends on the solubility of the coal derived species in the liquefaction solvent.
3. The optimum reactor + pre-heater configuration is primarily dependent on the initial solvent and coal composition:
  - A plug flow reactor + pre-heater provide optimum results for coal liquefaction in solvents similar to SRC oil,
  - An axially mixed reactor and pre-heater are best for coal liquefaction in donor rich solvents, provided the coal has a low hetero-atom content. Otherwise an axially mixed pre-heater followed by a plug flow reactor is preferred.

#### 5.4 The Role of Cobalt Molybdate Catalysts in DCL Reaction

##### Environments

Catalysts are ubiquitous actors in direct coal liquefaction reaction environments, as noted in Chapter 2. It is difficult to perform "catalyst free" or even "added catalyst free" experiments, when some mineral matter constituents and catecols, for example, act as catalysts. In addition, one must contend, experimentally, with the "memory effect" when employing Co-Mo catalysts. If a batch experiment is performed with this type of catalyst, and removed, the catalytic effect persists for 3 or 4 additional trials even if no more catalyst is added<sup>[120]</sup>. This effect

also contributes to the background level of catalysis.

Preliminary catalysis trials verified that catalyst support and the size of catalyst particles influences the effectiveness of a catalyst. Forestburg coal conversion, in the presence of 20 grams of whole  $\text{CoO-MoO}_3$  on  $\alpha$ -alumina pellets, for example, is 13.2 wt% less than in the presence of the same mass of finely ground catalyst pellets\*. One gram of ground catalyst appears to be equivalent to approximately 5.7 grams of whole catalyst pellets. An unsupported  $\text{MoO}_3 \cdot 1/2 \text{H}_2\text{O}$  powdered catalyst, containing the same number of moles of Mo + Co as 20 grams of supported catalyst, was also tested. Forestburg coal conversion was 5.6 wt% less in the presence of this catalyst than in the presence of ground catalyst pellets\*. Ground catalyst is twice as effective as the unsupported  $\text{MoO}_3 \cdot 1/2 \text{H}_2\text{O}$ , on an equi-molar basis.

Ground catalyst pellets were employed in all other catalysed trials. Other fixed experimental conditions included a reaction temperature of 698K, and a stirring rate of 16.67 Hz. 5 minute and 30 minute trials were performed with Forestburg sub-bituminous coals, 15 minute trials with Saskatchewan lignite, and 30 minute trials with Byron Creek bituminous coal. Results obtained from these experiments are shown on Figure 5.8 and noted below.

---

\* The experimental conditions were: temperature 698K, reaction time 30 minutes, stirring rate 16.67 Hz. Solvent 1 was employed for the first example; solvent 2 for the second one.

Figure 5.8 illustrates the sensitivity of coal and lignite conversion to the presence of added catalysts. In the absence of such catalysts, total coal conversion is radically reduced. The difference can be as great as 20 wt%. If excess catalyst is present a comparable reduction in total coal conversion may result. Gas yields from coals and lignites are also affected by added catalysts, but only when the coal or lignite is liquefied in a solvent that is not donor rich (i.e.) solvent 2. In this case, gas yield drops 1 to 2 wt% in the presence of added catalyst. Excess catalyst has no further effect on gas yield. If coals are liquefied in a donor rich solvent, gas yields are lower and added catalyst does not have a noticeable effect on gas yield - perhaps background catalytic effects are sufficient to minimize gas yield.

The sensitivity of total conversion, to the presence of added catalyst and particularly to the presence of excess catalyst, appears to be greatest for bituminous coals. Sub-bituminous coals are less sensitive and lignites least sensitive. Solvent composition also contributes to the sensitivity of coal conversion to the level of catalysis. Coal conversion is more adversely affected by non-optimal levels of catalysis when liquefied in solvent 1 than in solvent 2. This effect can be attributed to differences in the mean molar mass of the two solvents (solvent 1 comprising 70 wt% SRC oil and 30 wt% THN has a lower mean molar mass than solvent 2 which comprises 100 wt% SRC oil), and to the deportment of molecular species within the two solvents (section 5.6). It is not

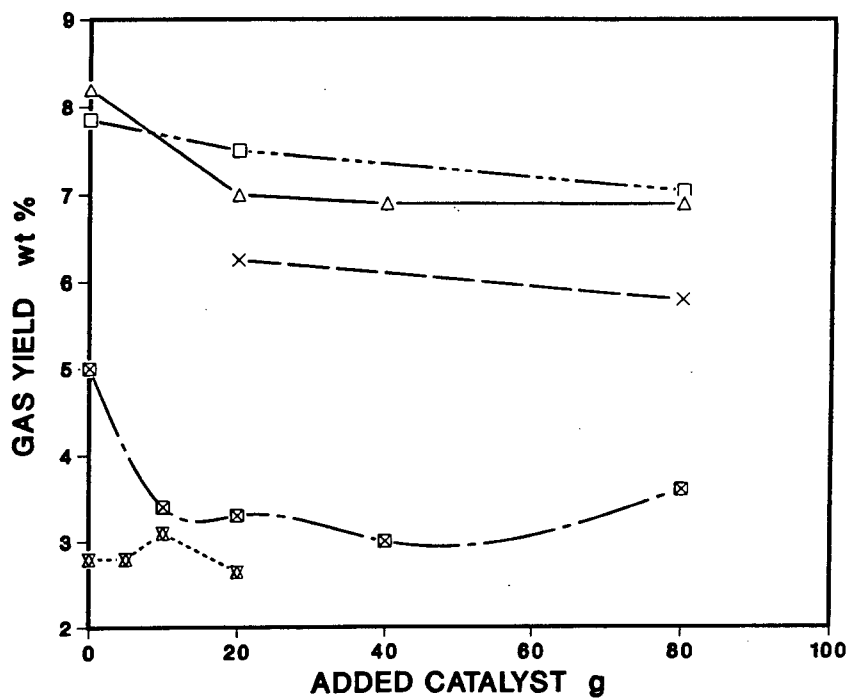
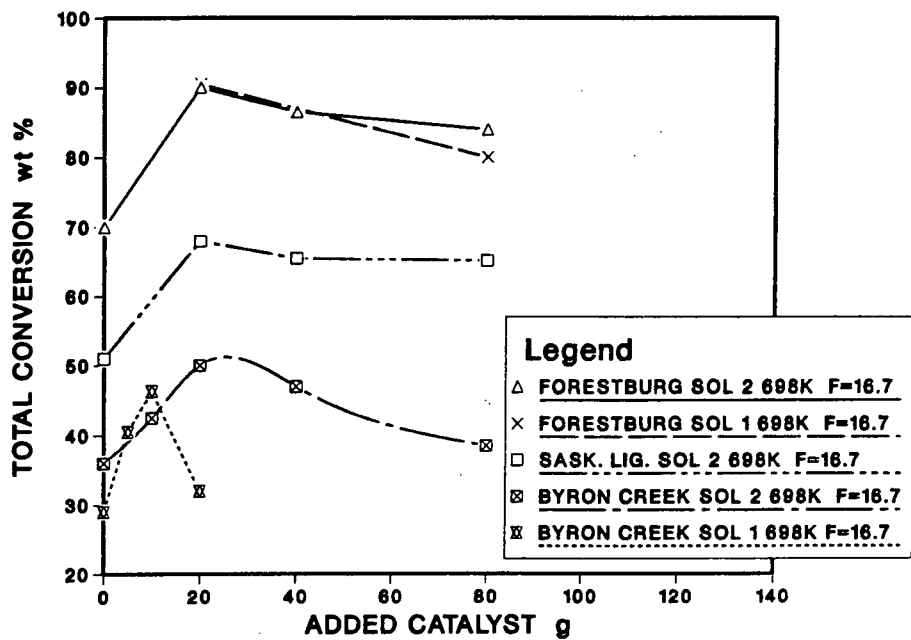


Figure 5.8: The Influence of Catalysis on Coal and Lignite Conversion

surprising, that the impact of catalysis, particularly excess catalysis, on coal conversion is dependent on coal type and solvent composition. Bituminous coals tend to generate larger molecular fragments than sub-bituminous coals and lignites. Larger molecules are less likely to be soluble in solvents undergoing catalysed hydrogenation/hydrogenolysis reactions as these reactions lead to rapid reduction in the mean molar mass of the solvent. The reduced solubility of coal derived molecular species in the carrier solvent yields lower coal conversions. This effect would be accentuated in a solvent with a lower initial mean molar mass.

The magnitude of the reduction in coal on lignite conversion, when non-optimum levels of catalysis are employed, is time dependent. The extent of Forestburg coal conversion, in solvent 2, is reduced by 25.85 wt% after 5 minutes, when zero grams of catalyst are added instead of 20.0 grams. This difference drops to 21.3 wt% after 30 minutes. A similar time dependence is noted for Forestburg coal conversion in solvent 1 with 20.0 vs 80.0 grams of added catalyst. After 5 minutes, there is a 15.3 wt% difference in coal conversion which reduces to 10.5 wt% after 30 minutes. So, not only is there an optimum level of catalysis for each coal/solvent system but one defined by initial coal solvent interactions.

Clearly, the optimum level of catalysis for reactor networks, employing plug flow pre-heaters, is defined by the pre-heater reaction environment, as long as the pre-heater exit temperature is greater than the temperature at which coal begins to undergo decomposition reactions. If

the pre-heater exit temperature is less than this temperature, the optimum level of catalysis will be defined by reaction conditions at the reactor inlet. For current and envisioned industrial DCL processes, optimum levels of catalysis are controlled by the reaction environment in pre-heaters. These results also indicate that for axially mixed reactors, or for reactors employing low-molar-mass solvents, only modest levels of "added catalyst" are warranted and excess catalysis should be avoided especially for bituminous coals.

### 5.5 The Intensity of Turbulence

The intensity of turbulence, which for autoclaves is defined by stirring rate and impeller geometry, is not considered to be a variable of consequence for direct coal liquefaction reactions. For laboratory reactors, employing hydrogen gas, for example, the literature asserts that it is only necessary to assure that the reactors are "well mixed" so that adequate gas-slurry mass transfer occurs. Stirring rates of 8.33 Hz are frequently employed for this purpose. The impact of stirring on the destruction of coal particles has only been treated in a qualitative manner. Whitehurst et al.<sup>[121]</sup> reviewed some of their own work and the work of others, and showed that coal particles remained intact with little or no apparent shrinkage, up to 80 wt% conversion, in the absence of agitation, but broke up rapidly when reacted in an agitated autoclave. They also showed that stirring rate had no influence on coal conversion to pyridine

soluble material, after 2 minutes of reaction at 698K.

In view of these findings, the results presented on Figure 5.9 are surprising. Coal conversion to tetrahydrofuran soluble material and gas yield are both affected by changes in stirring rate. For any given level of catalysis, coal conversion increases to a maximum then declines as stirring rate is increased. Total coal conversion can vary by as much as 8 wt%. There is no general trend for the dependence of gas yield on stirring rate but the fluctuations can exceed 1 wt%. The apparent contradiction between these results and previous findings is readily explained. Macerals present in raw coal are soluble in pyridine. Therefore, one would not expect pyridine solubility to reflect the degree of conversion of coal derived species. Raw coal is not soluble in tetrahydrofuran. Coal derived molecular species must undergo molar mass and/or hetero-atom content reduction before they are soluble in this solvent. Thus, THF solubility is sensitive to the degree of coal conversion. The results, presented on Figure 5.9, reflect this sensitivity. These results also highlight the interdependence of stirring rate (the intensity of turbulence) and the optimum level of catalysis. An optimum level of catalysis is only optimal at a single stirring rate. If one refers back to Figure 5.8, for example, 5 grams of catalyst at 16.67 Hz result in a greater total coal conversion than 10 grams of catalyst at 8.33 Hz, for Byron Creek coal liquefaction in solvent 1.



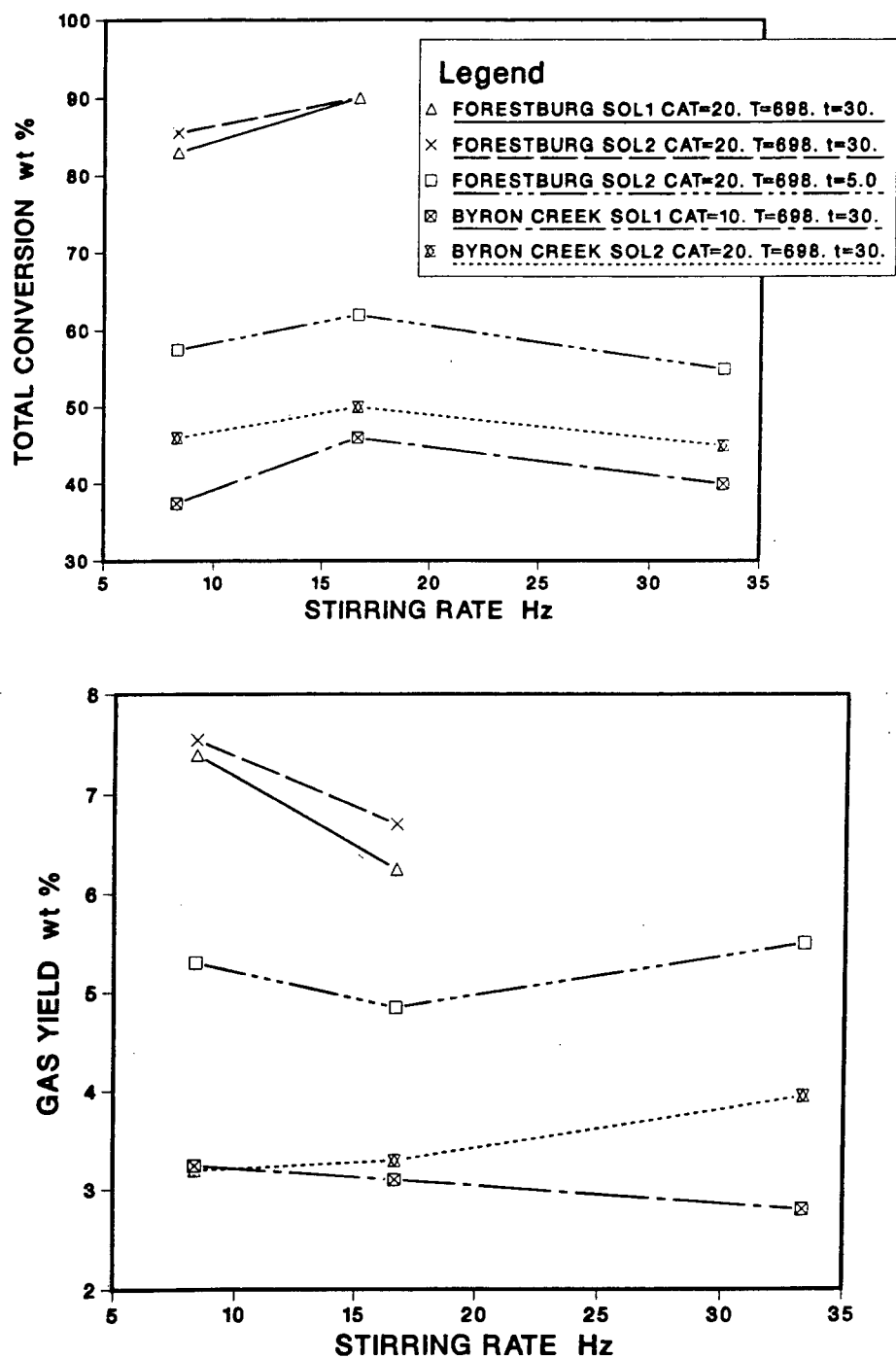


Figure 5.9: The Influence of Stirring Rate on Coal and Lignite Conversion

What experimental factors can account for the interdependence of these two variables? The only hint provided by the results is that the impact of non-optimum stirring rate-catalyst combinations on coal conversion persist from the initial sequence of liquefaction reactions. Figure 5.9 illustrates this effect for Forestburg coal liquefaction in solvent 2, at 698K, with 20 grams of catalyst. After 5 minutes the difference in coal conversion between 8.33 and 16.67 Hz is 4.75 wt%; after 30 minutes the difference is 4.46 wt%. One can only hypothesise that the intensity of turbulence influences the extent of coal particle break-up during the initial decomposition reactions. This would alter the coal-solvent interfacial area and affect the initial rates of the liquefaction reactions. Thus, changing the amount of catalyst at a constant stirring rate would be equivalent to changing the stirring rate while maintaining the same amount of catalyst. At a low stirring rate, little particle destruction occurs. Excess catalyst may be present and the extent of coal conversion is reduced as shown in section 5.4. At very high stirring rates, particles are reduced to fine powders. The rates of initial reactions are much higher, and if the amount of catalyst is insufficient, inadequate catalysis also leads to a reduction in coal conversion. At an intermediate stirring rate, the initial rate of coal dissolution and the amount of catalyst are well matched and a coal conversion optimum is observed.

This hypothesis was tested by Mr. G. Roemer, who examined residue particle size distributions, at constant conversion, as a function of

stirring rate. Particle size distributions for residue particles extracted from 5 minute liquefaction trials with Forestburg coal at 8.33, 16.67 and 33.3 Hz are shown on Figure 5.10 and can be compared with the initial coal particle size distribution, Figure 4.2. The total coal conversions for these trials are 57.3, 62.05, and 55.0 wt% respectively. The results indicate that the mean diameter of organic residua particles decreases from 16.4  $\mu\text{m}$  to 6.9  $\mu\text{m}$  to 5.9  $\mu\text{m}$  as the stirring rate increases from 8.33 to 16.67 to 33.3 Hz. The trend in these results is likely to be accurate. However, these results are best treated as tentative because the numerous steps in the analysis procedure provide ample opportunity for particle segregation:

1. Only small samples, comprising approximately 2000 particles, can be analysed.
2. Samples extracted from vials must be forced through a 90  $\mu\text{m}$  screen to break-up agglomerates which form during the residua filtration sequence
3. Only certain particle size fractions may disperse and remain on the slide for analysis

and only a fraction of the particles appear to undergo particle size reduction. Nevertheless, these results do corroborate the proposed relationship between stirring rate and the level of catalysis.

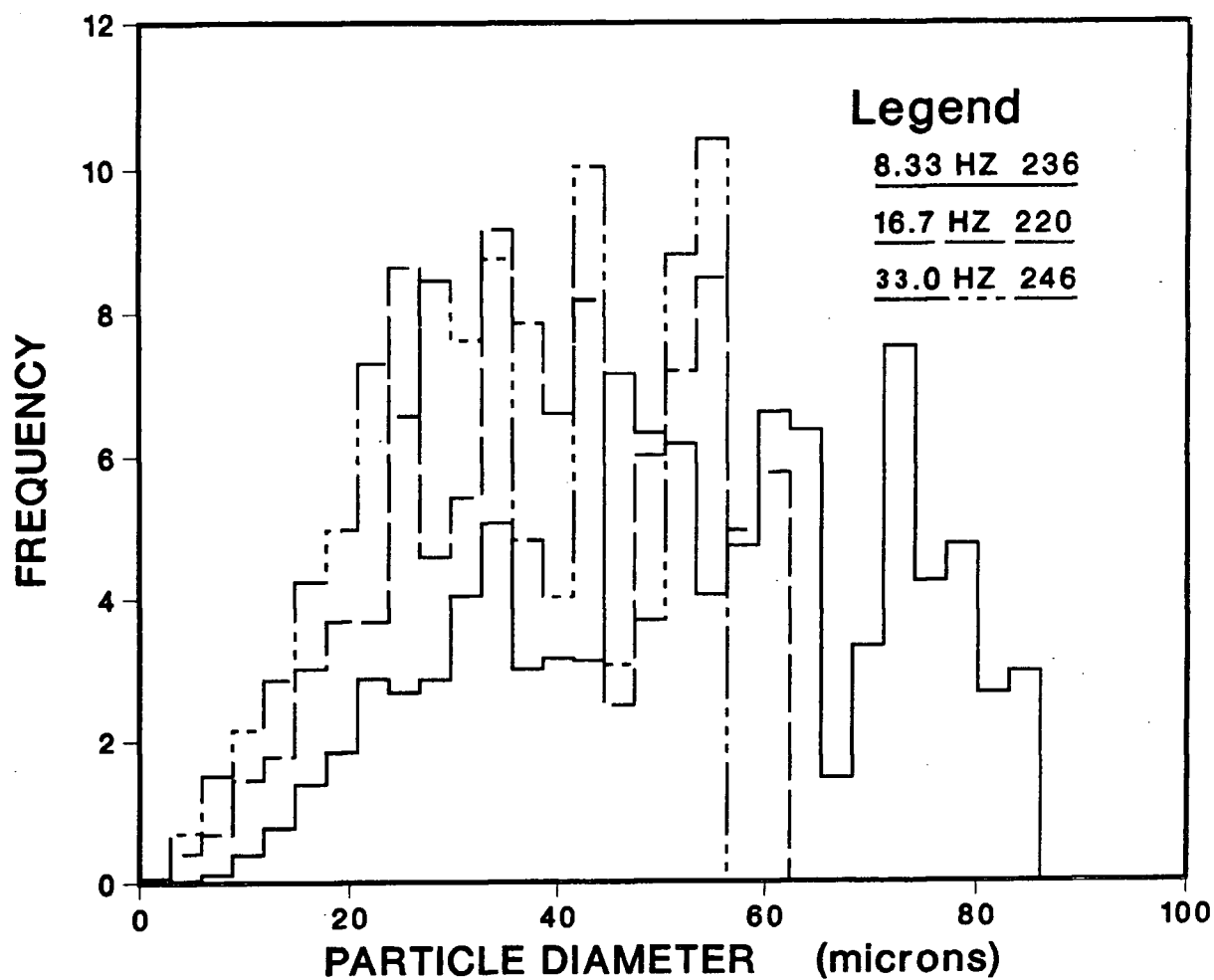


Figure 5.10: The Influence of Stirring Rate on the Residue Particle Size Distribution

As a further test of the hypothesis, the mechanical destruction of coal particles, at impeller surfaces was investigated. A 2000  $\mu\text{m}$  diameter coal particle was placed in a glass walled autoclave with water and stirred, for 2 hours, at 33.3 Hz. The autoclave and impeller geometry, for this test, were the same as for the liquefaction trials. No change in particle size was detected. Since much smaller coal particles were employed in liquefaction trials, mechanical break-up of inert coal particles should not occur in agitated DCL reactors.

The intensity of turbulence can only affect the break-up of partially reacted material, either dispersed liquid droplets, or particles comprising a loosely bonded solid skeleton. One would expect particles comprising a solid skeleton to break-up along predefined fault lines. The final particle size distribution need not be sensitive to the stirring induced stress intensity beyond a threshold value, whereas the size of fluid droplets would be sensitive to variations in stirring rate as shown by Calderbank<sup>[122]</sup>.

Compounds likely to be insoluble in liquefaction solvents have a high molar mass and hetero-atom content. These compounds may form viscous dispersed phase droplets at reaction temperature and solid particles at room temperature. The existence of such a phase would account for a number of observations noted, so far, in this chapter. Material in such a dispersed phase would account for:

1. reacted but "unconverted" coal,
2. the apparent reversibility of conversion,
3. the sensitivity of conversion to solvent composition,
4. retrogressive reactions
  - compounds most likely to undergo condensation or polymerization reactions are concentrated in droplets rather than dispersed in a hydrogenating environment.

The formation of a separate liquid phase, under reaction conditions, is the preferred explanation for observed liquefaction kinetics because molecular geometry does not lend itself to floc or micelle formation. Coal derived molecules tend to be planar sheets with distributed hetero-atom functionalities<sup>[119]</sup> rather than long chains with remote functional differences. Also, if such species were present, they would probably be too small to be affected by variations in stirring rate. Material, in dispersed phase droplets, may solidify rapidly, under reaction conditions, depending on the melting point of the molecules present and/or the rate of reverse reactions. At room temperature the "droplets" are certainly solid.

The existence of a dispersed organic phase, other than unreacted coal, is not unknown in the Direct Coal Liquefaction reaction environment. Asphaltene precipitation occurs in pre-heaters, under certain conditions. An "anti-solvent" is added to product liquids in the Lummus modification of the SRC process to separate ash and molecular species containing the

majority of the hetero-atoms from the remainder of the product liquids<sup>[123]</sup>. The rapid decrease in the solvency of a solvent as its critical point is approached is the principal method of operation of the critical solvent deashing process<sup>[124]</sup>. This work differs from previous research only in so far as the results suggest that a dispersed organic phase may persist throughout the reactor network. Further evidence of the existence of a persistent dispersed organic phase was obtained by close examination of the components comprising solvent 1. These results are reported in section 5.6.

#### 5.6 Observation of a Dispersed Phase in a Model Solvent

The results, presented in the previous sections of this chapter, provide little more than circumstantial evidence for the existence of a dispersed organic phase, in coal liquefaction solvents, under reaction conditions. Work reported in this section provides more direct evidence, even though reacted coal slurries were not analysed for the presence of a second organic phase. Ash, unreacted coal, and catalyst particles would have interfered with observations in such slurries, and had these problems been overcome, one would still have had to contend with the fact that these slurries are opaque even across thin sections. A model solvent, containing only organic material, with a translucent continuous phase was required. Such a solvent was devised from components present in solvent 1. This solvent contained approximately 95 wt% tetralin and 5 wt% SRC oil.

The bi-plex structure of the model solvent, at room temperature, is readily observed on Figure 5.11A. The dispersed phase, shown on this figure, contains solid particles and flocs, formerly SRC oil, which were first settled in a centrifuge from the tetralin matrix. Gentle rocking of the sample vial yielded the observed suspension. Vigorous agitation of the same sample vial yielded an opaque colloidal suspension, Figure 5.11B, which could only be resettled with difficulty. The bi-plex structure of this solvent persists up to about 703K, as shown by the series of photographs, Figure 5.12, which record a temperature time history of a sample heating trial. The solvent remained a solid suspension above 475K. By 575K, two separate liquid phases had emerged. Material transfer between these two bulk phases continued as the solvent was heated. The clear, tetralin-rich phase grew in size and SRC oil droplets gradually migrated to the opaque, SRC oil-rich phase. At about 703K, the two phases suddenly and violently recombined. When cooled to room temperature, it is uncertain whether the solvent formed a colloidal suspension or remained as a single phase.

These investigations have demonstrated the presence of a dispersed organic phase with solvent components frequently encountered in direct coal liquefaction reaction environments. Furthermore, they show that a dispersed phase may be fluid under reaction conditions and solid at room temperature. These findings provide crucial experimental verification for the hypothesis discussed in preceding sections and provide a sound basis for the coal liquefaction kinetic model proposed in Chapter 6.



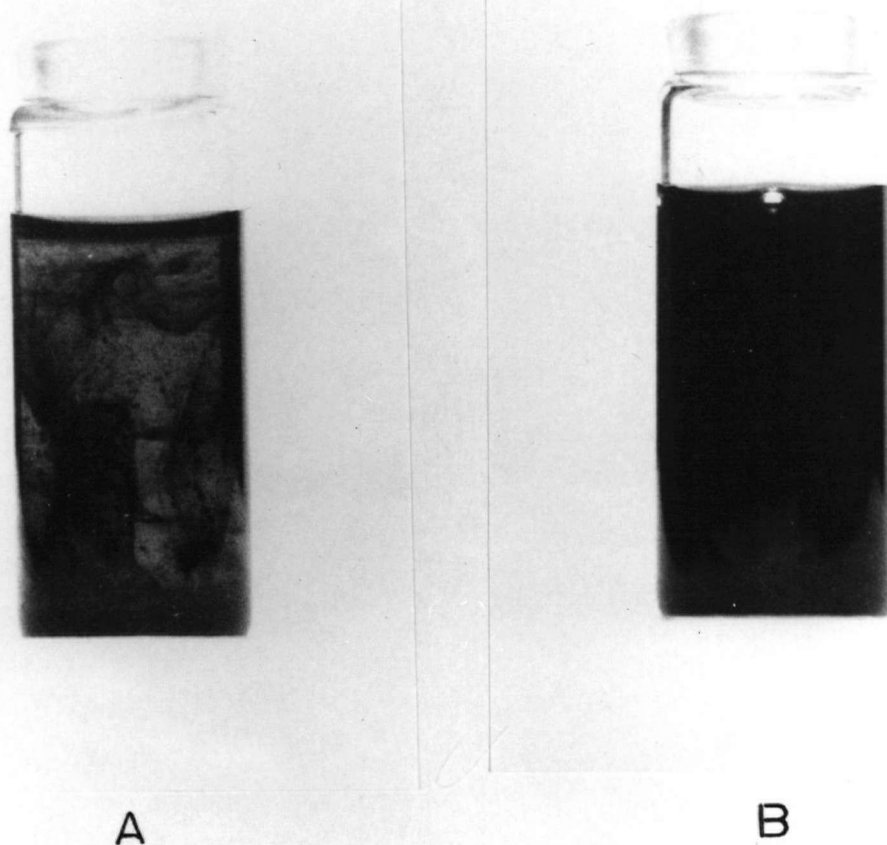


Figure 5.11: Phase Distributions in a Model Two Phase Liquefaction Solvent at Room Temperature ( A agglomerated SRC oil in tetralin, B a Colloidal Suspension of SRC oil in Tetralin)

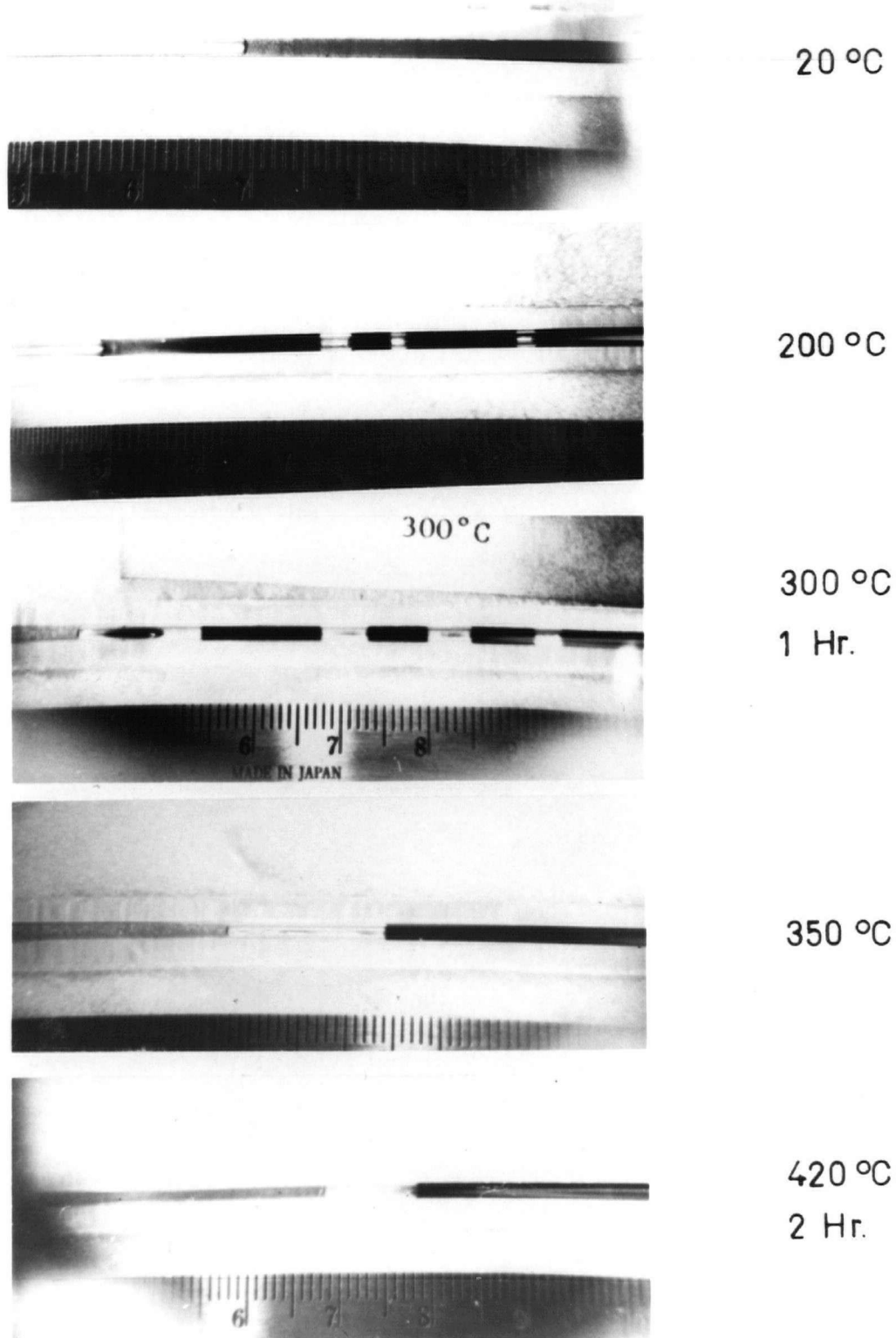


Figure 5.12: Phase Distributions in a Model Two Phase Liquefaction Solvent at Elevated Temperatures ( the tetralin rich phase is on the left, the SRC oil rich phase on the right).

## 5.7 Residual Solids Analysis

Composition analysis of residual solids and catalyst particles was only partially successful. The value of this work was limited by the resolving power of the JOEL MICROPROBE, and the ORTEC analyser attached to the ETEC scanning electron microscope.

Mr. G. Mojaphoko performed qualitative elemental analyses on residual particles and cross-sections of residual particles, with the SEM. The objectives of this work were to:

1. identify the various types of particles present,
2. observe, if possible, catalyst particles imbedded in organic residual particles (i.e.) investigate the possibility that dispersed phase reactions are catalysed.

He found that individual residual particles could be identified by the presence of characteristic elements. A high silicon content was invariably associated with mineral matter, cobalt with catalyst particles. It was hoped that organic residual particles would also be detectible in outline (i.e) as blank spaces surrounded by fine ash or catalyst particles, or in some other form. Unfortunately, these particles were indistinguishable from the background and catalyst penetration into the dispersed organic phase was not observable.

Elemental analysis of catalyst pellets, on the MICROPROBE, was equally inconclusive. Cobalt and molybdenum interfered with the aluminum determinations and it was not even possible to confirm the manufacturers specifications for the catalyst composition. Only the distribution of cobalt and molybdenum, in the raw catalyst, can be discussed with any certainty. These elements are distributed, in an equimolar ratio, throughout much of the catalyst. Fine fluorescent nodules, containing very high concentrations of molybdenum, were also observed. It is not certain whether these nodules also contain cobalt or aluminum. A cross-section of a spent catalyst pellet was also analysed on the MICROPROBE to determine the extent of catalyst sulphidation after a 30 minute exposure to the coal liquefaction environment. These results are shown on Figure 5.13. Seven mole % sulphur is required to completely sulphidize the catalyst. The maximum sulphur concentration observed was only 1.23 mole %. However, as these sulphur concentrations are averaged over a region, one would expect that an average sulphur concentration much less than 7 mole % would result in complete sulphidation of pore and external surfaces. So, even though the catalyst employed throughout this study was added as an oxide, it likely behaves as a sulphide catalyst in situ.

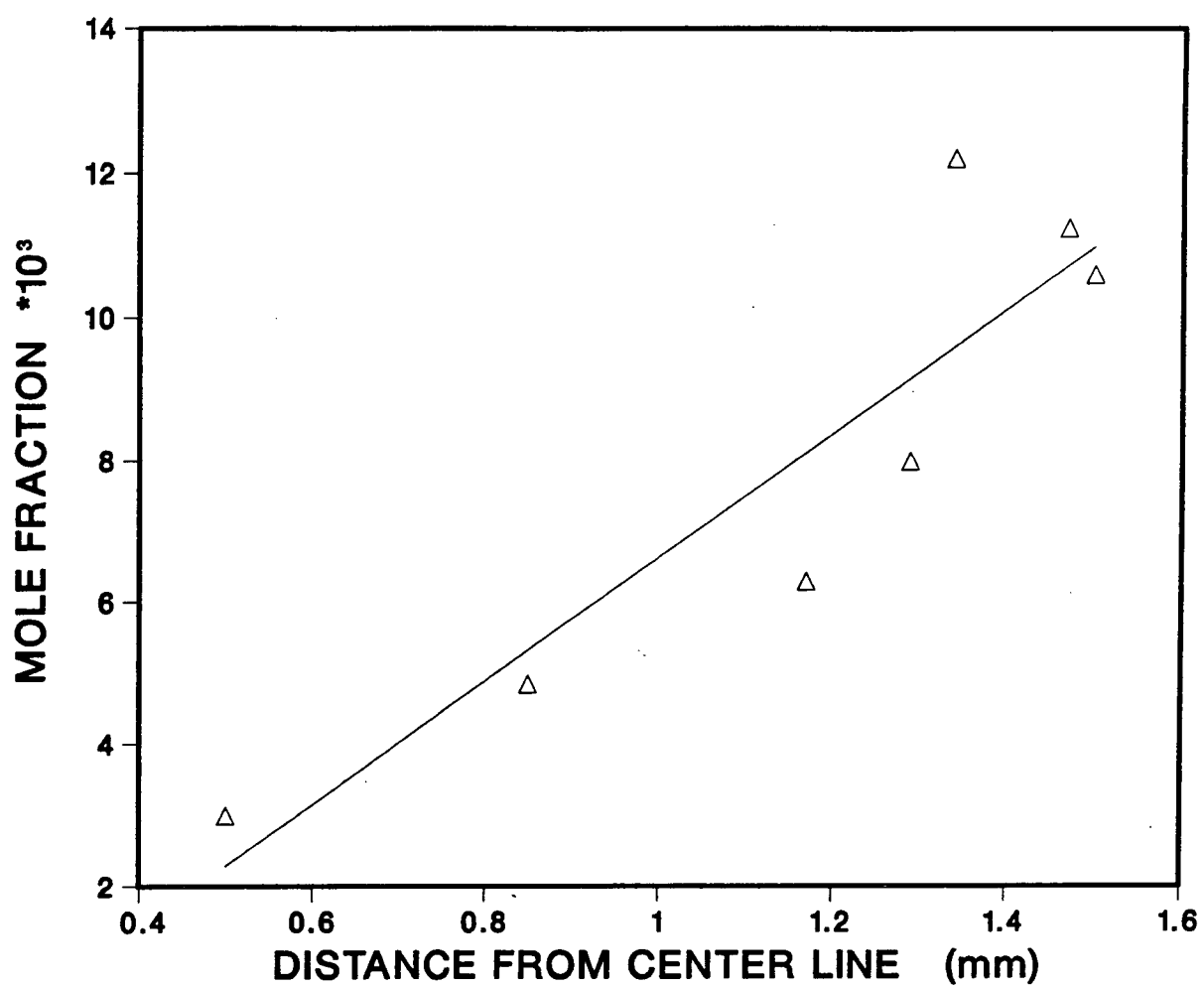


Figure 5.13: Sulphur Concentration Profiles in Spent Catalyst Particles

## 5.8 Summary

The experimental findings, presented in this chapter, provide a novel and detailed description of the Direct Coal Liquefaction reaction environment that accounts for the inability of existing coal liquefaction kinetic models to predict liquefaction results consistently or coherently. The results highlight the importance of a dispersed fluid phase, the intensity of turbulence, and mass transfer limited reaction kinetics during the opening moments of reaction on the overall kinetic scheme for coal liquefaction. Neither of these effects are included in existing DCL reaction models and consequently, these models are poor predictive tools. The results also show that optimization of coal-solvent-catalyst interactions by manipulating the intensity of turbulence, the level of catalysis and solvent composition may have a greater impact on the space time yields of desirable liquefaction products and the spectrum of products produced than variation of the extent of axial mixing per se. This latter parameter is frequently discussed in the literature without consideration of the many variables affected simultaneously.

## Chapter 6

### A Novel Reaction Model For Direct Coal Liquefaction Kinetics

#### 6.0 Introduction

The reaction models for Direct Coal Liquefaction, presented in Chapter 2, treat coal liquefaction as a purely kinetic process, controlled by intrinsic rates of product formation from specific coals. The experimental results summarized in the previous chapter demonstrate that this is an inappropriate basis for modelling reactions in such a complex reaction environment and account for the extreme specificity of these models. Non kinetic phenomena such as physical coal-solvent interactions, mass transfer effects, the intensity of turbulence, catalysis, etc. all have an influence on coal liquefaction kinetics. A novel reaction model, which quantifies the impact of these process variables on reaction kinetics, is presented in this chapter. The model predicts total conversion values, and employs as few as 4 parameters depending on the complexity of the reaction environment. Results obtained from a series of verification trials performed with bituminous and sub-bituminous coals and lignite, in diverse reaction environments are also reported.

## 6.1 An Outline of the Proposed Reaction Model

The proposed reaction model, Figure 6.1, conforms with experimental observations summarized in Chapter 5 and in the literature review, and is not radically different in appearance from previous models. If one compared this model with those listed on Table 2.9, for example, it would be best described as a combination of the models proposed by Curran et al, and Singh et al.. The major differences between the model proposed here and those proposed previously are related to the factors which control the rates of various liquefaction reactions rather than differences in the reaction scheme per se.

Three elements contribute to the formulation of the model:

1. A fraction of the coal or lignite is assumed to undergo "instantaneous" thermal decomposition yielding a spectrum of liquefaction products which include gases, liquids, partially converted material and coke. The fraction of the coal or lignite participating in these reactions is assumed to depend solely on its composition, while the product distribution is assumed to depend on the rate of hydrogen transfer to the coal or lignite particles, and the solubility of liquefaction products in the carrier solvent. In the absence of dissolved gaseous hydrogen, for example, the fraction of the coal reporting initially as liquid would decline, and the fraction reporting as coke would



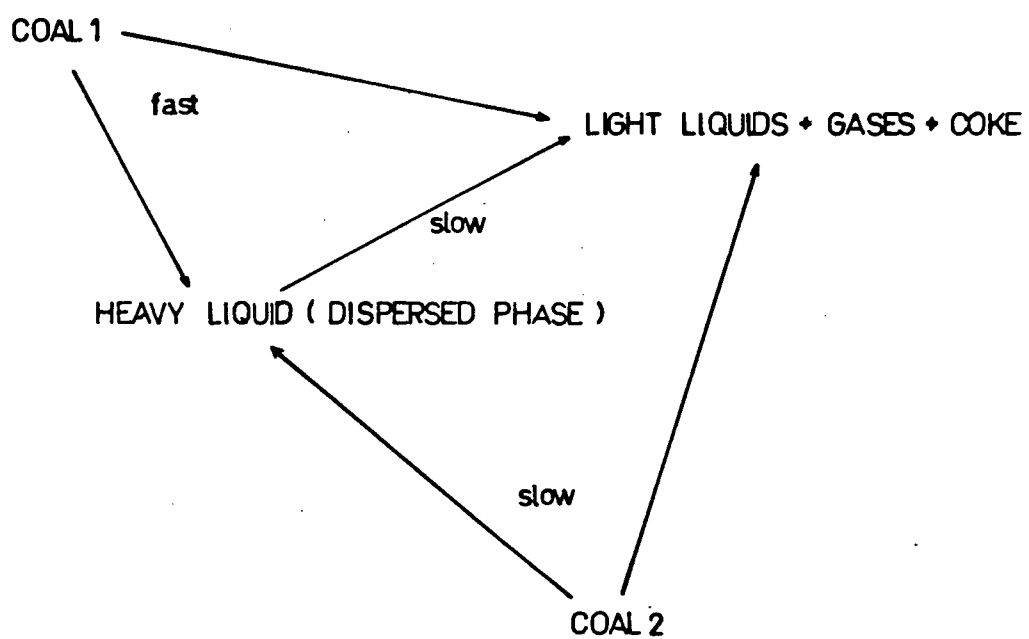


Figure 6.1: An Outline of the Model

increase, because polymerization and condensation reactions are more likely to occur under these conditions. The fraction reporting initially as partially converted material, which is insoluble in the carrier solvent, contributes to the formation of a dispersed fluid phase, and is primarily dependent on the solvency of the carrier solvent.

2. The remainder of the coal or lignite is assumed to undergo slow thermal decomposition into the various liquefaction products. These reactions are assumed to occur simultaneously with those described in 1 above. The necessity to subdivide coal into two reactive fractions can be addressed from either a maceral or molecular viewpoint. A series of liquefaction experiments performed with Byron Creek bituminous coal and vitrinite enriched Byron Creek coal for ESSO Canada Ltd., Appendix D, suggest that the vitrinite present in these coals reacts 10 times faster than the inertinite. On a molecular level, ether bond cleavage has been shown to be more rapid than alkyl (methyl) bond cleavage under DCL reaction conditions. The relative rates of these two liquefaction reactions are reflected in the relative rates of  $\text{CO}_2$ ,  $\text{CO}$ ,  $\text{CH}_4$  and  $\text{C}_2\text{H}_6$  production. Further segmentation of coal constituent reactivities, which more correctly correspond to the broad range of existing reactivities, must await more precise descriptions of coal composition and structure.

3. Material reporting to the dispersed phase initially is assumed to report eventually as either coke or converted material, depending on the rate of hydrogen transfer to the dispersed phase droplets, and variations in solvent composition with time. The rate of hydrogen transfer to the dispersed phase is proportional to the dissolved hydrogen concentration and inversely proportional to the mean droplet diameter, which is determined by the scale of turbulence. Solvent composition is altered by adduct formation, and catalytic hydrogenation and hydrogenolysis reactions.

These three elements comprise the basis for the proposed model and demonstrate the importance of the impact of process variables on liquefaction kinetics.

## **6.2 Mathematical Formulation of the Model**

### **6.2.0 Introduction**

When formulating the reaction model, it was necessary to resort, in part, to empirical correlations because general theories for predicting liquid-liquid solubility do not exist and because conversion is such a primitive measure of the extent of coal reaction.

"Unconverted" material, for example, includes the partially reacted material comprising the dispersed liquid phase, coke, and unreacted coal.

These components are not readily separated. So, in addition to being empirical, the model cannot distinguish material which always reports to the dispersed phase from unreacted coal. Only material which can either report to the continuous phase or the dispersed phase, depending on reaction conditions, is attributed to the dispersed phase. Thus, the model underestimates the influence of the dispersed phase on coal liquefaction reactions. The equations employed in the model reflect these shortcomings. Many of the equations were developed and refined by comparing model predictions with experimental conversion values during preliminary verification trials. Only the final equations are presented below.

### 6.2.1 Preliminary Reactions

The thermal decomposition of the most reactive species present in a coal or lignite is so rapid that it can be viewed as an instantaneous process. In the absence of dissolved gaseous hydrogen, these reactions may lead to negative conversions, if insoluble adducts are formed. In the presence of hydrogen, a greater fraction of the coal reports as converted material. The extent of the reduction in unconverted material is assumed to be proportional to the rate of hydrogen transfer to the coal particles. The rate of hydrogen transfer per unit mass of coal,  $K'$ , can be expressed as

$$K' = \frac{\bar{S}h^\circ D H A'}{\bar{d}^\circ \rho_{\text{coal}}} \rho_{\text{solvent}} \quad (6.1)$$

- where  $\bar{Sh}^\circ$  = the initial average Sherwood number
- $D$  = the diffusivity of hydrogen in the solvent
- $\bar{d}^\circ$  = the initial average mean diameter of the coal particles
- $\rho_{\text{solvent}}$  = the solvent density
- $\rho_{\text{coal}}$  = the bulk coal density
- $H$  = the dissolved hydrogen concentration per unit mass of solvent
- $A'$  = the surface area per unit volume of coal including pores

It should be noted here that  $A'$  varies appreciably with solvent composition and coal type, and can only be estimated within an order of magnitude. Thus for the purpose of the model, the coal fraction reporting initially as unreacted material,  $J_1$ , is defined as

$$J_1 = Y(2) - Y(4) \frac{D H \bar{Sh}^\circ}{\bar{d}^\circ \rho_{\text{coal}}} \rho_{\text{solvent}} \quad (6.2)$$

- where  $Y(2)$  = the fraction of the coal reporting as unreacted material in the absence of hydrogen
- $Y(4)$  = an empirical constant which relates hydrogen transfer to an extent of conversion.

In the absence of pertinent data this equation can be simplified to

$$J_1 = Y(2) - Y(4) D H \quad (6.3)$$

with a possible reduction in accuracy.

The coal or lignite fraction reporting to the dispersed phase initially is more difficult to estimate, as mentioned previously, and can only be observed if variables other than temperature and pressure are varied. It was noted in Chapter 5 that an optimum catalyst to stirring rate ratio exists. This was attributed to the existence of an optimum ratio of catalytic solvent hydrogenation to dispersed phase hydrogenation. At the optimum ratio of these reactions the amount of material reporting to the dispersed liquid phase is minimized. The dispersed phase, as defined by the model, ceases to exist at the optimum ratio. If one considers possible kinetic schemes for these two reactions, the rate of catalytic solvent hydrogenation,  $R_1$ , can be expressed as

$$R_1 = K_1 \text{ Cat } H \quad (6.4)$$

and the rate of dispersed droplet hydrogenation,  $R_2$ , can be expressed as

$$R_2 = \frac{K_2 D H \bar{S}h_{\text{drop}} \rho_{\text{solvent}}}{\bar{d}_{\text{drop}} \rho_{\text{drop}}} \quad (6.5)$$

where  $K_1$  and  $K_2$  are constants

Cat is the total mass of active catalyst present in the reactor

Droplet diameter is determined by the intensity of turbulence. The relationship between turbulence and drop diameter is well defined for stirred tanks. Calderbank<sup>[122]</sup> and Taverides et al<sup>[125]</sup> found that

$$d_{\text{droplet}}^{\text{max}} \propto F^{-1.2} \quad (6.6)$$

Taverides et al<sup>[125]</sup> also found that data, obtained by agitating oil-water mixtures with a six bladed turbine impeller, correlated well with

$$d_{\text{drop}}^{\text{max}} = .06 \frac{\sigma^{0.6} D^{-0.8} F^{-1.2}}{\rho^{0.6}} \quad (6.7)$$

where  $F$  = stirring frequency

$D$  = impeller diameter

$\sigma$  = interfacial tension

If one asserts that the mean droplet diameter is proportional to the maximum diameter the reaction rate ratio becomes

$$\frac{R_1}{R_2} = \frac{K_4}{D \text{ Sh}} \frac{\text{Cat}}{F^{2.4}} \quad (6.8)$$

This ratio is readily normalized with respect to an optimum by dividing it by the difference that would result if the intensity of turbulence were so large that droplets evolving from coal particles would not be broken up at the impeller. The fraction of the coal or lignite reporting to the dispersed phase,  $J_2$ , is proportional to some function of the ratio

$$J_2 \propto f \left( \frac{\left[ \frac{\text{Cat} + Y(6)}{\text{Sh}_o F_o^{2.4}} - Y(5) \right]}{\left[ \frac{\text{Cat} + Y(6)}{\text{Sh}_o F_o^{2.4}} - Y(5) \right]} \right) \quad (6.9)$$

where  $Y(6)$  = the residual catalytic effects present in the reactor  
+ the catalytic effect associated with minerals present  
in the coal

$Y(5)$  = the optimum reaction rate ratio

$F_o$  = the stirring rate at which droplets evolving from the  
coal become unstable

$\text{Sh}_o$  = the Sherwood Number associated with the droplets evolving  
from the coal

Experimentally, it was found that



$$\begin{aligned}
 J_2 &= Y3 & \text{if } F < F_o \equiv Y(1) \\
 J_2 &= Y3 \left( \frac{\left( \frac{\text{Cat} + Y(6)}{\text{Sh } F^{2.4}} - Y(5) \right)^2}{\left( \frac{\text{Cat} + Y(6)}{\text{Sh}_o F_o^{2.4}} - Y(5) \right)^2} \right) & \text{if } \frac{\text{Cat} + Y(6)}{\text{Sh } F^{2.4}} < Y(5) \\
 J_2 &= Y3 \left( \frac{\text{Cat} + Y(6)}{\text{Sh } F^{2.4} Y(5)} - 1 \right)^{0.5} & \text{if } \frac{\text{Cat} + Y(6)}{\text{Sh } F^{2.4}} > Y(5) \quad (6.10)
 \end{aligned}$$

where  $Y3 = Y(3) \cdot \text{TEMP} \cdot \text{Sh}_o H$

$Y3$  = a parameter relating divergence from the optimum ratio to the fraction of the coal reporting to the dispersed phase initially

One would expect  $Y(3)$  to vary primarily with solvent composition. Combining equations 6.2 and 6.10 yields the coal fraction reported as unconverted material at zero time,  $J$ .

$$J = J_1 + J_2 \quad (6.11)$$

### 6.2.2 Second Stage Reactions

Equations 6.2 and 6.10 describe the disposition of coal components at zero time. One might assume when designing the framework for subsequent, kinetically-controlled reactions that either a constant fraction of the coal or the initially unconverted coal is reactive under

Direct Coal Liquefaction reaction kinetics. However, this would ignore the possibility that polymerization and condensation reactions, which result in coke formation, are more likely to occur as the fraction of the coal reporting initially as "unconverted" material increases. Such retrogressive reactions are most likely to occur in the dispersed phase droplets, because these droplets contain high concentrations of large reactive molecules. One must expect the reactive fraction,  $Y_7$ , to decrease as the initially unconverted fraction increases. This assumption led to the development of equation 6.12

$$Y_7 = Y(7) + \frac{Y(8)}{J} \quad (6.12)$$

where  $Y(7)$  and  $Y(8)$  are parameters which are constant for any given coal.

A kinetic expression for the second stage reactions is defined in a straightforward manner.

The reaction rates for the dispersed phase and the slowly reacting coal cannot be distinguished. So, the reaction kinetics for these two types of material are combined in a single kinetic expression. First order reaction kinetics, a typical assumption in Direct Coal Liquefaction models, are also assumed in this model. Thus

$$\frac{\partial C}{\partial t} = - \kappa C \quad (6.13)$$

where C = the reactive fraction of a coal remaining unreacted  
at a given time

$\kappa$  = the rate constant

It would be natural, at this point, to assert that the rate constant,  $\kappa$ , has an Arrhenius temperature dependence. This assumption is frequently made in published models, despite the arbitrary definition of the rate constant. One would not expect such a rate constant to exhibit an Arrhenius temperature dependence, and this proved to be the case when the model was fitted to data selected from the literature - Figure 6.2. However, Arrhenius behaviour can be obtained if the rate constant is correlated by equation 6.14, as shown on Figure 6.3.

$$\kappa = [k_0 \exp(-\frac{E}{RT})]^{1/J_1} \quad (6.14)$$

The form of equation 6.14 suggests that only the aggregate behaviour of the coal follows an Arrhenius pattern and that the observed rate constant reflects the fact that coal constituents which do not react initially are more refractory than the coal itself. Consequently, the activation energy rises and the rate of liquefaction reactions slows. This equation conforms with the findings of Szladow et al<sup>[49]</sup> who showed that the apparent activation energy for liquefaction reactions increases with the extent of conversion. The slopes of the curves on Figure 6.3 are also noteworthy. Trials employing hydrogen gas have an Arrhenius slope

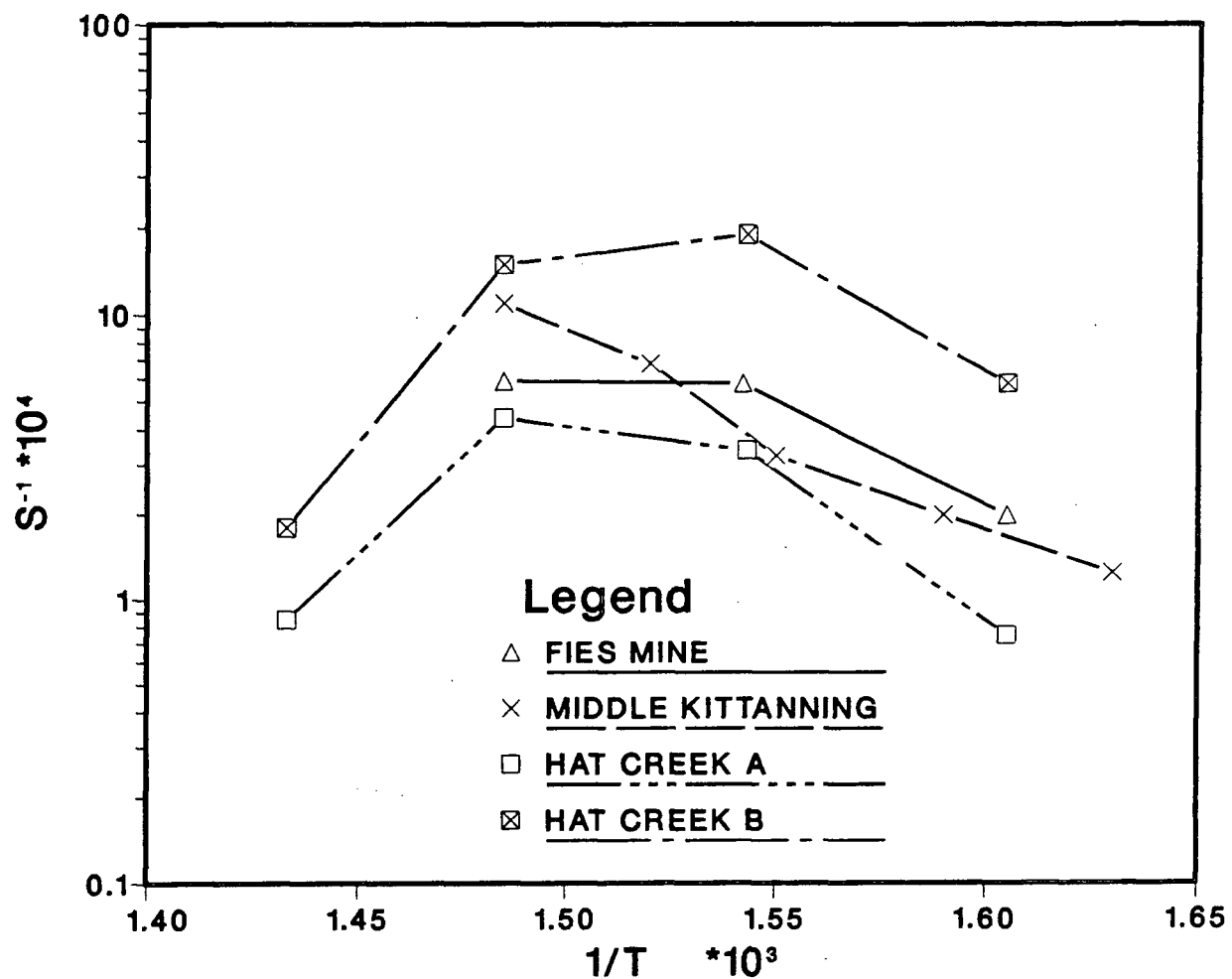


Figure 6.2: The Temperature Dependence of DCL Rate Constants

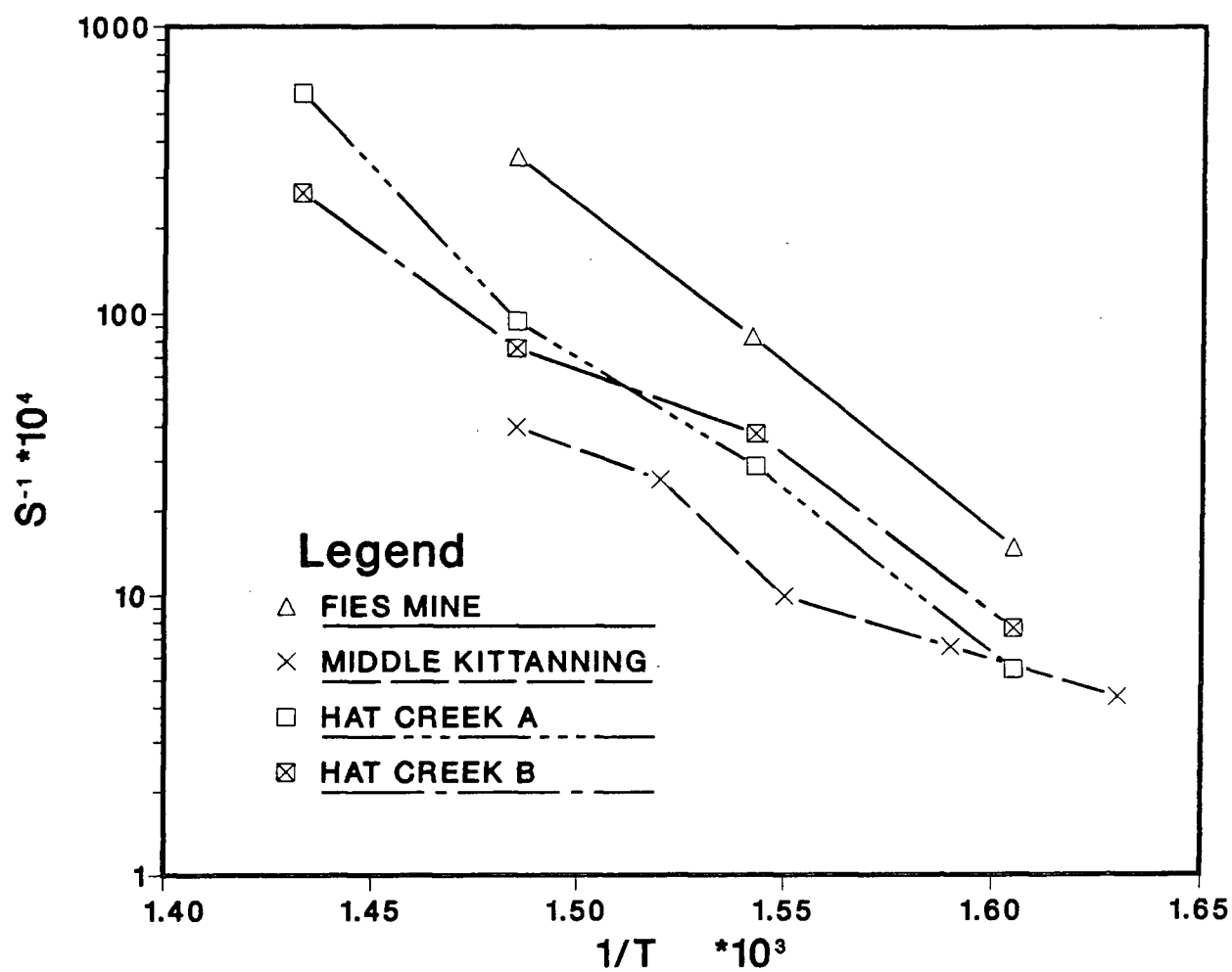


Figure 6.3: The Modified Arrhenius Dependence Of DCL Rate Constants

$\frac{E}{R} \approx -2.65 \times 10^4$ , while the trials not employing hydrogen have a slope of  $-1.38 \times 10^4$ . Despite the empirical nature of this correlation it is probable that the drop in activation energy is due to diffusion control of the liquefaction reaction kinetics in the latter case.

### 6.2.3 Residence Time Distributions

The final equation required in order to complete the model is one which couples the slurry residence time distribution with the kinetic expression, equation 6.13. Arbitrary slurry residence time distributions, which match distributions found in complex reactors, can be digitized and combined with the model. Simple distributions, such as the plug flow or dispersed flow distributions employed in the experimental program, can be resolved analytically to yield equations 6.15 and 6.16 respectively.

$$\% \text{ Conversion} = 100 - 100 J (e^{-kt} Y7 + 1.0 - Y7) \quad (6.15)$$

$$\% \text{ Conversion} = 100 - 100 J \left[ Y7 \left( \frac{e^{-kt_1} - e^{-kt_2}}{(t_2 - t_1)^{\kappa}} \right) + 1.0 - Y7 \right] \quad (6.16)$$

### 6.2.4 Summary

Equations 6.2, 6.10, 6.12, 6.14 comprise a novel reaction model for interpreting coal liquefaction data. Such a radical departure from the nature of existing models would not be feasible in the absence of the

liquefaction data summarized in Chapter 5. The influence of these findings, particularly the role of molecular hydrogen during the initial liquefaction sequence, and the presence of a dispersed liquid phase, on the understanding of DCL kinetics cannot be over emphasized.

### 6.3 Verification of the Model

#### 6.3.0 Introduction

The reaction model was verified by regressing sets of batch coal liquefaction data. The objective function was equation 6.17, where total coal conversion

$$\epsilon = \sum \left| \frac{TCC_{\text{exptl}} - TCC_{\text{predicted}}}{TCC_{\text{exptl}}} \right| \quad (6.17)$$

values estimated by equations 6.2, 6.10, 6.12, 6.14, and 6.15 were compared with experimental values. This function was minimized using a suite of non linear optimization programs, which adjusted  $Y(n)$  values subject to the constraint that each  $Y(n)$  must contribute significantly to the reduction in the percent difference between the experimental and predicted conversion values.

This work was hampered to varying degrees by the uncertainty of coal liquefaction data, the failure of some researchers to report

pertinent data, and the general lack of data with respect to the physical properties of coal liquids. Inaccurate data, for example, may lead to the selection of a set of parameters which fit the data but do not conform with expectation. Alternatively, a large number of parameter sets may be found to fit the inaccurate data equally well. Even when precise data are employed in verification trails, more than one set of optimum parameters may be found. However, in this case, the preferred set can be selected objectively. The parameter set with the most broadly distributed differences is preferred, unless there is some reason to question the accuracy of a single data point. This problem becomes most severe if the number of parameters is large, if there are few data points, or if the data is very imprecise.

The failure of investigators to report pertinent data or the absence of such data, necessitated a number of modifications in the equations which comprise the model. Hydrogen solubilities and diffusion coefficients in various liquefaction media, and the density of coal liquids are the principal physical properties required for input into the model. These data are frequently unavailable. In such cases, one must resort to approximations. Hydrogen concentration in a liquid is proportional to pressure over a narrow temperature range. Diffusion coefficients are proportional to temperature and inversely proportional to solvent viscosity, or proportional to the diffusion coefficient of another species. Consequently,  $J_1$  was correlated variously as



$$J_1 = Y(2) - Y(4) D H \quad (6.3)$$

$$J_1 = Y(2) - Y(4) \text{Temp } H \quad (6.18)$$

$$J_1 = Y(2) - Y(4) D \quad (6.19)$$

depending on the availability of data. The hydrogen concentration in the solvent, H, was assumed to be either equal to or proportional to the saturated hydrogen concentration in the various solvents. Hydrogen solubilities in tetralin were obtained from published data, Figure 2.19; hydrogen solubilities in SRC oil were estimated using equation 2.7. Considering the deportment of phases in Solvent 1, the continuous phase was assumed to be comparable to tetralin. Hydrogen solubilities were obtained accordingly. Viscosity data cannot be obtained or estimated with certainty so it was assumed to be constant in equation 6.18. This is only valid for a narrow range of temperatures. One set of data obtained from the literature did not employ hydrogen. The diffusivity of tetralin was assumed to be proportional to that of hydrogen, equation 6.19. The concentration of tetralin, expressed as moles  $\cdot \text{Kg}^{-1}$ , is constant by definition. These changes in the equations comprising the model may have a negative impact on the predictive accuracy of the model but were an essential element in the verification process.

### 6.3.1 Experimental

Verification trials were performed first with batch liquefaction results obtained from this work and from the literature. Results obtained from semi-batch coal liquefaction experiments, which were designed to simulate axially mixed reactors, were then subjected to qualitative verification trials in order to examine the impact of residence time distribution on model predictions. Liquefaction data obtained from flow apparatus were excluded from these tests because coal conversion, mean residence time and residence time distributions for slurries, and reactor temperature profiles are too poorly defined in these reactors.

The reaction conditions and reactor configurations associated with the data sets selected from the literature are listed on Table 6.1. These particular data sets were selected because:

1. tetralin was used as the liquefaction solvent.
  - tetralin is one of the few liquefaction solvents for which required physical properties are known or can be estimated. See section 2.4.
2. these data are extensive and include a broad range of temperatures.
3. the slurry residence times and residence time distributions are well defined.

TABLE 6.1

Data Sets Selected for Model Verification

Reference	Reactor	Coal	# Data Points	Reaction Conditions
Shalabi et al <sup>[45]</sup>	A Slurry Injected, 300 ml A.E. Autoclave -D = 3.2 cm -F = 25 s <sup>-1</sup>	Fies Mine Ky. Seam #9 (high volatile bituminous)	13	Solvent = tetralin Temp. = 350,375, 400°C Hydrogen Pressure = 13.2 MPa Analysis Solvent = THF
McElroy et al <sup>[126]</sup>	Shaken Micro-reactor containing steel balls	Hat Creek A (sub-bituminous)  Hat Creek B (sub-bituminous)	15  17	Solvent = tetralin Temp. = 350,375, 400, 425°C  Hydrogen Pressure = 5.5 MPa (cold) Analysis Solvent = Pyridine
Szladow et al <sup>[49]</sup>	Shaken Micro-reactor	Middle Kittanning (high volatile bituminous)	23	Solvent = tetralin Temp. = 340,355,370 385,400°C Hydrogen Pressure = 0.00 MPa Analysis Solvent = Pyridine

Four coals, two bituminous and two sub-bituminous coals, and three reactor types are represented.

### 6.3.2 Results and Discussion

The overall fit of the model, to the experimental data, as indicated by Figures 6.4 to 6.14, is quite good. The model accurately predicts total conversion values, for a variety of bituminous and sub-bituminous coals, and lignite, in diverse reaction environments. Only at long mean residence times does the model occasionally diverge from the experimental data. This divergence arises because the model does not include equations which account for the possible reduction in liquefaction product solubility in the carrier solvent over time. Nevertheless, the results confirm the generality of the proposed two stage reaction model. Shalabi et al<sup>[45]</sup>, for example, fitted a single stage coal dissolution model to their liquefaction results. The model, shown on Table 2.9, correlates total conversion values with 7 parameters obtained by regressing product distribution data. Even in this case, the model proposed here fits the data better, Figure 6.4, and employs only 4 parameters. Clearly, mass transfer controlled instantaneous decomposition followed by slow kinetically controlled dissolution of the remaining unconverted coal fraction provides a general framework for analysing liquefaction reactions.

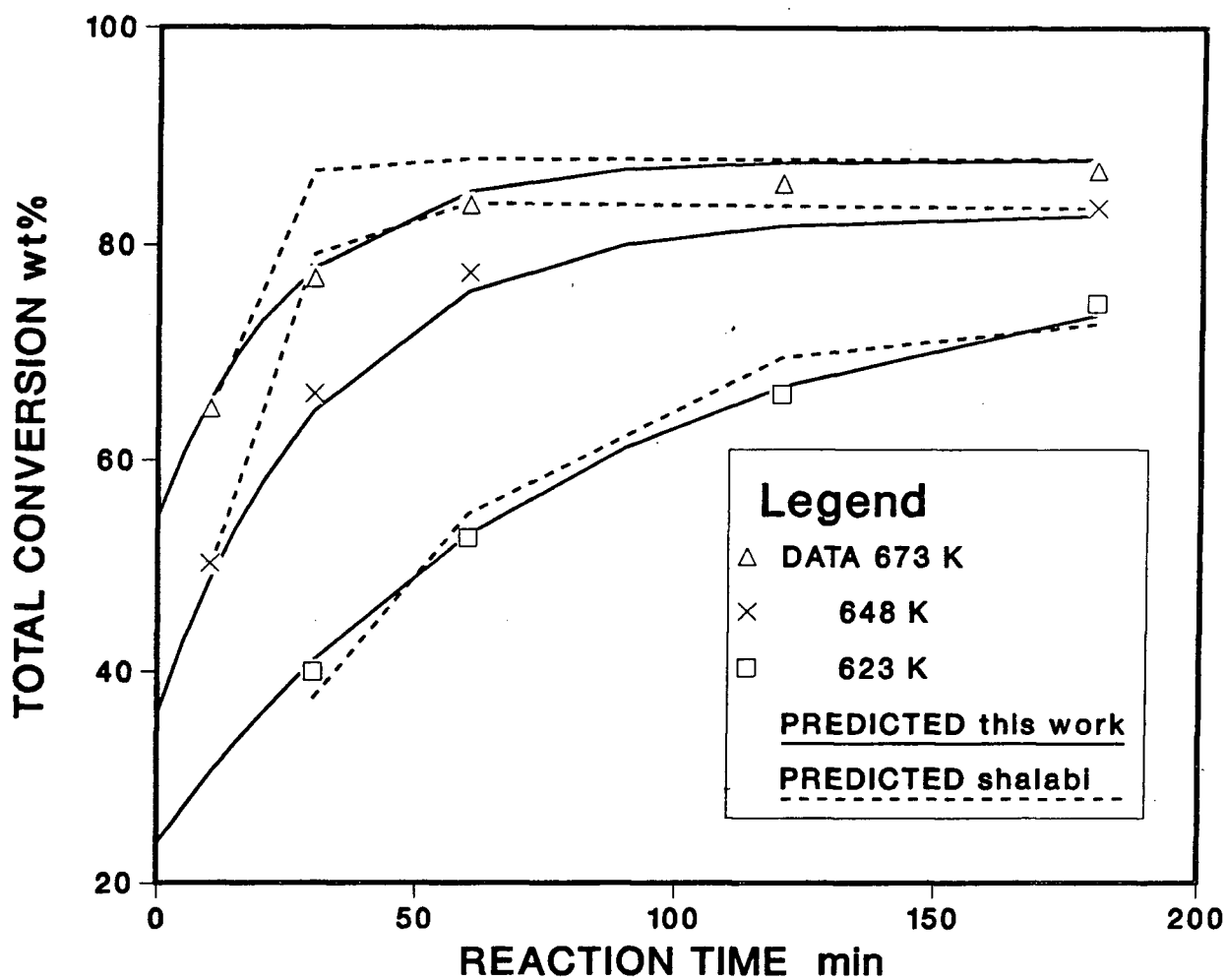


Figure 6.4: Result Summary for a Verification Trial with Fies Mine Coal

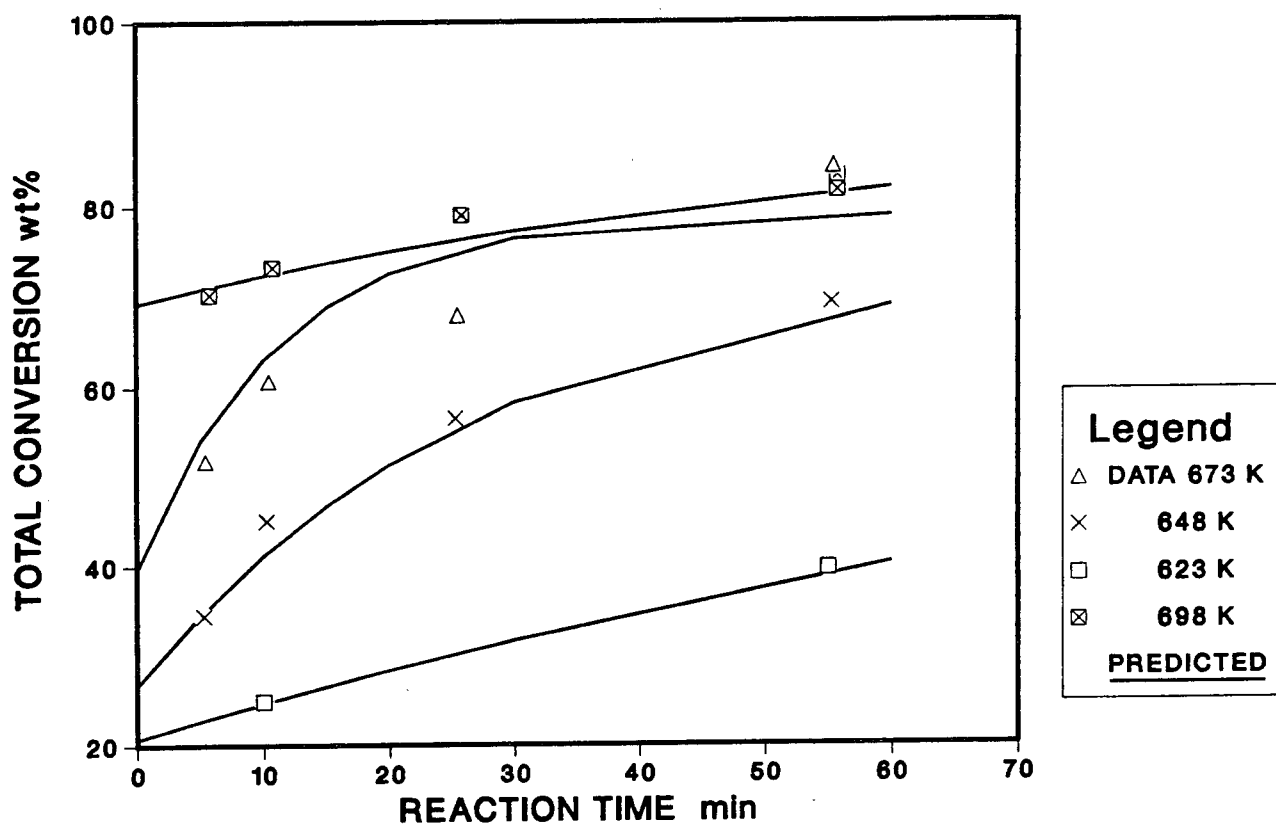


Figure 6.5: Result Summary for a Verification Trial with Hat Creek A Coal

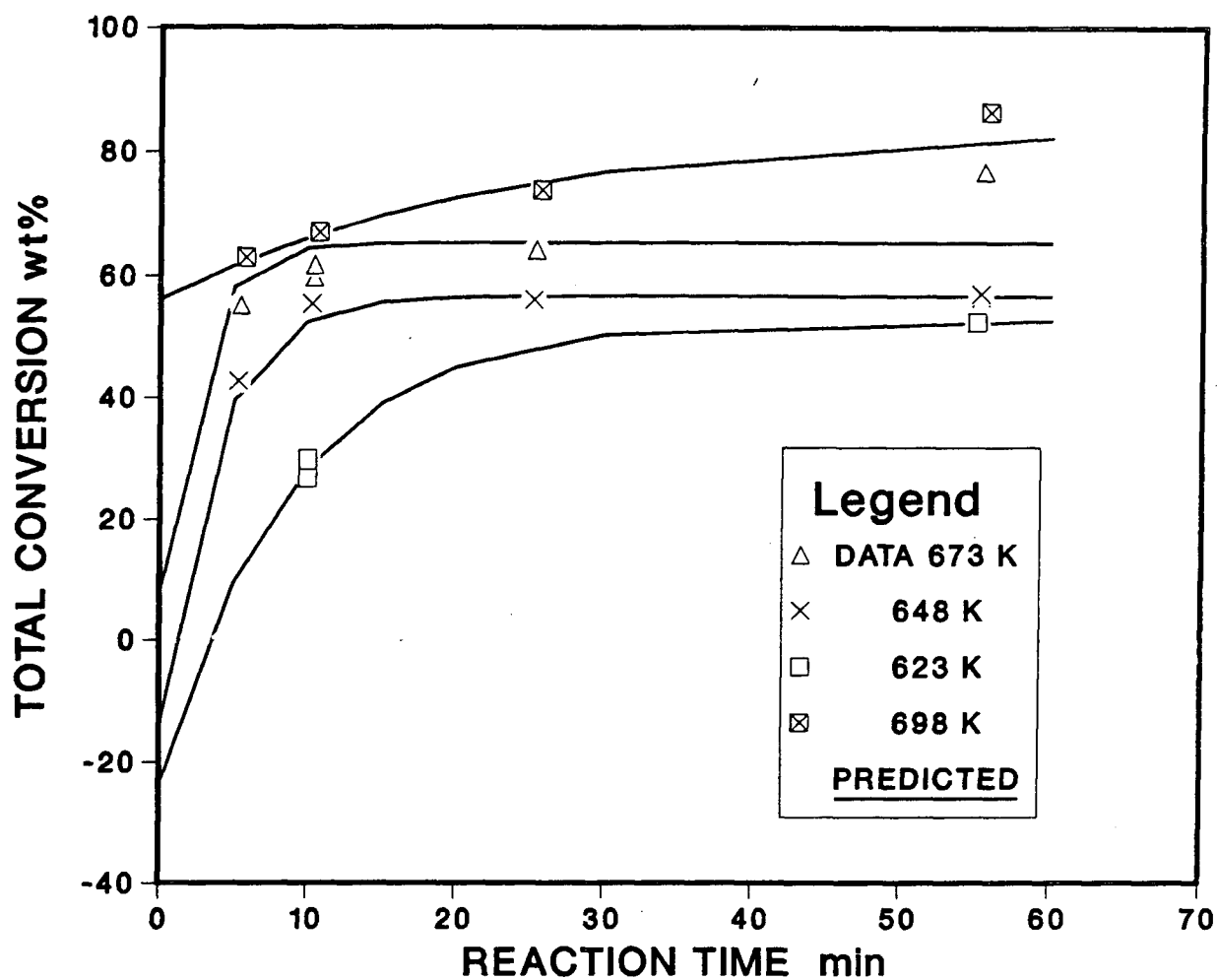


Figure 6.6: Result Summary for a Verification Trial with Hat Creek B Coal

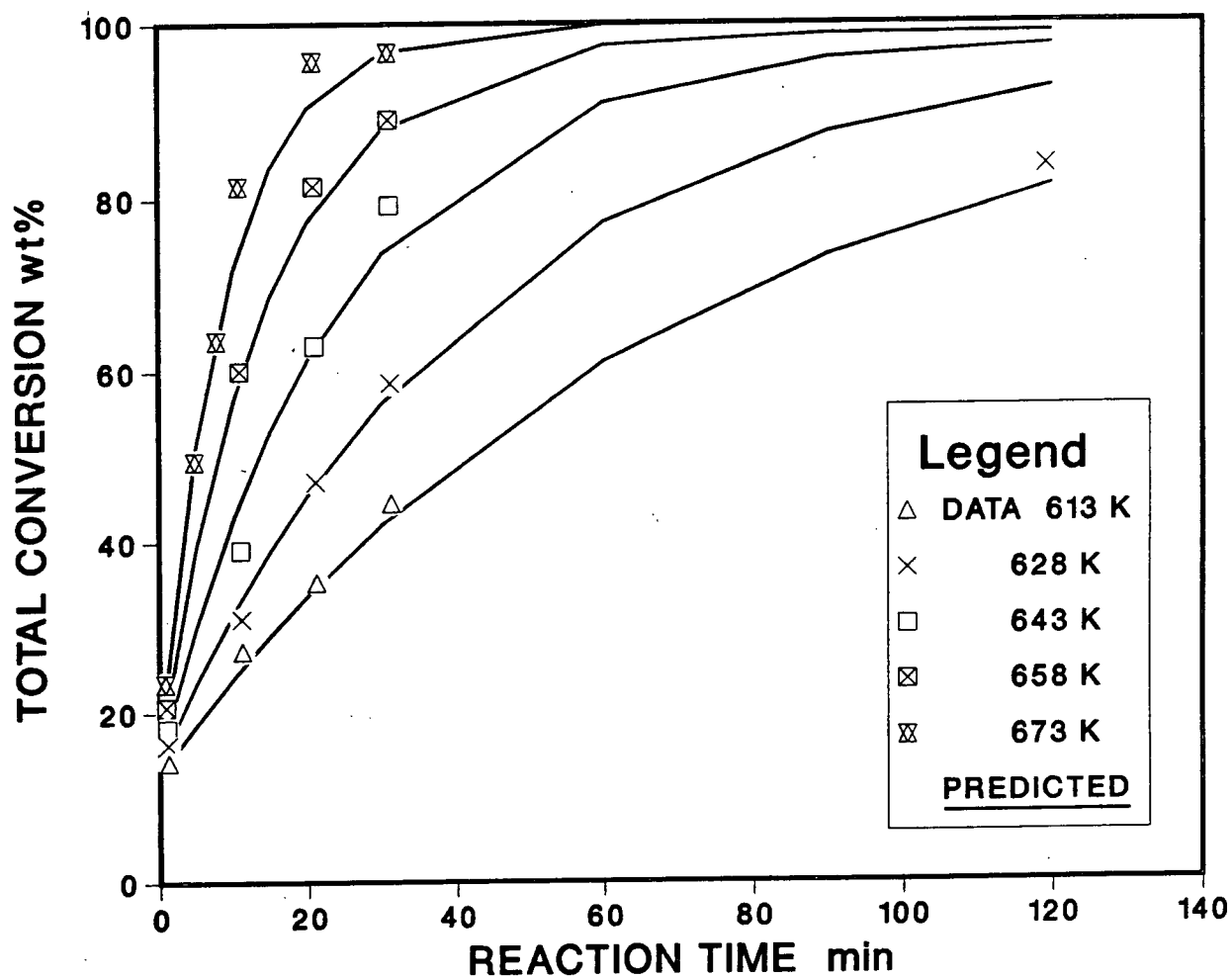


Figure 6.7: Result Summary for a Verification Trial with Middle Kittanning Coal



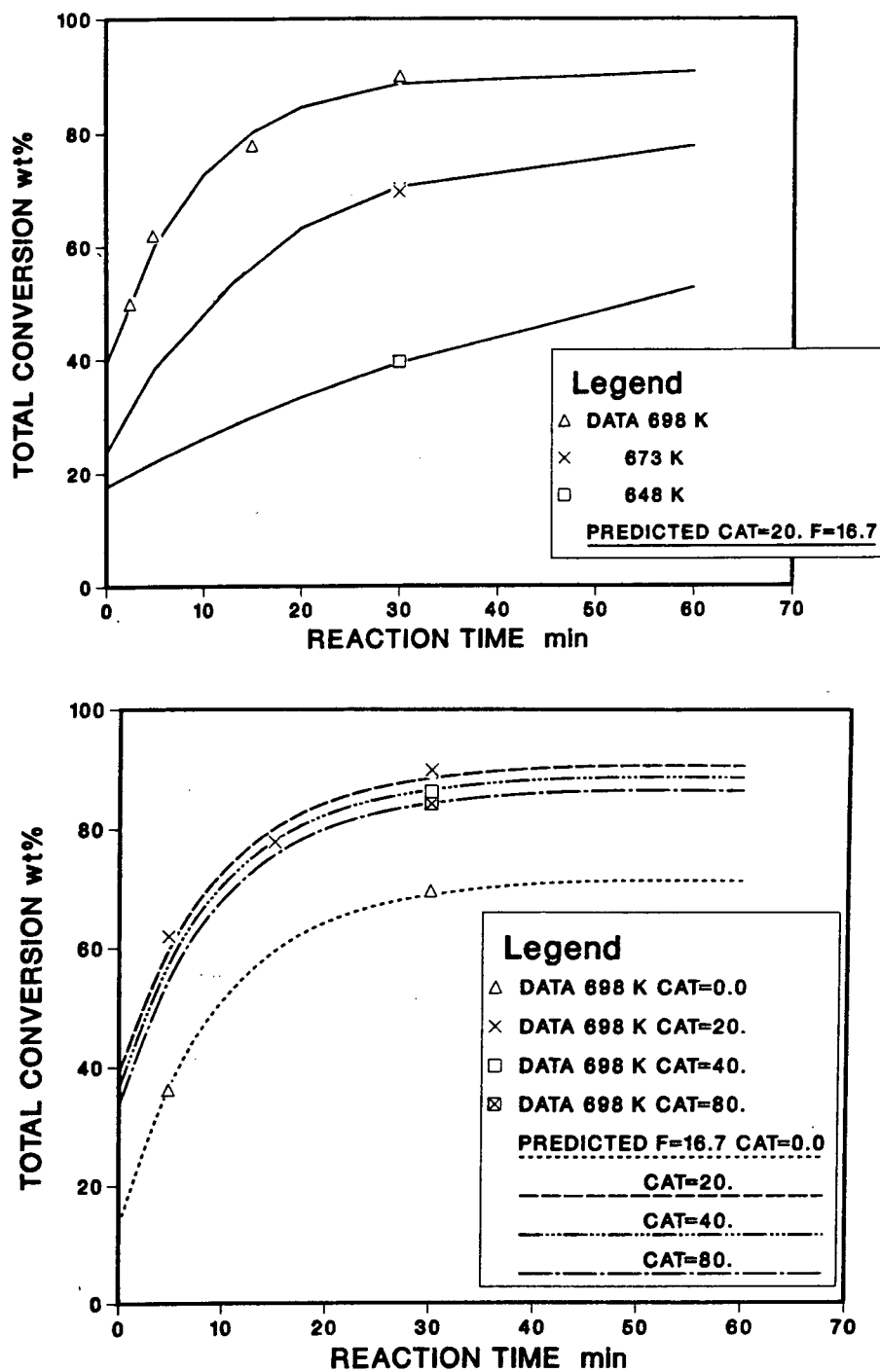


Figure 6.8: A Comparison of Predicted and Observed Results for Forestburg Coal Liquefied in Solvent 2 (I)

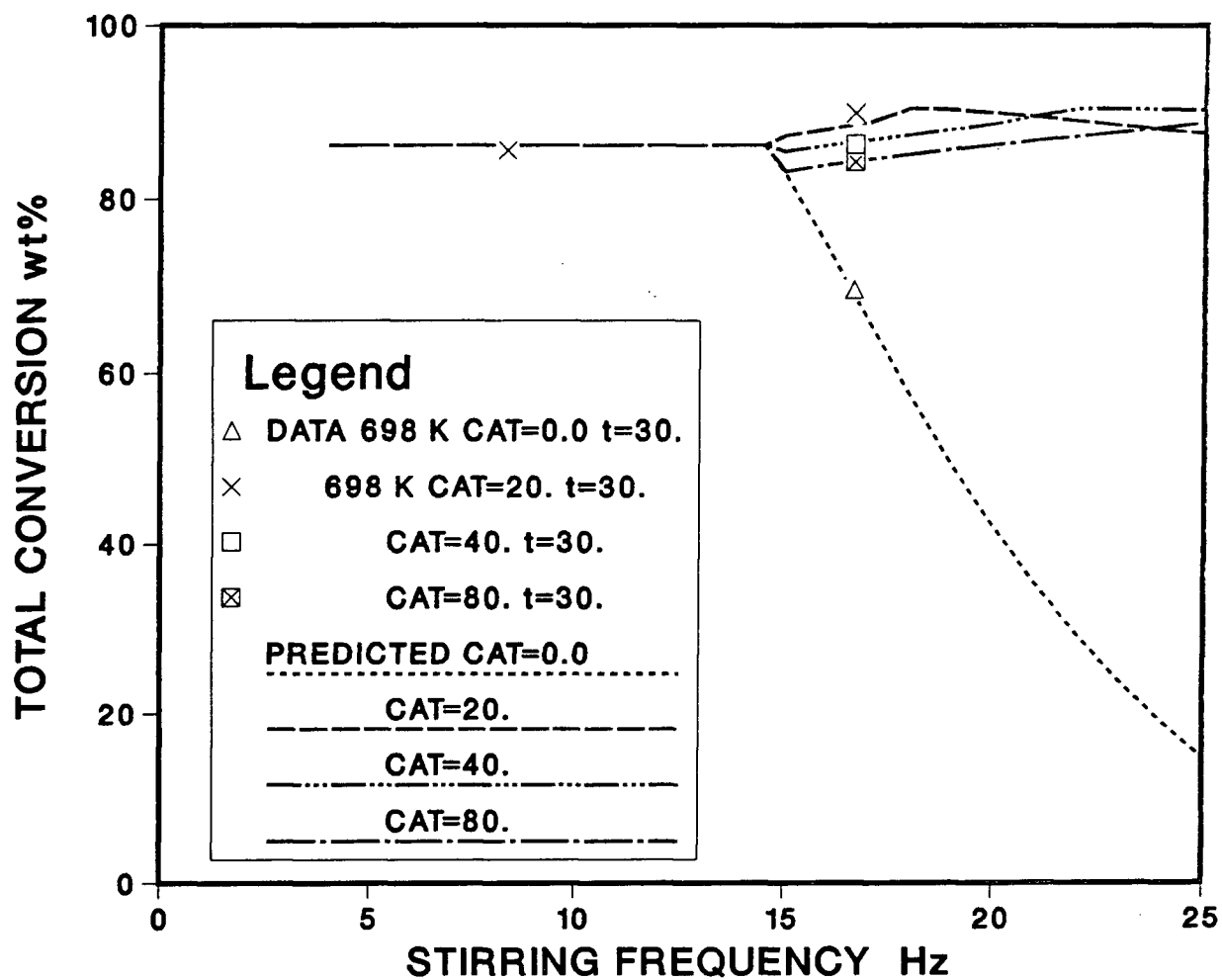


Figure 6.9: A Comparison of Predicted and Observed Results for Forestburg Coal Liquefied in Solvent 2 (II)

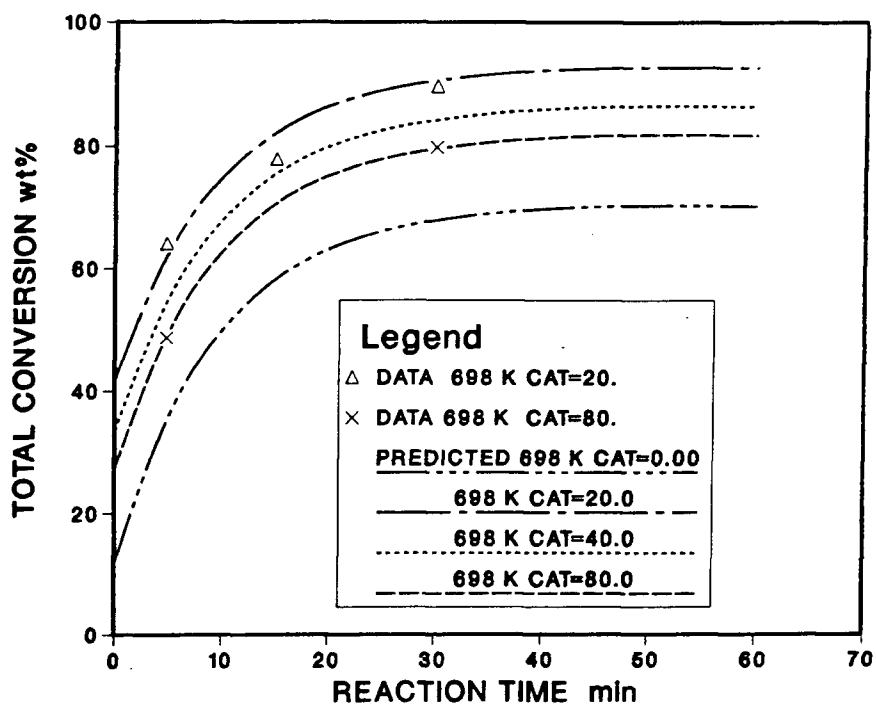
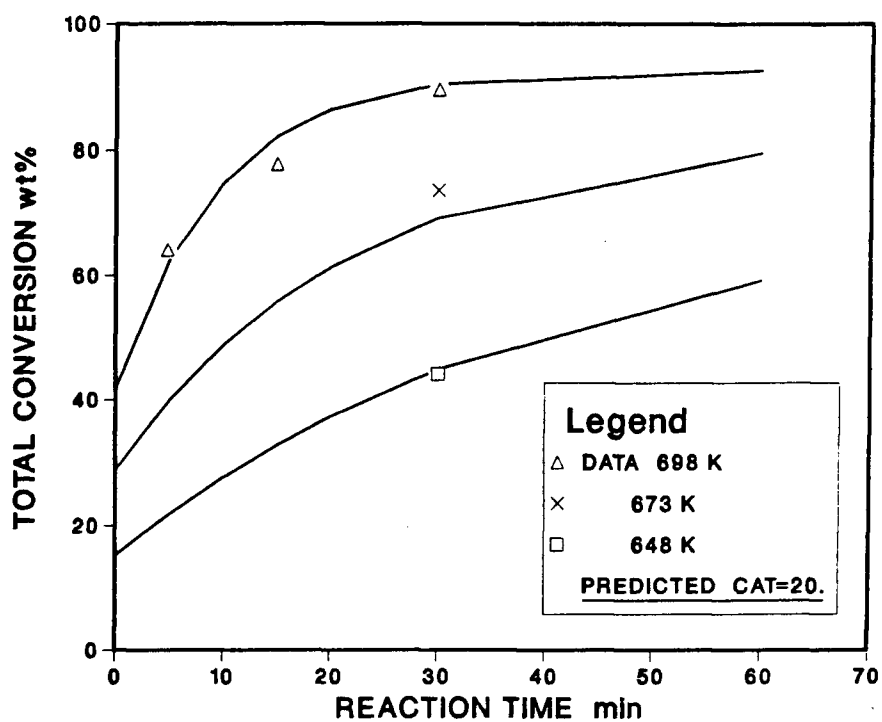


Figure 6.10: A Comparison of Predicted and Observed Results for Forestburg Coal Liquefied in Solvent 1 (I)

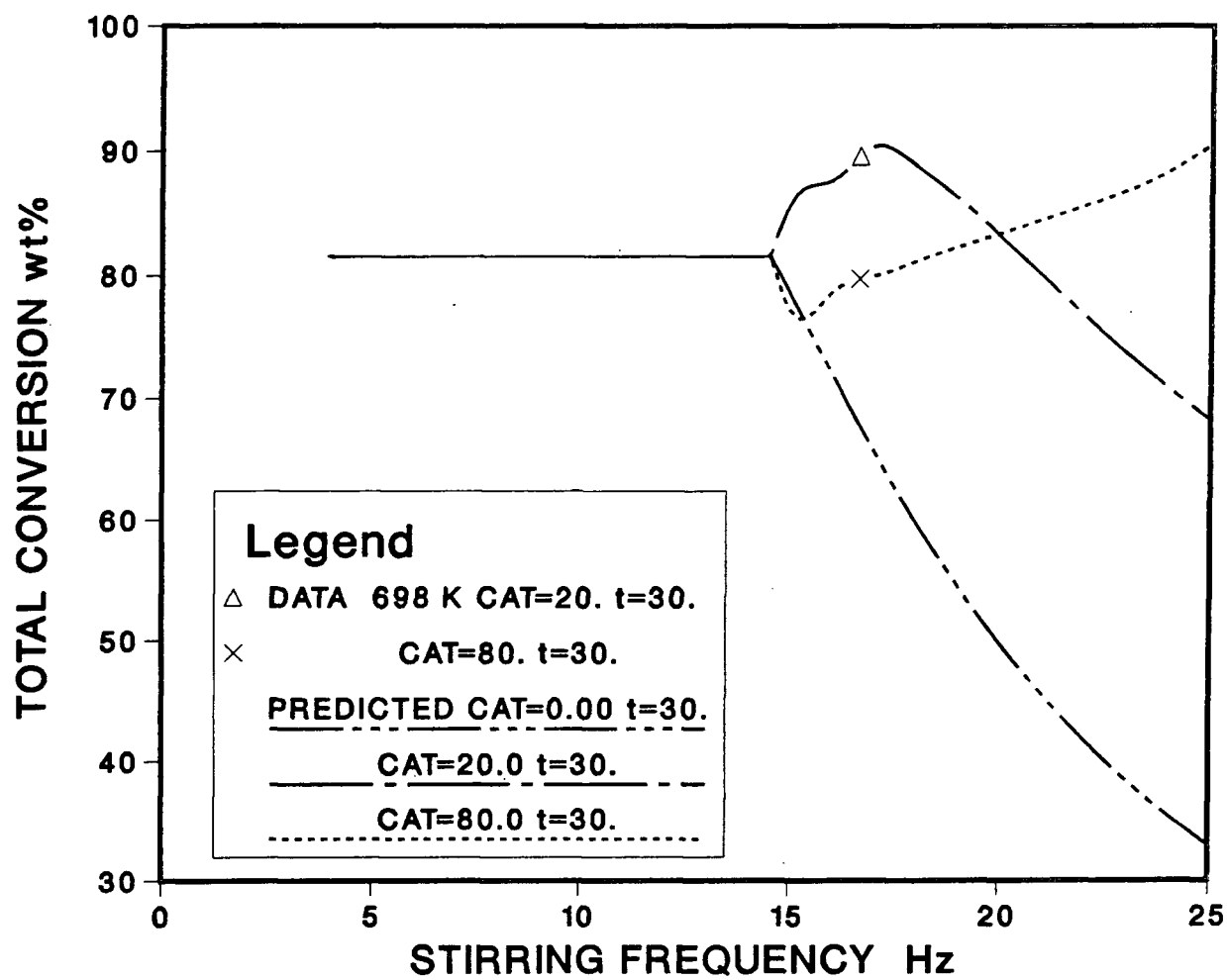


Figure 6.11: A Comparison of Predicted and Observed Results for Forestburg Coal Liquefied in Solvent 1 (II)

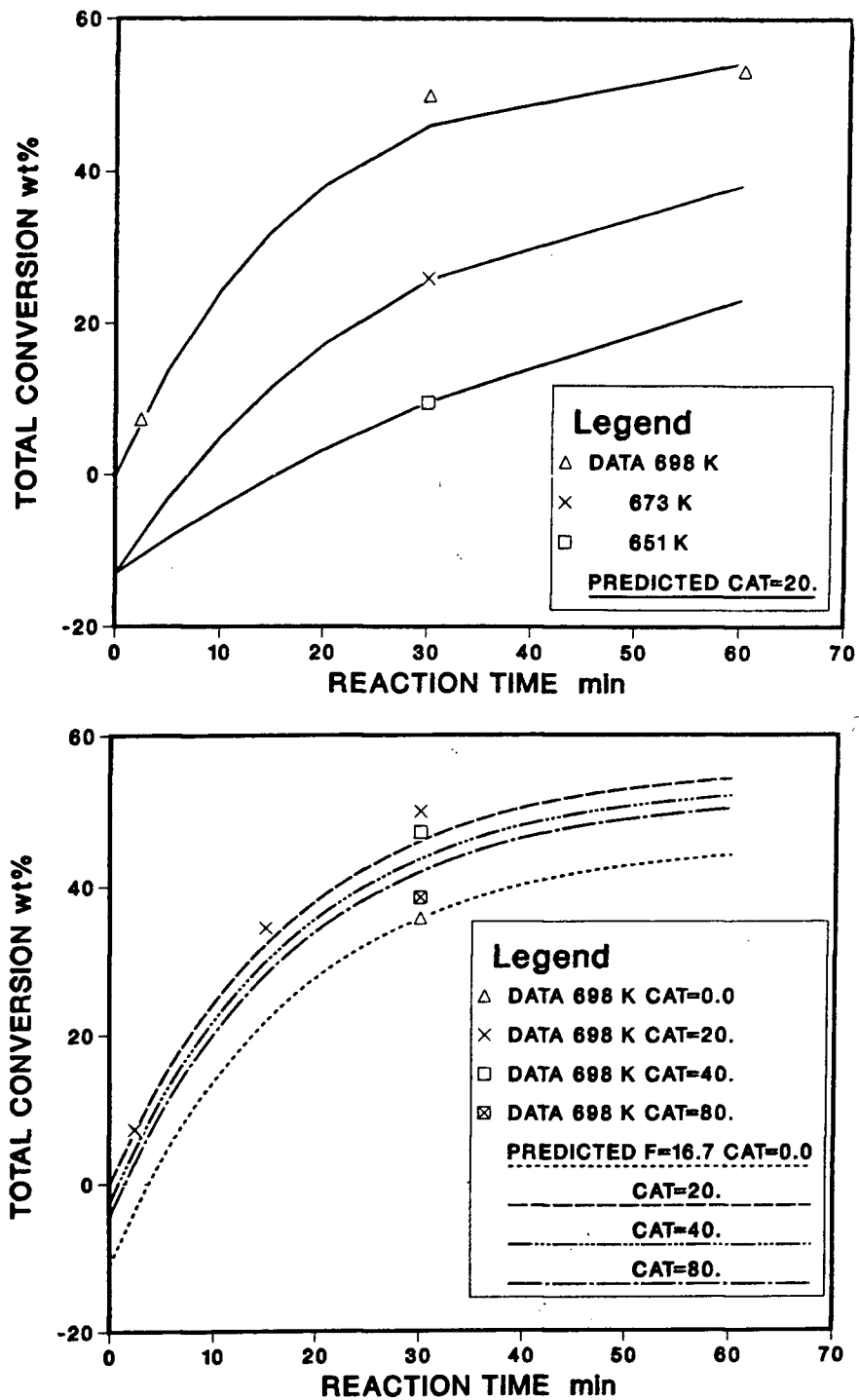


Figure 6.12: A Comparison of Predicted and Observed Results for Byron Creek Coal Liquefied in Solvent 2 (I)

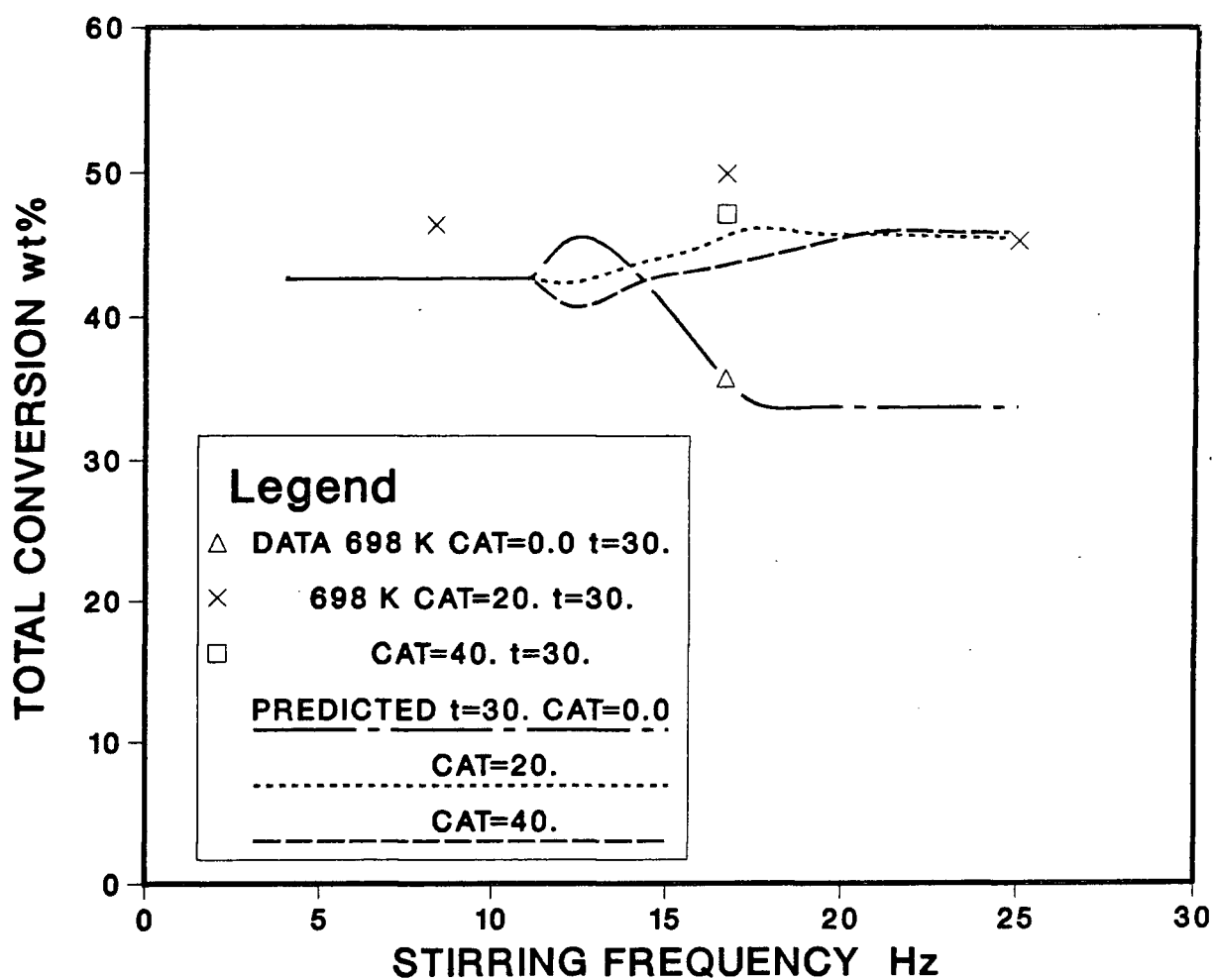


Figure 6.13: A Comparison of Predicted and Observed Results for Byron Creek Coal Liquified in Solvent 2 (II)

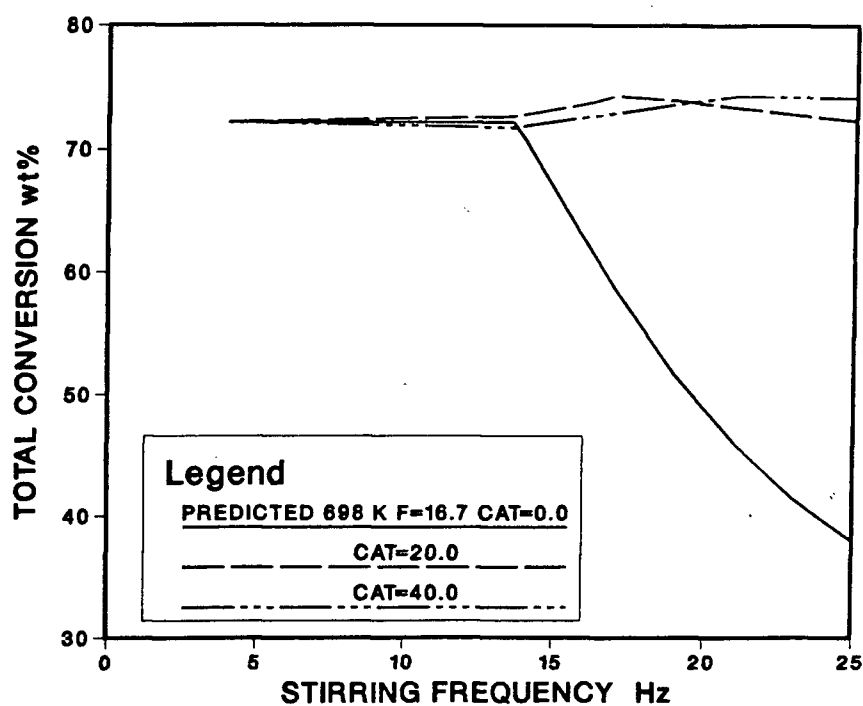
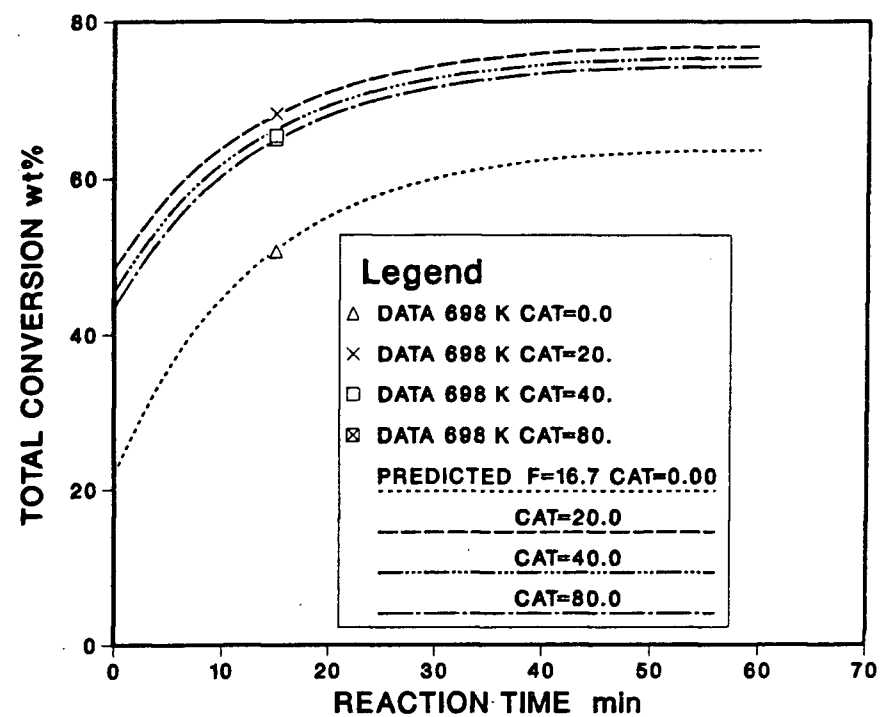


Figure 6.14: Result Summary for a Verification Trial with Saskatchewan Lignite

The optimum parameter sets for the batch verification trials, Table 6.2, also confirm the generality of the proposed two stage reaction model. Despite the large differences in the chemical composition and structure of these coals and lignite, and the many differences in the reaction environments, the liquefaction behaviour of these species can be characterized in a consistent and coherent manner.

The frequency factor for the rate constant,  $Y(9)$ , varies from  $7.6 \times 10^{14} \text{ s}^{-1}$  for the more slowly reacting sub-bituminous coals and lignite, up to  $4.6 \times 10^{15} \text{ s}^{-1}$  for the more quickly reacting high volatile bituminous coals. The only exceptions are Middle Kittanning coal, which was reacted in the absence of hydrogen (the rate of liquefaction reactions were assumed to be controlled by diffusion in this case) and Byron Creek coal which is a partially oxidized bituminous coal and consequently expected to react more slowly. The frequency factors correlate well with,  $Y(8)$ , the parameter that accounts for the tendency of the coal to undergo retrogressive reactions as the fraction of coal reporting initially as unconverted material increases. One would expect coals that have a lower tendency to undergo retrogressive reactions would have a higher net rate of production for "converted" material and this proves to be the case. Fies Mine and Hat Creek A coals are the least sensitive to  $Y(8)$  and have the greatest frequency factor. Hat Creek B coal, Saskatchewan Lignite, Forestburg and Byron Creek coals are progressively more sensitive to  $Y(8)$  and have reduced frequency factors.



TABLE 6.2

Optimum Parameters

Coal	Solvent	Parameters								
		$Y(1)_{s-1}$	Y(2)	Y(3)	Y(4)	Y(5)	Y(6)	Y(7)	Y(8)	$Y(9)_{s-1}$
Fies Mine (HVB)	Tetralin		1.049		$1002.1$ $(\sim 6.1 \times 10^{-4})^2$			0.7316	0.000	$4.60 \times 10^{15}$
Hat Creek A (SB)	Tetralin		0.918		$416.6^1$ $(\sim 2.8 \times 10^{-4})^2$			0.6531	0.000	$2.50 \times 10^{15}$
Hat Creek B (SB)	Tetralin		1.445		$690.4^1$ $(\sim 4.6 \times 10^{-4})^2$			0.6029	0.0195	$1.28 \times 10^{15}$
Middle Kittanning (HVB)	Tetralin		0.909	$3.46 \times 10^{-5}$	$153.6^3$ $(\sim 6.6 \times 10^{-4})^2$			0.04687	0.7938	$4.00 \times 10^6$
Forestburg (SB)	SRC oil	14.52	1.379	$2.88 \times 10^{-5}$	$8.09 \times 10^{-4}^2$	.01909	19.12	0.25254	0.3626	$7.617 \times 10^{14}$
	SRC oil + THN	14.52	1.154	$3.46 \times 10^{-5}$	$3.38 \times 10^{-4}^2$	.02285	19.12	0.25254	0.3626	$7.617 \times 10^{14}$
Byron Creek (B)	SRC oil	11.09	1.670	$1.75 \times 10^{-5}$	$6.79 \times 10^{-4}^2$	.0230	19.12	0.05886	0.5049	$0.228 \times 10^{14}$
	SRC oil + THN									
Saskatchewan Lignite	SRC oil	13.56		$2.03 \times 10^{-5}$		.02288	19.12	0.5075	0.0252	$1.00 \times 10^{15}$

1.  $J_1 = Y(2) - Y(4) D H$  (6.3)
2.  $J_2 = Y(2) - Y(4) (TEMP) (H)$  (6.18)
3.  $J_1 = Y(2) - Y(4) D$  (6.19)

Parameter Y(4), which relates the initial rate of hydrogen mass transfer to the coal fraction undergoing instantaneous conversion, also yields consistent results, even though different equations were used to correlate this parameter. Values obtained from the various correlations can be approximated by an equivalent value for equation 6.18. One would expect this parameter to vary with the porosity of the coal and the solubility of the initial liquefaction products in the carrier solvent. The parameter does vary, but only over a narrow range. The values range from  $3 \times 10^{-4}$  to  $8 \times 10^{-4} \text{ Kg} \cdot \text{mole}^{-1} \cdot ^\circ\text{K}^{-1}$ , if one assumes that tetralin is the diffusing species in the absence of molecular hydrogen. At sufficiently high hydrogen pressures, one might also expect to observe a switch from mass transfer to kinetic control of the "instantaneous" reactions. Such an effect was not observed.

Parameter Y(2), the amount of the organic material reporting as unconverted coal initially, in the absence of a hydrogenation agent,, suggests that negative conversion is not only possible but likely under these reaction conditions. If the liquefaction results for Middle Kittanning coal most closely resemble this situation, then Y(2) may overestimate the extent of adduct formation, in some cases. The Y(2) value reported for Byron Creek coal, 1.67, corresponds to a negative conversion of 67% and is clearly too large. This is an understandable shortcoming of an empirical model.

The maximum coal fraction which is predicted by the model to enter the dispersed phase is also proportional to the initial rate of hydrogen transfer to the coal. As noted previously, the model only detects marginal material which can report to either the liquid or dispersed phases. The constant of this proportionality,  $Y(3)$ , only varies from  $1.75 \times 10^{-5}$  to  $3.5 \times 10^{-5} \text{ Kg} \cdot \text{mole}^{-1} \cdot \text{K}^{-1}$  and is one order of magnitude smaller than  $Y(4)$ .

Parameter  $Y(5)$  is the optimum ratio of catalytic solvent hydrogenation reactions to dispersed phase hydrogenation reactions. The optimum ratio of these two reactions,  $Y(5)$ , appears to be fairly constant over broad ranges of solvent composition. Only one sequence of experiments, performed with Byron Creek coal in Solvent 1, contradict this statement. These experimental results indicate an optimum ratio of approximately 0.015 vs 0.02 to 0.023 for the other trials. However, Byron Creek coal liquefied in Solvent 1 encountered severe and progressive retrogressive reactions that are not anticipated by the model. A similar though less severe effect is encountered at longer mean residence times when Forestburg coal is liquefied, in Solvent 1. Had liquefaction results for Byron Creek coal in Solvent 1 been obtained at much shorter residence times, it is likely that the optimum ratio would be closer to .02.

Parameter  $Y(6)$ , is the background level of catalysis present in a well used reactor. This includes catalytic effects related to the memory

effect described previously, to the presence of catecols, to the mineral matter content of the coals liquefied. For the catalyst employed in this work, the memory effect predominates and it is not surprising that Y(6) equals 19.12 grams as this is very close to 20.09, the average level of catalyst employed in all runs conducted during the experimental program.

Parameter Y(1), the stirring rate, in Hz, at which phase droplets begin to be broken up, indicates that the reaction environment must be turbulent before the droplets are fragmented. If one were to employ equation 6.7 and assume that the solvent has a density of  $0.8 \text{ g cm}^{-3}$  and the interfacial tension is  $1 \text{ dynes cm}^{-2}$  the maximum droplet diameters for Byron Creek coal, Saskatchewan Lignite, and Forestburg coal are 10.6, 8.3, and  $7.6 \text{ }\mu\text{m}$  respectively. The volumetric mean particle diameters of these coals are approximately 10.3, 57.5 and  $40.5 \text{ }\mu\text{m}$  respectively, while the mean particle diameters are 4.6, 3.3,  $1.7 \text{ }\mu\text{m}$ . In the absence of a trend in the results it is only possible to conclude that the size of dispersed phase droplets must be related to the grain size of the maceral components in the pulverized coal.

Apart from the general similarity of the parameters listed on Table 6.2, and discussed above, the near identical values which characterize Forestburg coal liquefaction in Solvents 1 and 2 are noteworthy. If one takes into account anticipated differences in initial

product solubility all other parameters are the same. The same kinetic parameters (Y(7), Y(8), Y(9), for example, apply to both solvents. These results suggest that as long as retrogressive reactions do not play a major role in the liquefaction reaction sequence, shifts in the rates and extents of liquefaction reactions, resulting from radical changes in solvent composition can be predicted reliably.

The liquefaction results obtained from simulated axially mixed reactor and pre-heater trials, Table 5.3, can only be modelled qualitatively because the average hydrogen concentrations in the carrier solvents are unknown. An additional difference, with respect to modelling, is that the dissolved molecular hydrogen concentrations are likely to be equal to the saturated value rather than proportional to it as assumed for the batch injection trials. Quantitative verification of the model with respect to variations in residence time distribution must await more precise hydrogen solubility data.

Following the 30 minute axially mixed reactor simulation with Forestburg coal in Solvent 2, the apparent hydrogen solubility was measured as  $0.97 \times 10^{-3} \text{ moles} \cdot \text{Kg}_{\text{solvent}}^{-1} \cdot \text{Atm}^{-1}$ . This value is approximately one third the solubility in the starting solvent, and is too low to use equation 2.7 for extrapolation. At 698°K, the saturated hydrogen concentration is likely to be quite low and perhaps equal to or less than the initial hydrogen concentration encountered by coal particles

during batch trials. If one reduces the hydrogen concentration from 1.41 to 1.25 moles  $\text{Kg}^{-1}_{\text{solvent}}$  the model will duplicate the experimental conversion of 84.35 wt%.

A similar approach can be adopted for the axially mixed pre-heater simulation, also performed with Forestburg coal in Solvent 2. The hydrogen solubility in product liquids, measured at room temperature, drops below the detection limit for both batch and axially mixed trials with this solvent, following experiments with a 5 minute mean residence time. Consequently, one would expect the mean hydrogen concentration to be quite low. If a hydrogen solubility of 0.65 moles  $\text{Kg}^{-1}_{\text{solvent}} \cdot \text{Atm}^{-1}$  is employed, the model will duplicate the experimental conversion value.

The simulated axially mixed pre-heater trial performed with Forestburg coal in Solvent 1, presents the same situation as noted above for the axially mixed reactor simulation. The hydrogen solubility in the product liquids was measured at  $0.5 \times 10^{-3}$  moles  $\cdot \text{Kg}^{-1}_{\text{solvent}} \cdot \text{Atm}^{-1}$  which is between one half and one third of the solubility in the starting solvent. One finds that a hydrogen concentration of 2.48 moles  $\cdot \text{Kg}^{-1}_{\text{solvent}}$ , vs 2.42 for batch trials, permits the model to duplicate the experimental conversion value.

Due to the absence of accurate hydrogen solubility data on hydrogen concentration data, the results of these verification trials can

only be treated as qualitative. However, the results are self consistent, and conform with experimental observations, thus, providing sufficient grounds to suggest that the model may be applied to axially mixed as well as batch reactors. The only caution which must be mentioned is that if the solvent is subject to rapid hydrogenation hydrogenolysis reactions which degrade the solvent, the model will not predict a catastrophic reduction in product yield.

#### 6.4 Summary

The novel coal liquefaction reaction model presented and verified in this chapter has been shown to provide a general framework for describing the liquefaction behaviour of coals and lignite. A variety of reaction environments were modelled successfully and the model appears to be applicable for both axially mixed and batch reactors. However, the generality of the model is bounded by two important limitations. Retrogressive reactions are treated as a liquid-liquid insolubility problem involving the solvent and the initial liquefaction products arising from instantaneous decomposition of a coal. The tendency for larger coal derived molecules to precipitate progressively with time as the solvent undergoes hydrogenolysis reactions is not modelled, and cannot be modelled until more general theories for liquid-liquid solubility are developed. Retrogressive reactions can play an important role in determining the liquefaction reaction sequence. Under conditions where this occurs the model is not applicable. A second restriction, envisioned

when the model was formulated, is that the transition zone between labile hydrogen diffusion and molecular hydrogen mass transfer control of the initial "instantaneous" liquefaction reactions would be difficult to model. The model has been shown to work well if either of these modes of reaction dominate, but the transition zone, occurring over a range of hydrogen concentrations, not yet identified, must be found and quantified if the model is to be rendered as general as possible.



## Chapter 7

### Direct Coal Liquefaction Reactor Design

#### 7.0 Introduction

The experimental results and the coal liquefaction reaction model, which comprise the two previous chapters, focus on an analysis and description of direct coal liquefaction environments from a microscopic perspective. The impact of these findings on the design of pre-heaters, the use of catalysts, and the selection of slurry residence time distributions are discussed in this chapter. Current DCL reactor designs, Table 2.1 and Figures 2.1 to 2.8, are then re-examined and a novel reactor design, which optimizes the production of liquid products, is proposed.

#### 7.1 Pre-heater Design

Pre-heaters, an often overlooked component of DCL reactors, play two important roles in liquefaction processes. The reaction conditions prevailing in pre-heaters determine the rate and maximum extents of subsequent liquefaction reactions. Pre-heaters also serve their design function as a heat transfer device. Proposed industrial pre-heater designs, Chapter 2, are typically coal or natural gas fired boilers with a single heat transfer tube, in the shape of a helix. These pre-heaters

are operated in slug flow and act as plug flow reactors with respect to the slurry phase. As shown in Chapter 5, this configuration is optimal if heavy oils or coal liquids are used as a liquefaction solvent. One could only recommend, in this particular case, that the highest possible hydrogen pressure be employed, and that the slurry residence time in this device be maximized. For lighter solvents, (i.e.) hydrogenated middle and heavy distillate oils, or solvents with a reduced tendency to form adducts during initial reactions, such a design was shown to be non-optimal, and separation of the heat transfer and reaction initiation functions must be considered.

The heat transfer function, served by pre-heaters, is essential, even though liquefaction reactions are exothermic. The cleavage of various organic bonds, followed by hydrogen saturation of the resulting radicals, yields approximately 13.0 Kcal per mole of hydrogen consumed. The cleavage of aryl or alkyl carbon-carbon bonds, followed by hydrogenation yields between 12. and 13. Kcal·mole  $H_2^{-1}$ . Comparable values for CO, CO<sub>2</sub> and H<sub>2</sub>O formation are ~ 10, < 20, 10-15 Kcal·mole  $H_2^{-1}$ , respectively. The amount of energy released varies with the overall molecular structure. If the hydrogen consumption behaviour of Forestburg sub-bituminous coal, at 698°K, is taken as representative, 9 moles of H<sub>2</sub> are consumed per kilogram of MAF coal within the first 2.4 minutes of reaction; 15 moles·Kg<sup>-1</sup> MAF Coal are consumed within 5 minutes and 20 moles

after 30 minutes of reaction. Pilot plant trials suggest that up to 35 moles of  $H_2$  per kilogram of MAF coal can be consumed - Table 2.1. The maximum temperature rise resulting from initial reactions is approximately  $50^\circ K$ , for a 40 wt% slurry, and the maximum overall temperature rise is less than  $180^\circ K$ . Consequently, the coal slurry must be pre-heated to at least  $573^\circ K$  before entering a reactor. Since this temperature is below the threshold for liquefaction reactions, the two functions of the pre-heater can be separated, in principle.

Judicious selection of operating conditions may permit a sustainable temperature rise in excess of  $100^\circ K$  between the pre-heater exit and the reactor operating temperatures. As shown in Chapters 5 and 6, the initial extent and rate of liquefaction reactions, in light solvents are maximized in a reactor with a broad slurry residence time distribution and a mean residence time between 5 and 10 minutes. The inclusion of such a reactor, with a hydrogen consumption in excess of 20 moles  $\cdot Kg^{-1}$ , would maximize the initial rate of hydrogen consumption and heat evolution, and minimize the heat exchange requirement.

## 7.2 Reactor Design

The optimum liquefaction reactor design for heavy solvents, is one where the slurry has a plug flow residence time distribution. Apart from the first few minutes of reaction, a similar design is also preferred

when light carrier solvents are employed. In fact, the use of axially mixed reactors with light solvents may lead to radical reductions in product yield. Heavy solvents are less subject to such coal-solvent interactions and the plug flow optimum is only shallow. Two additional parameters which must be considered are:

1. the intensity of turbulence - a level of turbulence sufficient to break-up residual coal particles and dispersed phase droplets must be maintained throughout the reactor.
2. the catalyst to turbulence ratio - an optimum ratio must be maintained.

Industrial Designs cannot employ agitators, as were used in this study. These devices are too costly for such applications. Gas bubbles and jets must be used to create turbulence. Currently, there are no published papers relating gas flux or mean bubble diameter to the size of dispersed phase droplets in liquid-liquid-gas systems. Fundamental investigations must be performed before optimum gas distributors can be designed and DCL pilot plant trials can be conducted.

### **7.3 Catalysts**

The experimental program has demonstrated the importance of added catalysts. Added catalyst must be present wherever coal is undergoing reaction, if coal conversion is to be maximized. The optimum level of

catalyst is determined by the intensity of turbulence. If reactions are initiated in pre-heaters, flow through catalysts are preferred. If catalyst is to be contained inside a reactor, the pre-heater temperature should not exceed 573°K.

#### **7.4 A Re-Evaluation of Existing DCL Reactor Designs**

Despite the absence of complete sets of operating data for the various liquefaction processes, Table 2.1, it is clear that they all violate the optimum design criteria proposed above. The SRC I process, for example, operates at a low hydrogen pressure, and does not employ an added catalyst. Consequently, adduct formation and "coking" are dominant modes of reaction, and little upgrading of liquid products occurs. The catalytic effect of mineral matter is enhanced in the SRC II process and a lighter carrier solvent is employed. Higher hydrogen concentrations are encountered in the carrier solvent, and catalytic hydrogenation also occurs. The product distribution is shifted from solids to lighter liquid and gaseous components. The H-Coal process does not employ a flow through catalyst. The coal entering the reactor has a minimum net conversion as irreversible coke formation occurs in the pre-heater. The pre-heater is then followed by an ebulated bed reactor, which further reduces the maximum extent of liquid formation. Little data is available for the EDS Process, which employs a light solvent. Added catalysts are not employed in the liquefaction sequence, and a plug flow pre-heater is used. The reactor, a multi-stage tank reactor, approximates a plug flow

residence time distribution for the reacting slurry. Significant improvements in space time yield would result from the introduction of catalyst and a distributed residence time for the initial reactions. The liquid yield of the Dow process could be improved by using a higher hydrogen pressure, and by segmenting the reactor. The Saarbergwerke and Ruhrkohle Processes both employ flow through catalysts, a high hydrogen pressure, and a multi-stage reactor design. These design features are appropriate for the selection of heavy oil as a carrier solvent. Improvements could only be made in these processes if a non optimal catalyst to turbulence ratio is currently used, or if the hydrogen concentration in the latter stages of the reactors could be reduced to minimize synthetic natural gas production. Of the piloted Direct Coal Liquefaction Processes, only the Saarbergwerke and Ruhrkohle Processes are sufficiently close to design optimum to permit optimization without significant design changes. These two processes may or may not be competitive with the reactor design proposed in the next section which is centered on an alternative design optimum.

### **7.5 An Optimum Direct Coal Liquefaction Reactor Design**

As noted in Chapter 5, reactors employing heavy oils as the carrier solvent yield optimum rates of liquid product formation when the slurry residence time distribution approximates plug flow. The productivity optimum for lighter solvents occurs when a backmixed reactor with a short mean residence time precedes a plug flow reactor with a

a longer mean residence time. The Saarbergwerke and Ruhrkohle Processes approximate the former optimum. The design proposed here approximates the latter optimum and affords two potential advantages over the German Processes. The size of heat exchangers and the hydrogen recycle load are reduced significantly.

The proposed reactor, Figure 7.1, is preceded by a pre-heater and/or heat exchangers which pre-heat the slurry to approximately 573K. Hydrogen saturated coal slurry, hydrogen gas and catalyst enter at the base of a co-current up flow tubular reactor with a mean residence time of approximately 5 minutes. This reactor is imbedded within another tubular reactor which is the second stage of the reactor network. The slurry exits at the top of the first stage and enters the second stage. The slurry passes downwards within the annulus and exits the second stage after an additional 10 to 20 minutes. The partially consumed hydrogen stream, which contains  $\text{CO}$ ,  $\text{H}_2\text{O}$ ,  $\text{CO}_2$ , also exits at the top of the first stage. This gas is re-compressed and fed to the base of the second stage of the reactor. A plug flow slurry residence time is maintained in the second stage by forcing the gas injected at the base of the second stage through a series of sieves with progressively smaller hole diameters. In order to maintain a constant intensity of turbulence, this gas flow is augmented by gas jets attached to the external wall of the reactor.

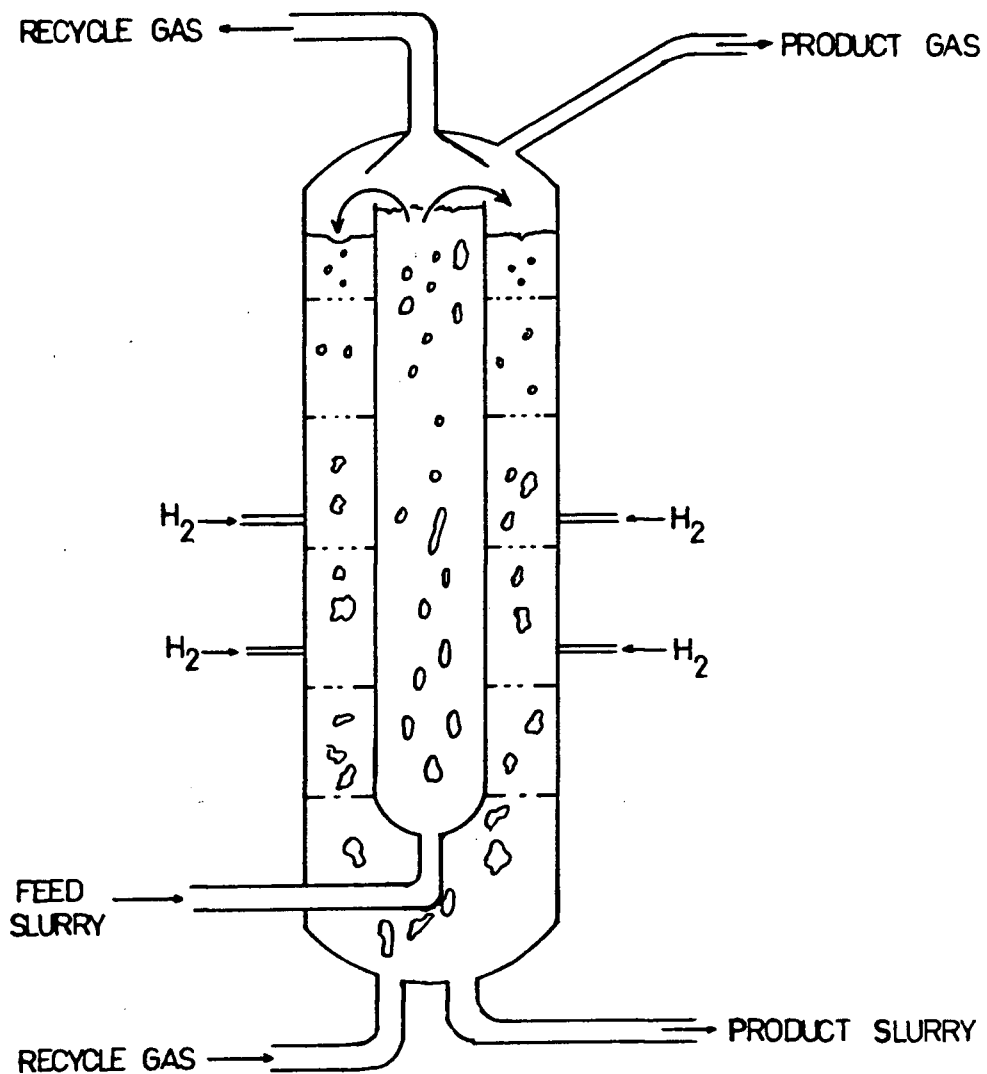


Figure 7.1: A Novel Coal Liquefaction Reactor Design



Such a design maximizes the conversion, the hydrogen consumption and the temperature rise in the first stage of the reactor. Thus, there would be less need to recycle hydrogen. The gas entering the second stage is at the same pressure as in the first stage but with a substantially reduced hydrogen fraction. This helps to reduce excess synthetic natural gas formation. Since there is no pressure gradient, the containment walls of the first stage can be quite thin (i.e. the sieve tray supports can also be used to support the tube) and high rates of heat transfer can be realized. This reduces the requirement for external high pressure heat exchange equipment by over 30%. The overall mean residence time would also be less than in the German Processes because liquefaction reactions are more rapid in lighter liquefaction solvents.

## 7.6 Summary

The experimental findings of this thesis indicate the existence of two reactor design optima for Direct Coal Liquefaction Processes, which maximize the rate and extent of liquid product formation. One design optimum is approximated by the Saarbergewerke and Ruhrkohle Processes. An alternative and potentially competitive design optimum is proposed in section 7.5.

## Chapter 8

### 8. Summary

#### 8.1 Conclusions

A series of direct coal liquefaction trials performed with coals and lignite revealed that both bituminous and sub-bituminous coals and lignite undergo a comparable sequence of reactions in DCL reaction environments. The maximum rate and extent of conversion was found to depend on the initial rate of hydrogen transfer to reacting coal particles, and on the ratio of catalyst to the intensity of turbulence. This latter finding led to the discovery of a persistent dispersed liquid phase which was unknown prior to this work. The finding that the initial rate of hydrogen mass transfer had such a demonstrable effect on the rate and maximum extent of liquefaction reactions is inconsistent with the view, prevalent in the literature, that the rates and maximum extents of product formation are determined intrinsically by coal composition and structure.

These findings provided important insights into the nature of DCL reaction environments and permitted the development of a general, though empirical, coal liquefaction reaction model. This model, which couples the experimental findings with a simple kinetic scheme, correlated the liquefaction behaviour of bituminous and sub-bituminous coals, and

lignite in diverse reaction environments. Coal liquefaction reaction models, based solely on kinetics, rarely correlate the liquefaction behaviour of more than a single coal in a particular reaction environment.

The results of the experimental program and the reaction model were used to formulate design criteria for Direct Coal Liquefaction reactors. These analyses led to identification of two DCL reactor design optima. One design optimum is approximated by two existing processes: the Saarbergewerke and Ruhrkohle processes. The second optimum, a novel 2 stage reactor configuration, also conforming with the experimental findings, is potentially a superior alternative.

## **8.2 Suggestions for Further Study**

Design and development of Direct Coal Liquefaction processes is far from complete. A detailed description of liquefaction kinetics, and a precise definition of optimum geometries for liquefaction reactors must await future developments. This work suggests that studies related to the following areas are warranted:

1. The acquisition and correlation of physical property data for complex organic mixtures at high temperatures.
  - the lack of data pertaining to the physical properties of complex organic mixtures inhibited some aspects of this work.

Solvent density, viscosity, and interfacial tension data, in particular, were found to be lacking.

2. The analysis of gas-liquid-liquid three phase flow.

- studies relating to the impact of gas flux, and bubble size on the size of dispersed liquid droplets are of the greatest potential importance for Direct Coal Liquefaction Reactor Design.

3. The improvement of analysis methods for coal and residual solid particles.

- maceral distributions in finely divided coal cannot be defined with certainty, and fine unreacted coal particles are difficult to distinguish from "coke". Improvements in this area would permit the development of more precise reaction models for DCL Processes.

4. The novel two stage liquefaction reactor design.

- this design should be subjected to further development and testing using a continuous bench scale reactor.

## REFERENCES

1. Conrad, J., Victory, Penguin Books, Harmondworth, England, p. 1, (1979).
2. Strobel, B., Romey, I., Kolling, G.: "German Routes to Coal Hydrogenation", Advances in Coal Technology, Louisville, Kentucky, U.S.A., p. 291-316, (May 1979).
3. Storch, H.H.: "Hydrogenation of Coal and Tar", Chemistry of Coal Utilization, ed. H.H. Lowry, Wiley and Sons, N.Y., Vol. 2, p 1750-1756, (1945).
4. Bergius, F.: "The Transformation of Coal Into Oil by Means of Hydrogenation", Can. Chem. and Met., Vol. 10, p. 275-279, (1926).
5. Wolk, R.H.: "Overview of Liquefaction Process Technology", Advances in Coal Utilization Technology, Louisville, Kentucky, U.S.A., p. 273-290, (May 1979).
6. Whitehurst, D.D., Mitchell, T.O., Farcasiu, M.: Coal Liquefaction: The Chemistry and Technology of Thermal Processes, Academic Press, N.Y., p. 355, (1980).
7. Ibid, p. 346-370.
8. Neworth, M.B.: "Development of a Two-Stage Liquefaction Process", Advances in Coal Technology, Louisville, Kentucky, U.S.A., 18, p. 345-358, (May 1979).
9. Berkowitz, N.: An Introduction to Coal Technology, Academic Press, New York, p. 303-314, 1979.
10. Alpert, S.B., Wolk, R.H., "Liquefaction Processes", Chemistry of Coal Utilization, ed. M.A. Elliott, Wiley-Interscience, N.Y., 2nd Sup. Vol., p. 1919-1990, (1981).
11. Lee, M.H. Guin, J.A., Tarrer, A.R.: "A Dispersion Model for the SRC Process", Ind. Eng. Chem. Process Des. Dev., Vol. 17, No. 2, p. 127-34, (1978).
12. Abou-El-Hassan, M.E.: "Mixing and Phase Distributions in Two and Three Phase Bubble Column Reactors", Proc. 3rd European Conference on Mixing, BHRA Fluid Engineering, Cranfield, Bedford, England, Vol. 1, F2, p. 303-324, (April 1979).

13. Taitel, Y., Bornia, D., Dukler, A.E.: "Modelling Flow Pattern Transitions for Steady Upward Gas-Liquid Flow in Vertical Tubes", *AICHE Journal*, Vol. 26, No. 3, p. 345-354, (May 1980).
14. Vince, M.A., Lahey, R.T.: "On the Development of an Objective Flow Regime Indicator", *Int. J. Multiphase Flow*, Vol. 8, No. 2, p. 93-124, (1982).
15. Barnea, D., Shohan, O., Taitel, Y., Dukler, A.E.: "Flow Pattern Transition for Horizontal and Inclined Pipes: Experimental and Comparison with Theory", *Int. J. Multiphase Flow*, Vol. 6, p. 217-225, (1980).
16. Levenspiel, O.: *Chemical Reaction Engineering*, 2nd, Wiley, New York, p. 272-290, (1972).
17. Han, K.W., Wen, C.Y.: "Initial Stage (Short Residence Time) Coal Dissolution", *FUEL*, Vol. 58, p. 779-82, (Nov. 1979).
18. Whitehurst, D.D. Mitchell, T.O., Farcasiu, M.: *Coal Liquefaction The Chemistry and Technology of Thermal Processes*, Academic Press, N.Y., p. 366-368, (1980).
19. Han, K.W., Dixit, V.B., Wen, C.Y.: "Analysis and Scale-Up Consideration of Bituminous Coal Liquefaction Rate Processes", *Ind. Eng. Chem. Process Des. Dev.*, Vol. 17, No. 1, p. 16-21, (1978).
20. Moschopedis, S.E., Speight, J.R.: "The Co-Processing of Heavy Oil and Coal", *Proc. 32nd Can. Chml. Eng. Con.*, Vancouver, B.C., Vol.1, p. 490-496, (Oct. 1982).
21. Bickel, T.C., Thomas, M.G.: "Catalyst Deactivation in the H-Coal Liquefaction Process. 1. Catalyst Residence Time Distribution", *Ind. Eng. Chem. Process Des. Dev.*, Vol. 21, p. 377-381, (1982).
22. Grace, J.R.: "Fluidized Bed Hydrodynamics", *Handbook of Multiphase Systems*, ed. G. Hetsroni, Hemisphere, New York, p. 8.15, (1982).
23. Levenspiel, O.: "The Chemical Reactor Omnibook", Oregon State University Press, Corvallis, Oregon, Ch. 68, (1979).
24. Peters, B.C.: *Dow Chemical Internal Report*, Dow-F-R-363, F-1534-50, (1977). *Chem. Abstract* N 79-11166.

25. Freel, J., Jackson, D.M., Schmid, B.K.: "SRCII Demonstration Project", Chem. Eng. Progress, p. 86-91, (May 1981).
26. Shah, Y.T., Carr, N.L.: "New Experimental Techniques for High Pressure High Temperature Gas-Liquid-Solid Reactors", Proc. 2nd World Congress of Chemical Engineering, Montreal, Canada, V.3, p. 138-141, (1981).
27. Moll, N.G., Quarderer, G.J.: "The Dow Coal Liquefaction Process", CEP, p. 46-51, (Nov. 1979).
28. Goethel, G.F., Klein, W., Hosang, H.: "Coal Liquefaction and Heavy Oil Processing ... Veba Oil", Proc. 32nd Can. Chml. Eng. Con., Vancouver, B.C., Vol. 2, (Oct. 1982).
29. Fajner, D., Magelli, F., Pasqualli, G.: "Modelling of Non-Standard Mixers Stirred with Multiple Impellers", Chem. Eng. Commun., Vol. 17, p. 285-295, (1982).
30. Taunton, J.W., Trachte, K.L., Williams, R.D.: "Coal Feed Flexibility in the EDS Coal Liquefaction Process", FUEL, Vol. 60, p. 788-794, (Sept. 1981).
31. Rosenthal, J.W., Danlberg, A.J., Kuehler, C.W., Cash, D.R., Freedman, W.: "The Chevron Coal Liquefaction Process (CCLP)", FUEL, Vol. 61, p. 1045-1050, (October 1982).
32. Schindler, H.D., Sze, M.C., Long, R.H. Unger, H.: "Advanced Coal Liquefaction Processes Emphasize Low Hydrogen Consumption", Proc. 15th Intersociety Energy Conversion Engineering Conference, Seattle, Washington, Vol. 2, p. 1543-1556, (August 1980).
33. Abichandani, J.S., Shah, Y.T., Cronauer, D.C., Ruberto R.G.: "Kinetics of Thermal Liquefaction of Coal", FUEL, Vol. 61, p. 276-282, (March 1982).
34. Cronauer, D.C., Shah, Y.T., Ruberto, R.G.: "Kinetics of Thermal Liquefaction of Belle Ayr Sub-bituminous Coal", Ind. Eng. Chem. Process Des. Dev., Vol. 17, No.3, p. 281-287, (1978).
35. Mohan, G., Silla, H.: "Kinetics of Donor Solvent Liquefaction of Bituminous Coals in Nonisothermal Experiments", Ind. Eng. Chem. Process Des. Dev., Vol. 20, p. 349-358, (1981).

36. Droege, J.W., Stickford, G.H., Chauhan, S.P.: "Thermophysical Properties of Pre-heater Slurries", Proc. 16th Intersociety Energy Conversion Engineering Conference, Atlanta, Vol. 2, p. 1085-1091, (August 1981).
37. Thurgood, J.R., Hanks, R.W., Oswald, G.E., Youngblood, E.L.: "The Rheological Characterization of Coal Liquefaction Pre-heater Slurries", AIChE Journal, Vol. 28, No. 1, p. 111-116, (January 1982).
38. Okutani, T., Yokoyama, S., Maekawa, Y.: "Viscosity of Coal Paste Under High Hydrogen Pressure", FUEL, Vol. 59, p. 67-69, (January 1980).
39. Turian, R.M., Yuan, T.F.: "Flow of Slurries in Pipelines", AIChE Journal, Vol. 23, No. 3, p. 232-242, (May 1977).
40. Weinberg, V.L., Yen, T.F.: "Solubility Parameters in Coal and Coal Liquefaction Products", FUEL, Vol. 59, p. 287-289, (May 1980).
41. Hombach, H.P.: "General Aspects of Coal Solubility", FUEL, Vol. 59, p. 465-470, (July 1980).
42. Shibaoka, M., Stephens, J.F., Russel, N.J.: "Microscopic Observations of the Swelling of a High-Volatile Bituminous Coal in Response to Organic Solvents", FUEL, Vol. 58, p. 515-522, (July 1979).
43. Habermehl, D., Orywel, F., Beyer, H.D.: "Plastic Properties of Coal", Chemistry of Coal Utilization, ed. M.A. Elliot, Wiley, N.Y., 2nd Sup. Vol. p. 354, (1981).
44. Derbyshire, F.J., Whitehurst, D.D.: "Study of Coal Conversion in Polycondensed Aromatic Compounds", FUEL, Vol. 60, p. 655-662, (August 1981).
45. Shalabi, M.A., Baldwin, R.M., Bain, R.L., Gary, J.H., Golden, J.D.: "Non Catalytic Coal Liquefaction in a Donor Solvent. Rate of Formation of Oil, Asphaltenes, and Preasphaltenes", Ind. Eng. Chem. Process Des. Dev., Vol. 18, No. 3, p. 474-479, (1979).
46. Yarzab, R.F., Given, P.H., Spackman, W., Davies, A.: "Dependence of Coal Liquefaction Behavior on Coal Characteristics. 4. Cluster Analysis for Characteristics of 104 Coals", FUEL, Vol. 59, p. 81-92, (Feb. 1980).



47. Smith, G.C., Cook, A.C.: "Coalification Paths of Exinite, Vitrinite, and Inertite", FUEL, Vol. 59, p. 641-646, (Sept. 1980).
48. Gun, S.R., Same, J.K., Chowdhury, P.B., Muklerjee, S.K., Muklerjee, D.K.: "A Mechanistic Study of Hydrogenation of Coal. 1", FUEL, Vol. 58, p. 171-175, (March 1979).
49. Szladow, A.J., Given, P.H.: "Models and Activation Energies for Coal Liquefaction Reactions", Ind. Eng. Chem. Process Des. Dev., Vol. 20, p. 27-33, (1981).
50. Kuhlmann, E., Boerwinkle, E., Orchin, M.: "Solubilization of Illinois Bituminous Coal: The Critical Importance of Methylene Group Cleavage", FUEL, Vol. 60, p. 1002-1004, (Nov. 1981).
51. Carson, D.W., Ignasiak, B.S.: "Polymeric Structure of Coal. 3. Re-examination of the Role of Ether Bonds in Reduction of Molecular Weight of a Low-rank Vitrinite Treated with Hydrogen Donor", FUEL, Vol. 59, p. 757-761, (Nov. 1980).
52. Deno, N.C., Greigger, B.A., Jones, A.D., Raktisky, W.G., Whitehurst, D.D., Mitchell, T.O.: "Structural Changes Occurring in Coal Liquefaction", FUEL, Vol. 59, p. 701-703, (October 1980).
53. Curran, G.P., Struck, R.T., Gorin, G.: "Mechanism of the Hydrogen-Transfer Process to Coal and Coal Extract", Ind. Eng. Chem. Process Des. Dev., Vol. 6, No.2, p. 166-173, (April 1967).
54. Vernon, L.W. "Free Radical Chemistry of Coal Liquefaction: Role of Molecular Hydrogen", FUEL, Vol. 59, p. 102-106, (February 1980).
55. Petrakis, L., Grandy, D.W.: "Free Radicals in Coals and Coal Conversion 2. Effect of Liquefaction Processing Conditions on the Formation and Quenching of Coal Free Radicals", FUEL, Vol. 59, p. 227-232, (1980).
56. Franz, J.A., Camaioni, D.I.: "Fragmentations and Rearrangements of Free Radical Intermediates during Hydro-liquefaction of Coals in Hydrogen Donor Media", FUEL, Vol. 59, p. 803-805, (Nov. 1980).
57. Derbyshire, F.J., Varghese, P., Whitehurst, D.D.: "Synergistic Effects between Light and Heavy Solvent Components during Coal Liquefaction", FUEL, Vol. 61, p. 859-864, (1982).
58. Houalla, M., Broderick, D.H., Sapre, A.V., Nag, N.K., de Beer, V.H.J., Gates, B.C., Kwart, H.: "Hydrodesulphurization of Methyl Substituted Dibenzothiophenes Catalyzed by Sulphided Co-Mo/ $\alpha$ -Al<sub>2</sub>O<sub>3</sub>", Journal of Catalysis, Vol. 61, p. 523-527, (1980).

59. Yoshii, T., Yaginuma, R., Yoshikaura, H., Utoh, Soichi: "Unusual Effects of Catechol upon the Hydro-liquefaction of Coal", FUEL, Vol. 61, p. 865-866, (September 1982).
60. Painter, P.C., Yamada, Y., Jenkins, R.G., Coleman, M.M., Walker, P.L.: "Investigation of Retrogressive Reactions leading to Carbonization of Solvent-Refined Coal", FUEL, Vol. 58, p. 293-297, (April 1979).
61. Mochida, I., Takarabe, A., Takeshita, K.: "Solvolytic Liquefaction of Coals with a series of Solvents", FUEL, Vol. 58, p. 17-23, (January 1979).
62. Longanback, J.R.: "Short-Contact-Time Coal Liquefaction: "Effect of Coal Rank and Solvent Source on Conversions and Heptane Insoluble Product Formation", ACS Symp. Ser., 169, (New Approaches Coal Chem.) p. 131-152, (1981).
63. Whitehurst, D.D., Farcasiu, M., Mitchell, T.O., Dickert, J.J., EPRI AF-480 Ann. Rep., (1977) Ch. 8, (see ref. 64).
64. Benjamin, B.M., Hagaman, E.W. Raaen, V.F., Collins, C.J.: "Pyrolysis of Tetralin", FUEL, Vol. 58, p. 386-390, (May 1979).
65. Hooper, R.J. Battaerd, H.A.J., Evans, D.G.: "Thermal Dissociation of Tetralin between 300 and 450°C, FUEL, Vol. 58, p. 132-138, (February 1979).
66. Guin, J.A., Tarrer, A.R., Prather, J.W., Johnson, D.R., Lee, J.M.: "Effects of Coal Minerals on the Hydrogenation, Desulphurization and Solvent Extraction of Coal", Ind. Eng. Chem. Process Des. Dev., Vol. 17, No. 2, p. 118-126, (1978).
67. Guin, J.A., Tarrer, A.R., Lee, J.M., Van Backle, H.F., Curtis, C.W.: "Further Studies of Catalytic Activity of Coal Minerals in Coal Liquefaction<sup>2</sup>", Ind. Eng. Chem. Process Des. Dev., Vol. 18, No. 4, p. 631-637, (1979).
68. Ross, D.S., Blessing, J.E.: "Alcohols as H-Donor Media in Coal Conversion", FUEL, Vol. 58, p. 433-437, (June 1979).
69. Guin, J.A., Tarrer, A.R., Lee, J.M., Lo, L., Curtis, C.W.: "Verification of Catalytic Activity of Mineral Matter by Model Compound Studies", Ind. Eng. Chem. Process Des. Dev., Vol. 18, No. 3, p. 371-376, (1979).

70. Weigold, H.: "Behavior of Co-Mo-Al<sub>2</sub>O<sub>3</sub> Catalysts in the Hydro-deoxygenation of Phenols", FUEL, Vol. 61, p. 1021-1026, (October 1982).
71. Rollmann, L.D.: "Catalytic Hydrogenation of Model Nitrogen, Sulfur, and Oxygen Compounds", Journal of Catalysis, Vol. 46, p. 243-252, (1977).
72. Weisser, O., Landa, S.: "Sulfide Catalysts, Their Properties and Applications", Pergamon Press, Oxford, (1973).
73. Ouchi, K., Chicada, T., Itoh, H.: "Pressure and Temperature Effect on the Mean Chemical Structure of Coal Hydrogenolysis Product", FUEL, Vol. 58, p. 37-42, (January 1979).
74. Ratnasamy, P., Ramaswamy, A.V., Sivasanker, S.: "Basic Molecules as Probes for the Study of Mo-Alumina Catalysts", Journal of Catalysis, Vol. 61, p. 519-522, (1980).
75. Rudnick, L.R., Whitehurst, D.D.: "The Effect of Solvent Composition on the Liquefaction Behavior of Western Sub-bituminous Coal", A.C.S. Symp. Ser., 169 (New Approaches to Coal Chem.), p. 153-171, (1981).
76. Kershaw, J.R., Gray, D.: "Ageing Studies on Coal Hydropyrolysis Liquids", FUEL, Vol. 59, p. 436-438, (June 1980).
77. Hara, T., Jones, L., Li, N.C., Tewari, K.C.: "Ageing of SRC Liquids", FUEL, Vol. 60, p. 1143-1148, (December 1981).
78. Brown, F.R., Karn, F.S.: "Stability Studies of Coal-Derived Liquids", FUEL, Vol. 59, p. 431-435, (June 1980).
79. Krishnamurthy, S., Shah, Y.T., Stiegel, G.J.: "Pyrolysis of Coal Liquids", FUEL, Vol. 59, p. 738-746, (November 1980).
80. Mukherjee, S.K., Mukherjee, D.K.: "Coking Characteristics of Heavy Oil From Coal Hydrogenation", Indian Journal of Technology, 15 (9), p. 381-388 (89:132175h), (1977).
81. Badilla-Ohlbaum, R., Prtt, K.C., Trimm, D.L.: "A Study of Nickel-Molybdate Coal Hydrogenation Catalysts Using Model Feed Stocks", FUEL, Vol. 58, p. 309-314, (1979).

82. Sapre, A.V., Gates, B.C.: "Hydrogenation of Aromatic Hydrocarbons Catalyzed by Sulfided  $\text{CoO-MoO}_3/\gamma\text{-Al}_2\text{O}_3$ . Reactivities and Reaction Networks", Ind. Eng. Chem. Process Des. Dev., Vol. 20, p. 68-73, (1980).
83. Rottendorf, H., Wilson, M.A.: "Effects of In-Situ Mineral Matter and a Nickel-Molybdenum Catalyst on Hydrogenation of Liddel Coal", FUEL, Vol. 59, p. 175-180, (1980).
84. Mackison, F.W., Stricoff, R.C., Partridge, L.J. Jr.: NIOSH/OSHA Pocket Guide to Chemical Hazards, DHEW (NIOSH) Publication No. 78-210, (August 1980).
85. Burke, F.P., Winschel, R.A., Pochapsky, T.C.: "Composition and Performance of Distillate Recycle Solvents from the SRC-1 Process", FUEL, Vol. 60, p. 562-572, (July 1981).
86. Whitehurst, D.D., Mitchell, T.O., Farcasiu, M.: Coal Liquefaction: The Chemistry and Technology of Thermal Processes, Academic Press, N.Y., p. 280-284, (1980).
87. Katoh, T., Yokoyama, S., Sanada, Y.: "Analysis of a Coal-Derived Liquid using High-Pressure Liquid Chromatography and Synchronous Fluorescence Spectrometry", FUEL, Vol. 59, p. 845-850, (December 1980).
88. Liu, T.-C., Anthony, R.G.: "Reaction Model for the Dissolution of Large Particles of Texas Lignite", Ind. Eng. Chem. Process Des. Dev., Vol. 20, p. 609-615, (1981).
89. Batchelder, R.F., Fu, Y.C.: "Evaluation of Use of Syngas for Coal Liquefaction", Ind. Eng. Chem. Process Des. Dev., Vol. 18, No. 4, p. 594-599, (1979).
90. Johnson, C.A., Chervenak, M.C., Johanson, E.S., Stotler, H.H., Winter, O., Wolk, R.H.: "Present Status of the H-Coal Process", Proc. 2nd Symp. Clean Fuels from Coal, Inst. Gas Technol., Chicago, Ill, p. 525-551, (1975).
91. Stotler, H.H., Schutter, R.T.: "Status and Plans of the H-Coal Pilot Plant", Coal Processing Technology, Vol. V, ed. CEP, AICHE, New York p. 73-77, (1979).

92. Fettweis, G.B.: World Coal Resources - Methods of Assessment and Results, Elsevier Publishing, New York, , p. 318-323, (1976).
93. Struck, R.T., Clark, W.E., Dudt, P.J., Rosenhoover, W.A., Zielke, C.W., Gorin, E.: Ind. Eng. Chem Process Des. Dev., 8, p. 546, (1969).
94. Falkum, E., Glenn, R.A.: FUEL, 31, p. 133, (1952).
95. Vaclav, P., Kubicek, I., Kucler, J.: Chem. Prum., 31 (2), p. 61-66, (1981), (Chem. Abs. 94-177257-F).
96. Sharma, M.M.: CES, 38 (1), p. 21-28, (1983).
97. Data Tables, Chemistry of Coal Utilization: Supplemental Volume, Ed. H.H. Lowry, Wiley and Sons, N.Y., 1963.
98. Lin, H., Sebastian, H.M., Simmik, J.J., Chao, K.: "Solubilities of Hydrogen and Methane in Coal Liquids", Ind. Eng. Chem. Process Des. Dev., 20, pp. 253-256, (1981).
99. IUPAC: Solubility Data Series, Vol. 5/6, Hydrogen and Deuterium, Pergamon Press, Oxford, England, (1981).
100. IUPAC: Solubility Data Series, Vol. 4, Argon, Pergamon Press, Oxford, England, (1980).
101. IUPAC: Solubility Data Series, Vol. 9, Ethane, Pergamon Press, Oxford, England, (1982).
102. IUPAC: Solubility Data Series, Vol. 10, Nitrogen and Air, Pergamon Press, Oxford, England, (1982).
103. Kriz, J.F.: "Some Effects of Carbon Monoxide in Hydro-processessing of Heavy Feedstocks", 32nd CSChE Conference, Vancouver, B.C., (1982).
104. Oldshue, J.Y.: "Fluid Mixing Technology and Practice", Chem. Eng., pp. 82-108, June 13 (1983).
105. Sekizawa, T., Kubota, H.: "Liquid Mixing in Multistage Bubble Columns", J. Chem. Eng. Japan, Vol. 7, No. 6, pp. 441-446, (1974).
106. Ozum, B., Gibb, W.J., du Plessis, M.P.: "Modeling of Liquefaction Reactors", Proc. 32nd Can. Che. Eng. Conference, Vol. 1, p. 514-525, (October 1982).

107. Timmermans, D.: Physico-Chemical Constants of Binary Systems, Vol. 1, Interscience Pub., New York, (1959).
108. Reid, R.C., Prausnitz, J.M., Sherwood, T.K.: The Properties of Gases and Liquids, 3rd Ed., McGraw-Hill, New York, p. 359, (1977).
109. Ibid, p. 68-68.
110. Ibid, p. 435-462.
111. Gertenbach, D.D., Baldwin, R.M., Bain, R.L.: "Modelling of Bench-Scale Coal Liquefaction Systems", Ind. Eng. Chem. Process Des. Dev., Vol. 21, p. 490-500, (1982).
112. Shah, Y.T., Cronauer, D.L., McIlvried, H.G., Paraskos, J.A.: "Kinetics of Catalytic Liquefaction of Big Horn Coal in a Segmented Reactor", Ind. Eng. Chem. Process Des. Dev., Vol. 17, No. 3, p.288-301, (1978).
113. Singh, C.P.P., Shah, Y.T., Carr, N.L., Prudich, M.E.: "Liquefaction of Coal by SRC-II Process (I)", Can. J. Che. Eng., Vol. 60, p. 248-260, (April, 1982).
114. Singh, C.P.P., Shah, Y.T., Carr, N.L., Prudich, M.E.: "Liquefaction of Coal by SRC-II Process (II)", Can. J. Che. Eng., Vol. 60, p. 261-271, (April 1982).
115. Singh, C.P.P., Shah, Y.T., Carr, N.L., Prudich, M.E.: "Liquefaction of Coal by SRC-II Process (III)", Can. J. Che. Eng., Vol. 60, p. 659-665, (October 1982).
116. Singh, C.P.P., Shah, Y.T., Carr, N.L., Prudich, M.E.: "Liquefaction of Coal by SRC-II Process (IV)", Can. J. Che. Eng., Vol. 60, p. 831-841, (December 1982).
117. Singh, C.P.P., Shah, Y.T., Carr, N.L., Prudich, M.E.: "Liquefaction of Coal by SRC-II Process (V)", Can. J. Che. Eng., Vol. 60, p. 842-852, (December 1982).
118. Singh, C.P.P., Shah, Y.T., Carr, N.L., Prudich, M.E.: "Process Simulation of an SRC-II Plant", Ind. Eng. Chem. Des. Dev., Vol. 22, pp. 104-118, (1983).
119. Longanbach, J.R.: "The Effects of Heavy Recycle Solvents on Coal Liquefaction", CEP, Vol. 80, No. 11, p. 29-32, (1984).

120. Tarrer, A., Guin, J., Pitts, W., Henley, J., Prather, J., Styles, G.: "Effect of Coal Minerals on Reaction Rates During Coal Liquefaction", Liquid Fuels from Coal, Ed. R.T. Ellington, Academic Press, N.Y., p. 45-61, (1977).
121. Whitehurst, D., Mitchell, T., Farcasiu, M.: Coal Liquefaction; The Chemistry and Technology of Thermal Processes, Academic Press, N.Y., p. 93-112, (1980).
122. Calderbank, P.H.: Mixing, ed. Uhl, V.W., Gray, J.B., Vol. II, p.28-33.
123. Pelso, M., Ogren, D.F.: "Anti-Solvent Deashing", CEP, Vol. 75, No. 6, p. 41-44, (1979).
124. Adams, R.M., Knebel, A.H., Rhodes, D.E.: "Critical Solvent Deashing", CEP, Vol. 75, No.6, p. 44-48, (1979).
125. Taverides, L.L., Stamatoudis, M.: "The Analysis of Interphase Reactions and Mass Transfer in Liquid-Liquid Dispersions", Advances in Chemical Engineering, Vol. II, p. 199-268, (1980).
126. McElroy, R.: A private communication.

**APPENDICES**



## APPENDIX A: HYDRODYNAMIC CALCULATIONS

### APPENDIX A.1: HYDRODYNAMIC CALCULATIONS FOR THE H-COAL REACTOR

Data: (PDU Reactor)

Slurry concentration	(25-40) wt%	C
Slurry density	1 gcm <sup>-3</sup>	(assumed) $\rho_s$
Reactor x-sectional area	371.6 cm <sup>2</sup>	a
Coal Flow Rate		
(i) syncrude	76.9 l-hr <sup>-1</sup>	F
(ii) fuel oil	225. l-hr <sup>-1</sup>	
Catalyst Extrudate		
(i) length	4.86 mm	$\ell$
(ii) diameter	(.3-.5)mm	D
(iii) density	1.7 gcm <sup>-3</sup>	$\rho_p$
Slurry Viscosity	(1-2) cp	$\mu$

Calculations:

$$(1) \text{ Superficial slurry velocity} = \frac{F}{c} \cdot \rho_s^{-1} \cdot a^{-1} \cdot \frac{454}{36.00}$$

$$\text{syncrude mode} = (.06 - .10) \text{ cm s}^{-1}$$

$$\text{fuel oil mode} = (.19 - .30) \text{ cm s}^{-1}$$

$$(2) \text{ Minimum fluidization velocity: } U_{mf}$$

Although the reactor is not a fluidized bed, fluidization equations can provide an estimate for the velocity required to fluidize the "ebullated catalyst bed".

$$Re_{mf} = (27.2^2 + 0.0408 Ar)^{1/2} - 27.2$$

$$A_r = \frac{\rho_s (\rho_p - \rho_s) g \bar{d}_p^3}{\mu_s^2}$$

$$\bar{d}_p = (1.5 \cdot \lambda)^{1/3} (D)^{2/3}$$

$$u_{mf} = \frac{Re_{mf} \mu_s}{\bar{d}_p \rho_s}$$

$$u_{mf} = (2.25 - 3.5) \text{ cm s}^{-1}$$


---

## APPENDIX A.2: AXIAL MIXING IN THE SRC I REACTOR

Data: Wilsonville Reactor<sup>[11]</sup>

Gas velocity	1.8 cm s <sup>-1</sup>
Slurry velocity	0.335 cm s <sup>-1</sup>
reactor length	7.0 m
$\rho$ , density	1.0 gcm <sup>-3</sup>
$\mu$ , viscosity	1.0 cp

Calculations:

$$(1) \text{ Dispersion number } D = v \cdot 800 \left\{ \log \left( g^{1/3} \frac{Q}{v^{5/3}} \right) - 4.331 \right\}^{3.2}$$

$$(2) \sigma^2 = 2 \left( \frac{D}{uL} - \left( \frac{D}{uL} \right)^2 \right) \left( 1 - \exp \left( - \frac{uL}{D} \right) \right)$$

(from the dispersion model)

$$(3) N \approx \frac{1}{\sigma^2}$$

$$N \approx 1.24$$

Note: In order to obtain  $N = 2$  the gas phase velocity must be reduced by a factor of 14.

### APPENDIX A.3: AXIAL MIXING IN THE RUHRKOHL REACTOR

Data: B-F Reactor

#### Reactor Dimensions

- length	2.0 m
- volume	11.0 l

#### Reactor Temperature

total gas flow	1600. $\text{sm}^2 \text{ day}^{-3}$
pressure	30. MPa

#### Slurry

- density	1.0 $\text{gcm}^{-3}$
- viscosity	1. cp

Calculations:

$$(1) D = v.800 \log \left\{ \left( g^{1/3} \frac{Q}{v^{5/3}} \right) - 4.311 \right\}^{3.2}$$

$$(2) \sigma^2 = 2 \left( \frac{D}{uL} - \left( \frac{D}{uL} \right)^2 \right) \left( 1 - \exp \left( - \frac{uL}{D} \right) \right)$$

$$(3) N \approx \frac{1}{\sigma^2}$$

$$\underline{N \approx 1.3}$$

## APPENDIX B: CORRELATION DERIVATIONS

### APPENDIX B.1: GAS SOLUBILITY CORRELATION

In regions removed from the critical point, (i.e.)  $T_r < 0.95$ , the solubility of a gas in a pure compound is approximated by

$$\log S = a + b \log T_r \quad (\text{B.1})$$

or

$$S = A e^{b \log T_r} \quad (\text{B.2})$$

Substituting equation B.2 into equation 2.6

$$S_{\text{mix}} \cong \prod_{i=1}^n S_i^{x_i} \quad (\text{2.6})$$

yields

$$S_{\text{mix}} \cong \prod_{i=1}^n (A_i e^{b_i \log T_{ri}})^{x_i} \quad (\text{B.3})$$

which can be simplified further to

$$S_{\text{mix}} \cong A e^{\bar{b} \log \bar{T}_r} \quad (\text{B.4})$$

where  $\bar{A}$ ,  $\bar{b}$ ,  $\bar{T}_r$  are weighted averages overall the components which preserve the basic log-linear character of the solubility-temperature relationship. The only thermal complication is the evaluation of  $\bar{T}_r$  for a specific solvent as  $\bar{A}$  and  $\bar{b}$  are constants for all solvent components drawn from the same or similar classes.

For pure solvents the critical temperature is proportional to the boiling temperature.

$$T_c \approx \frac{T_B}{(0.67 \pm .02)} \quad (\text{B.5})$$

Thus a pseudo critical temperature can be defined for complex solvents as

$$\bar{T}_c \approx \frac{T_{B50}}{0.67} = 1.495 T_{B50} \quad (\text{B.6})$$

where  $T_{B50} \equiv$  the temperature at which 50 wt% of the solvent is distilled at one atmosphere pressure.

Since boiling range data is frequently supplied along with other solvent properties in the literature,  $\bar{T}_c$  is readily obtained.

Gas solubilities, in complex mixtures, should correlate approximately according to

$$S_{\text{mix}} = \bar{A} \exp \left\{ \frac{\bar{b} T}{1.495 T_{B50}} \right\} \quad (\text{B.7})$$

**APPENDIX C****LIQUEFACTION TRIAL DATA**

TABLE C.1

## Trial Summary for Forestburg Coal

Run	Operating Conditions						Gas Production (Consumption) g/Kg MAF Coal					Mass Balance grams		% Conversion		
	°C	RPM	CAT. g	SOLVENT	MRT min.	SIM	(H <sub>2</sub> )	CH <sub>4</sub>	CO	C <sub>2</sub> H <sub>6</sub>	CO <sub>2</sub>	MAF Coal Input	Entrained Slurry	Gas	Liq.	Total
201	475	1000	20.0	1	30.0	PF	20.2	10.5	6.6	5.1	35.2	168.31	85.0	5.74	70.9	76.7
204	475	1000	20.0	1	30.0	PF	35.8	12.6	8.0	5.5	37.7	151.6	13.4	6.38	84.2	90.5
205	475	1000	20.0	1	30.0	PF	31.6	12.0	8.3	5.1	40.9	155.8	32.2	6.62	83.0	89.6
208	475	1000	20.0	2	30.0	PF	33.4	12.0	5.0	5.9	40.5	163.6	60.3	6.30	83.8	90.1
209	475	1000	20.0	2	30.0	PF	35.4	14.1	4.7	5.2	46.5	157.5	64.1	7.03	83.0	90.0
210	475	1000	20.0	2	30.0	PF	34.3	10.4	5.0	5.7	37.0	159.8	73.8	5.81	84.1	89.9
212	475	1000	20.0	2	30.0	PF	28.9	13.6	7.5	7.3	44.8	160.2	41.7	7.31	77.1	84.4
213	475	1000	20.0	1	30.0	PF	30.8	11.1	7.5	5.7	38.4	152.7	26.3	6.26	83.6	89.9
214	375	1000	20.0	2	30.0	PF	17.7	1.7	2.9	0.8	30.1	156.5	19.2	3.55	36.1	39.6
215	375	1000	20.0	1	30.0	PF	15.9	1.8	2.8	0.5	29.5	138.6	59.8	3.46	40.8	44.2
216	375/425	1000	20.0	1	30.0	PF	28.4	8.0	7.6	3.9	34.6	133.9	75.4	5.41	79.3	84.7
217	425	1000	20.0	2	30.0	PF	38.2	13.5	5.40	7.1	48.4	163.0	91.3	7.44	82.1	89.5
218	425	1000	20.0	2	30.0	PF	39.1	16.4	8.4	13.6	43.5	148.0	40.4	8.19	83.2	91.4
219	425	1000	20.0	1	5.0	PF	24.1	5.0	5.1	3.0	36.5	121.3	39.1	4.96	59.2	64.1
220	425	1000	20.0	2	5.0	PF	30.0	6.4	5.1	3.5	33.4	167.5	76.8	4.83	57.3	62.1
221	400	1000	20.0	2	30.0	PF	30.3	5.7	3.8	3.1	36.6	173.7	133.6	4.91	65.5	70.4
222	400	1000	20.0	1	30.0	PF	27.1	5.1	6.7	2.7	35.3	128.0	37.5	4.97	68.4	73.4
223	400	1000	20.0	2	30.0	PF	28.3	5.3	5.3	2.8	39.4	161.4	18.7	5.28	64.4	69.7
224	425	1000	40.0	2	30.0	PF	39.1	13.7	4.1	7.1	45.0	157.8	23.9	6.98	79.2	86.2



225	425	1000	80.0	2	30.0	PF	39.9	14.2	1.7	7.7	45.1	154.4	29.7	6.87	77.4	84.3
226	425	1000	40.0	2	30.0	PF	37.7	13.8	2.9	6.4	44.9	161.1	28.6	6.80	79.6	86.4
227	425	1000	80.0	Pre	30.0	PF	29.2	5.1	3.3	3.1	31.9	116.6	52.4	4.34	53.9	58.2
				hydrog.												
229	425	1000	80.0	1	30.0	PF	33.4	8.0	4.3	5.2	30.8	125.7	58.6	4.83	44.0	48.8
230	425	1000	0.0	2	30.0	PF	17.7	14.1	7.8	7.9	52.3		55.0	8.21	61.5	69.7
231	425	1000	0.0	2	30.0	PF	6.90	5.5	5.7	2.9	44.3	147.4	29.3	5.83	30.4	36.2
232	425	500	20.0	2	30.0	PF	35.1	13.6	5.3	7.6	48.4	152.3	52.9	7.48	78.1	85.6
233	425	500	20.0	1	30.0	PF	35.3	14.1	5.5	8.1	46.4	127.4	22.6	7.40	75.5	82.9
234	425	1000	20.0	2	30.0	2	26.4	5.4	6.0	2.7	38.9	160.6	20.9	5.30	54.3	59.6
235	425	1000	20.0	1	30.0	2	24.5	5.4	6.3	3.0	37.3	157.8	28.6	5.19	59.5	64.7
236	425	500	20.0	2	30.0	PF	27.3	6.3	3.9	3.5	39.3	152.7	79.5	5.29	52.0	57.3
237	425	1000	20.0	1	15.0	PF	29.4	8.9	7.1	4.5	39.0	160.8	85.0	5.94	72.0	77.9
238	425	1000	20.0	2	30.0	2	38.1	14.9	4.0	7.7	46.4	159.5	89.9	7.30	77.1	84.4
239	425	1000	80.0	1	30.0	PF	36.7	11.1	3.9	5.5	37.2	160.9	33.1	5.77	74.0	79.8
240	425	1000	20.0	High												
				Sol.	15.0	PF	31.1	9.2	7.0	5.0	40.8	160.8	93.6	6.19	74.4	80.6
241	425	1000	20.0	2	2.44	2	17.3	4.6	6.0	2.2	33.1	161.8	63.9	4.59	45.4	50.0
242	425	1000	20.0	1	45.0	PF	36.6	14.2	5.7	6.2	40.7	158.5	20.0	6.68	81.2	87.9
243	425	1000	20.0	2	30.0	PF	37.0	14.2	5.3	6.2	44.1	162.6	62.2	6.99	80.0	87.0
244	425	1000/														
		500	20.0	2	30.0	PF	34.2	7.2	4.9	7.1	47.1	165.0	62.2	6.63	78.3	84.9
245	425	1000	20.0	2	30.0	PF	36.0	12.1	5.2	9.4	70.0	157.6	78.3	9.66	71.0	80.7
246	425	2000	20.0	2	5.0	PF						160.68				55.0

TABLE C.2

## Trial Summary for Byron Creek Coal

Run	Operating Conditions						Gas Production (Consumption) g/Kg MAP Coal					Mass Balance grams		Z Conversion		
	°C	RPM	CAT. g	SOLVENT	MRT min.	SIM	(H <sub>2</sub> )	CH <sub>4</sub>	CO	C <sub>2</sub> H <sub>6</sub>	CO <sub>2</sub>	MAF Coal Input	Entrained Slurry	Gas	Liq.	Total
312	425	1000	20.0	1	2.44	2	12.7	9.3	1.31	2.49	8.88	166.7	33.7	1.60	15.1	16.7
313	425	1000	0.0	2	30.0	PF	7.7	12.2	2.61	5.85	29.5	170.9	19.5	5.02	30.7	35.8
314	425	1000	20.0	2	30.0	PF	24.4	15.4	2.56	7.49	7.79	171.1	40.3	3.32	46.6	50.0
315	425	1000	40.0	2	30.0	PF	25.2	13.5	2.78	6.06	7.41	156.4	24.7	2.97	44.2	47.2
316	425	1000	80.0	2	30.0	PF	25.5	15.2	1.28	12.8	7.10	166.4	21.0	3.64	34.9	38.6
317	425	1000	20.0	2	2.44	2						169.6				13.9
320	425	1000	20.0	2	2.44	2	14.5	3.9	1.58	3.16	8.67	168.6	41.7	1.73	5.59	7.3
321	425	1000	10.0	2	30.0	PF	19.6	13.0	3.66	7.26	10.5	171.4	31.6	3.44	39.0	42.5
322	425	1000	0.0	1	30.0	PF	4.4	9.7	2.75	4.10	11.2	165.4	34.2	2.78	26.3	29.1
323	425	1000	10.0	1	30.0	PF	15.0	10.6	3.91	5.67	10.7	169.2	12.1	3.09	42.7	45.8
324	425	1000	20.0	1	30.0	PF	17.8	10.0	2.58	5.29	8.65	161.3	7.60	2.65	29.4	32.0
325	400	1000	10.0	1	30.0	PF	12.7	2.97	1.46	1.29	7.33	167.2	22.1	1.31	18.6	19.9
326	425	1000	20.0	2	60.0	PF	29.3	21.1	2.42	11.7	12.8	174.8	41.8	4.80	48.5	53.3
327	378	1000	20.0	2	30.0	PF	11.8	1.4	0.96	0.56	6.48	163.2	14.7	0.94	8.60	9.50
328	425	2000	20.0	2	30.0	PF	25.8	13.5	3.28	10.5	12.5	160.6	11.3	3.94	41.4	45.3
329	425	500	20.0	2	30.0	PF	23.2	13.0	2.73	7.80	8.82	165.7	0.00	3.24	43.2	46.4
330	425	1000	20.0	2	15	PF	20.3	9.6	2.29	9.53	13.6	170.5	26.3	3.51	27.9	31.4
331	425	1000	5.0	1	30.0	PF	14.2	10.4	3.08	5.39	9.19	163.1	38.5	2.80	36.6	39.4
332	425	2000	10.0	1	30.0	PF	11.7	8.7	2.60	4.91	11.1	166.9	14.2	2.74	37.4	40.1
333	425	500	10.0	1	30.0	PF	14.6	10.0	2.85	6.92	12.8	162.4	18.5	3.25	34.0	37.3
334	425	1000	10.0	1	15	PF	12.0	5.0	2.44	1.87	6.95	169.6	18.0	1.63	32.8	34.4
335	400	1000	20.0	2	30.0	PF	16.8	4.6	1.74	2.21	6.91	165.9	20.0	1.55	24.1	25.7
336	425	1000	20.0	2	38	2	25.2	16.2	3.43	8.41	9.39	162.9	23.5	3.74	44.1	47.8
337	425	1000	10.0	1	38	2	15.2	13.5	4.02	7.21	10.6	162.2	6.00	3.53	48.0	51.6
338	425	1000	10.0	1	60	PF	15.1	10.3	3.33	4.75	8.23	167.2	11.0	2.66	41.0	43.7

TABLE C.3

Trial Summary for Saskatchewan Lignite

Run	Operating Conditions						Gas Production (Consumption) g/Kg MAF Coal					Mass Balance grams		% Conversion		
	°C	RPM	CAT. g	SOLVENT	MRT min.	SIM	(H <sub>2</sub> )	CH <sub>4</sub>	CO	C <sub>2</sub> H <sub>6</sub>	CO <sub>2</sub>	MAF Coal Input	Entrained Slurry	Gas	Liq.	Total
401	425	1000	0.0	2	15	PF	10.3	8.88	6.04	4.72	58.8	153.4	32.7	7.85	42.9	50.8
402	425	1000	20.0	2	15	PF	29.4	8.92	4.73	5.38	55.2	154.4	0.00	7.42	60.9	68.4
403	425	1000	40.0	2	15	PF	33.2	8.93	4.39	6.23	64.8	146..7	6.72	8.43	57.2	65.6
404	425	1000	80.0	2	15	PF	34.3	9.59	3.74	6.37	51.0	150.7	17.68	7.07	58.1	65.2

TABLE C.4:

Solubility Data for Trials with Forestburg Coal

Trial	Apparent Solubility      moles $\cdot$ Kg <sup>-1</sup> <sub>solvent</sub> $\cdot$ Atm <sup>-1</sup> $\times 10^3$						
	Ar	N <sub>2</sub>	CH <sub>4</sub>	CO	C <sub>2</sub> H <sub>6</sub>	CO <sub>2</sub>	H <sub>2</sub>
224	2.9	1.5	6.5	1.9	30.	29.	4.3
225	3.3	2.3	5.5	1.9	19.	15.	3.4
226	2.1	1.2	4.3	1.9	17.	13.	2.1
227	11.	6.0	22.	9.3	95.	68.	5.4
229	20.	12.	42.	13.	168.	118.	11.0
230	14.	4.6	12.0	18.	204.	139.	5.5
231	8.5	4.0	22.	5.8	108.	76.	2.3
232	4.4	2.1	9.8	3.2	47.	31.	2.7
233	14.	6.0	37.	9.6	230.	153.	8.0
235	1.9	0.9	4.3	1.2	22.	15.	0.6
237	1.6	0.8	4.2	1.0	24.	16.	2.3
238	1.3	0.6	3.1	1.1	16.	11.	1.1
239	11.	5.2	24.	9.6	100.	68.	6.2
240	8.4	4.2	20.	6.0	96.	69.	4.1
241	8.7	5.5	17.	6.1	73.	53.	4.1
242	12.	5.9	28.	11.	127.	88.	7.4
243	3.1	1.6	6.4	2.1	25.	18.	2.1
244	1.6	0.8	6.9	1.1	14.	10.	1.0
245	8.1	5.9	15.	6.7	50.	38.	4.6

TABLE C.5

Solubility Data for Trials with Byron Creek Coal

Trial	Apparent Solubility      moles • Kg <sup>-1</sup> <sub>solvent</sub> • Atm <sup>-1</sup> x 10 <sup>3</sup>						
	Ar	N <sub>2</sub>	CH <sub>4</sub>	CO	C <sub>2</sub> H <sub>6</sub>	CO <sub>2</sub>	H <sub>2</sub>
312	9.0	4.1	19.	7.6	69.	58.	2.7
313	5.0	3.8	9.1	3.4	-	-	2.8
314	2.3	1.4	5.8	2.7	24.	21.	1.1
315	2.6	1.2	5.3	2.0	1.1	15.	1.4
316	15.	8.8	29.	9.8	111.	79.	6.0
320	5.8	3.1	12.0	4.6	40.	32.	2.1
321	5.1	2.6	10.	4.0	46.	34.	2.1
322	2.9	1.6	6.4	2.2	29.	21.	0.9
323	7.1	4.0	15.	3.0	46.	43.	2.4
324	5.8	2.6	10.	4.5	46.	32.	1.8
325	8.1	4.7	17.	6.1	22.	17.	3.1
326	6.6	3.3	12.	4.6	61.	43.	4.0
328	13.	7.7	23.	11.	92.	62.	6.4
329	7.8	3.9	16.	7.3	68.	45.	3.6
330	14.	7.0	29.	12.	83.	111.	5.2
331	3.7	1.7	6.6	1.9	30.	23.	1.0
332	7.4	4.4	15.	4.2	72.	50.	2.8
333	8.6	4.4	19.	4.3	85.	56.	2.9
336	3.7	2.3	7.1	2.6	26.	20.	1.8
337	8.4	5.9	16.	4.4	60.	48.	3.0
338	4.0	2.6	8.0	2.1	25.	21.	1.6

TABLE C.6

Solubility Data for Trials with Saskatchewan Lignite

Trial	Apparent Solubility      moles $\cdot$ Kg <sup>-1</sup> <sub>solvent</sub> $\cdot$ Atm <sup>-1</sup> $\times 10^3$						
	Ar	N <sub>2</sub>	CH <sub>4</sub>	CO	C <sub>2</sub> H <sub>6</sub>	CO <sub>2</sub>	H <sub>2</sub>
401	2.2	1.8	3.6	1.6	11.	9.5	1.3
402	3.7	2.3	7.0	3.1	30.	14.	2.5
403	6.0	3.3	12.	5.0	43.	32.	2.7
404	3.1	1.8	5.9	2.9	19.	15.	2.7

## APPENDIX D

Direct Coal Liquefaction Characteristics of Byron Creek Coal and  
Vitrinite enriched Byron Creek Coal.SUMMARY

The liquefaction characteristics of a Byron Creek Coal sample and a vitrinite enriched sample, concentrated from the same coal, were compared under several different experimental conditions related to the H-coal liquefaction process. The general conclusions are that (a) vitrinite is not more than 50% liquifiable, while inertinite is probably 100% liquifiable; (b) vitrinite reacts about 14 times more quickly than inertinite, in terms of a first-order constant for the liquefiable fraction of each maceral.

A model that could account for these results is one in which vitrinite dissolves in coal solvent much faster than it can be hydrogenated, leading to precipitation of unreactive polymers, while inertinite dissolves much more slowly and so can be hydrogenated to permanently soluble products much more reliably.

## EXPERIMENTAL

### Materials:

Byron Creek coal (BC) and vitrinite enriched Byron Creek coal (VBC) were obtained from the same raw coal sample. Petrographic, proximate, and ultimate analyses of these two coals were supplied by Esso Canada Ltd. These analyses are summarized on Table 1. The catalyst 12% MoO<sub>3</sub>, 3% CoO supported on an alumina matrix, was manufactured by Alpha products. The liquefaction solvent comprised 90 wt% SRC oil, from Kerr Magee Corp., a product of the Wilsonville, Alabama SRT-1 pilot plant, and 10 wt% reagent grade tetrahydronaphthalene. The standard grade hydrogen, used in these experiments, was purchased locally, and is at least 99.9% pure.



TABLE 1. COAL ANALYSES

COAL		VITRINITE ENRICHED BYRON CREEK	BYRON CREEK
Petrographic	Vitrinite	61.6 2 sd = 5	43.5 2 sd = 5
Analysis	Inertinite	36.6 2 sd = 5	53.3 2 sd = 5
Vol% (MMF)	Liptinite	1.8 2 sd = 1	3.2 2 sd = 1
As Received	Moisture	0.5	0.41
Analysis, wt%	Ash	9.21	23.99
MAF Analysis	Volatiles	27.19	28.77
wt%	Fixed Carbon	72.81	71.23
	Carbon	87.54	85.21
	Hydrogen	4.84	4.87
	Nitrogen	1.27	1.27
	Difference	6.53	8.65

## Experiments:

Two types of experiments were performed during this study:

- i) batch experiments; where coal, solvent, catalyst and hydrogen are charged into a cold autoclave and heated to reaction conditions
- ii) injection experiments; where cold coal slurry is fed rapidly into a preheated autoclave previously charged with hydrogen, catalyst and a small quantity of solvent.

Batch liquefaction experiments were performed because they are a standard laboratory test. Such experiments have a number of drawbacks including poorly defined total reaction time, and relatively long heat-up periods, during which solvent composition can change and coal can begin to react. Slurry injection experiments simulate industrial liquefaction schemes by virtually eliminating heat-up time and by providing more precise control of total reaction time.

## Procedure:

Both batch and injection experiments were performed with the same autoclave and approximately the same amount of reagents and catalyst. A typical charge comprised:

450.0g SRC-011  
50.0g tetralin  
200.0g raw coal  
5.0g catalyst  
5.3g hydrogen  
2.5:1 oil: coal ratio

Total reaction time was measured from the time the autoclave reached reaction temperature (685K), for batch experiments, and from the midpoint of the injection cycle for injection experiments. All experiments were terminated by quenching the reactor to room temperature. Gas and slurry samples were obtained, once the autoclave was cool. Gas samples were analysed for CO, CO<sub>2</sub>, C<sub>2</sub>H<sub>6</sub>, C<sub>3</sub>H<sub>8</sub> using a gas chromatograph. Slurry samples were extracted with tetrahydrofuran to determine a baseline for liquefaction yield.

## RESULTS

Experimental results are summarized on Table 2 along with associated operating data. Based on previous experience with the apparatus and analysis procedures, the total conversion statistics reported on this table are reproducible to within  $\pm 0.3$  wt%. The gas yields are very small, less than 2.2 wt%, and consequently, the probable error is relatively large -  $\pm 20\%$  of the value reported. Liquid yield is determined by difference, and the probable error varies from  $\pm (.4-.7)$ wt%, depending on the gas yield. A further, systematic error is also associated with liquid yield, as water, a compound not readily separated from the reaction products, is included as part of the liquid yield.

### MAF Coal Conversion to Gases and Liquids:

Liquid yield is typically the best indicator of the overall suitability of a coal for direct coal liquefaction, as coal liquids are, in general, more valuable than the fuel gases produced by liquefaction reactions. In the present case, gas yield is less than 5% of the total yield and the discussion is greatly simplified if total conversion is used as a basis for comparison.

After 15 minutes the total conversion of vitrinite enriched Byron Creek coal (27.5 wt%) is much greater than the conversion of Byron Creek coal (18.34 wt%), whereas after 60 minutes the relationship is less

TABLE 2: EXPERIMENTAL RESULTS

Experiment		301	302	303	304	305	307	308	309
Operating Conditions	Temp. (°C)	412	412	412	412	412	412	412	412
	reaction time (min)	15	60	60	15	60	60	15	60
	catalyst (g)	5.03	0.00	5.01	5.03	5.04	5.04	5.00	5.00
	run type	batch	batch	batch	batch	batch	injection	injection	injection
	coal	VBC	VBC	VBC	BC	BC	VBC	VBC	BC
Gas Production (consumption) per Kg MAF coal	CH <sub>4</sub>	2.74	8.32	9.65	3.30	9.39	8.09	3.73	9.86
	CO	0.28	-	0.949	-	0.681	0.582	0.305	1.13
	C <sub>2</sub> H <sub>6</sub>	1.17	5.13	6.91	1.70	3.24	4.60	1.83	4.32
	CO <sub>2</sub>	1.23	2.90	4.13	2.70	1.71	1.95	1.48	2.54
	H <sub>2</sub>	(8.21)	(3.68)	(14.13)	(5.67)	(13.06)	(10.69)	(5.63)	(13.46)
MAF Conversion wt %	gas	0.54	1.63	2.16	0.77	1.50	1.52	0.73	1.79
	liquid	26.97	34.24	37.21	17.57	41.33	37.66	23.04	33.75
	total	27.51	35.87	39.37	18.34	42.83	39.18	23.77	35.53

significant and reversed (42.8 wt% conversion for Byron Creek coal, and only 39.4 wt% conversion for vitrinite enriched Byron Creek coal). These results show that vitrinite reacts more quickly than inertinite but to a lesser extent. The injection experiments lead to the same conclusion. After 15 minutes of reaction, there is a small difference between the liquefaction results obtained from batch and injection experiments for vitrinite enriched Byron Creek coal. This difference is eliminated after 60 minutes of reaction, despite the additional 3 to 5 minutes of kinetically active pre-heating time for the batch experiment. The unenriched Byron Creek coal, comprised principally of the more slowly reacting maceral inertinite, had insufficient reaction time, even after 1 hr, to attain the same total conversion level as obtained from the batch experiment.

#### A Semi-Empirical Reaction Model:

In an effort to quantify the observed reactivity difference between the three macerals (vitrinite, inertinite, liptinite) present in Byron Creek coal, a semi-empirical kinetic model, equation 1, was devised and fitted to the experimental conversion data.

$$\begin{aligned} \text{Total MAF Conversion} &= \sum_{i=1}^3 \left( X_i M_i - X_i M_i \exp [X_i^1 (t_i + t^1)] \right) \quad (1) \\ &= \text{potential liquefiable material} - \text{unreacted by potentially liquefiable material} \end{aligned}$$

- where  $X_i$  = the mass fraction of a maceral which can be liquefied
- $M_i$  = the MAF mass fraction of a maceral in the coal
- $X_i^1$  = the pseudo first order rate constant for the liquefaction reaction of a maceral
- $t$  = the measured reaction time
- $t^1$  = the reaction time equivalent of the kinetically active heat-up time (batch runs only)

The assumptions implicit in this model include:

- i) only a fraction of each maceral is potentially liquefiable.
- ii) each maceral reacts separately according to a first order irreversible reaction to produce gaseous and liquid products.
- iii) mass transfer or other effects do not interfere with reaction kinetics.

The first assumption is encountered frequently in the literature. However, the second two grossly over simplify the complex reaction kinetics of direct coal liquefaction. Despite the simplicity of the model, the mean deviation between the predicted and realized conversions is less than 8%, and much of this deviation can be traced to the uncertainty associated with the petrographic analysis. The model is imperfect but it can still be used to address the questions raised during this study.

The optimum values of the model parameters, Table 3, are sensitive to petrographic composition. Thus, the kinetic data presented can only provide order of magnitude estimates for maceral reactivities. The model results conform to the conclusions of the more qualitative discussion found in the previous section. Vitrinite reacts 14 times more

TABLE 3: OPTIMIZED KINETIC MODEL PARAMETERS

MACERAL	VITRINITE	INERTINITE	LIPTINITE
Mass Fraction which can potentially be liquefied ( $X_i$ )	0.506	1.00	0.202
Pseudo first order rate constant ( $X_i$ , $\text{min}^{-1}$ )	0.0674	0.00487	0.00414
Reaction time equivalent of the heat-up time for batch runs ( $t_i$ , min)	3.96		



rapidly than inertinite, according to the model, but only half of the vitrinite is potentially liquefiable, whereas most of the inertinite is potentially liquefiable. Liptinite reacts at about the same rate as inertinite but very little of it appears to be liquefiable.

CONCLUSIONS:

1. The vitrinite present in Byron Creek coal is only about 50% liquifiable but the reactive fraction reacts about 14 times as fast as inertinite in the same coal.
2. The inertinite in Byron Creek coal appears to be completely liquifiable, but reacts very much more slowly.
3. Results for liptinite would indicate that it is quite unreactive. However, there is too little liptinite in the coal to obtain reliable results.